Western Graduate&PostdoctoralStudies

Western University
Scholarship@Western

Electronic Thesis and Dissertation Repository

1-30-2017 12:00 AM

Expert-in-the-Loop Multilateral Telerobotics for Haptics-Enabled Motor Function and Skills Development

Mahya Shahbazi
The University of Western Ontario

Supervisor
Dr. Rajni V. Patel
The University of Western Ontario

Graduate Program in Electrical and Computer Engineering
A thesis submitted in partial fulfillment of the requirements for the degree in Doctor of Philosophy
© Mahya Shahbazi 2017

Follow this and additional works at: https://ir.lib.uwo.ca/etd

Part of the Biomedical Commons, Controls and Control Theory Commons, and the Robotics Commons

Recommended Citation

Shahbazi, Mahya, "Expert-in-the-Loop Multilateral Telerobotics for Haptics-Enabled Motor Function and Skills Development" (2017). *Electronic Thesis and Dissertation Repository*. 4387.
https://ir.lib.uwo.ca/etd/4387

This Dissertation/Thesis is brought to you for free and open access by Scholarship@Western. It has been accepted for inclusion in Electronic Thesis and Dissertation Repository by an authorized administrator of Scholarship@Western. For more information, please contact wlswadmin@uwo.ca.

Abstract

Among medical robotics applications are Robotics-Assisted Mirror Rehabilitation Therapy (RAMRT) and Minimally-Invasive Surgical Training (RAMIST) that extensively rely on motor function development. Haptics-enabled expert-in-the-loop motor function development for such applications is made possible through multilateral telerobotic frameworks. While several studies have validated the benefits of haptic interaction with an expert in motor learning, contradictory results have also been reported. This emphasizes the need for further in-depth studies on the nature of human motor learning through haptic guidance and interaction. The objective of this study was to design and evaluate expert-in-the-loop multilateral telerobotic frameworks with stable and human-safe control loops that enable adaptive "hand-over-hand" haptic guidance for RAMRT and RAMIST.

The first prerequisite for such frameworks is active involvement of the patient or trainee, which requires the closed-loop system to remain stable in the presence of an adaptable time-varying dominance factor. To this end, a wave-variable controller is proposed in this study for conventional trilateral teleoperation systems such that system stability is guaranteed in the presence of a time-varying dominance factor and communication delay. Similar to other wave-variable approaches, the controller is initially developed for the Velocity-force Domain (VD) based on the well-known passivity assumption on the human arm in VD. The controller can be applied straightforwardly to the Position-force Domain (PD), eliminating position-error accumulation and position drift, provided that passivity of the human arm in PD is addressed. However, the latter has been ignored in the literature. Therefore, in this study, passivity of the human arm in PD is investigated using mathematical analysis, experimentation as well as user studies involving 12 participants and 48 trials. The results, in conjunction with the proposed wave-variables, can be used to guarantee closed-loop PD stability of the supervised trilateral teleoperation system in its classical format. The classic dual-user teleoperation architecture does not, however, fully satisfy the requirements for properly imparting motor function (skills) in RAMRT (RAMIST). Consequently, the next part of this study focuses on designing novel supervised trilateral frameworks for providing motor learning in RAMRT and RAMIST, each

customized according to the requirements of the application.

The framework proposed for RAMRT includes the following features: a) therapist-in-the-loop mirror therapy; b) haptic feedback to the therapist from the patient side; c) assist-as-needed therapy realized through an adaptive Guidance Virtual Fixture (GVF); and d) real-time task-independent and patient-specific motor-function assessment. Closed-loop stability of the proposed framework is investigated using a combination of the Circle Criterion and the Small-Gain Theorem. The stability analysis addresses the instabilities caused by: a) communication delays between the therapist and the patient, facilitating haptics-enabled tele- or in-home rehabilitation; and b) the integration of the time-varying nonlinear GVF element into the delayed system. The platform is experimentally evaluated on a trilateral rehabilitation setup consisting of two Quanser rehabilitation robots and one Quanser HD^2 robot.

The framework proposed for RAMIST includes the following features: a) haptics-enabled expert-in-the-loop surgical training; b) adaptive expertise-oriented training, realized through a Fuzzy Interface System, which actively engages the trainees while providing them with appropriate skills-oriented levels of training; and c) task-independent skills assessment. Closed-loop stability of the architecture is analyzed using the Circle Criterion in the presence and absence of haptic feedback of tool-tissue interactions. In addition to the time-varying elements of the system, the stability analysis approach also addresses communication delays, facilitating tele-surgical training. The platform is implemented on a dual-console surgical setup consisting of the classic *da Vinci* surgical system (Intuitive Surgical, Inc., Sunnyvale, CA), integrated with the da Vinci Research Kit (dVRK) motor controllers, and the dV-Trainer master console (Mimic Technology Inc., Seattle, WA).

In order to save on the expert's (therapist's) time, dual-console architectures can also be expanded to accommodate simultaneous training (rehabilitation) for multiple trainees (patients). As the first step in doing this, the last part of this thesis focuses on the development of a multi-master/single-slave telerobotic framework, along with controller design and closed-loop stability analysis in the presence of communication delays. Various parts of this study are supported with a number of experimental implementations and evaluations.

The outcomes of this research include multilateral telerobotic testbeds for further studies on the nature of human motor learning and retention through haptic guidance and interac-

tion. They also enable investigation of the impact of communication time delays on supervised haptics-enabled motor function improvement through tele-rehabilitation and mentoring.

Keywords: Expert-in-the-loop motor skills development; haptics-enabled motor learning; multilateral teleoperation; robotics-assisted surgical training; robotics-assisted mirror rehabilitation therapy; supervised telerobotics.

Co-Authorship Statement

The thesis presented here has been written by Mahya Shahbazi under the supervision of Dr. Rajni V. Patel. Parts of the material in this thesis were published in peer-reviewed journal and conference papers, or are under review. The research published in each paper has been mainly conducted and written by the principal author. For the research reported in all of the papers, Dr. Patel was the project leader and supervisor, guiding and directing the study in every aspect, including idea development, theoretical and experimental evaluations, writing and revising the papers.

The material presented in Chapter 2 will be submitted for publication:

- Mahya Shahbazi, Rajni V. Patel, "A Systematic Review of Multilateral Teleoperation Systems", To be submitted to *IEEE Transactions on Haptics*, 2016.

The material presented in Chapter 3 has been published as:

- Mahya Shahbazi, Heidar A. Talebi, Rajni V. Patel, "Networked Dual-User Teleoperation with Time-Varying Authority Adjustment: A Wave Variable Approach", *IEEE/ASME International Conference on Advanced Intelligent Mechatronics (AIM)*, pp. 415-420, 2014.
    - Mahya Shahbazi developed the idea, designed the controller, and experimentally implemented the framework. She also conducted experiments, evaluated the results and wrote the manuscript.
    - Dr. H.A. Talebi was an academic collaborator in this work. He contributed in development of the theory.

The material presented in Chapter 4 is currently under review for publication:

- Mahya Shahbazi, Seyed Farokh Atashzar, Mahdi Tavakoli and Rajni V. Patel, "Position-Force Domain Passivity of Human Arm in Telerobotics Systems", Submitted to *the International Journal of Robotics Research: Special Issue on Human-Robot Interaction*, 2016.

- Mahya Shahbazi was the primary contributor to the development of the idea and the research hypothesis, experimental implementation of the idea, user-data collection, data analysis and evaluation of results, and writing the manuscript.
- Seyed Farokh Atashzar helped in preparing the experimental setup, and user-data collection.
- Dr. Mahdi Tavakoli was an academic collaborator in this work. He helped in the development of the research hypothesis and in planning the user study. Mahya Shahbazi was a visiting research scholar in Dr. Tavakoli's lab for a 6-month period, during which a part of the work was carried out. This work was supported by joint grants awarded to Dr. R.V. Patel and Dr. M. Tavakoli.

The material presented in Chapter 5 has been published as:

- Mahya Shahbazi, Seyed Farokh Atashzar, Mahdi Tavakoli and Rajni V. Patel, "Robotics-Assisted Mirror Rehabilitation Therapy: A Therapist-in-the-Loop Assist-as-Needed Architecture", *IEEE/ASME Transactions on Mechatronics*, vol. 21, no. 14, pp. 1954-1965, 2016.

- Mahya Shahbazi, Seyed Farokh Atashzar, Mahdi Tavakoli and Rajni V. Patel, "Therapist-In-The-Loop Robotics-Assisted Mirror Rehabilitation Therapy: An Assist-As-Needed Framework", *IEEE International Conference on Robotics and Automation (ICRA)*, pp. 5910-5915, 2015

- Mahya Shahbazi, Seyed Farokh Atashzar, and Rajni V. Patel, "A Framework for Supervised Robotics-Assisted Mirror Rehabilitation Therapy", *IEEE/RSJ International Conference on Intelligent Robots and Systems (IROS)*, pp.3567-3572, 2014.

  - Mahya Shahbazi was the primary contributor to the development of the idea, design and experimental implementation of the proposed framework, development of the theoretical aspects including the stability analysis, conducting experiments and writing the manuscript.
  - Seyed Farokh Atashzar helped in preparing the experimental setup, and designing and conducting the experiments.

- Dr. Mahdi Tavakoli was an academic collaborator in this work. He contributed to the development of the experimental platform, and some of the theory. Mahya Shahbazi was a visiting research scholar in Dr. Tavakoli's lab for a 6-month period, during which a part of the work was conducted. This was supported by joint grants awarded to Dr. R.V. Patel and Dr. M. Tavakoli.

The material presented in Chapter 6 is currently under review for publication:

- Mahya Shahbazi, Seyed Farokh Atashzar, Christopher Ward, Heidar Ali Talebi, Rajni V. Patel, "Multimodal Sensorimotor Integration for Expert-in-the-Loop Telerobotic Surgical Training", Submitted to *IEEE Transactions on Robotics*, 2016.

A part of the material in this Chapter was published in

- Mahya Shahbazi, Seyed Farokh Atashzar, Heidar Ali Talebi and Rajni V. Patel, "An Expertise-Oriented Training Framework for Robotics-Assisted Surgery", *IEEE International Conference on Robotics and Automation (ICRA)*, pp. 5902-5907, 2014.

- Mahya Shahbazi, Seyed Farokh Atashzar, and Rajni V. Patel, "A dual-user teleoperated system with Virtual Fixtures for robotic surgical training", *IEEE International Conference on Robotics and Automation (ICRA)*, pp. 3639-3644, 2013.

  - Mahya Shahbazi was the primary contributor to the development of the idea, design and experimental implementation of the proposed framework, development of the theory including the stability analysis, conducting the experiments and writing the manuscript.
  - Seyed Farokh Atashzar helped in designing and conducting the experiments.
  - Christopher Ward helped in preparing the experimental setup, and wrote a section describing the setup.
  - Dr. Heidar Ali Talebi was an academic collaborator in this work. He contributed in the development of the theoretical aspect of the work.

The material presented in Chapter 7 has been published in

- Mahya Shahbazi, Seyed Farokh Atashzar, Heidar Ali Talebi and Rajni V. Patel, "Novel Cooperative Teleoperation Framework: Multi-Master/Single-Slave System", *IEEE/ASME Transactions on Mechatronics*, vol. 20, no. 4, pp. 1668-1679, 2014.

- Mahya Shahbazi, Seyed Farokh Atashzar, Heidar Ali Talebi and Rajni V. Patel, "A Multi-Master /Single-Slave Teleoperation System", *ASME Dynamic Systems and Control Conference (DSCC)*, pp. 107-112, 2012.

  - Mahya Shahbazi was the primary contributor to the development of the idea, design and experimental implementation of the proposed framework, development of the theoretical aspects including the stability analysis, conducting experiments and writing the manuscript.

  - Seyed Farokh Atashzar helped to prepare the experimental setup, and conduct the experiments.

  - Dr. H.A. Talebi was an academic collaborator in this work. He helped in the development of the idea and the stability analysis.

To Maryam and Roholla,

without whom I would not be me;

and

to my Dearest Grandparents,

whose love has left an indelible impression on my heart.

Acknowledgments

This thesis would not have been possible without the invaluable support of so many different people around the world.

First and foremost, I would like to express my sincere gratitude and appreciation to my brilliant supervisor, Dr. Rajni Patel, for his continuous support and encouragement, insightful vision and supervision, as well as constructive advice. It was under his skillful mentorship that I was able to flexibly pursue my interests and build on my strengths without losing sight of my goals. He is a living exemplar of a truly humane scientist.

I would like to sincerely thank my former supervisors in Iran, Drs. Hamid D. Taghirad and Heidar Ali Talebi, who taught me the basics of research in the first place. Special thanks also go to Dr. Mahdi Tavakoli for his support, guidance and encouragement along the way. I would also like to thank my examiners, Dr. S.E. Salcudean, Dr. I. Polushin, Dr. A.L. Trejos and Dr. L. Ferraira, for taking the time to review (and evaluate) my thesis and for providing valuable comments.

I would also like to acknowledge several Canadian granting agencies and industries, without whose generous financial support my research would not have been possible. This includes the Canadian Institutes of Health Research (CIHR) and the Natural Sciences and Engineering Research Council (NSERC) of Canada through the Collaborative Health Research Projects (CHRP) Grant #316170, the NSERC Collaborative Research and Development Grant #CRDPJ411603-10, and the NSERC Discovery Grant #RGPIN1345; the AGE-WELL Network of Centres of Excellence through the project AW-CRP2015-WP5.3; the Canada Foundation for Innovation through Grant LOF 28241, Quanser Inc. (Markham, ON, Canada), as well as the Ontario Graduate Scholarship (OGS) and the NSERC Collaborative Research and Training Experience (CREATE) programs.

Special thanks go to Christopher Ward, Abelardo Escoto, Dr. Ali Talasaz and Karen Siroen for their technical support during this study. I am also grateful to all of my friends at CSTAR and in London, especially Dr. Iman Khalaji, Dr. Ali Asadian, Dr. Mahta Khoshnam Tehrani, Behnaz Poursartip, Dr. Peyman Yadmellat, Dr. Nima Najmaei, Saeed Bakhshmand, Sahar Shahbazi, Vahid Mehrabi, Pouya Soltani Zarrin, Dr. Ran Xu, Linda Andrews, Dr. Nazanin

Pourmand, Dr. Mehrnoosh Kaffashi, Dr. Zeinab Birjandian, Dr. Omid Mola, Dr. Meysam Haghshenas, and Dr. Maysam Mirahmadi for their support and friendship over the past several years.

I am enormously thankful to Ayda Bashiri, Dr. Samaneh Kazemifar, Behnaz Poursartip, Razieh Karimi, Dr. Laleh Nazari, Dr. Mohammad Ali Tavallaei, Dr. Amir Owrangi, Dr. Iman Owrangi, and Dr. Sadra Souzanchi for their true friendship, and all the great moments we have shared. Miles apart from my family, the daily grind would have been harder without their heartwarming and revitalizing presence as my second family in Canada.

Very special acknowledgments go out to my fiercely devoted mom, Maryam Jafarpour, for being the angel to lift me to my feet whenever my wings had trouble remembering how to fly. I would not have been where I am now if it had not been for her and the sacrifices she has made for me throughout her life.

Endless thanks go to my unbelievably dedicated dad, Rohollah Shahbazi, for continuously believing in me and my capabilities, no matter the circumstances, and for all the courage and strength he taught me to have in the face of difficulties. The world would be a better and safer place to live in if it had more supportive dads like him.

Special thanks go to Jamileh Zerehgar and Dr. Heshmat Atashzar, the world's most amazing parents-in-law, for their unconditional love, countless expressions of support and boundless inspiration. I am truly blessed to be a part of such a caring and loving family. This journey would have been more difficult if it had not been for them.

I would like to express special thanks to Mohamad Shahbazi for being the perfect brother one might ask for, someone who makes my world a brighter and more beautiful place to live, and also to Hasty and Nazly Ataszhzar for being the kind and lovely sisters whom I had always wished to have. I am so lucky to have them in my life. I also want to thank the rest of my family in Iran, especially Mehrnoosh and Golrokh Jafarpour, and Haydeh Zerehgar for their endless love and encouragement.

Finally, I want to express my most sincere gratitude to Dr. Seyed Farokh Atashzar, my wonderful husband, my best friend, my greatest colleague and, in a single word, my soulmate. This journey would not have been possible without his ceaseless support and limitless love. Farokh, you were the source of my strength and inspiration when I was too tired to take another

step. Thanks for all the hope, motivation and encouragement you gave me. Thank you for all the great memories we have shared, all the dreams and wishes, ups and downs, laughter and tears, and, above all, your very enjoyable companionship during the past decade. Thanks for being a true blessing in my life.

Contents

List of Figures

List of Tables

List of Acronyms

2D	Two Dimensional
ANMT	Assist-as-Needed Mirror Therapy
ANT	Assist-as-Needed Therapy
BMI	Body Mass Index
DM/SS	Dual-Master/Single-Slave
DOF	Degree Of Freedom
DOM	Degree Of Mobility
DURC	Dual-User Redundancy Control
DUSC	Dual-User Shared Control
dVRK	da Vinci Research Kit
EE	End-Effector
EIL	Expert-In-the-Loop
EZW	Extended Zeheb–Walach
FDA	Food and Drug Administration
FDPC	Frequency-Domain Passivity Controller
FIS	Fuzzy Interface System
GUI	Graphical User Interface
GVF	Guidance Virtual Fixture
HF	High Frequency
HOH	Hand-Over-Hand
IOS	Input-Output Stable
LAN	Local Area Network
LF	Low Frequency
LH	Left Hand
LOG	Level Of Guidance

MIME	Mirror Image Movement Enabler
MIS	Minimally Invasive Surgery
MM/MS	Multi-Master/Multi-Slave
MM/SS	Multi-Master/Single-Slave
MS	Movement Smoothness
MSA	Mass-Spring Array
MT	Mirror Therapy
MTM	Master Tool Manipulator
PCC	Pearson product-moment Correlation Coefficient
PD	Position-force Domain
PDP	Position-force Domain Passivity
PE	Persistently Exciting
PFL	Patient's Functional Limb
PIL	Patient's Impaired Limb
PR	Positive Real
PS	Performance Symmetry
PSD	Positive Semi-Definite
PSM	Patient Side Manipulator
QLA	Quad Linear Amplifier
RAMIS	Robotics-Assisted Minimally Invasive Surgery
RAMIST	Robotics-Assisted Minimally Invasive Surgical Training
RAMT	Robotics-Assisted Mirror Therapy
RART	Robotics-Assisted Rehabilitation Therapy
RAS	Robotics-Assisted Surgery
RH	Right Hand
RHP	Right Half Plane
SAW	Surgical Assistant Workstation

SM/MS	Single-Master/Multi-Slave
SM/SS	Single-Master/Single-Slave
SPR	Strictly Positive Real
TASC	Teleoperative-Autonomous Shared Control
TCT	Therapist-Commanded Trajectory
TDPC	Time-Domain Passivity Controller
TIL	Therapist-in-the-Loop
TPL	Total Path Length
TTI	Tool-Tissue Interaction
UDP	User Datagram Protocol
UMI	User Macro Interface
VD	Velocity-force Domain
VDP	Velocity-force Domain Passivity
VIM	Virtual Internal Model
VR	Virtual Reality
ZW	Zeheb–Walach

Chapter 1

Introduction

A robotics-based teleoperation system (henceforth called a telerobotic or teleoperation system) extends an operator's sensing and manipulation capabilities to a remote location. It facilitates off-site performance of a desired task through a set of robotic consoles, which provides operators with safety and accessibility. A telerobotic system consists of three main components: 1) a slave console, performing a desired task on a designated environment; 2) a master console manipulated by an operator, remotely controlling the slave console [1], [2]; and 3) a communication channel, to transmit data between the master and slave consoles that may be located at some distance [3]. Telerobotic systems have been broadly used in a wide range of applications from mining, space and underwater exploration, to medicine [3], [4], [5], [6]. The application of telerobotic systems to medicine includes Robotics-Assisted Minimally Invasive Surgery (RAMIS) [5], [6] and Robotics-Assisted Rehabilitation Therapy (RART) [7], [8], [9], which have received a great deal of attention during the past couple of decades. Although telerobotic systems offer considerable benefits to various aspects of medical interventions, when it comes to motor function and skills development, their conventional Single-Master/Single-Slave (SM/SS) structure imposes limitations and there are constraints that need to be addressed. This research focuses on two main applications of a telerobotic system for motor function development in two medical interventions, RART and RAMIS, in terms of the limitations imposed by an SM/SS structure, and it proposes solutions for both of these applications. To discuss each application in further detail, each topic will be elaborated on separately.

1.1 Robotics-Assisted Rehabilitation Therapy

Annually 15 million people worldwide suffer from stroke, a sudden loss of brain function caused by the rupture of blood vessels in the brain (hemorrhagic stroke) or the interruption of blood flow to the brain (ischemic stroke). As a result of a stroke, brain cells (neurons) in the affected area are deprived of oxygen and begin to die [10]. With a survival rate of about 70%– about 10 million people per year– stroke is known to be a major leading cause of long-term disabilities and severe impairments [11]. The significant number of patients recovering from stroke, in addition to other neurological disorders, has led to a growing need for rehabilitation services in order to induce neuroplasticity in patients. Neuroplasticity is referred to as the reorganization ability of the brain by developing new neural connections through sensory inputs, experience, and learning, which allows the brain's neurons to compensate for injury and disease [12]. Achieving brain neuroplasticity from rehabilitation therapy is a labor-intensive process, which necessitates not only a therapist's expertise and knowledge, but also reproducible movements and stereotyped exercises. This has led to a paradigm shift towards Robotics-Assisted Rehabilitation (RAR), offering novel recovery-assessment approaches along with patient-targeted rehabilitation therapies [13, 14]. MIT-MANUS [13], ARMin [15], Pneu-WREX [16], RUPERT [16], [17] are some examples of robotics-assisted rehabilitation systems. As an effective rehabilitation approach, Mirror Therapy (MT) has also found its way into the robotics-assisted rehabilitation world [18, 19].

1.1.1 Mirror Therapy

Mirror therapy (Fig. 1.1) refers to the use of a mirror to create a reflective illusion of a Patient's Impaired Limb (PIL) moving in accordance with the Patient's Functional Limb (PFL), in order to trick the brain into thinking the movement has occurred at the impaired/affected side [20].
It has been shown in several studies that observing or imagining an action activates the same cortical areas of the brain as during execution of the same action [21], [22], [23], [24]. Based on this mechanism, mirror therapy has been shown to be effective by providing the patient with a visual illusion of his/her impaired limb moving, thus activating the cortical areas involved in the task execution and inducing neuroplasticity.

Figure 1.1: Conventional mirror therapy (©North Coast Medical Inc.; source: https://www.ncmedical.com/item_2444.html).

Moreover, through mirror-symmetric (or any other coordinated bimanual) movement pattern for the two limbs in mirror therapy, the unimpaired hemisphere of the brain interacts with the impaired hemisphere, thereby inducing reorganization of the motor cortex networks and facilitating cortical neuroplasticity through a second mechanism [25, 26].

The effectiveness of mirror-symmetric *bimanual* therapy has been shown in comparison with conventional *unimanual* therapy to result in an increase in the functional ability as well as a decrease in movement completion times for the PIL [27]. Mirror therapy has also been shown to be effective in terms of improving the accuracy, active range of motion, dexterity and grip strength of the limb [28–31].

1.1.2 Robotics-Assisted Mirror Therapy (RAMT)

To benefit from the indisputable advantages of RAR, the robotic form of mirror therapy has evolved during the past decade. During robotics-assisted mirror therapy, motions of the patient's functional limb are mirrored through a telerobotic medium to the patient's impaired limb, promoting the functional recovery of the impaired limb through the spatial coupling effect between the two limbs, resulted from the tendency of one limb to adopt the spatial features of the other limb [26, 32, 33]. Fig. 1.2 illustrates an overall scheme of robotics-assisted mirror therapy. Existing RAMT systems, such as Mirror Image Movement Enabler (MIME) [34], pro-

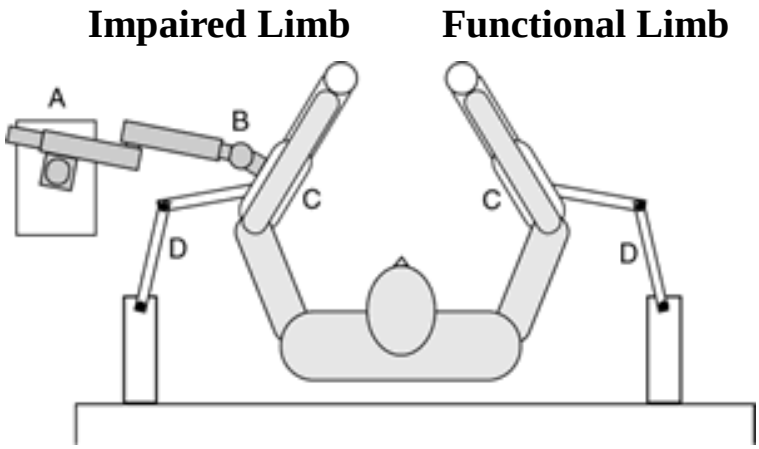

Figure 1.2: Robotics-assisted mirror therapy [19].

vide a bilateral– i.e., single-master/single-slave– telerobotic framework in order for the PIL to move in accordance with the mirror-image motions of the PFL. This gives patients some level of control over the therapy through the involvement of their functional limb. However, due to the inherently restrictive structure of SM/SS systems used in conventional RAMT (Fig. 1.3), the PIL interacting with the slave robot can only receive commands from the PFL interacting with the master robot. This means that a therapist cannot be directly involved in the rehabilitation loop to apply corrective movements or to monitor/assess the PIL performance through haptic feedback. Presence of an expert in the loop of the therapy is essential in promoting the patient's functional recovery not only because of the therapist's knowledge and expertise, but also due to the possible effect of haptic interaction with an expert on the patient's learning curve, as discussed in [35]. This haptic interaction between the therapist and the patient is, however, not achievable through the limiting SM/SS structure of the conventional RAMT system.

1.2 Robotics-Assisted Minimally Invasive Surgery

In a RAMIS operation, as a particular form of minimally invasive surgery, surgical instruments are introduced into the patient's body through tiny incisions, where surgeons perform surgical intervention by remotely manipulating the instruments through a master/slave telerobotic platform. Besides the benefits provided to patients by non-robotic minimally invasive surgery, i.e.,

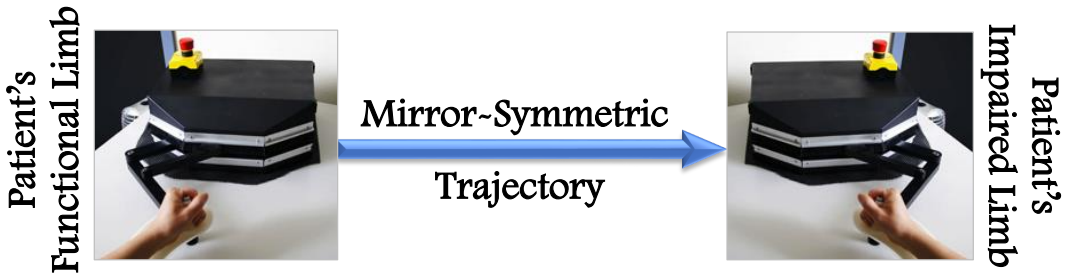

Figure 1.3: The overall scheme of the conventional robotics-assisted mirror therapy with respect to the interconnection between the PFL and the PIL [36] (©[2016] IEEE).

Figure 1.4: The *da Vinci* surgical robotic system (©[2006] Intuitive Surgical, Inc.).

less post-operative pain and significantly faster recovery time as result of reduced trauma, and improved cosmesis [37], RAMIS also offers several advantages to surgeons by 1) improving dexterity in manipulating surgical instruments, 2) providing HD stereovision capabilities, 3) filtering out their hand tremor, and 4) scaling down their hand motions resulting in enhanced precision [38], [37] [39]. The *da Vinci*® surgical system (Fig. 1.4) from Intuitive Surgical Inc. [40] is an FDA-approved RAMIS system which has been used in more than 200,000 surgeries to date.

1.2.1 Robotics-Assisted Minimally Invasive Surgical Training (RAMIST)

While this form of surgery has significant advantages for patients, it could be challenging for novice surgeons and residents to perform, and achieving technical competence requires a

Figure 1.5: The dual-console *da Vinci*® Si surgical robotic system (©[2009] Intuitive Surgical, Inc.).

well-planned learning strategy. For successful RAMIS, effective surgical training is necessary for novice surgeons to acquire appropriate psychomotor skills [41]. There have been several RAMIS-related adverse events reported to the U.S. Food and Drug Administration (FDA) during the past 15 years. One reason cited for this is a lack of proper training; affirming the necessity of developing appropriate RAMIST frameworks [42].

In order to provide on-demand training to RAMIS trainees, Intuitive Surgical Inc. has developed the *da Vinci*® Skills Simulator [40] which is operated from the surgeon's console of the *da Vinci*®. The Simulator incorporates a virtual reality (VR)-based simulation platform from Mimic [43] and provides the trainee with the look and feel of the *da Vinci*® Surgical System.

A more recent development by Intuitive Surgical Inc., the dual-console *da Vinci*® Si Surgical System [44], shown in Fig. 1.5, addresses questions that normally arise regarding fidelity of the simulation environment by providing a feature that enables a trainee to be involved in an actual surgical procedure. This system offers two master consoles each manipulated individually by a surgeon, one of which can be a trainee. However, at each time, the slave console receives commands only from one master console. Therefore, to involve the trainee in the procedure, it is required to switch from the expert's console to the trainee's. Therefore, when the trainee has control over the procedure, the expert does not have any authority over the surgery,

which may increase potential risks to the patient. This constraint is mainly imposed due to the inherent SM/SS structure of the system. Although two master consoles are integrated into the system, the whole system is a combination of two SM/SS systems independently working in series/parallel, rather than a cohesive Dual-Master/Single-Slave (DM/SS) framework. In addition, the system provides the trainee, using a see-and-repeat model [44], with no direct supervision and control on the trainee through haptic-based interaction between the expert and the trainee. Such haptic interactions can enhance and speed up the motor learning process compared to when practicing the task alone for the same duration [35].

1.3 Research Statement

The aforementioned challenges for RAMT and RAMIS necessitate development of appropriate supervised haptics-enabled multilateral frameworks tailored based on the requirements of each application in order to cultivate proper motor function (skills). The potency of expert-in-the-loop dyadic haptic interaction in advancing motor function (skills), as compared to practicing the learning task alone for the same duration, has been investigated in many studies, although in the absence of communication delay. While several have validated the benefits of supervised haptic augmentation in motor learning processes [35], [45], [46], [47], contradictory outcomes have also been reported possibly due to the *fixed-gain* nature of the error-reducing haptic guidance provided and/or the forcefulness insufficiency of the haptic guidance resulting from the limited stability margin of the dyadic frameworks under investigation [48], [49]. These controversies emphasize the need for further in-depth and conclusive studies on the nature of human motor learning and retention through haptic guidance and dyadic interactions. An exemplary testbed for these purposes should enable active involvement of the operator as well as skills-oriented assignment of the haptic guidance [48], while preserving closed-loop stability in the presence of sufficiently high level of haptic interaction [49]. Therefore, this thesis aims at the design and development of appropriate expert-in-the-loop haptics-enabled teleoperation frameworks that facilitate further informative studies on the nature of human motor learning and retention in both RAMT and RAMIS areas.

1.3.1 Time-Varying Dominance Distribution

To achieve the above-mentioned goal, the first requirement for the trilateral telerobotic system would be to allow for time-varying dominance/authority distribution between the two operators (expert/novice or therapist/patient). This allows the patient (novice) to actively engage in the therapy (training) process depending on their level of impairment (skills). Toward this end, ensuring closed-loop stability of the dual-user system in the presence of a time-varying dominance factor is a necessity. Therefore, the first part of this thesis aims at development of a wave variable control approach for conventional haptics-enabled dual-user teleoperation systems such that system stability is guaranteed in the presence of a time-varying dominance factor as well as communication time delay. The proposed controller includes a local impedance-based controller adopted from the literature for each robot and a wave transformation modified for the dual-user system with a time-varying dominance-factor. In order to investigate closed-loop stability, passivity theory has been applied and it has been shown that the proposed wave-variable-based controller guarantees system stability in the presence of a time-varying dominance factor, while the communication channels have constant time delays. Validity of the controller has been demonstrated via experiments.

1.3.2 Position-Force Domain Passivity

Similar to other passivity-based approaches, the above-mentioned wave-variable methodology is initially developed for velocity-force domain, due to the well-known assumption of passivity of the human arm in this domain. However, the framework is straightforwardly extendable to position-force domain, which enhances performance by eliminating position-error accumulation and position drift, provided that the human-arm terminal also remains passive in this domain. Unlike velocity-force domain passivity of the human arm, position-force domain passivity of the human-arm terminal has not, however, been studied in the literature. Therefore, the next part of this thesis focuses on investigating passivity of the human arm in position-force domain, explored through mathematical analysis, experimentation and statistical user studies involving 12 subjects and 48 trials. It is shown that, unlike in velocity-force domain, passivity of the human arm in position-force domain is frequency-dependent and thereby, considera-

tion should be given for a framework to be applied in the position-force domain. For future design of suitable controllers, statistical analyses are performed to investigate correlations between the levels of position-force domain passivity of the left and the right arms of the human participants, as well as the levels of passivity of the subjects' arms and their physical characteristics, e.g., weight, height, and body mass index. Possible control strategies through which the passivity of the operator termination can be guaranteed are also discussed.

1.3.3 Novel Trilateral Teleoperation Frameworks

Integrating the above-mentioned position-force domain passivity analysis with the proposed wave-variable methodology will facilitate time-varying adjustment of the dominance factor for the conventional trilateral teleoperation framework in position-force domain. While this will address instability challenges of a conventional dual-user framework in the presence of a time-varying dominance factor, the classic dual-user architecture has still some limitations that make it inadequate for properly inducing motor function/skills in RAMT and RAMIS. Consequently, the next parts of this thesis focus on design and implementation of novel supervised trilateral frameworks for inducing motor learning in RAMT and RAMIS, each customized/tailored according to the requirements of the application. Rigorous stability analyses have also been performed to ensure closed-loop stability of the frameworks in the presence of various destabilizing factors, including communication time delays.

The framework proposed for each application provides the following innovations:

Robotics-Assisted Mirror Therapy

1. Therapist-in-the-loop MT, which enhances the PIL motor recovery process through the cross-cortex coupling effect between limbs, as well as the expertise and direct supervision of the therapist over the treatment to provide appropriate corrective movements.

2. PFL-mediation, which allows for the supervision/impact of the patient over the treatment through their PFL medium in order to guarantee the patient's safety and comfort by avoiding the application of excessive pressure and pain on the PIL.

3. Haptic feedback to the therapist from the patient side, which allows the therapist to better

decide on the intensity of the therapy administered to the patient.

4. Assist-as-needed therapy, realized through an adaptive Guidance Virtual Fixture (GVF), which promotes active involvement of the patient in the treatment.

5. Task-independent and patient-specific motor-function assessment, which facilitates adaptive adjustment of the therapy based on the patient's impairment level.

Another contribution of this part of the thesis is an investigation of the closed-loop stability of the proposed framework. This was done using a combination of the Circle Criterion and the Small-Gain Theorem, which leads to a set of sufficient stability conditions. The proposed stability analysis also addresses instabilities caused by communication delays between the therapist and the patient, which facilitates the case of haptics-enabled tele/in-home rehabilitation.The proposed procedure also addresses extra stability challenges raised by the integration of the time-varying nonlinear GVF element into the delayed closed-loop system. Several experiments are conducted in order to evaluate the proposed framework.

Robotics-Assisted Minimally Invasive Surgical Training

1. Expert-in-the-loop surgical training with multimodal sensorimotor integration, which speeds up the learning curve through haptic interaction between the novice and the expert.

2. Adaptive expertise-oriented training, realized through a Fuzzy Interface System (FIS)– which actively engages the trainee, while providing them with appropriate level/format of training, depending on their level of proficiency over the task.

3. Task-independent motor skills assessment, which facilitates adaptive expertise-oriented training;

4. Haptic feedback from the surgical site to the expert surgeon, which enables the expert to transparently perceive the surgical environment, disregarding the trainee's level of skills and participation.

5. concurrent conduct of a surgical procedure by an expert providing multimodal training to a trainee at any stage of motor-skills learning, without jeopardizing patient safety.

Another contribution of this part is an investigation of the closed-loop stability of the proposed framework using the Circle Criterion, in the presence and absence of tool-tissue interaction haptic feedback, which leads to sufficient stability conditions. In addition to the time-varying elements of the system, the stability analysis approach also addresses communication time delay, facilitating tele-surgical training. Experimental evaluations are presented in support of the proposed platform through the implementation of a dual-console surgical setup consisting of the classic *da Vinci*® surgical system (Intuitive Surgical, Inc., Sunnyvale, CA) and the dV-Trainer® master console (Mimic Technology Inc., Seattle, WA).

1.3.4 Novel Multi-Master/Single-Slave Teleoperation Framework

The above-mentioned dual-console telerobotic architectures provide expert-in-the-loop motor function development training to one patient/trainee at a time. In order to save on the therapist/surgeon time, the dual-console architectures can be extended to accommodate for multiple patients/trainees. As the first of step of doing so, the next part of this thesis focuses on development of a multi-master/single-slave telerobotics framework. The desired objectives for the MM/SS system are presented in such a way that both cooperative and training applications, e.g. surgical teleoperation and surgical training, can benefit. Passivity of the system is investigated and it is shown that an ideal MM/SS system, depending on its structure, may not always be passive unlike a conventional SM/SS system. An impedance-based control methodology is developed to satisfy the desired objectives of the MM/SS system in the presence of communication delays. The Small-Gain theorem is used to analyze closed-loop stability, deriving a sufficient condition to guarantee system stability in the presence of time delays. Experimental results conducted on an MM/SS system are presented to evaluate the performance of the proposed methodology.

1.4 Thesis Structure

The structure of the rest of the thesis is as follows:

Chapter 2 Presents a systematic literature review on multilateral (trilateral and higher) telerobotic systems. It classifies the existing state-of-the-art architecture based on topologies, applications (including motor function development in robotic surgical training and rehabilitation), and closed-loop stability analysis approaches. For each category, the review discusses control strategies used for various architectures as well as control challenges (e.g., closed-loop instability as a result of a delay in the communication network, etc.) addressed by each methodology.

Chapter 3 Presents a wave-variable control approach developed for the conventional dual-user teleoperation system, such that closed-loop stability is guaranteed in the presence of a time-varying dominance factor as well as communication delays.

Chapter 4 Investigates human-arm passivity in position-force domain. It shows through analytical, experimental and user trial studies that unlike in the velocity-force domain, passivity of the human arm in the position-force domain is frequency-dependent and thereby, consideration should be given for a framework to be applied in the position-force domain. The chapter concludes with suggestions for ensuring passivity of the arm terminal in the aforementioned domain.

Chapter 5 Presents the design and implementation of the proposed supervised trilateral framework for robotics-assisted mirror rehabilitation therapy. Closed-loop stability analysis of the framework using a combination of the Circle Criterion and the Small-Gain Theorem, as well as experimental evaluations are also presented.

Chapter 6 Discusses the design and implementation of the supervised dual-console architecture proposed for robotic minimally invasive surgical training. Closed-loop stability analysis of the proposed architecture in the presence and absence of tool-tissue interaction haptic feedback is also discussed and sufficient stability conditions are derived. The experimental evaluation of the architecture on a dual-console platform consisting of the classic *da Vinci*® surgical system (Intuitive Surgical, Inc., Sunnyvale, CA) and the dV-Trainer® master console (Mimic Technology Inc., Seattle, WA) is also presented.

Chapter 7 Presents the proposed multi-master/single-slave teleoperation framework. An impedance-based control methodology is adopted to satisfy the desired objectives of the MM/SS system in the presence of communication delays. Closed-loop stability analysis of the framework in the presence of time delays and using the Small-Gain theorem as well as experimental evaluation of the proposed platform are also given.

Chapter 8 Highlights the contributions of this thesis and provides suggestions for future work.

Bibliography

[1] Y. Ye and P. X. Liu, "Improving trajectory tracking in wave-variable-based teleoperation," *IEEE/ASME Transactions on Mechatronics*, vol. 15, no. 2, pp. 321–326, 2010.

[2] V. Chawda and M. K. OMalley, "Position synchronization in bilateral teleoperation under time-varying communication delays," *IEEE/ASME Transactions on Mechatronics*, vol. 20, no. 1, pp. 245–253, 2015.

[3] C. Melchiorri, "Robotic telemanipulation systems: An overview on control aspects," in *Proceedings of the 7th IFAC Symposium on Robot Control*, vol. 1, 2003, pp. 707–716.

[4] M. Tavakoli, R. Patel, M. Moallem, and A. Aziminejad, *Haptics for Teleoperated Surgical Robotic Systems*. New Frontiers in Robotics, World Scientific, 2008.

[5] A. D. Greer, P. M. Newhook, and G. R. Sutherland, "Human–machine interface for robotic surgery and stereotaxy," *IEEE/ASME Transactions on Mechatronics*, vol. 13, no. 3, pp. 355–361, 2008.

[6] J. Burgner, D. C. Rucker, H. B. Gilbert, P. J. Swaney, P. T. Russell, K. D. Weaver, and R. J. Webster, "A telerobotic system for transnasal surgery," *IEEE/ASME Transactions on Mechatronics*, vol. 19, no. 3, pp. 996–1006, 2014.

[7] A. Gupta and M. K. O'Malley, "Design of a haptic arm exoskeleton for training and rehabilitation," *Mechatronics, IEEE/ASME Transactions on*, vol. 11, no. 3, pp. 280–289, 2006.

[8] P. R. Culmer, A. E. Jackson, S. Makower, R. Richardson, J. A. Cozens, M. C. Levesley, and B. B. Bhakta, "A control strategy for upper limb robotic rehabilitation with a dual

robot system," *IEEE/ASME Transactions on Mechatronics*, vol. 15, no. 4, pp. 575–585, 2010.

[9] S. F. Atashzar, I. G. Polushin, and R. V. Patel, "Networked teleoperation with non-passive environment: Application to tele-rehabilitation," in *2012 IEEE/RSJ International Conference on Intelligent Robots and Systems (IROS)*. IEEE, 2012, pp. 5125–5130.

[10] Z. Corbyn, "Stroke: a growing global burden," *Nature*, vol. 510, no. 7506, pp. S2–S3, 2014.

[11] http://www.strokecenter.org/patients/about-stroke/stroke-statistics/.

[12] B. B. Johansson, "Brain plasticity and stroke rehabilitation the Willis lecture," *Stroke*, vol. 31, no. 1, pp. 223–230, 2000.

[13] H. I. Krebs, N. Hogan, M. L. Aisen, and B. T. Volpe, "Robot-aided neurorehabilitation," *IEEE Transactions on Rehabilitation Engineering*, vol. 6, no. 1, pp. 75–87, 1998.

[14] R. Colombo, F. Pisano, S. Micera, A. Mazzone, C. Delconte, M. C. Carrozza, P. Dario, and G. Minuco, "Robotic techniques for upper limb evaluation and rehabilitation of stroke patients," *IEEE Transactions on Neural Systems and Rehabilitation Engineering*, vol. 13, no. 3, pp. 311–324, 2005.

[15] T. Nef, M. Guidali, V. Klamroth-Marganska, and R. Riener, "Armin-exoskeleton robot for stroke rehabilitation," in *World Congress on Medical Physics and Biomedical Engineering, September 7-12, 2009, Munich, Germany*. Springer, 2009, pp. 127–130.

[16] R. Sanchez Jr, E. Wolbrecht, R. Smith, J. Liu, S. Rao, S. Cramer, T. Rahman, J. Bobrow, and D. Reinkensmeyer, "A pneumatic robot for re-training arm movement after stroke: Rationale and mechanical design," in *Rehabilitation Robotics, 2005. ICORR 2005. 9th International Conference on*. IEEE, 2005, pp. 500–504.

[17] J. He, E. Koeneman, R. Schultz, D. Herring, J. Wanberg, H. Huang, T. Sugar, R. Herman, and J. Koeneman, "RUPERT: a device for robotic upper extremity repetitive therapy," in *27th Annual International Conference of the IEEE Engineering in Medicine and Biology Society*. IEEE, 2005, pp. 6844–6847.

[18] S. Hesse, G. Schulte-Tigges, M. Konrad, A. Bardeleben, and C. Werner, "Robot-assisted arm trainer for the passive and active practice of bilateral forearm and wrist movements in hemiparetic subjects," *Archives of physical medicine and rehabilitation*, vol. 84, no. 6, pp. 915–920, 2003.

[19] C. G. Burgar, P. S. Lum, P. C. Shor, and H. M. Van der Loos, "Development of robots for rehabilitation therapy: the palo alto va/stanford experience," *Journal of rehabilitation research and development*, vol. 37, no. 6, pp. 663–674, 2000.

[20] H. Thieme, J. Mehrholz, M. Pohl, J. Behrens, and C. Dohle, "Mirror therapy for improving motor function after stroke," *Stroke*, vol. 44, no. 1, pp. e1–e2, 2013.

[21] L. Fadiga, L. Fogassi, G. Pavesi, and G. Rizzolatti, "Motor facilitation during action observation: a magnetic stimulation study," *Journal of neurophysiology*, vol. 73, no. 6, pp. 2608–2611, 1995.

[22] S. De Vries and T. Mulder, "Motor imagery and stroke rehabilitation: a critical discussion," *Journal of Rehabilitation Medicine*, vol. 39, no. 1, pp. 5–13, 2007.

[23] M. Iacoboni, R. P. Woods, M. Brass, H. Bekkering, J. C. Mazziotta, and G. Rizzolatti, "Cortical mechanisms of human imitation," *Science*, vol. 286, no. 5449, pp. 2526–2528, 1999.

[24] C. Keysers, B. Wicker, V. Gazzola, J.-L. Anton, L. Fogassi, and V. Gallese, "A touching sight: Sii/pv activation during the observation and experience of touch," *Neuron*, vol. 42, no. 2, pp. 335–346, 2004.

[25] J. H. Cauraugh and J. J. Summers, "Neural plasticity and bilateral movements: a rehabilitation approach for chronic stroke," *Progress in Neurobiology*, vol. 75, no. 5, pp. 309–320, 2005.

[26] H. Kim, L. M. Miller, I. Fedulow, M. Simkins, G. M. Abrams, N. Byl, and J. Rosen, "Kinematic data analysis for post-stroke patients following bilateral versus unilateral rehabilitation with an upper limb wearable robotic system," *IEEE Transactions on Neural Systems and Rehabilitation Engineering*, vol. 21, no. 2, pp. 153–164, 2013.

[27] J. J. Summers, F. A. Kagerer, M. I. Garry, C. Y. Hiraga, A. Loftus, and J. H. Cauraugh, "Bilateral and unilateral movement training on upper limb function in chronic stroke patients: a TMS study," *Journal of the Neurological Sciences*, vol. 252, no. 1, pp. 76–82, 2007.

[28] E. L. Altschuler, S. B. Wisdom, L. Stone, C. Foster, D. Galasko, D. M. E. Llewellyn, and V. S. Ramachandran, "Rehabilitation of hemiparesis after stroke with a mirror," *The Lancet*, vol. 353, no. 9169, pp. 2035–2036, 1999.

[29] J. A. Stevens and M. E. P. Stoykov, "Using motor imagery in the rehabilitation of hemiparesis," *Archives of Physical Medicine and Rehabilitation*, vol. 84, no. 7, pp. 1090–1092, 2003.

[30] J. A. Stevens and M. Ellen Phillips Stoykov, "Simulation of bilateral movement training through mirror reflection: a case report demonstrating an occupational therapy technique for hemiparesis," *Topics in stroke rehabilitation*, vol. 11, no. 1, pp. 59–66, 2004.

[31] K. Sathian, A. I. Greenspan, and S. L. Wolf, "Doing it with mirrors: a case study of a novel approach to neurorehabilitation," *Neurorehabilitation and Neural Repair*, vol. 14, no. 1, pp. 73–76, 2000.

[32] A. R. Luft, S. McCombe-Waller, J. Whitall, L. W. Forrester, R. Macko, J. D. Sorkin, J. B. Schulz, A. P. Goldberg, and D. F. Hanley, "Repetitive bilateral arm training and motor cortex activation in chronic stroke: a randomized controlled trial," *The Journal of the American Med. Association*, vol. 292, no. 15, pp. 1853–1861, 2004.

[33] M. E. Michielsen, M. Smits, G. M. Ribbers, H. J. Stam, J. N. van der Geest, J. B. Bussmann, and R. W. Selles, "The neuronal correlates of mirror therapy: an fMRI study on mirror induced visual illusions in patients with stroke," *Journal of Neurology, Neurosurgery & Psychiatry*, vol. 82, no. 4, pp. 393–398, 2011.

[34] P. Lum, C. G. Burgar, M. Van der Loos, P. Shor, M. Majmundar, and R. Yap, "The mime robotic system for upper-limb neuro-rehabilitation: results from a clinical trial in subacute stroke," in *9th International Conference on Rehabilitation Robotics*, 2005, pp. 511–514.

[35] G. Ganesh, A. Takagi, R. Osu, T. Yoshioka, M. Kawato, and E. Burdet, "Two is better than one: Physical interactions improve motor performance in humans," *Scientific reports, Nature Publishing Group*, vol. 4, 2014.

[36] M. Shahbazi, S. Atashzar, M. Tavakoli, and R. Patel, "Robotics-assisted mirror rehabilitation therapy: A therapist-in-the-loop assist-as-needed architecture," *IEEE/ASME Transactions on Mechatronics*, DOI: 10.1109/TMECH.2016.2551725, 2016.

[37] C. Preusche, T. Ortmaier, and G. Hirzinger, "Teleoperation concepts in minimal invasive surgery," *Control Engineering Practice*, vol. 10, no. 11, pp. 1245–1250, 2002.

[38] J. Rosen, B. Hannaford, M. P. MacFarlane, and M. N. Sinanan, "Force controlled and teleoperated endoscopic grasper for minimally invasive surgery-experimental performance evaluation," *IEEE Transactions on Biomedical Engineering*, vol. 46, no. 10, pp. 1212–1221, 1999.

[39] A. Talasaz, "Haptics-enabled teleoperation for robotics-assisted minimally invasive surgery," Ph.D. dissertation, Western University, 2012.

[40] http://www.intuitivesurgical.com/products/skills_simulator/.

[41] C. Feng, H. Haniffa, J. Rozenblit, J. Peng, A. Hamilton, and M. Salkini, "Surgical training and performance assessment using a motion tracking system," in *Proceedings of the 2nd European Modeling and Simulation Symposium. EMSS*, 2006, pp. 647–652.

[42] H. Alemzadeh, R. K. Iyer, Z. Kalbarczyk, N. Leveson, and J. Raman, "Adverse events in robotic surgery: A retrospective study of 14 years of FDA data," *ArXiv Preprint ArXiv:1507.03518*, 2015.

[43] http://www.mimicsimulation.com/training/.

[44] http://www.intuitivesurgical.com/products/davinci_surgical_system/davinci_surgical_system_si/ dualconsole.html.

[45] K. Reed, M. Peshkin, M. J. Hartmann, M. Grabowecky, J. Patton, and P. M. Vishton, "Haptically linked dyads are two motor-control systems better than one?" *Psychological science*, vol. 17, no. 5, pp. 365–366, 2006.

[46] R. Groten, D. Feth, A. Peer, M. Buss, and R. Klatzky, "Efficiency analysis in a collaborative task with reciprocal haptic feedback," in *IEEE/RSJ International Conference on Intelligent Robots and Systems*. IEEE, 2009, pp. 461–466.

[47] D. Feth, B. A. Tran, R. Groten, A. Peer, and M. Buss, "Shared-control paradigms in multi-operator-single-robot teleoperation," in *Human Centered Robot Systems*. Springer, 2009, pp. 53–62.

[48] Y. Li, V. Patoglu, and M. K. O'Malley, "Negative efficacy of fixed gain error reducing shared control for training in virtual environments," *ACM Transactions on Applied Perception*, vol. 6, no. 1, p. 3, 2009.

[49] Y. Che, G. M. Haro, and A. M. Okamura, "Two is not always better than one: Effects of teleoperation and haptic coupling," in *2016 6th IEEE International Conference on Biomedical Robotics and Biomechatronics (BioRob)*. IEEE, 2016, pp. 1290–1295.

Chapter 2

Literature Review

A teleoperation system consists of at least one master robot locally manipulated by an operator, and at least one slave robot that remotely mimics the maneuvers of the master robot in order to perform the operation on an environment. A communication network connects the master and the slave robots, transferring necessary information between the two sites (Fig. 2.1). A telerobotic framework with one master robot and one slave robot is called Single-Master/Single-Slave (SM/SS) teleoperation system, which establishes unilateral or bilateral information flow between the two agents. The first SM/SS teleoperator was build in the mid 1940s by Geortz. Since then, several state-of-the-art studies have been conducted on SM/SS teleoperators and various control frameworks have been developed for such systems, as discussed in [1, 2]. By extending the human capability to remote or unaccessible sites, teleoperation has been found to be effective in a wide range of applications, from underwater and space exploration, mining and handling toxic materials, to robotics-assisted rehabilitation and telesurgery [1].

As the field of telerobotics grows, multilateral (trilateral and beyond) frameworks have also received much attention during the past few decades. A multilateral framework not only allows for one-to-one correspondence between the operator-master and the slave-environment sets, but also realizes collaborative scenarios between multiple operator-master sets and/or multiple slave robots. As with human behaviour [3], collaborative performance of a task can enhance efficacy, precision, dexterity, loading capacity and handling capability [4].

In an SM/SS system, the teleoperator can be modeled as an *1-port* or *2-port* network, depending on the type of interactions between the operator and the environment. As shown in

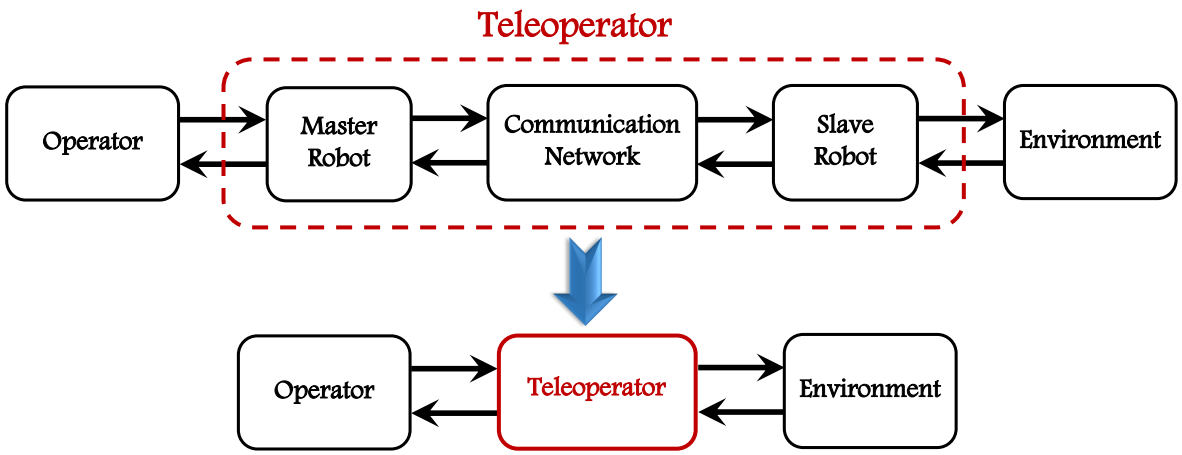

Figure 2.1: Schematic representation of components of an SM/SS teleoperation system.

Figure 2.2: Schematic representation of a unilateral SM/SS teleoperation system.

Figure 2.3: Schematic representation of a bilateral SM/SS teleoperation system.

Fig. 2.2, having a one-directional interaction between the operator and the environment results in an *1-port* teleoperator network, called a unilateral system. Establishing a two-directional interaction between the operator and the environment transforms the teleoperator into a *2-port* network, and therefore the system is a bilateral one (Fig. 2.3). Having more than 2 robotic agents (master and slave robots), i.e., $n >= 3$, the teleoperator can be modeled as an *n-port* network and therefore, is an n-lateral framework. Based on the analogy used in the literature, a multilateral teleoperation system with 3 robotics agents interacting is called a trilateral framework.

The research conducted on multilateral (trilateral and higher) teleoperation systems can be categorized into four main divisions, as follow:

1. Trilateral, which refers to the interconnection of a total of three human-master sets and

slave robots,

2. Multi-Master/Single-Slave (MM/SS), which allows for collaboration between multiple operators in order to control/manipulate one slave robot through their corresponding master robots,

3. Single-Master/Multi-Slave (SM/MS), which enables control of multiple slave robots through one master robot manipulated by one operator,

4. Multi-Master/Multi-Slave (MM/MS), which, as the name implies, realizes collaboration of multiple operators and robots in general.

It should be noted that in this context, *multilateral* refers to *trilateral and higher*, but not *bilateral* SM/SS framework. Bilateral systems have been extensively discussed in excellent surveys including [1, 2]. To the best knowledge of the authors, this article is the first to provide an overview and classification of the state-of-the-art literature on multilateral teleoperation systems. As the field is very broad with no specific borderlines, we do not claim that the survey covers every aspect of the field, but we believe that it presents the most important attributes.

The rest of this chapter is organized as follows: Sections 2.1-2.4 present an overview of existing state-of-the-art multilateral frameworks classified based on the architectures. Section 2.1 discusses existing trilateral teleoperation systems, as the widest category of multilateral frameworks, in three classifications. Sections 2.2, 2.3, and 2.4, respectively, present multilateral MM/SS, SM/MS, and MM/MS teleoperation frameworks with more than three robotic agents. Section 2.5 gives an overview of the state-of-the-art topology-interdependent stability analysis for general multilateral teleoperation systems. Section 2.6 concludes the chapter and provides an overview of future research directions on multilateral teleoperation systems.

2.1 Trilateral Architectures

A trilateral architecture is the most common form of a multilateral teleoperation system, in which three master and slave agents interact. Depending on the number of agents and their interaction configuration, we have classified trilateral teleoperation systems into three main categories, namely:

- Teleoperated-Autonomous Shared Control (TASC),
- Dual-User Shared Control (DUSC),
- Dual-User Redundancy Control (DURC),

as discussed below.

2.1.1 Teleoperated-Autonomous Shared Control (TASC)

This type of shared control strategy refers to a combination of teleoperated and autonomous modes, in which an operator and an autonomous agent can collaboratively perform a task [5]. In such frameworks, the operation outcome benefits from not only the supervision and decision making capabilities of the operator, but also a considerably shorter completion time and possibly enhanced precision as a result of the autonomous mode [6, 7].

In [8], Zaatri developed a cooperative error recovery scheme for such frameworks. By providing a Graphical User Interface (GUI) to the operator, the scheme creates a dialog between the operator and the autonomous agent in order to recover errors, avoid failures, and save time. In this context, an error or failure was defined as the occurrence of an unexpected and/or exceptional event. Handling delicate objects is an application that, upon proper selection of types and methods of feedback (force, visual and audio), can benefit from a TASC framework [9]. There are also several other applications for which several TASC frameworks have been developed to date, as categorized below:

Space

Assembly, maintenance and repair processes for space satellites are among applications in which a TASC strategy is very beneficial [10]. While autonomous agents are incapable of dealing with large uncertainties, major re-planning, re-tooling or making common-sense decisions, pure teleoperation also necessitates the terrestrial teleoperator to be predictive in sending commands to the remote station in order to handle large communication delays (expected to be larger than 8 seconds round trip) [11]. This makes a TASC architecture suitable for space applications, by combining advantages of both teleoperated and autonomous control modes.

In 1989, Hayati [6] developed a two-level hierarchical shared control framework that accepts commands from either an autonomous planner or a teleoperator alone, or a combination of the two. The architecture was designed for general applications, while also specifically modified for space applications; and to cover both possible approaches: 1) modifying nominal autonomous trajectories by a teleoperator, or 2) autonomously modifying nominal teleoperator trajectories.

In [7], a User Macro Interface (UMI) for the TASC architecture was implemented to enable the operator to interactively set up a task-execution environment, specify input parameters for a variety of task primitives, and to stop task execution at any time. The UMI interface was designed to serve at a local command site in order to prepare and send operator's commands to a remote space robot.

A general TASC telerobotic architecture was presented in [5] for real-time, sensor-based Cartesian control of remote manipulator systems. The framework allows simultaneous control inputs from various components including haptics-enabled joystick, vision controller, position controller, and force controller. The system was experimentally implemented at the National Aeronautics and Space Administration (NASA) Langley Research Center.

Haptics-Enabled Training in Virtual Environment

Training a novice based on haptic guidance/assistance is another application of TASC mode. This enables a trainee to share control of a telerobotic system with a virtual or actual expert, while receiving haptic cues. In [12], Powell *et al.* used a shared control methodology to classify and investigate the efficacy of various haptic-based training paradigms. In this study, the control was shared between a novice and an autonomous virtual expert interacting to perform tasks in a Virtual-Reality (VR) environment. In a similar work [13], Li *et al.* studied the efficacy of haptic guidance during training in VR environments using the TASC framework. The evaluation was performed on a target-hitting task and based on fixed-gain error-reducing haptic guidance. The outcome emphasized the necessity of adaptive time-varying, and possibly skill-oriented, haptic guidance, rather than fixed-gain assistance with continuous presence in order to preserve the trainee's active involvement, thereby, their motor pathway activity.

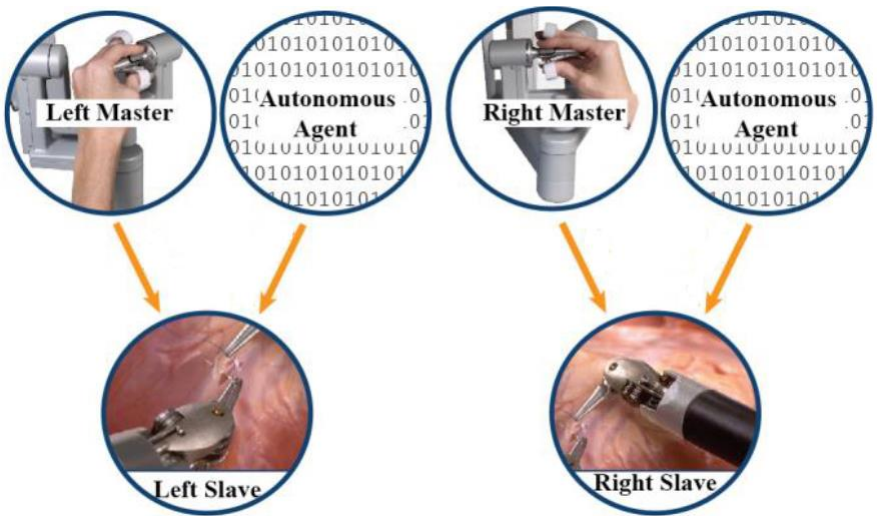

Figure 2.4: Schematic representation of a TASC framework for surgical procedures [14] (©[2015] IEEE).

Supervised Autonomous Surgical Procedures

While inherently delicate in terms of manipulating deformable tissues in a very dynamic environment, robotic surgical producers involve several repetitive tasks, e.g., cutting, suturing, palpating and debriding. Incorporating some degree of automation (Fig. 2.4) to perform such kinematically complex and repetitive tasks can decrease the processing and physical burdens on surgeons, while speeding up the operation without degrading the outcome. In [14], Shamaei *et al.* presented a teleoperated TASC framework that integrates a surgeon supervision and an autonomous agent to perform surgical tasks. The architecture, which is designed independent of the automation algorithm, includes: 1) a dominance factor to enable the surgeon to take control over the slave robot, and 2) an aggressiveness factor which specifies the pace of the autonomous agent, assigning either leader, synchronous, or follower roles to the slave robot. In this study, the autonomous agent was defined to be a linear mapping to coordinate a trajectory-following task. The adjustment process of the dominance and the aggressiveness factors as well as a systematic adaptation rule for the automation agents was not presented.

2.1.2 Dual-User Shared Control (DUSC)

This strategy refers to control and manipulation of a slave robot by two human operators through a shared/collaborative framework (Fig. 2.5). It is shown that through a shared dyadic

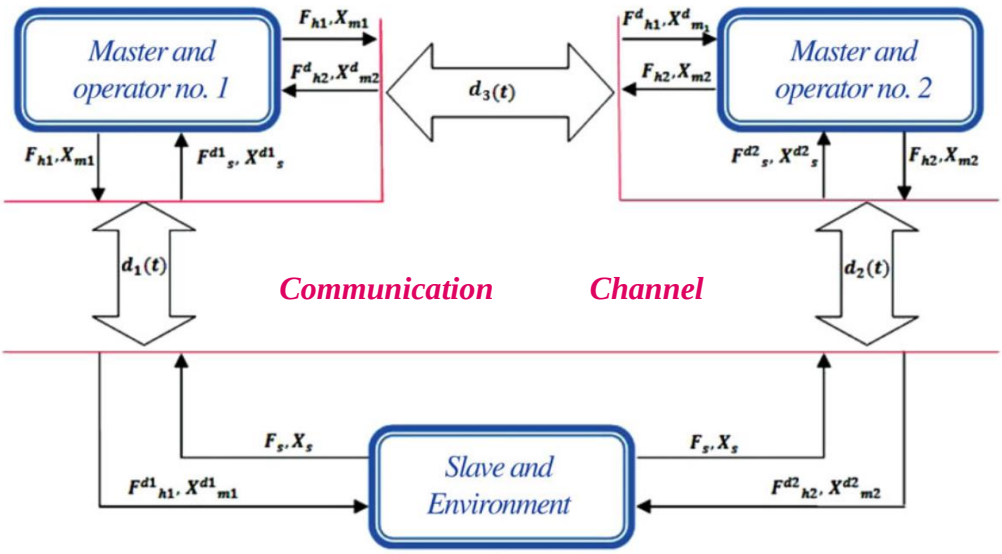

Figure 2.5: Schematic representation of a general trilateral DUSC framework, including two operator-master sets and one slave-environment set, communicating through a network [16] (©[2012] Cambridge University Press).

framework, a dyad can quickly negotiate a more effective task-performance strategy that enhances the outcome, compared to individually executing the task by either operator. This negotiation is apparently at a level below the awareness of the operators and must happen through a haptic interaction channel [15]. Compared to other categories of trilateral teleoperation systems, prior art on DUSC frameworks is relatively greater and can be classified into two main divisions, frameworks developed for general purpose with a focus on control challenges (e.g., closed-loop stability), and specific applications, which in turn can be classified into more subcategories based on the particular application (e.g., supervised robotics-assisted surgical training and rehabilitation therapy), as described below:

Control Strategies for General DUSC Architectures

Khademian and Hashtrudi-zaad [17] presented a six-channel DUSC framework to enable interaction between two operators, collaboratively controlling a slave robot through a dominance/authority factor. The architecture was designed such that two desired objectives (position-based and force-based) are defined to simultaneously satisfy for each operator/master set as well as the slave robot. The framework requires all positions and forces to be exchanged

among the three agents, the balance of which were set to be shaped through the dominance factor. By developing a number of kinesthetic measures, the impact of the dominance factor on the transparency level of the system with a delay-free communication network was also investigated. In [18], an H_∞ force-position controller was developed for such a framework in order to ensure robust stability of the system in the absence of communication delay, but the presence of uncertainties in operators and environment dynamics. A robust controller based on μ-synthesis was developed in [19] in order to address instabilities caused by known and constant communication delay between the masters and the slave sides, as well as dynamic uncertainties in the system.

In [20], a DUSC framework was developed to satisfy 1) a position-based desired objective at the slave side (incorporating the dominance factor) in order to ensure shared control of the operators over the slave robot through a dominance factor, and 2) a force-based desired objective at each master side, providing the operators with haptic feedback from the environment.

A decentralized adaptive impedance controller as well as a sliding-mode control methodology along with a passivity-based analysis approach were developed in [20] and [16], respectively, to ensure closed-loop stability of the nonlinear DUSC system in the presence of unknown and constant communication time delay. The definition of the ideal hybrid matrix for DUSC frameworks integrated with the dominance factor was initially introduced in [16]. A higher order sliding-mode impedance controller was also developed in [21] for the DUSC system with unknown and constant communication time delay.

An adaptive fuzzy control approach and an adaptive neural network controller were developed, respectively, in [22] and [23] for motion/force synchronization in dual-master control of a single holonomic-constrained slave robot. The controllers were designed such that stability of the teleoperation system is preserved in the presence of stochastic time-varying communication delay, dynamics/kinematics uncertainties and external disturbance. In [24], Ghorbanian *et al.* developed a DUSC framework with two distinct dominance factors. To address instability caused by time-varying communication delays, two controllers were presented: 1) Proportional with dissipative gains, and 2) Proportional and Derivative with dissipative gains.

A time domain passivity controller was developed in [25] for DUSC frameworks subject to communication delays. The controller was designed in a generic way, such that any control ar-

chitecture and communication channel characteristics in a peer-to-peer system are allowed. It was shown experimentally that the proposed approach can be used well for round-trip delays up to 200ms. In [26], a wave-variable-based control methodology was developed to ensure closed-loop stability of a DUSC framework in the presence of a time-varying dominance-factor (which enables real-time adjustment of the operators' authority over the task) as well as constant communication time delays. The concept of time-varying authority adjustment for operators was originally introduced in [27] by Shahbazi *et al.* In [28], a passivity-based approach based on the Port-Hamiltonian method was adopted for DUSC framework with a time-varying dominance factor. An asymmetric DUSC framework with three dominance factors was introduced in [29], and stability conditions were derived for the system in the presence of an unknown communication delay.

Application-Specific DUSC Architectures: Therapist-In-the-Loop (TIL) Rehabilitation Therapy

Rehabilitation therapy is a labor-intensive process, that necessities not only a therapist's expertise and knowledge, but also reproducible movements and stereotyped exercises [30]. This has resulted in a paradigm shift in past decades towards supervised robotic rehabilitation, which brings knowledge and supervision of a therapist into the loop of robotics-assisted rehabilitation therapy [31]. Along with bilateral SM/SS frameworks, DUSC architectures have also found their way to supervised robotic rehabilitation, where they also enable tele and in-home therapy procedures, so that a therapist can remotely provide rehabilitation to a patient.

Carignan *et al.* [32] developed a DUSC framework that enables a therapist and a patient to remotely interact through a virtual environment. The virtual task was defined as collaboratively manipulation of a virtual beam by the therapist and the patient, while providing them with interaction forces reflected back from the virtual environment. A control methodology based on wave variables was presented to counter the destabilizing effect of communication and processing time delays.

In [33], Shahbazi *et al.* presented a therapist-in-the-loop DUSC framework for robotics-assisted mirror rehabilitation. The framework (Fig. 2.6), designed for patients with hemiparesis and/or hemispatial neglect, includes adaptive assist-as-needed therapy adjusted based on the

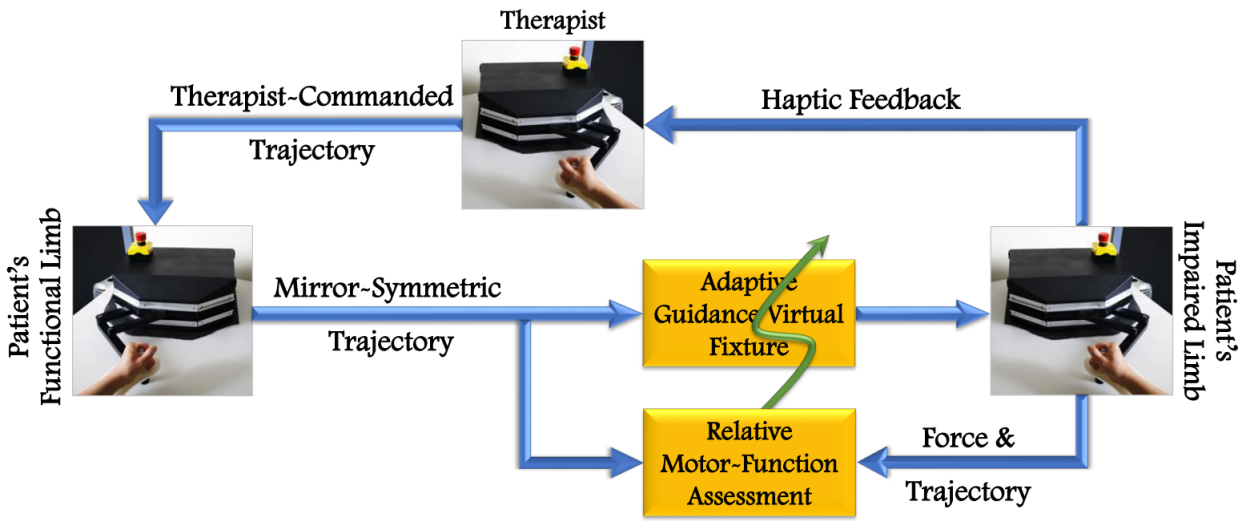

Figure 2.6: Schematic representation of a trilateral DUSC framework for therapist-in-the-loop rehabilitation therapy [33] (©[2016] IEEE).

impairment level of the patient's affected limb. Through such a DUSC framework, a patient benefits from an enhanced motor-recovery process as a result of integrating the following features: 1) the cross-cortex coupling effect between the patient's impaired and functional limbs induced by the mirror therapy; 2) the expertise and direct supervision of, as well as the haptic feedback delivered to, the therapist in the loop enabling them to provide appropriate corrective movements; 3) the supervision of the patient over the treatment through their functional limb medium, which ensures the patient's safety and comfort by limiting excessive pain and pressure on the patient's impaired limb; and 4) active involvement of the patient in the treatment through the adaptive assist-as-needed therapy. A combination of the Small Gain theorem and the Circle Criterion was used to analyze closed-loop system stability in the presence of communication delays to also facilitate tele and in-home rehabilitation.

Application-Specific DUSC Architectures: Expert-in-the-Loop Haptics-Enabled Training

Haptics-based interaction with an expert when learning a motor task has been shown to consistently enhance a trainee's motor skills and performance, compared to when practicing the task individually for the same duration [34], [35]. Through the DUSC telerobotics frameworks, it is

possible to bring the supervision and involvement of an expert into a training loop to capitalize on the impact of haptic interactions on the trainee's learning curve.

Yano [36] was among the first researchers to incorporate haptics interaction between an expert and a trainee through a DUSC framework such that they can simultaneously work in a virtual environment with force feedback. The system was designed so as to have a "haptic coupling" between their hands to assist skills development in virtual environments.

Nudehi *et al.* [37] developed a DUSC training architecture for minimally invasive surgery. The framework was designed to enable an expert surgeon to mentor a trainee through a fixed-gain error-based haptic interaction between the expert and the trainee. The concept of the dominance factor for DUSC frameworks was initially introduced in this paper, which allows providing partial levels of control authority over the task to each user. A control approach based on H_∞ was presented to ensure robust stability and performance of the architecture in the presence of constant communication delay.

In [38], Chebbi *et al.* outlined the high level design of a collaborative virtual surgical environment that allows haptic tele-mentoring of a trainee by an expert during performance of simple surgical tasks. The paper discussed various aspects of the simulated graphical unit, including graphical rendering, physical simulation, and collision detection inside the virtual environment. The DUSC framework was designed so as to include the following control modes: 1) independent mode in which each operator can independently perform simple virtual surgical tasks; 2) tele-mentoring mode, in which the expert can guide the movements of the trainee; 3) tele-evaluation mode, in which the trainee has control over the movements of the expert; and 4) bilateral tele-mentoring mode which provides the expert and the trainee with a two-way interaction such that both can feel the movements of each other.

In [39], a tele-collaborative VR environment was presented and evaluated for dual-user surgical training, through which a novice and an expert can remotely communicate and collaborate. The simulated VR application, which involves a gall bladder removal, allows both the trainee and the expert to simultaneously work in the same virtual space. Withstanding latencies of around 200 millisecond, the tele-collaborative virtual environment was evaluated between an expert located in USA and some trainees in Australia.

In [40], a dual-user framework was presented for haptics-enabled training, where two mas-

ter robots are manipulated by an expert and a trainee, while the slave robot makes contact with the environment. The architecture was designed such that each robot follows the trajectory of another robot, creating a chain of leader-follower behavior. The framework can be considered as a closed-loop interconnection of two SM/SS frameworks placed in series, where the slave robot of the first SM/SS framework acts as the master robot for the second architecture, the slave robot of which acts as the master robot for the first framework. To realize the framework, a decoupled controller was applied to each robot in differential-position mode.

In [41], the controller design for a trainer-trainee collaboration in haptics-enabled virtual environments was addressed. Adaptive nonlinear controls were developed to enforce desired mapping between the operators and the virtual environment, which can be either impedance or admittance type, in the presence of parametric dynamic uncertainties in the operator's hand. A Lyapunov function was used to investigate performance of the closed-loop system, while also analyzing closed-loop stability using the Nyquist envelopes of the interval plants and an off-axis circle criterion. The approach provided for the analysis of closed-loop stability requires *a priori* knowledge of the bounds on the users' and environment's parameters.

In [42], Khademian *et al.* presented a DUSC architecture for haptics-enabled training in a simulated environment. In this architecture, a virtual slave robot is collaboratively controlled by a trainee and a trainer through their partial authority levels over the task. The framework sets two simultaneous desired objectives for each user and his/her corresponding master robot based on: 1) the weighted sum of positions of the virtual slave and the second master robots, and 2) the in-contact haptic force generated at the slave side. This can result in simultaneous exertion of two different forces on the users' hands. A mechanism based on which the users can decouple and discriminate between these forces, however, was not presented. Closed-loop stability of the architecture was analyzed against uncertainties in the environment and the user's dynamics, using the Llewellyn's unconditional stability criterion. This was done by 1) finding the continuous-domain equivalent of the discrete-time virtual slave robot using the Tustin transformation; 2) obtaining an equivalent two-port network model from the original three-port framework by considering the environment as a load termination; and 3) applying Llewellyn's criterion to the resulting two-port network. The kinesthetic performance of the architecture was also evaluated through numerical analysis and in terms of transparency under various operating

conditions, including types of environments and users' grasps.

In [27], Shahbazi *et al.* developed a DUSC framework for haptics-enabled training of a novice concurrently with the execution of a surgical procedure by an expert in the loop. The kinesthetic haptic guidance was proposed to be adaptively adjusted in real-time and based on the performance level of the trainee in order to keep the trainee actively engaged. Thus, to objectively quantify the trainee's performance in real time, a relative skills-assessment approach was developed. The concept of time-varying adaptive dominance factor was originally presented in this paper, enabling real-time adjustment of the authority level of the trainee over the surgical task based on his/her level of expertise. An impedance-based control methodology was applied and closed-loop stability was investigated. By applying the Small Gain theorem, a sufficient condition was derived that guarantees closed-loop stability of the architecture in the presence of a non-negligible time-varying communication delay. In [43], the authors took a further step by proposing a real-time expertise-oriented surgical training architecture. The expertise-oriented framework was designed such that it provides novice trainees with haptic guidance/cueing, while trainees with a sufficient level of expertise receive haptic tool-tissue interaction force reflected back from the patient side that enables the trainees to get acquainted with the range of forces applied to the surgical instruments in the patient's body. This was realized through a Fuzzy interface system, which adaptively specifies the type and level of the haptic guidance/feedback as well as the appropriate authority level of the trainee over the procedure based on to his/her level of expertise in real time. Closed-loop stability of the expertise-oriented framework was investigated in the presence of constant communication delays and a sufficient stability condition was derived.

A trilateral DUSC architecture was developed by Shamaei *et al.* [44] for robotic training. The framework (consisting of two master robots manipulated by a trainee and an expert as well as one slave robot) includes a dominance factor, through which the trainee's authority level over the slave robot can be controlled. In addition, an observation factor was incorporated, through which the desired force/velocity inputs to the trainee can be adjusted. The architecture consists of six velocity- and force-based desired objectives, two for each master and slave robots. A discussion on how to assign both velocity and force values simultaneously was not given. Stability and transparency of the framework was analyzed numerically for a specific

version of the architecture run in position-position-position mode.

2.1.3 Dual-User Redundancy Control (DURC)

Kinematic redundancy of a robotic manipulator makes it appropriate for use in unstructured and complex environments, and enables simultaneous multitasking [45]. Involving human operator(s) in controlling a kinematically redundant robot through teleoperated frameworks brings the human intelligence, expertise and sensory inputs into the loop, while it requires appropriate strategies for redundancy resolution. A solution to this is to incorporate two master robots in order to control a kinematically redundant slave robot, such that each master robot can be assigned to perform a part of the task [46].

Unlike symmetric trilateral teleoperation systems, in asymmetric DUSC frameworks there is no one-to-one mapping between the Degrees Of Mobility (DOMs) of the master robot(s) and the slave robot. DOM is defined as the minimum number of independent variables that uniquely determines the robot motion. In [46], Malysz and Sirouspour developed an asymmetric DURC approach, in which two master robots can control a kinematically redundant slave robot in delay-free applications (Fig. 2.7). The architecture was designed such that the first master robot controls a primary task control frame (e.g. the slave end-effector frame), while the second master robot manipulates a secondary task (e.g. avoiding collision with obstacles in the environment) without affecting the primary task. This was achieved through a joint-space Lyapunov-based adaptive controller with local velocity-level redundancy resolution and task-space coordinating reference commands. The approach was also extended in [47] to dual-user control of a kinematically deficient slave robot.

An application to such frameworks is robotic rehabilitation. In [48], Culmer *et al.* developed a DURC strategy for upper-limb robotic rehabilitation in which two 3-Degree-Of-Freedom (DOF) robotics systems were used to control a human arm in 6-DOF and to perform rehabilitative tasks in a virtual user interface environment. A main challenge in such an application is to ensure that the master robots are controlled in unison with each other, and also with the patient's arm in order to safely coordinate arm movements. For this purpose, a 6-DOF model of the upper limb was used to form the controller's coordinate system and an admittance-based cooperative control strategy was applied.

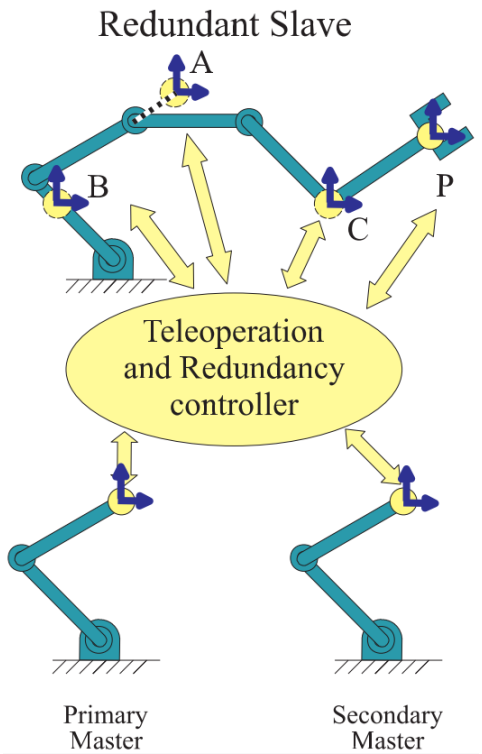

Figure 2.7: Schematic representation of a trilateral asymmetric DURC framework [46] (©[2011], SAGE Publications).

2.2 MM/SS Architectures

MM/SS teleoperation frameworks are, in fact, an extended class of dual-user teleoperation systems in which multiple operators can collaboratively control a slave robot, resulting in an improved-dexterity human-machine interface. This can involve shared/cooperative user control of a slave robot with either an equal number of DOFs or kinematic redundancy in order to enhance operability in complex environments [49], [50].

Goldberg *et al.* [51] were among the first researchers to develop an MM/SS framework that enables multiple operators to collaboratively teleoperate an industrial robotic arm over the Internet. In order to fuse the inputs from all operators, input averaging was applied. Based on the Central Limit Theorem, input averaging for multiple operators with similar levels of expertise may lead to a more effective control signal than that from an individual.

Katsura *et al.* [52] presented a control framework for MM/SS systems in the spatial mode coordinate system to compensate for differences in the structure and the number of DOF between the master robots and the slave robot. For this purpose, a spatial mode transformation

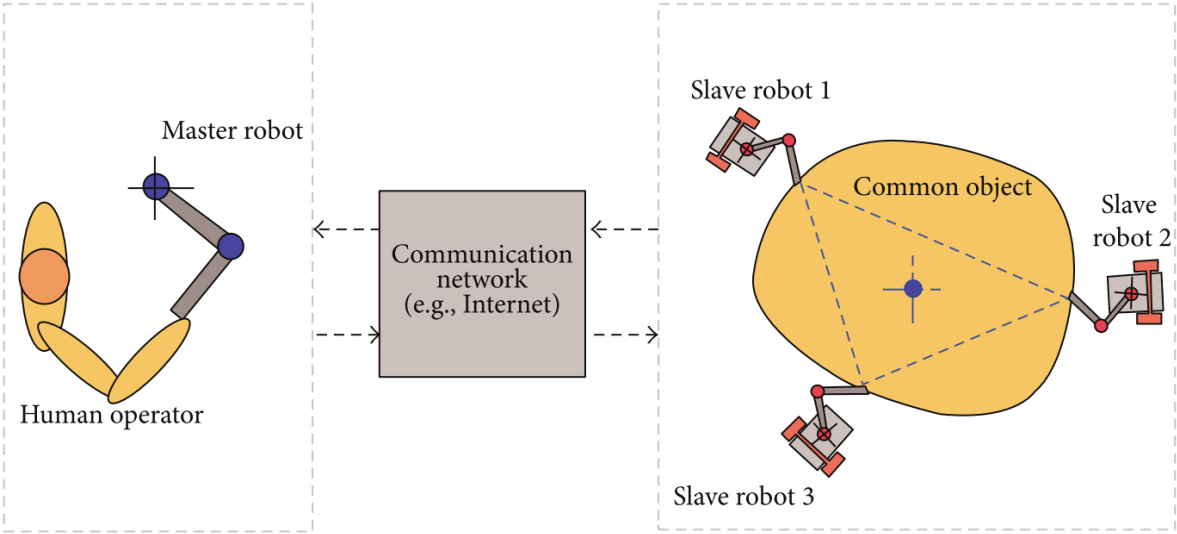

Figure 2.8: Schematic representation of an SM/MS teleoperation system with three slave robots handling a common object [53] (©[2005] IEEE).

was introduced based on decoupled modes of a task (e.g., translation, rotation, and grasp). An acceleration-based controller was designed to facilitate position regulation at the slave side and force servoing at the masters side.

In [49], projective force mappings were introduced for MM/SS frameworks to facilitate dividing the teleoperation control of the slave end-effector into a number of potentially overlapping subtasks. A systematic way to obtain corresponding projective matrices was presented based on which the master robots can be allocated shared or decoupled control over the slave robot. An adaptive controller was applied to implement the projective force mapping objectives. The approach does not include environment force feedback to the operators.

In [54], Shahbazi *et al.* presented a set of desired objectives for MM/SS teleoperation frameworks, through which both mutli-user cooperative and training applications (e.g., surgical training to a class of trainees) can be realized. The definition of the hybrid matrix as well as the desired hybrid matrix for such a framework was initially given in this paper. Passivity of the framework was investigated and it was shown that, unlike SM/SS systems, passivity of an MM/SS system is architecture-dependent and determined based on the desired objectives of the architecture. An impedance-based control approach was developed to satisfy the desired objectives defined for the system in the presence of communication delays. Using the Small-

Gain theorem, closed-loop stability of the framework was investigated and a sufficient stability condition in the presence of communication time delays was derived.

2.3 SM/MS Architectures

An SM/MS system enables an operator to remotely control multiple slave robots performing a common task. The coordination of slave robots in such frameworks increases the load capacity, dexterity and rigidity of the system. An SM/MS system is applicable in tasks such as manipulating a heavy object, or assembling a bolt-nut pair, where multiple slave arms are required to accomplish the task, while one operator would suffice to control the position/orientation as well as the interface force/moment of the target point. Fig. 2.8 shows a schematic representation of an SM/MS framework with three slave robots.

In [55], a task-oriented control approach was proposed for SM/MS systems using a Virtual Internal Model (VIM). The framework enables the operator to concentrate on the task itself in the 6-DOF space, while the VIM-based controller automatically resolves the task-oriented variables into the motion of each slave arm. The control framework requires some level of knowledge about the task in order to specify the internal force/moment interactions.

When handling a kinematically-unknown object using an SM/MS system, grasping safety is a critical aspect. Grasping should be maintained securely and precisely in order to avoid dropping the object. In [56], Lee and Spong proposed a passivity-based control framework for SM/MS that ensures a secure and tight cooperative grasping among the slave robots regardless of the communication time delay, operator command, and behavior of the object. Applying a passive decomposition, the dynamics of the slave robots is first decomposed into two decoupled systems, namely a shape system and a locked system. The shape system is then controlled by disturbance cancellation to ensure a secure grasp, while the locked system (describing the overall behavior of the slave robots) is controlled in accordance with the operator's commands. The passivity-based control framework was designed such that the operator can receive haptic force feedback, while ensuring safety and stability of the interaction in the presence of communication delay using the scattering variables. In [57], a wave-variable-based controller was also developed for nonlinear SM/MS systems to guarantee position synchronization and force

reflection in the presence of time-varying communication delays.

2.4 MM/MS architectures

MM/MS systems enables multiple operators to remotely control multiple slave robots in a common environment over the network. Such frameworks are applicable in cooperative teleoperation, which offers several advantages including increased dexterity, enhanced handling capability and loading capacity, as well as improved robustness as a result of possible redundancy [4]. Fig. 2.9 shows a schematic representation of such a framework for a specific case of two operators remotely manipulating two slave robots to perform a collaborative physical task. One of the main challenges with such systems in the presence of considerable communication time delays is to cope with delayed visual perception in order to avoid collision between the slave robots [58]. To ensure a collision-free collaboration between the slave robots, in [59], a real-time predictive graphics simulator was developed for such frameworks, in which the slave robots move based on a predictive trajectory generated by the simulator at the operators' sites.

In [60], an Internet-based distributed multi-behavior MM/MS system was presented, including three layers of hierarchical system software, namely: 1) the robot application layer, 2) the robot task layer, and 3) robot execution layer. The multi-behavior structure of the system enables performance of simple tasks (e.g., executing a primitive action) as well as complex operations (e.g., dealing with unexpected events such as possible collisions).

Lo *et al.* [61] developed a distributed event-based control methodology for MM/MS systems in the presence of Internet communication time delay. The controller was developed such that each operator/master independently controls a slave robot, while real-time force feedback was used to render the interactions among the robots and the operators.

In [4], Sirouspour developed a multilateral MM/MS teleoperation framework that 1) takes the dynamic interaction of slave robot with the tool/environment into account, and 2) allows force and position information flow between all master and slave robots, rather than merely between each corresponding master-slave unit, in order to facilitate task coordination and execution. A μ-synthesis robust control methodology was also developed to ensure stability of the framework in the presence of unknown, but passive, operators and environment dynam-

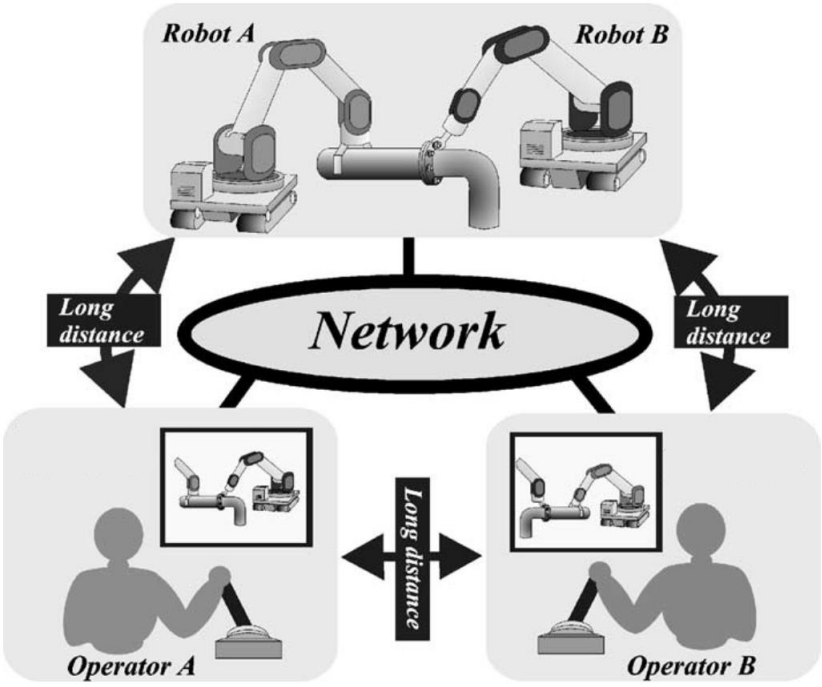

Figure 2.9: Schematic representation of a multilateral cooperative teleoperation framework[1] [59].

ics. In [62], a model-based adaptive nonlinear controller was developed for the same MM/MS framework. The Lyapunov analysis was used to analyze closed-loop stability of the framework in free motion, and in contact with flexible and rigid environments. In [63], Setoodeh *et al.* developed an event-based distributed controller for such a framework subject to a known constant communication delay. The control strategy included model-based Linear Quadratic Gaussian (LQG) controllers for free and in-contact phases with switching according to the operation phase. The Nyquist technique was used to investigate robustness of the system with respect to parametric uncertainties.

In [64], the concept of model-mediated MM/MS cooperative frameworks was adopted in order to incorporate knowledge about the environment into the system. In this framework, an estimated model of the environment was rendered on the master site, rather than transmitting force/velocity signals, in order to enhance the bandwidth of the overall system. The framework, integrated with a centralized position-based admittance controller, was developed for a specific 1-DOF MM/MS system with two master-slave pairs communicating through a delay-free com-

[1]Reprinted from: A collaborative multi-site teleoperation over an ISDN, vol. 13, no. 8, N.Y. Chong, et al., Mechatronics, pp.957-979., ©(2003), with permission from Elsevier.

munication network. Feth *et al.* [65] improved on this by proposing prediction algorithms for dyadic haptic interaction, such that no *a-priori* knowledge about the task, the remote environment or the teleoperator dynamics is required.

Using information graphs and consensus algorithms, Tumerdem *et al.* [66] presented a multilateral teleoperation platform that is robust to dynamical changes in the network topology, as long as the network structure remains connected and balanced. Capitalizing on the stability of consensus algorithms under switching conditions, the system was designed such that the controller law at each robot site also switches in correspondence with the dynamical changes in the network topology, while tolerating communication failures.

In [67], Kanno and Yokokohji presented a wave-variable-based controller for MM/MS systems with arbitrary number of master/slave robots. By introducing a wave node (to which multiple wave-variable-based transmission lines can be connected), the controller guarantees passivity of the system in the presence of communication delay regardless of the dynamics characteristics of the master/slave robots. The controller also includes a wave-integral-error feedback in order to compensate position drift resulted by the communication delay.

In [68], a general multilateral control framework based on passivity was presented to enable energy coupling of n operator-master sets and m environment-slave sets through a delayed communication network. This framework includes three main elements: 1) nodes: generalized effectors or agents, e.g. human-master set, autonomy agent, and/or environment-slave set; 2) segment: the energy flow between each two nodes; and 3) track: a control medium that enables the flow of energy between each two nodes. This high-level modular topology, integrated with a passivity-based controller, uses power-correlated signals transferred between each two nodes independently of the nature of the agents, eliminating the necessity of precise modeling of the agents. A generalized modular representation of MM/SS framework was also given in [69], based on the flow/effort concept in mechanical-electrical network analogy. A time domain passivity controller was developed to stabilize the closed-loop framework in the presence of communication time delay, regardless of the number of master-slave robots, the control architecture and dynamic uncertainties.

Chen *et al.* [70] presented an adaptive robust controller for a general MM/MS system with n master-operators to remotely manipulate n slave robots cooperatively handling an object. The

framework replaces the environment force feedback by using an estimation of environment parameters at the master side in order to address the non-passivity caused by the conventional bilateral delayed communication channel. The adaptive robust controller addresses dynamics nonlinearities and parametric uncertainties of the robots and the environment.

2.5 Topology-Free Stability Analysis of Multilaretal Teleoperation Frameworks

Closed-loop stability is one of the main objectives in designing control strategies for teleoperation systems, and this is particularly important for multilateral frameworks. This section presents an overview of the state-of-the-art stability analysis approaches for general multilateral teleoperation systems independent of their topology and architectural interconnections, through modeling the systems as *n-port* networks.

In [71], Mendez *et al.* presented a necessary and sufficient criterion for passivity analysis of coupled multi-DOF multilateral teleoperation/haptic systems, which in turn ensures stability of the closed-loop system. Considering the multilateral framework as an *n-port* network, the criterion was developed based on the analysis of immittance (impedance, admittance, hybrid or inverse-hybrid) parameters of the *n-port* network. For the *n-port* network to remain passive, the proposed criterion necessitates 2n conditions for the immittance parameters and their residues to satisfy. It was shown in the paper that for $n = 2$, the proposed passivity criterion reduces to Raisbeck's criterion for a *two-port* network. Although the proposed passivity criterion provides a conservative approach to stability analysis, it does not require information on the operators' and the environment's impedance characteristics as long as they remain passive.

In [72], an approach for unconditional stability analysis of dual-user teleoperation systems (which can be modeled by *3-port* networks as shown in Fig. 2.10) was presented. The proposed framework is based on reducing the *3-port* network to an equivalent *2-port* network (schematically shown in Fig. 2.11), to which Llewellyn's unconditional stability criterion can be applied. For this purpose, one of the three terminations of the network (operator 1, operator 2 or environment) should be considered as a load termination (zero excitation) and absorbed into the *3-port* network. Among the three terminations, the environment is the best candidate

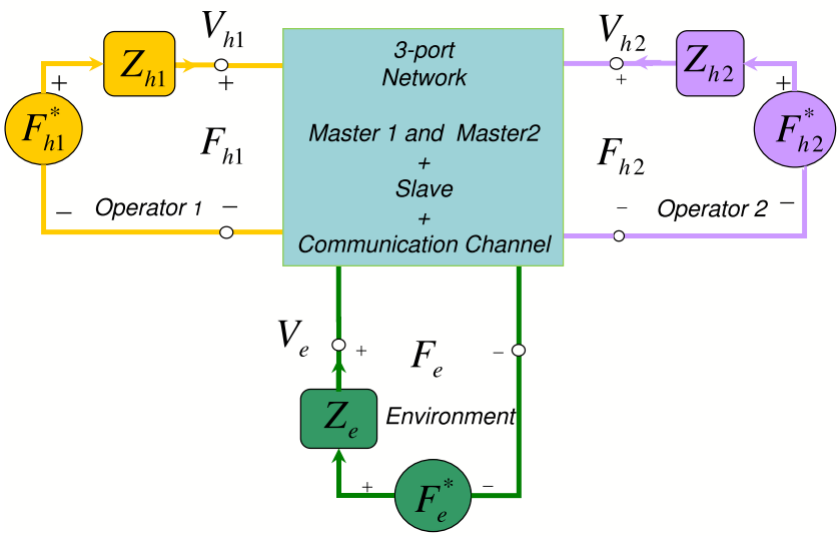

Figure 2.10: Schematic representation of a trilateral teleoperation system modeled by a *3-port* network [72] (©[2010] IEEE).

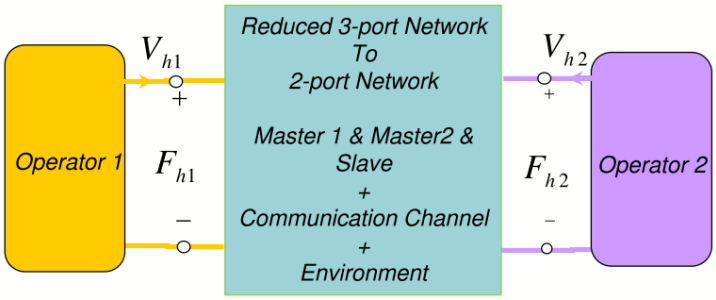

Figure 2.11: Schematic representation of the reduced *2-port* network, by considering the environment as the load termination [72] (©[2010] IEEE).

for load termination as, unlike the two operators, it does not generate exogenous input or excitation. Choosing the environment as the load termination, the equivalent *2-port* network can be then calculated through algebraic manipulations. Afterward, Llewellyn's criterion can be applied to the equivalent *2-port* network to find the stability criterion. In addition to the immittance (impedance, admittance, hybrid or inverse-hybrid) parameters of the original *3-port* network, the resultant stability criterion also depends on the dynamics of the environment (load termination) absorbed into the equivalent *2-port* network, which, thereby, should be known.

Remark: *In this context, a 2-port network is said to be unconditionally (absolutely) stable, if it is stable for all possible passive terminations [73].*

A similar approach was adopted in [73] to develop a stability analysis framework for multilateral MM/MS teleoperation frameworks (which can be modeled by an *n-port* network).

Based on this approach, two ports of the network should be arbitrary chosen as the network's sources, while all other ports will be considered as load terminations and absorbed into the network, resulting in a reduced *2-port* network. The next step would be to apply unconditional stability analysis methods such as Llewellyn's criterion or stability circles in the scattering domain to the equivalent *2-port* network. The stability conditions derived using this method will depend on not only the *n-port* network parameters, but also the port terminations. The stability analysis approach requires the dynamics of all terminations, except for one of the source terminations, to be approximated by linear models.

In [74], Li *et al.* took one step further by presenting an absolute stability condition for trilateral systems in a closed-form expression. In this work, a set of necessary and sufficient conditions was directly derived for trilateral systems based on the impedance (admittance) matrix of the equivalent *3-port* network, without first reducing to a *2-port* network. In addition to the set of stability conditions, the proposed criterion also necessitates the network impedance (admittance) matrix to satisfy a symmetrization condition, which involves the actual values of the teleoperator parameters. The stability criterion was expanded in [50] to also cover a class of multilateral MM/SS teleoperation systems, in which multiple master robots control one slave robot provided that the total number of DOFs in master robots is equal to the that of the slave robot. similar to the trilateral version, the stability analysis framework proposed for multilateral systems requires the immittance matrix of the equivalent *n-port* network to also satisfy a specific symmetrization condition, which can be satisfied by proper adjustment of the controller gains. The stability analysis framework allows for dynamic coupling across different DOFs of the robots, the operators and the environment.

Razi *et al.* [75] also set out a framework for coupled stability analysis of linear trilateral teleoperation systems (modeled by a *3-port* network). The analysis framework was based on an extended version of Zeheb–Walach (ZW) criteria and applies to the immittance parameters of the *3-port* network. An Extended ZW (EZW) theorem was developed such that, unlike the original ZW, it allows poles on the imaginary axis, which makes it applicable to robotic systems with position feedback.

In [76], the passivity criterion vs. the absolute stability criterion for trilateral teleoperation systems was compared analytically and through simulations/experiments. It was concluded

that, in the position-tracking mode for such systems, the absolute stability criterion is less conservative compared to the passivity criterion. It was also shown that the two criteria become the same for a trilateral framework with a symmetric immittance matrix.

2.6 Discussion and Future Direction

In this chapter, a review of multilateral frameworks was given, classifying the existing state-of-the-art architectures. The higher layer of classification was made based on the existing topologies, dividing the frameworks into the following general categories: 1) trilateral, 2) MM/SS, 3) SM/MS and 4) MM/MS frameworks. Then, the state-of-the-art results in each category were discussed in terms of applications, control strategies and challenges. An overview of topology-free stability analysis approaches for multilateral teleoperation framework was also presented.

As described in the chapter, coping with dynamic uncertainties for human operator(s) and the environment was among the control challenges addressed by prior studies on multilateral frameworks. Several studies also addressed control challenges associated with communication time delays, including closed-loop instability. Effect of communication delays (and other degrading aspects of communication networks, e.g., packet loss and jitter) on system performance/transparency have not, however, received much attention. Similar to SM/SS frameworks, and as also verified in [77] for a specific trilateral framework with a shared virtual environment, it is expected that communication delays have a destructive effect on performance of haptics-enabled multilateral systems as well. However, to what extent performance of multilateral teleoperation can be affected by communication delays, considering system topology, compared to that of a SM/SS system, requires more experimental and analytical investigations. Khademian *et al.* [78], Bacocco and Melchiorri [79], Powell *et al.* [12] are some of the publications that have discussed performance and efficacy of multilateral frameworks in the absence of communication delays. A part of future work can be focused on studying performance of delayed multilateral teleoperation systems as well as how having multiple operators in the loop, as compared to in classical SM/SS systems, can impact and possibly improve the outcome. The results of this type of investigative studies can then be used to enhance the operators telepresence and improve the task outcome for various multilateral architectures. Towards increasing

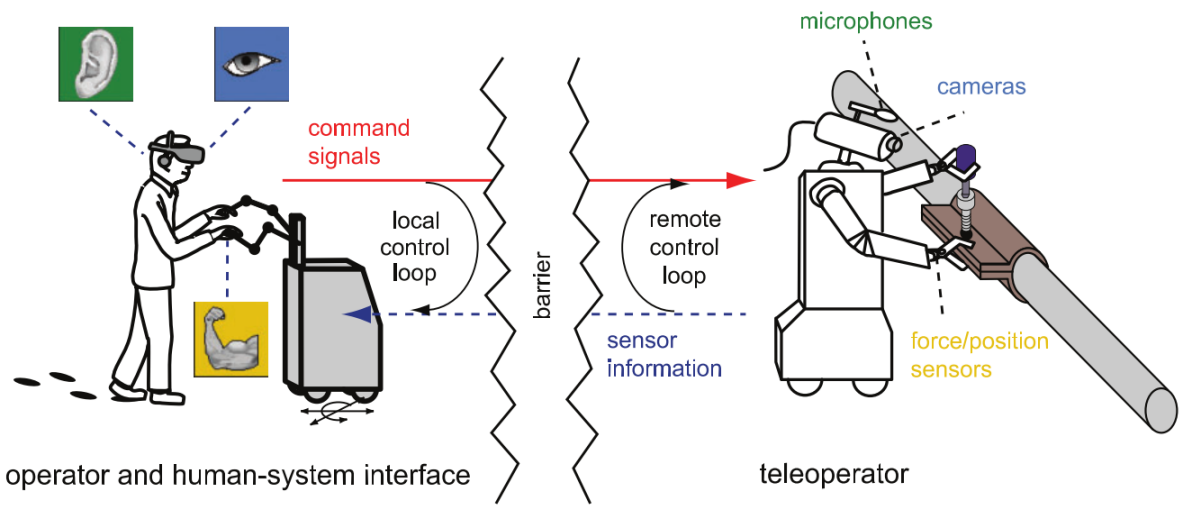

Figure 2.12: Schematic representation of a multi-modal telepresence system with visual, auditory and haptic feedback augmentation [80] (©[2009], SAGE Publications).

the operators telepresence and enhancing interaction between operators in a multi-user teleoperation framework, Buss *et al.* [80] developed a multi-modal system by augmenting visual, auditory and haptic feedback components into the framework (Fig. 2.12). For this purpose, a high-fidelity interpolation technique was developed to render three-dimensional sound scenes, a video system was designed to allow modeling and rendering of the remote environment in real time, and admittance-based haptic system was implemented to improve the operators telepresence.

As discussed earlier, haptics-enabled expert-in-the-loop motor skills development (including robotics-assisted surgical training [37], [38], [81] and rehabilitation therapy [32], [33]) as well as haptics-enabled training of a class of trainees [54] are among applications made possible through multilateral teleoperation frameworks. Effectiveness of haptic feedback from the environment was shown in [82], in terms of enhancing users performance as well as their sense of co-presence and awareness in a cooperative virtual environment. The potency of dyadic haptic interaction between two operators in enhancing the motor skills, as compared to practicing the task alone for the same duration, has also been investigated in many studies in the absence of communication delays. While several have validated the benefits of haptic augmentation in motor learning [34], [35], [83], [84], possible dependencies of the outcome on the task type and difficulty, the operator's ability, as well as the modality and the level of the haptic feedback

have also been discussed [13], [85], [86]. This emphasizes the need for further exploration of the extent of task-dependence as well as the impact of the forcefulness level and the type of haptic guidance. In addition, studies should be conducted to investigate the impact of large communication delays on the process of motor skills development through long-distance haptic interactions. Frameworks with a stable and human-safe control loop, as proposed in this thesis (which enables adaptive skills-oriented haptic guidance, without imposing limitations on the level of guidance force), realize appropriate testbeds for further studies on the nature of human motor learning and retention through haptic guidance and dyadic interactions. Frameworks with limited stability margin and *fixed-gain* error-reducing haptic guidance may not suffice for in-depth and conclusive studies [13], [85].

Another interesting area to explore would be the process of dominance/authority distribution between multiple operators as well as the impact of such distribution on the performance of shared multilateral frameworks. Shahbazi *et al.* [81], presented a real-time adjustment profile for the dominance factor for a trilateral framework developed for surgical training applications. Groten *et al.* [87] experimentally investigated the dominance distribution procedure between two operators for an object handling task. Future studies can be conducted to explore such issues (e.g., the development of a systematic adjustment procedure for the dominance distribution) for a wider range of applications, while ensuring closed-loop stability and thereby, safety of human-robot interaction.

Bibliography

[1] P. F. Hokayem and M. W. Spong, "Bilateral teleoperation: An historical survey," *Automatica*, vol. 42, no. 12, pp. 2035–2057, 2006.

[2] C. Passenberg, A. Peer, and M. Buss, "A survey of environment-, operator-, and task-adapted controllers for teleoperation systems," *Mechatronics*, vol. 20, no. 7, pp. 787–801, 2010.

[3] A. P. Melis, "The evolutionary roots of human collaboration: coordination and sharing of resources," *Annals of the New York Academy of Sciences*, vol. 1299, no. 1, pp. 68–76, 2013.

[4] S. Sirouspour, "Modeling and control of cooperative teleoperation systems," *IEEE Transactions on Robotics*, vol. 21, no. 6, pp. 1220–1225, 2005.

[5] R. L. Williams, F. W. Harrison, D. I. Soloway *et al.*, "Shared control of multiple-manipulator, sensor-based telerobotic systems," in *IEEE International Conference on Robotics and Automation*, vol. 2. IEEE, 1997, pp. 962–967.

[6] S. Hayati and S. Venkataraman, "Design and implementation of a robot control system with traded and shared control capability," in *IEEE International Conference on Robotics and Automation*. IEEE, 1989, pp. 1310–1315.

[7] P. G. Backes and K. S. Tso, "UMI: An interactive supervisory and shared control system for telerobotics," in *IEEE International Conference on Robotics and Automation*. IEEE, 1990, pp. 1096–1101.

[8] A. Zaatri and H. Van Brussel, "Investigations in telerobotics using cooperative supervisory modes of control," in *Intelligent Systems & Advanced Manufacturing*. International Society for Optics and Photonics, 1997, pp. 41–52.

[9] W. B. Griffin, W. R. Provancher, and M. R. Cutkosky, "Feedback strategies for shared control in dexterous telemanipulation," in *IEEE/RSJ International Conference on Intelligent Robots and Systems*, vol. 3. IEEE, 2003, pp. 2791–2796.

[10] S. Hayati, T. Lee, K. Tso, P. Backes, and J. Lloyd, "A testbed for a unified teleoperated-autonomous dual-arm robotic system," in *IEEE International Conference on Robotics and Automation*. IEEE, 1990, pp. 1090–1095.

[11] P. G. Backes, "Supervised autonomous control, shared control, and teleoperation for space servicing," *NASA Technical Report, Sixth Annual Workshop on Space Operations Applications and Research*, vol. 2, pp. 720–731, 1993.

[12] D. Powell and M. K. O'Malley, "The task-dependent efficacy of shared-control haptic guidance paradigms," *IEEE Transactions on Haptics*, vol. 5, no. 3, pp. 208–219, 2012.

[13] Y. Li, V. Patoglu, and M. K. O'Malley, "Negative efficacy of fixed gain error reducing shared control for training in virtual environments," *ACM Transactions on Applied Perception*, vol. 6, no. 1, p. 3, 2009.

[14] K. Shamaei, Y. Che, A. Murali, S. Sen, S. Patil, K. Goldberg, and A. M. Okamura, "A paced shared-control teleoperated architecture for supervised automation of multilateral surgical tasks," in *IEEE/RSJ International Conference on Intelligent Robots and Systems*. IEEE, 2015, pp. 1434–1439.

[15] K. B. Reed, M. Peshkin, M. J. Hartmann, J. Patton, P. M. Vishton, and M. Grabowecky, "Haptic cooperation between people, and between people and machines," in *IEEE/RSJ International Conference on Intelligent Robots and Systems*. IEEE, 2006, pp. 2109–2114.

[16] M. Shahbazi, S. F. Atashzar, H. A. Talebi, F. Towhidkhah, and M. Yazdanpanah, "A sliding-mode controller for dual-user teleoperation with unknown constant time delays," *Robotica*, vol. 31, no. 04, pp. 589–598, 2013.

[17] B. Khademian and K. Hashtrudi-Zaad, "Dual-user teleoperation systems: New multilateral shared control architecture and kinesthetic performance measures," *IEEE/ASME Transactions on Mechatronics*, vol. 17, no. 5, pp. 895–906, 2012.

[18] ——, "A robust multilateral shared controller for dual-user teleoperation systems," in *Canadian Conference on Electrical and Computer Engineering*, 2008.

[19] M. Shahbazi, H. Talebi, and F. Towhidkhah, "A robust control architecture for dual user teleoperation system with time-delay," in *36th Annual Conference on IEEE Industrial Electronics Society*. IEEE, 2010, pp. 1419–1423.

[20] M. Shahbazi, H. Talebi, S. Atashzar, F. Towhidkhah, R. Patel, and S. Shojaei, "A new set of desired objectives for dual-user systems in the presence of unknown communication delay," in *IEEE/ASME International Conference on Advanced Intelligent Mechatronics*. IEEE, 2011, pp. 146–151.

[21] H. Santacruz-Reyes, L. Garcia-Valdovinos, H. Jimenez-Hernandez, T. Salgado-Jimenez, and L. Garcia-Zarco, "Higher order sliding mode based impedance control for dual-user bilateral teleoperation under unknown constant time delay," in *IEEE/RSJ International Conference on Intelligent Robots and Systems*. IEEE, 2015, pp. 5209–5215.

[22] Z. Li, L. Ding, H. Gao, G. Duan, and C.-Y. Su, "Trilateral teleoperation of adaptive fuzzy force/motion control for nonlinear teleoperators with communication random delays," *IEEE Transactions on Fuzzy Systems*, vol. 21, no. 4, pp. 610–624, 2013.

[23] Z. Li, Y. Xia, D. Wang, D.-H. Zhai, C.-Y. Su, and X. Zhao, "Neural network-based control of networked trilateral teleoperation with geometrically unknown constraints," *IEEE Transactions on Cybernetics*, vol. 46, no. 5, pp. 1051–1064, 2016.

[24] A. Ghorbanian, S. Rezaei, A. Khoogar, M. Zareinejad, and K. Baghestan, "A novel control framework for nonlinear time-delayed dual-master/single-slave teleoperation," *ISA Transactions*, vol. 52, no. 2, pp. 268–277, 2013.

[25] M. Panzirsch, J. Artigas, A. Tobergte, P. Kotyczka, C. Preusche, A. Albu-Schaeffer, and G. Hirzinger, "A peer-to-peer trilateral passivity control for delayed collaborative teleoperation," in *Haptics: Perception, Devices, Mobility, and Communication*. Springer, 2012, pp. 395–406.

[26] M. Shahbazi, H. A. Talebi, and R. V. Patel, "Networked dual-user teleoperation with time-varying authority adjustment: A wave variable approach," in *IEEE/ASME International Conference on Advanced Intelligent Mechatronics*. IEEE, 2014, pp. 415–420.

[27] M. Shahbazi, S. F. Atashzar, and R. V. Patel, "A dual-user teleoperated system with virtual fixtures for robotic surgical training," in *IEEE International Conference on Robotics and Automation*. IEEE, 2013, pp. 3639–3644.

[28] L. Fei, A. Lelevé, D. Eberard, and T. Redarce, "A dual-user teleoperation system with online authority adjustment for haptic training." in *Annual International Conference of the IEEE Engineering in Medicine and Biology Society*, vol. 2015, 2015, p. 1168.

[29] P. Huang and Z. Lu, "Auxiliary asymmetric dual-user shared control method for teleoperation," in *International Conference on Ubiquitous Robots and Ambient Intelligence*. IEEE, 2015, pp. 267–272.

[30] M. Shahbazi, S. F. Atashzar, and R. V. Patel, "A framework for supervised robotics-assisted mirror rehabilitation therapy," in *IEEE/RSJ International Conference on Intelligent Robots and Systems*. IEEE, 2014, pp. 3567–3572.

[31] M. Shahbazi, S. F. Atashzar, M. Tavakoli, and R. V. Patel, "Therapist-in-the-loop robotics-assisted mirror rehabilitation therapy: An assist-as-needed framework," in *Robotics and Automation (ICRA), 2015 IEEE International Conference on*. IEEE, 2015, pp. 5910–5915.

[32] C. R. Carignan and P. A. Olsson, "Cooperative control of virtual objects over the internet using force-reflecting master arms," in *IEEE International Conference on Robotics and Automation*, vol. 2. IEEE, 2004, pp. 1221–1226.

[33] M. Shahbazi, S. Atashzar, M. Tavakoli, and R. Patel, "Robotics-assisted mirror rehabilitation therapy: A therapist-in-the-loop assist-as-needed architecture," *IEEE/ASME Transactions on Mechatronics*, DOI: 10.1109/TMECH.2016.2551725, 2016.

[34] K. Reed, M. Peshkin, M. J. Hartmann, M. Grabowecky, J. Patton, and P. M. Vishton, "Haptically linked dyads are two motor-control systems better than one?" *Psychological science*, vol. 17, no. 5, pp. 365–366, 2006.

[35] G. Ganesh, A. Takagi, R. Osu, T. Yoshioka, M. Kawato, and E. Burdet, "Two is better than one: Physical interactions improve motor performance in humans," *Scientific reports*, vol. 4, 2014.

[36] H. Yano and H. Iwata, "Cooperative work in virtual environment with force feedback," *Transactions-Society of Instrument and Control Engineers*, vol. 31, pp. 1495–1501, 1995.

[37] S. S. Nudehi, R. Mukherjee, and M. Ghodoussi, "A shared-control approach to haptic interface design for minimally invasive telesurgical training," *IEEE Transactions on Control Systems Technology*, vol. 13, no. 4, pp. 588–592, 2005.

[38] B. Chebbi, D. Lazaroff, F. Bogsany, P. X. Liu, L. Ni, and M. Rossi, "Design and implementation of a collaborative virtual haptic surgical training system," in *IEEE International Conference Mechatronics and Automation*, vol. 1. IEEE, 2005, pp. 315–320.

[39] C. Gunn, M. Hutchins, D. Stevenson, M. Adcock, and P. Youngblood, "Using collaborative haptics in remote surgical training," in *First Joint Eurohaptics Conference and Symposium on Haptic Interfaces for Virtual Environment and Teleoperator Systems*. IEEE, 2005, pp. 481–482.

[40] S. Katsura and K. Ohnishi, "A realization of haptic training system by multilateral control," *IEEE Transactions on Industrial Electronics*, vol. 53, no. 6, pp. 1935–1942, 2006.

[41] S. Moghimi, S. Sirouspour, and P. Malysz, "Haptic-enabled collaborative training with generalized force and position mappings," in *2008 Symposium on Haptic Interfaces for Virtual Environment and Teleoperator Systems*. IEEE, 2008, pp. 287–294.

[42] B. Khademian and K. Hashtrudi-Zaad, "Shared control architectures for haptic training: Performance and coupled stability analysis," *The International Journal of Robotics Research*, p. 0278364910397559, 2011.

[43] M. Shahbazi, S. F. Atashzar, C. Ward, H. A. Talebi, and R. V. Patel, "Multimodal sensorimotor integration for expert-in-the-loop telerobotic surgical training," *Submitted to IEEE Transactions on Control System Technology*, 2016.

[44] K. Shamaei, L. H. Kim, and A. M. Okamura, "Design and evaluation of a trilateral shared-control architecture for teleoperated training robots," in *37th Annual International Conference of the IEEE Engineering in Medicine and Biology Society*. IEEE, 2015, pp. 4887–4893.

[45] R. V. Patel and F. Shadpey, *Control of redundant robot manipulators: theory and experiments*. Springer Science & Business Media, 2005, vol. 316.

[46] P. Malysz and S. Sirouspour, "Trilateral teleoperation control of kinematically redundant robotic manipulators," *The International Journal of Robotics Research*, vol. 30, no. 13, pp. 1643–1664, 2011.

[47] ——, "A kinematic control framework for single-slave asymmetric teleoperation systems," *IEEE Transactions on Robotics*, vol. 27, no. 5, pp. 901–917, 2011.

[48] P. R. Culmer, A. E. Jackson, S. Makower, R. Richardson, J. A. Cozens, M. C. Levesley, and B. B. Bhakta, "A control strategy for upper limb robotic rehabilitation with a dual robot system," *IEEE/ASME Transactions on Mechatronics*, vol. 15, no. 4, pp. 575–585, 2010.

[49] P. Malysz and S. Sirouspour, "Cooperative teleoperation control with projective force mappings," in *IEEE Haptics Symposium*. IEEE, 2010, pp. 301–308.

[50] J. Li, M. Tavakoli, and Q. Huang, "Stability of cooperative teleoperation using haptic devices with complementary degrees of freedom," *Control Theory & Applications*, vol. 8, no. 12, pp. 1062–1070, 2014.

[51] K. Goldberg, B. Chen, R. Solomon, S. Bui, B. Farzin, J. Heitler, D. Poon, and G. Smith, "Collaborative teleoperation via the internet," in *IEEE International Conference on Robotics and Automation*, vol. 2. IEEE, 2000, pp. 2019–2024.

[52] S. Katsura, T. Suzuyama, and K. Ohishi, "A realization of multilateral force feedback control for cooperative motion," *IEEE Transactions on Industrial Electronics*, vol. 54, no. 6, pp. 3298–3306, 2007.

[53] D. Lee, O. Martinez-Palafox, and M. W. Spong, "Bilateral teleoperation of multiple cooperative robots over delayed communication networks: Application," in *IEEE International Conference on Robotics and Automation*. IEEE, 2005, pp. 366–371.

[54] M. Shahbazi, S. F. Atashzar, H. A. Talebi, and R. V. Patel, "Novel cooperative teleoperation framework: multi-master/single-slave system," *IEEE/ASME Transactions on Mechatronics*, vol. 20, no. 4, pp. 1668–1679, 2015.

[55] K. Kosuge, J. Ishikawa, K. Furuta, and M. Sakai, "Control of single-master multi-slave manipulator system using vim," in *IEEE International Conference on Robotics and Automation*. IEEE, 1990, pp. 1172–1177.

[56] D. Lee and M. W. Spong, "Bilateral teleoperation of multiple cooperative robots over delayed communication networks: theory," in *IEEE International Conference on Robotics and Automation*. IEEE, 2005, pp. 360–365.

[57] D. Sun, F. Naghdy, and H. Du, "Stability control of force-reflected nonlinear multilateral teleoperation system under time-varying delays," *Journal of Sensors*, vol. 2016, 2015.

[58] N. Y. Chong, S. Kawabata, K. Ohba, T. Kotoku, K. Komoriya, K. Takase, and K. Tanie, "Multioperator teleoperation of multirobot systems with time delay: Part i—aids for collision-free control," *Presence: Teleoperators and Virtual Environments*, vol. 11, no. 3, pp. 277–291, 2002.

[59] N. Y. Chong, T. Kotoku, K. Ohba, K. Komoriya, K. Tanie, J. Oaki, H. Hashimoto, F. Ozaki, K. Maeda, and N. Matsuhira, "A collaborative multi-site teleoperation over an ISDN," *Mechatronics*, vol. 13, no. 8, pp. 957–979, 2003.

[60] X.-G. Wang, M. Moallem, and R. V. Patel, "An internet-based distributed multiple-telerobot system," *IEEE Transactions on Systems, Man and Cybernetics, Part A: Systems and Humans*, vol. 33, no. 5, pp. 627–634, 2003.

[61] W.-t. Lo, Y. Liu, I. H. Elhajj, N. Xi, Y. Wang, and T. Fukuda, "Cooperative teleoperation of a multirobot system with force reflection via internet," *IEEE/ASME Transactions on Mechatronics*, vol. 9, no. 4, pp. 661–670, 2004.

[62] S. Sirouspour and P. Setoodeh, "Multi-operator/multi-robot teleoperation: an adaptive nonlinear control approach," in *IEEE/RSJ International Conference on Intelligent Robots and Systems*. IEEE, 2005, pp. 1576–1581.

[63] P. Setoodeh, S. Sirouspour, and A. Shahdi, "Discrete-time multi-model control for cooperative teleoperation under time delay," in *IEEE International Conference on Robotics and Automation*. IEEE, 2006, pp. 2921–2926.

[64] C. Passenberg, A. Peer, and M. Buss, "Model-mediated teleoperation for multi-operator multi-robot systems," in *IEEE/RSJ International Conference on Intelligent Robots and Systems*. IEEE, 2010, pp. 4263–4268.

[65] D. Feth, A. Peer, and M. Buss, "Enhancement of multi-user teleoperation systems by prediction of dyadic haptic interaction," in *Experimental Robotics*. Springer, 2014, pp. 855–869.

[66] U. Tumerdem and K. Ohnishi, "Multi-robot teleoperation under dynamically changing network topology," in *IEEE International Conference on Industrial Technology*. IEEE, 2009, pp. 1–6.

[67] T. Kanno and Y. Yokokohji, "Multilateral teleoperation control over time-delayed computer networks using wave variables," in *IEEE Haptics Symposium*. IEEE, 2012, pp. 125–131.

[68] M. Panzirsch, J. Artigas, J.-H. Ryu, and M. Ferre, "Multilateral control for delayed teleoperation," in *International Conference on Advanced Robotics*. IEEE, 2013, pp. 1–6.

[69] H. Van Quang and J.-H. Ryu, "Stable multilateral teleoperation with time domain passivity approach," in *IEEE/RSJ International Conference on Intelligent Robots and Systems*. IEEE, 2013, pp. 5890–5895.

[70] Z. Chen, Y.-J. Pan, and J. Gu, "Integrated adaptive robust control for multilateral teleoperation systems under arbitrary time delays," *International Journal of Robust and Nonlinear Control*, 2015.

[71] V. Mendez, M. Tavakoli, and J. Li, "A method for passivity analysis of multilateral haptic systems," *Advanced Robotics*, vol. 28, no. 18, pp. 1205–1219, 2014.

[72] B. Khademian and K. Hashtrudi-Zaad, "Unconditional stability analysis of dual-user teleoperation systems," in *IEEE Haptics Symposium*. IEEE, 2010, pp. 161–166.

[73] ——, "A framework for unconditional stability analysis of multimaster/multislave teleoperation systems," *IEEE Transactions on Robotics*, vol. 29, no. 3, pp. 684–694, 2013.

[74] J. Li, M. Tavakoli, and Q. Huang, "Absolute stability of multi-DOF multilateral haptic systems," *IEEE Transactions on Control Systems Technology*, vol. 22, no. 6, pp. 2319–2328, 2014.

[75] K. Razi and K. Hashtrudi-Zaad, "Analysis of coupled stability in multilateral dual-user teleoperation systems," *IEEE Transactions on Robotics*, vol. 30, no. 3, pp. 631–641, 2014.

[76] J. Li, M. Tavakoli, V. Mendez, and Q. Huang, "Passivity and absolute stability analyses of trilateral haptic collaborative systems," *Journal of Intelligent & Robotic Systems*, vol. 78, no. 1, pp. 3–20, 2015.

[77] M. Fotoohi, S. Sirouspour, and D. Capson, "Stability and performance analysis of centralized and distributed multi-rate control architectures for multi-user haptic interaction," *The International Journal of Robotics Research*, vol. 26, no. 9, pp. 977–994, 2007.

[78] B. Khademian and K. Hashtrudi-Zaad, "Performance issues in collaborative haptic training," in *IEEE International Conference on Robotics and Automation*. IEEE, 2007, pp. 3257–3262.

[79] R. Bacocco and C. Melchiorri, "A performance and stability analysis for cooperative teleoperation systems," in *Proceedings of the 18th IFAC World Congress*, 2011, pp. 1096–1101.

[80] M. Buss, A. Peer, T. Schauß, N. Stefanov, U. Unterhinninghofen, S. Behrendt, J. Leupold, M. Durkovic, and M. Sarkis, "Development of a multi-modal multi-user telepresence and teleaction system," *The International Journal of Robotics Research*, vol. 29, no. 10, pp. 1298–1316, 2010.

[81] M. Shahbazi, S. F. Atashzar, H. A. Talebi, and R. V. Patel, "An expertise-oriented training framework for robotics-assisted surgery," in *IEEE International Conference on Robotics and Automation*. IEEE, 2014, pp. 5902–5907.

[82] S. Ullah, P. Richard, S. Otmane, M. Naud, and M. Mallem, "Haptic guides in cooperative virtual environments: Design and human performance evaluation," in *IEEE Haptics Symposium*. IEEE, 2010, pp. 457–462.

[83] R. Groten, D. Feth, A. Peer, M. Buss, and R. Klatzky, "Efficiency analysis in a collaborative task with reciprocal haptic feedback," in *IEEE/RSJ International Conference on Intelligent Robots and Systems*. IEEE, 2009, pp. 461–466.

[84] D. Feth, B. A. Tran, R. Groten, A. Peer, and M. Buss, "Shared-control paradigms in multi-operator-single-robot teleoperation," in *Human Centered Robot Systems*. Springer, 2009, pp. 53–62.

[85] Y. Che, G. M. Haro, and A. M. Okamura, "Two is not always better than one: Effects of teleoperation and haptic coupling," in *2016 6th IEEE International Conference on Biomedical Robotics and Biomechatronics (BioRob)*. IEEE, 2016, pp. 1290–1295.

[86] D. P. Losey, L. H. Blumenschein, and M. K. O'Malley, "Improving the retention of motor skills after reward-based reinforcement by incorporating haptic guidance and error

augmentation," in *2016 6th IEEE International Conference on Biomedical Robotics and Biomechatronics (BioRob)*. IEEE, 2016, pp. 857–863.

[87] R. Groten, D. Feth, H. Goshy, A. Peer, D. A. Kenny, and M. Buss, "Experimental analysis of dominance in haptic collaboration," in *IEEE International Symposium on Robot and Human Interactive Communication*. IEEE, 2009, pp. 723–729.

Chapter 3

Time-Varying Dominance Distribution: A Wave-Variable Approach

The material presented in this chapter was published in the Proceedings of the IEEE/ASME International Conference on Advanced Intelligent Mechatronics (AIM), pp. 415-420, France, 2014.

3.1 INTRODUCTION

A teleoperation system makes it possible for a human to perform a task remotely with no need for the operator to be present at the task side. Therefore, teleoperation systems can be used for hazardous tasks and out of reach areas; such as in space exploration, undersea tasks, mining, and handling of hazardous materials [1]. An important recent application of teleoperation is in the medical field, and more specifically, in the performance of Minimally Invasive Surgery (MIS).

In teleoperation systems, stability and transparency are the main control objectives. However, these objectives are usually at odds with each other, meaning that an improvement in one can degrade the other. Addressing this problem usually necessitates a trade-off in the controller design procedure. The controller design gets more complicated and challenging if the

©[2014] IEEE. Reprinted, with permission, from [Mahya Shahbazi, H.A. Talebi, R.V. Patel," Networked Dual-User Teleoperation with Time-Varying Authority Adjustment: A Wave Variable Approach", IEEE/ASME International Conference on Advanced Intelligent Mechatronics (AIM), 2014.]

master and the slave robots are located far from each other. In fact, long distances can introduce considerable communication delays, which are difficult to deal with [1], [2], [3]. In order to deal with communication delays in Single-Master/Single-Slave (SM/SS) teleoperation systems, several control structures are presented in the literature, as summarized in [4]. In an SM/SS system, as the name implies, one operator holding one master robot performs a task through one slave robot. Building on this conventional category of teleoperation systems, dual-user systems have also been introduced. In this category, two operators perform a common task through a set of two master robots and one slave robot [5], [6]. In dual-user teleoperation systems, each operator can affect the operation based on his/her expertise. The authority of each operator over the task can be adjusted by a "dominance factor", which can be set depending on the task and expertise of the operators. A dual-user teleoperation system is primarily applicable in cooperative tasks and training applications, e.g., rehabilitation and surgical training [7], [8], [9]. Work on dual-user teleoperation systems is relatively recent and there are only a few studies to date on the subject. In [10], a control architecture is proposed to control a kinematically redundant slave manipulator controlled by two master robots. In this architecture, the scheme is different from the dual-user task mentioned above. Each master performs a separate task, a primary and a secondary, while in the problem addressed in this chapter, the master robots perform a common task cooperatively. In [11], two multilateral shared control architectures are presented for dual-user systems, which provide increased maneuverability and enhanced sense of the environment to the users. A force-position multilateral shared controller has been proposed for dual-user teleoperation systems in [12]. The controller is robustly stable in the presence of uncertainties of hand dynamics and environmental impedance. Although the above-mentioned studies as well as most of the other previous research present control methodologies for dual-user systems, they do not address the issue of communication delays.

A robust controller based on μ-synthesis has been proposed for a dual-user system in the presence of communication delays in [5]. In this architecture, the time delay between the slave robot and each master robot is assumed to be known and constant, while delay-free communication is assumed between the master robots.

A potential application of a dual-user system is in two-handed tele-rehabilitation therapy,

where the patient is asked to involve his/her healthy arm to cooperate with the therapist's arm in order to train the patient's impaired arm [13]. This approach, which increases the effectiveness of therapy, necessitates two master robots one held by the therapist and the other by the patient's healthy arm in order to manipulate one slave robot held by the patient's impaired arm. A suitable therapy would allow the therapist to specify the impact level of the patient's healthy arm over his/her impaired arm during the task. This necessitates the closed-loop system to remain stable in the presence of a time-varying dominance factor. Another potential application of a dual-user system could be in training for Robotics-Assisted Minimally Invasive Surgery (RAMIS), e.g., when two surgeon's consoles are available as in the new da Vinci Si from Intuitive Surgical Inc., where one is operated by a mentor and the other by a trainee to manipulate the slave robotic system at the patient side. A useful feature of such a system would be to provide the expert with the ability to adjust the authority of the trainee over the task in a real-time fashion. This also requires the system to remain stable in the presence of the time-varying dominance factor.

Work on dual-user teleoperation systems is relatively recent, and applications involving *variation* of the dominance factor have not been considered in previous research. In [14], a dual-user training approach for RAMIS was proposed by the authors which benefits from the variation of the dominance factor. However, the structure proposed there and the closed-loop stability analysis were task-specific, developed for training applications and cannot be straightforwardly generalized to other applications such as tele-rehabilitation therapy. Therefore, in this chapter, a dual-user system with a time-varying dominance factor is studied, while preserving system generality. In order to make the communication channels passive, a modified version of the conventional wave transformation approach used for the SM/SS system [15] is proposed, guaranteeing closed-loop stability of the dual-user system with a time-varying dominance factor in the presence of a constant delay. Controller validity is demonstrated by experimental results.

The rest of the chapter is organized as follows: The system dynamics and desired objectives are presented in Section 3.2. Section 3.3 describes the controller design and the modified wave transformation for the dual-user system. The stability analysis and experimental results are given in Section 3.4 and 3.5, respectively. Section 3.6 concludes the chapter.

3.2 System Dynamics and Desired Objectives

3.2.1 System Dynamics

In a dual-user teleoperation system, two operators use two master robots in order to perform a task through a slave robot. Both master robots and the slave robot have nonlinear dynamics [16]:

$$D_\gamma(x_\gamma)\ddot{x}_\gamma + C_\gamma(x_\gamma,\dot{x}_\gamma)\dot{x}_\gamma + G_\gamma(x_\gamma) = F_{c\gamma} - F_{ext\gamma} \tag{3.1}$$

where $\gamma = m_1$ and $\gamma = m_2$, for master #1 and master #2, respectively, while for the slave robot, $\gamma = s$. In addition, x_γ stands for the positions of the robots' end-effectors, D_γ is the mass matrix, $C_\gamma(x_\gamma,\dot{x}_\gamma)$ corresponds to the velocity-dependent elements and $G_\gamma(x_\gamma)$ represents the position-dependent forces such as gravity. Furthermore, $F_{c\gamma}$ stands for the control signal and $F_{ext\ \gamma}$ for the external force acting at the robot end-effector. The external force acting on each master robot corresponds to the hand force of its operator. The operator's hand dynamics are modeled by a second-order linear time-invariant system [17]. Therefore, the operators' hand forces F_{h_i} $(i = 1,2)$ are given by:

$$\begin{aligned} F_{ext\ m_i} = -F_{h_i} = \\ -\left(F^*_{h_i} - M_{h_i}\ddot{x}_{h_i} - B_{h_i}\dot{x}_{h_i} - K_{h_i}[x_{h_i} - x_{h_i0}]\right) \end{aligned} \tag{3.2}$$

where M_{h_i}, B_{h_i} and K_{h_i} $(i = 1,2)$ denote the mass, damping and stiffness of the operators' hands, respectively and $F^*_{h_i}$ represents the users exogenous force. In addition, x_{h_i} $(i = 1,2)$ refers to the position of the operators' hands, while the subscript 0 refers to the initial value, i.e., x_{h_i} at $t = 0$. Since, each operator holds a master robot with his/her hand; we have the following equality between the operators' hand positions and the end-effector positions of the master robots:

$$x_{h_i} = x_{m_i} \quad (i = 1,2) \tag{3.3}$$

The external force acting on the slave end-effector corresponds to the environment force. Since the environment can be modelled as a second-order linear time-invariant system [17], the envi-

ronment force F_e is given by:

$$F_{ext\ s} = F_e = M_e\ddot{x}_e + B_e\dot{x}_e + K_e(x_e - x_{e0}) \tag{3.4}$$

where M_e, B_e and K_e refer to the mass, damping and stiffness of the environment respectively; x_e corresponds to the position of the environment and the subscript 0 refers to the initial value (at $t = 0$). Since the slave robot interacts with the environment, the following equality holds between the slave position and the environment position:

$$x_s = x_e \tag{3.5}$$

3.2.2 Desired Objective in Dual-User Systems

In dual-user systems, two operators perform the task cooperatively. Therefore, it is desired for the slave robot to follow a combination of the positions of the master robots. This combination is adjusted through the dominance factor "α". Therefore, the desired position for the slave robot is as follows [11]:

$$x_{sd} = \alpha x_{m_1} + (1-\alpha)x_{m_2} \tag{3.6}$$

where x_{m_1}, x_{m_2} and x_s represent the positions of masters and slave robots and subscript "d" refers to the desired value for the slave robot. In addition, α the dominance factor varies between 0 and 1 which determines the authority of each user over the task. Setting $\alpha = 1$, and consequently $1-\alpha = 0$, full authority will be given to the first operator, while the second operator will have no authority over the task. In another case, considering equal authority for the operators, we have $\alpha = 1-\alpha = 0.5$ and the slave position will be the average of the master robots' positions. If the operators perform the task completely similar to each other that is $x_{m_1} = x_{m_2}$, as can be seen in (3.6), the effect of the dominance factor will be eliminated; therefore, regardless of the value of α, in this case we will have: $x_{sd} = x_{m_1} = x_{m_2}$.

In addition to the desired objectives for the slave position, it is desired for the operators to feel the environment force to have transparent operations. Therefore, two other desired

objectives for the dual-user system are as follows [11]:

$$F_{h_1 d} = F_e \tag{3.7}$$

$$F_{h_2 d} = F_e \tag{3.8}$$

where the subscript "d" refers to the desired value of F_{h_1} and F_{h_2}, the operators' hand forces.

3.3 The Proposed Wave-Variable-Based Controller

In order to satisfy the desired objectives for the dual-user system, a decentralized impedance-based control methodology is adopted [18]. For this purpose, three impedance surfaces are defined as the desired closed-loop systems and an impedance controller is designed to satisfy these impedance surfaces. Note that the impedance controller can be replaced by an adaptive impedance controller if the robots' physical parameters are not exactly known. The impedance equations for master #1, master #2 and the slave robot are defined as follows:

$$M_{1,d}\ddot{x}_{m_1} + B_{1,d}\dot{x}_{m_1} + K_{1,d}x_{m_1} = F_{h_1} - F_e \tag{3.9}$$

$$M_{2,d}\ddot{x}_{m_2} + B_{2,d}\dot{x}_{m_2} + K_{2,d}x_{m_2} = F_{h_2} - F_e \tag{3.10}$$

$$x_s = \alpha x_{m_1} + (1-\alpha)x_{m_2} \tag{3.11}$$

where $M_{i,d}$, $B_{i,d}$ and $K_{i,d}$ $(i = 1,2)$ correspond to the desired inertia, damping and stiffness for master #1 and master #2. By satisfying (3.9) and (3.10) as the closed-loop system of the master robots, it can be seen that the operators' hand forces, F_{h_i}, will follow the environment force, F_e, with an error. This error is relative to the position of the corresponding master robot as well as the desired impedance parameters $M_{i,d}$, $B_{i,d}$ and $K_{i,d}$. Therefore, by setting these parameters to small values, the force tracking error can be reduced to an acceptable value, although it cannot be totally eliminated.

The adopted impedance-based control methodology can guarantee system stability in the presence of negligible time delay. However, it is well-understood that a significant communication delay can easily make the overall closed-loop system unstable. Therefore, in this chapter,

the conventional wave transformation (applicable to the SM/SS system) is modified so as to guarantee the closed-loop stability for the dual-user system in the presence of the *time-varying* dominance factor and constant communication delays.

The proposed wave transformations for the communication channels between the slave robot and the master #1 and #2 in a dual-user system with a time-varying dominance factor are given by (3.12) and (3.13), respectively:

$$\begin{cases} f_{m_1} = b_1\dot{\alpha}x_{m_1} + b_1\alpha\dot{x}_{m_1} - \sqrt{2b_1}v_{m_1} \\ \qquad = b_1\left(\alpha x_{m_1}\right)' - \sqrt{2b_1}v_{m_1} \\ \\ u_{m_1} = -v_{m_1} + \sqrt{2b_1}\dot{\alpha}x_{m_1} + \sqrt{2b_1}\alpha\dot{x}_{m_1} \\ \qquad = -v_{m_1} + \sqrt{2b_1}\left(\alpha x_{m_1}\right)' \\ \\ \dot{x_{s_1}} = \sqrt{\dfrac{2}{b_1}}u_{s_1} - \dfrac{1}{b_1}f_{s_1} \\ \\ v_{s_1} = u_{s_1} - \sqrt{\dfrac{2}{b_1}}f_{s_1} \end{cases} \tag{3.12}$$

$$\begin{cases} f_{m_2} = b_2\dot{x_{m_2}} - b_2\dot{\alpha}x_{m_2} - b_2\alpha\dot{x}_{m_2} - \sqrt{2b_2}v_{m_2} \\ \qquad = b_2\Big((1-\alpha)x_{m_2}\Big)' - \sqrt{2b_2}v_{m_2} \\ \\ u_{m_2} = -v_{m_2} - \sqrt{2b_2}\dot{\alpha}x_{m_2} - \sqrt{2b_2}\alpha\dot{x}_{m_2} + \sqrt{2b_2}\dot{x}_{m_2} \\ \qquad = -v_{m_2} + \sqrt{2b_2}\Big((1-\alpha)x_{m_2}\Big)' \\ \\ \dot{x_{s_2}} = \sqrt{\dfrac{2}{b_2}}u_{s_2} - \dfrac{1}{b_2}f_{s_2} \\ \\ v_{s_2} = u_{s_2} - \sqrt{\dfrac{2}{b_2}}f_{s_2} \end{cases} \tag{3.13}$$

where $(\cdot)'$ refers to the $\dfrac{d}{d\tau}(\cdot)$ operation; u_{m_i} and v_{m_i} $(i = 1,2)$ are the wave variables used at the master robots sides; u_{s_i} and v_{s_i} $(i = 1,2)$ are the wave variables used at the slave robot

side and we have $u_{s_i}(t) = u_{m_i}(t - T_i)$ and $v_{m_i}(t) = v_{s_i}(t - T_i)$, where T_i indicate the constant time delay between master robot #i and the slave robot; Moreover, b_i $(i = 1,2)$ indicate the characteristic wave impedances for the wave transformation between master #i and the slave robot. Furthermore, f_{s_i} $(i = 1,2) = F_e$. Signals with the subscript i=1 correspond to those used for the communication channel between the slave robot and master #1, while $i = 2$ refers to the signals through the communication channel between the slave robot and master #2. In addition, T_i $(i = 1,2)$ denotes the communication delay between the slave robot and master #i . Fig. 1 shows the overall dual-user system including the wave variables. By applying these transformations, at the masters sides, instead of F_e, we will receive f_{m_1} and f_{m_2} sent from the slave side. Therefore, it is required to replace F_e by f_{m_1} and f_{m_2} in (3.9) and (3.10), respectively.

In addition, based on the definition of the wave variables in (3.12) and (3.13), the slave robot will receive $\dot{x}_{s_1}$ and $\dot{x}_{s_2}$ instead of $\dot{\alpha}x_{m_1} + \alpha\dot{x}_{m_1}$ and $-\dot{\alpha}x_{m_2} + (1-\alpha)\dot{x}_{m_2}$ as the signals sent from master #1 and master #2, respectively. Therefore, αx_{m_1} and $(1-\alpha)x_{m_2}$ in (3.11) are required to be replaced with the integral of $\dot{x}_{s_1}$ and $\dot{x}_{s_2}$, respectively.

The presence of $\dot{\alpha}$ in (3.12) and (3.13), the proposed wave transformation necessitates bounded first-derivative for the dominance factor $\alpha(t)$, which should be considered in the dominance-factor design process. Different parameters may contribute to the adjustment of a dominance factor depending on the application. For example in training a novice for a RAMIS, the quantified expertise level of the trainee over the task [19] may be included in the online automatic adjustment of the dominance factor. Therefore, the more expertise the trainee demonstrates during the task, the more authority could be given to her/him over the task. Besides the trainee's expertise level, the expert surgeon still can be given the ability to overrule the automatic adjustment when necessary. The various design scenarios to adjust the dominance factor in an online fashion during the task with regard to the application turns the subject into a fascinating area to study, which is the future focus of this research.

3.4 Stability Analysis

In order to investigate the closed-loop stability, passivity theory is used. A passive teleoperator can be shown to be stable despite the nonlinear behavior of the operators and the environment

as long as they are passive, but otherwise arbitrary [20], [21]. Therefore, by the assumption of passivity of the environment and the operators with respect to the velocity-force input-output pair, in order to have a passive system, the overall communication-channel specified by the red dashed line in Fig. 3.1 (including the communication channels Ψ_1 and Ψ_2, and wave transformations) and the transformation blocks Ω_1 and Ω_2 are required to be separately passive. A general time-varying n-port system with zero initial energy storage is passive if [22], [23]:

$$\varepsilon(t) = \int_0^t P_{in}(\tau)d\tau = \int_0^t x^T(\tau).y(\tau)d\tau \geq 0 \tag{3.14}$$

where $x(\tau) \in R^n$ and $y(\tau) \in R^n$ correspond to the input and output of the network, respectively. For the overall communication channel, $x(\tau)$ and $y(\tau)$ are defined as:

$$\begin{aligned} x(\tau) &= \begin{bmatrix} \frac{d}{d\tau}(\alpha x_{m_1}(\tau)) & \frac{d}{d\tau}((1-\alpha)x_{m_2}(\tau)) & F_e(\tau) & F_e(\tau) \end{bmatrix}, \\ y(\tau) &= \begin{bmatrix} f_{m_1}(\tau) & f_{m_2}(\tau) & \frac{d}{d\tau}x_{s_1}(\tau) & \frac{d}{d\tau}x_{s_2}(\tau) \end{bmatrix} \end{aligned} \tag{3.15}$$

Consequently, for passivity of the communication channel, it is required to have:

$$\begin{aligned} \varpi(t) = \int_0^t \Big(&(\alpha x_{m_1})'.f_{m_1} + ((1-\alpha)x_{m_2})'.f_{m_2} + x'_{s_1}.F_e \\ &+ x'_{s_2}.F_e \Big) d\tau \geq 0 \end{aligned} \tag{3.16}$$

This condition can be written down in a conservative format, which refers to a sufficient condition for (3.16), as follows:

$$\begin{cases} \varpi_1(t) = \int_0^t \Big((\alpha x_{m_1})'.f_{m_1} + x'_{s_1}.F_e \Big) d\tau \geq 0 \\ \varpi_2(t) = \int_0^t \Big(((1-\alpha)x_{m_2})'.f_{m_2} + x'_{s_1}.F_e \Big) d\tau \geq 0 \end{cases} \tag{3.17}$$

In fact, if $\varpi_1(t) \geq 0$ and $\varpi_2(t) \geq 0$, then $\varpi = \varpi_1(t) + \varpi_2(t) \geq 0$. According to Fig. 1, this conservative condition indicates that passivity of the overall communication channel, shown by the red dashed line, can be satisfied if the communication channels Ψ_1 and Ψ_2 (including the wave transformations) are separately passive.

To investigate passivity of Ψ_1 and Ψ_2, by a change of the variables $\delta_{m_1} = \alpha x_{m_1}$ and $\delta_{m_2} =$

$(1-\alpha)x_{m_2}$, the wave variables f_{m_i} and $u_{m_i}(i=1,2)$ given by (3.12) and (3.13) can be rewritten as (3.18) and (3.19). Now, the simplified wave transformations for the communication channels between each master robot and the slave robot are in the form of the conventional wave transformation [15], [24].

$$\begin{cases} f_{m_1} = b_1\dot{\delta}_{m_1} - \sqrt{2b_1}v_{m_1} \\ u_{m_1} = -v_{m_1} + \sqrt{2b_1}\dot{\delta}_{m_1} \\ \dot{x_{s_1}} = \sqrt{\dfrac{2}{b_1}}u_{s_1} - \dfrac{1}{b_1}f_{s_1} \\ v_{s_1} = u_{s_1} - \sqrt{\dfrac{2}{b_1}}f_{s_1} \end{cases} \tag{3.18}$$

$$\begin{cases} f_{m_2} = b_2\dot{\delta}_{m_2} - \sqrt{2b_2}v_{m_2} \\ u_{m_2} = -v_{m_2} + \sqrt{2b_2}\dot{\delta}_{m_2} \\ \dot{x_{s_2}} = \sqrt{\dfrac{2}{b_2}}u_{s_2} - \dfrac{1}{b_2}f_{s_2} \\ v_{s_2} = u_{s_2} - \sqrt{\dfrac{2}{b_2}}f_{s_2} \end{cases} \tag{3.19}$$

Therefore, the overall communication channels between the slave robot and the master robots (Ψ_1 and Ψ_2 including the wave transformations) are passive. Fig. 3.2 shows the network connections of the simplified wave transformations for the communication channel Ψ_i $(i=1,2)$.

In addition to passivity of the overall communication channel shown by the red dashed line in Fig. 3.1, two transformation blocks Ω_1 and Ω_2 also need to be passive. To investigate passivity of these blocks, the inputs and the outputs of the 2-port system Ω_1 and Ω_2 can be defined as in (3.20) and (3.21), respectively. Note that, based on the standard passivity theorem [25], [26], the conditions of passivity can be applied to input/output pairs sent/received through the n-port network.

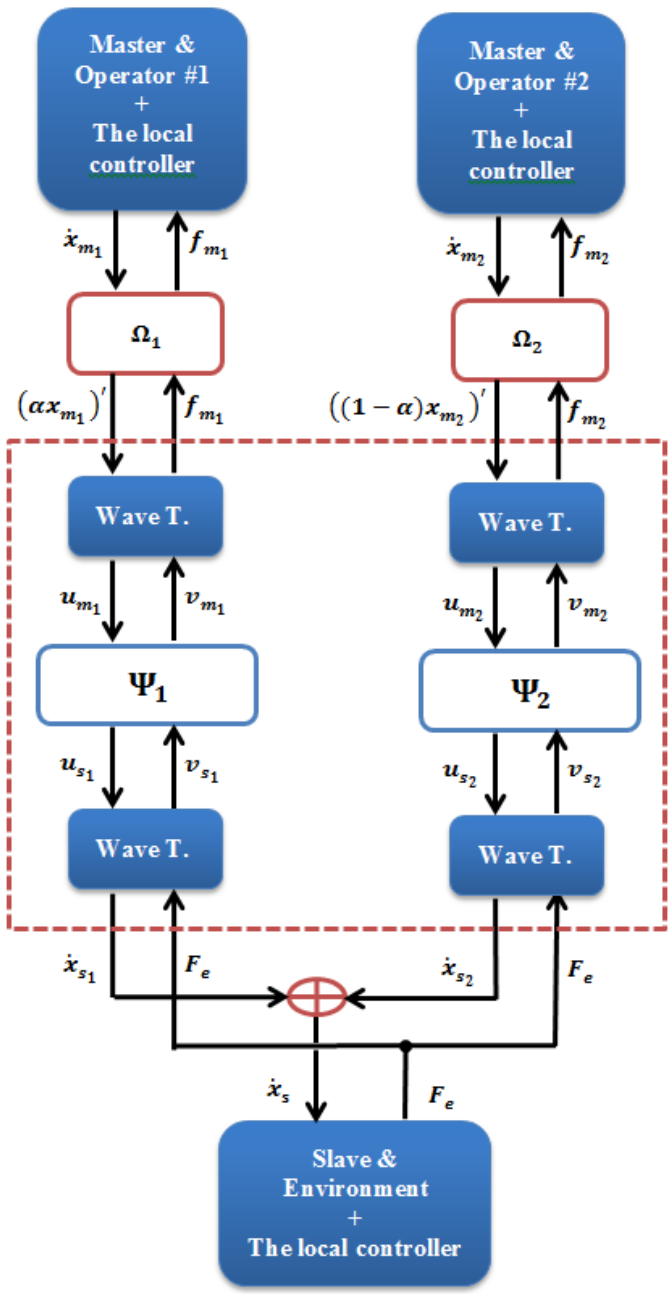

Figure 3.1: The overall scheme of the dual-user system focusing on the signals transmitted, where Wave T.s refers to the proposed wave transformations; Ψ_1 and Ψ_2 denote the communication channels between the master robots and the slave robot; $v_{m_1}(t) = v_{s_1}(t-T_1)$, $u_{s_1}(t) = u_{m_1}(t-T_1)$, $u_{s_2}(t) = u_{m_2}(t-T_2)$, $v_{m_2}(t) = v_{s_2}(t-T_2)$, where T_1 and T_2 are the constant time delays in Ψ_1 and Ψ_2 respectively. Ω_1 and Ω_2 illustrate two sub-systems transforming x_{Ω_i} to y_{Ω_i}, $i = 1,2$, as elaborated below in (3.20) and (3.21).

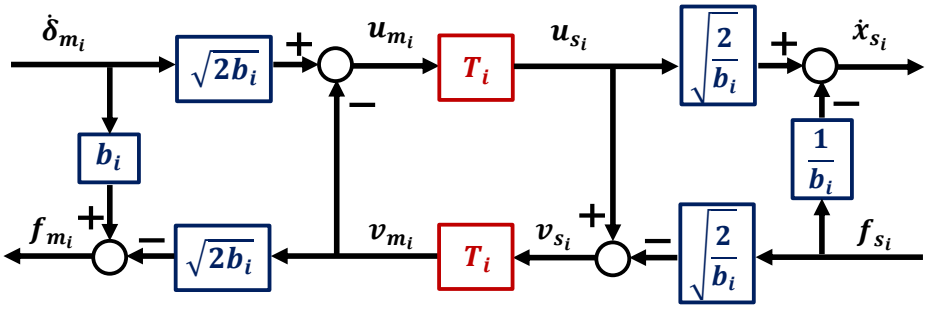

Figure 3.2: Network connection of the simplified wave transformation for communication channel Ω_i $(i = 1,2)$ given in (3.18) and (3.19), which is in the form of the conventional wave transformation.

$$\begin{cases} x_{\Omega_1}(\tau) = \left[\frac{d}{d\tau}x_{m_1}(\tau) \;\; f_{m_1}(\tau)\right] \\ y_{\Omega_1}(\tau) = \left[\frac{d}{d\tau}\alpha x_{m_1}(\tau) \;\; f_{m_1}(\tau)\right] \end{cases} \tag{3.20}$$

$$\begin{cases} x_{\Omega_2}(\tau) = \left[\frac{d}{d\tau}x_{m_2}(\tau) \;\; f_{m_2}(\tau)\right] \\ y_{\Omega_2}(\tau) = \left[\frac{d}{d\tau}(1-\alpha)x_{m_2}(\tau) \;\; f_{m_2}(\tau)\right] \end{cases} \tag{3.21}$$

Consequently, for passivity of Ω_1 and Ω_2, it is required, for $i = 1,2$, to have:

$$\Xi_{\Omega_i}(t) = \int_0^t \left(x_{\Omega_i}^T(\tau).y_{\Omega_i}(\tau)\right) d\tau \geq 0 \tag{3.22}$$

which can be rewritten as:

$$\Xi_{\Omega_i}(t) = \int_0^t \left(x_{m_i}^{'}(\tau).\left(\alpha_i(\tau).x_{m_i}(\tau)\right)^{'} + f_{m_i}(\tau).f_{m_i}(\tau)\right) d\tau \geq 0 \tag{3.23}$$

where $\alpha_i = \begin{cases} \alpha & i = 1 \\ 1-\alpha & i = 2 \end{cases}$.

Therefore, for passivity of Ω_i, it is enough to have: $\int_0^t \left[x_{m_i}^{'}(\tau).\left(\alpha_i(\tau).x_{m_i}(\tau)\right)^{'}\right] d\tau \geq 0$, which can be straightforwardly shown by the assumption of slow variation profile for α_i. Therefore, by the assumption of passivity of the environment and the operators, and also by ensuring passivity of both Ω_1 and Ω_2, as well as passivity of the overall communication channel in-

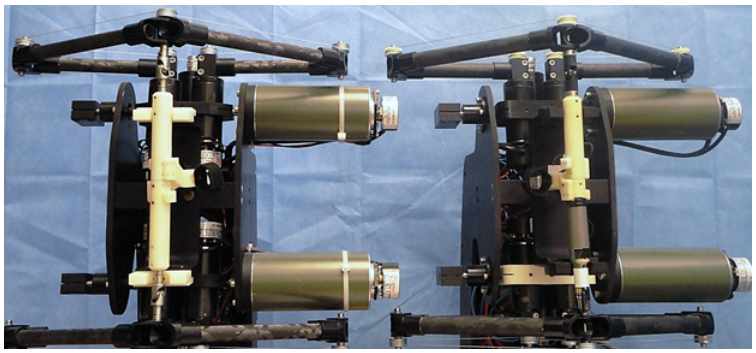

(a) Customized Quanser haptic wands.

(b) Mitsubishi PA10-7C slave robot.

Figure 3.3: The experimental setup.

cluding the wave transformations, shown by the red dashed line in Fig. 3.1, it follows that the entire closed-loop system remains passive, and hence stable in the presence of a time-varying dominance factor and constant time delays.

3.5 Experimental Results

In this section, experimental results are given to demonstrate the validity of the proposed scheme. The experimental setup, as shown in Fig. 3.3, consists of two customized Quanser Haptic Wands as the master robots and one Mitsubishi PA10-7C robot with a rod as the operation tool attached at the tip as the slave robot. An ATI Gamma six-DOF force sensor has been mounted between the wrist of the PA10-7C robot and the rod to measure the environment force exerted at the tool tip. The User Datagram Protocol is used to transmit data between the master robots and the slave robot. The manipulators' controllers and the communication are implemented at a sampling frequency of 1kHz [27].

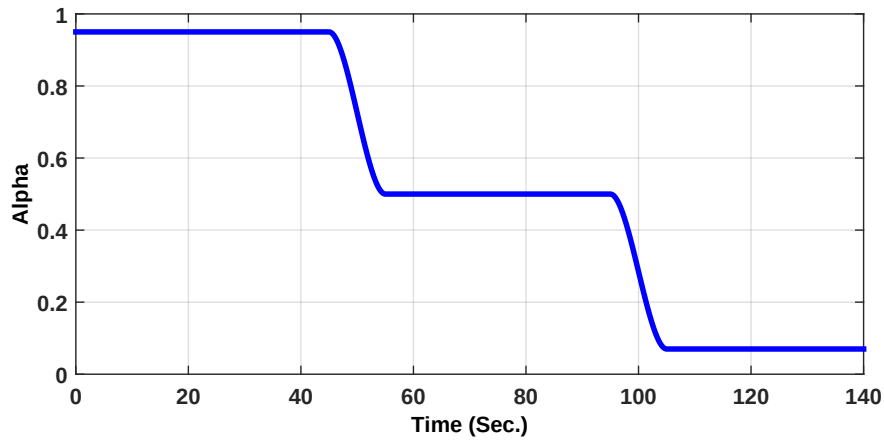

Figure 3.4: Time-varying dominance factor α used in the experiment.

In the conducted experiments, the communication channels had constant time-delays as follow: $T_1 = 140ms$, $T_2 = 110ms$. In addition, the dominance factor α was designed to change according to Fig. 3.4. As can be seen, between $t = 0s$ and $t = 45s$ the dominance factor was set to 0.95 which refers to high authority of operator #1 where operator #2 had authority of $1 - \alpha = 0.05$. Between $t = 45s$ and $t = 55s$ the dominance factor started to decrease to 0.5 and had the value of 0.5 till $t = 95s$. Therefore, between $t = 55s$ and $t = 95s$, $\alpha = 1 - \alpha = 0.5$ which refers to equal authority of both operators over the task. At $t = 95s$, the dominance factor α started to decrease and reached to the value 0.05 at $t = 105s$ and kept its value until $t = 140s$. Between $t = 105s$ and $t = 140s$, operator #1 had her lowest authority level from the beginning of the experiment, while operator #2 had his maximum authority over the task. To include in-contact motions in the experiment, a silicone tissue phantom was placed at $x_s > 0$. Fig. 3.5 shows the experimental results.

As can be seen in Fig. 3.5a, between $t = 0s$ and $t = 45s$, the slave robot is mostly guided by operator #1 who had the most level of authority. Although operator #2 moved his hand totally differently from operator #1, he was unable to skew the slave robot motion due to his low authority over the task. It should be noted that, between $t = 20s$ and $t = 40s$ where the slave robot was in contact with tissue, it did not completely track the position of master #1 although operator #1 had the full authority. This tracking error is due to existence of the tissue which did not allow the slave robot to move further along $x_s \geq 0$. Consequently, as shown in Fig. 3.5b, the environment force increased and was reflected back to operators' hands. After $t = 45s$, the

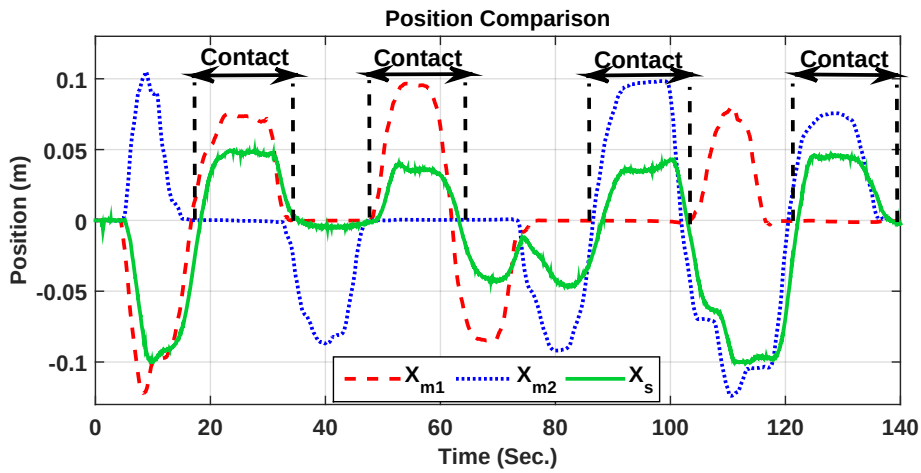

(a) Position comparison.

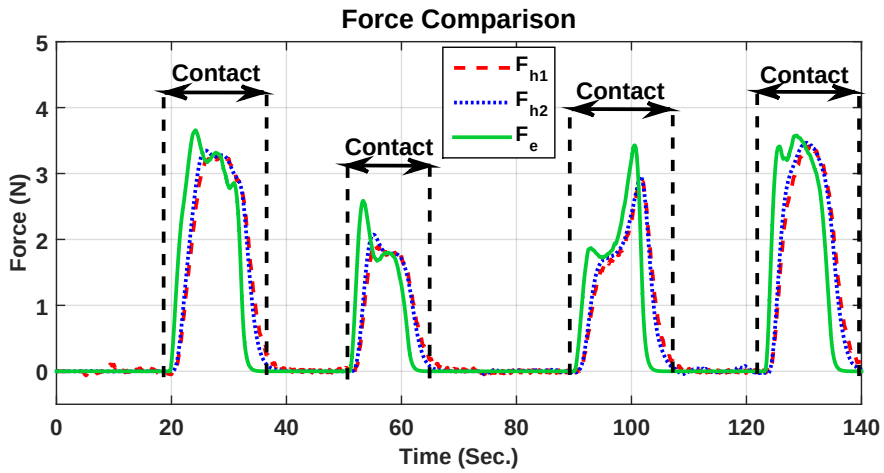

(b) Force comparison.

Figure 3.5: Experimental results in the presence of time delays.

dominance factor α started to decrease and reached to 0.5 at $t = 55s$. As can be seen in Fig. 3.5a, although operator #1 generated larger motions inside the tissue in this time interval, the slave robot moved less inside the tissue comparing with the first in-contact motion. This is due to the decrease of operator #1's authority, α, and increase of operator #2's, $1-\alpha$. Therefore, with regard to the fact that operator #2 was keeping his master robot at $x_s = 0$, a smaller motion was generated for the slave robot. Consequently, since the slave robot moved less inside the tissue, less environment force was generated compared to the previous in-contact motion, as shown in Fig. 3.5b.

Between $t = 55s$ and $t = 95s$, both operators had equal authority $(\alpha = 1-\alpha = 0.5)$ and consequently they both had equal impacts on the slave robot. As shown in Fig. 3.5a, the slave robot tracked the α-based combination of the master robots position, which is their average in that time interval. At $t = 95s$, the dominance factor α started to decrease and reached to 0.05 at $t = 105s$ and kept its value till $t = 140s$. Fig. 3.5a, shows that the authority of operator #1 over the slave robot started to decrease, where after $t = 105s$ her authority over the task is totally removed. Consequently, at the last phase of the experiment, the slave robot was manipulated by operator #2 regardless of the motions generated by operator #1.

During the experiment, whenever the slave robot was guided inside the tissue, the environment force increased and was reflected back to both operators' hands (Fig. 3.5b). Consequently, both operators experienced good transparency irrespective of their authority level over the task.

It is noteworthy that, the variation profile of the dominance factor was designed just to evaluate the controller performance at different levels of authority. In an actual task, the dominance factor should be adjusted systematically with regard to various parameters specific to the task. For example, in a training application, the dominance factor adjustment should include quantified expertise levels of the trainee over the task in an online fashion. A systematic design of the profile variation for the dominance factor with regard to the application will be the focus of our future work.

3.6 Conclusions

In order to have a mechanism for transferring authority from a therapist (expert surgeon) to a patient (trainee) and vice versa, the dominance factor needs to be changed online during the procedure. The adjustment mechanism of the dominance factor could include various parameters such as the expertise level of the trainee. This chapter addressed the problem of including a time-varying dominance factor in a dual-user system. A wave-variable-based controller was presented to guarantee system stability in the presence of the time-varying dominance factor, while the communication channels had constant time delays. By applying passivity theory, it was shown that the wave-transformation-based approach makes the communication channels passive, which ensures stability of the dual-user system. Validity of the controller was demonstrated by experimental results.

Similar to other passivity-based approaches, the proposed wave-variable methodology is primarily developed for velocity-force domain, due to the well-known passivity assumption for the human arm in this domain. However, the framework is straightforwardly extendable to position-force domain, provided that the human-arm terminal also remains passive in this domain. Unlike velocity-force domain passivity of the human arm, position-force domain passivity has not been studied in the literature. Therefore, the next chapter investigates passivity of the human arm in position-force domain through mathematical analysis, experimentation and statistical user studies.

Bibliography

[1] K. Hashtrudi-Zaad and S. E. Salcudean, "Analysis of control architectures for teleoperation systems with impedance/admittance master and slave manipulators," *The International Journal of Robotics Research*, vol. 20, no. 6, pp. 419–445, 2001.

[2] K. Hashtrudi-Zaad, F. Mobasser, and S. Salcudean, "Transparent implementation of bilateral teleoperation controllers under rate mode," in *Proceedings of the American Control Conference*, vol. 1. IEEE, 2003, pp. 161–167.

[3] D. A. Lawrence, "Stability and transparency in bilateral teleoperation," *IEEE Transactions on Robotics and Automation*, vol. 9, no. 5, pp. 624–637, 1993.

[4] P. F. Hokayem and M. W. Spong, "Bilateral teleoperation: An historical survey," *Automatica*, vol. 42, no. 12, pp. 2035–2057, 2006.

[5] M. Shahbazi, H. Talebi, and F. Towhidkhah, "A robust control architecture for dual user teleoperation system with time-delay," in *36th Annual Conference on IEEE Industrial Electronics Society*. IEEE, 2010, pp. 1419–1423.

[6] M. Shahbazi, H. A. Talebi, S. F. Atashzar, F. Towhidkhah, R. V. Patel, and S. Shojaei, "A novel shared structure for dual user systems with unknown time-delay utilizing adaptive impedance control," in *IEEE International Conference on Robotics and Automation*. IEEE, 2011, pp. 2124–2129.

[7] B. Chebbi, D. Lazaroff, and P. X. Liu, "A collaborative virtual haptic environment for surgical training and tele-mentoring," *International Journal of Robotics & Automation*, vol. 22, no. 1, p. 69, 2007.

[8] S. S. Nudehi, R. Mukherjee, and M. Ghodoussi, "A shared-control approach to haptic interface design for minimally invasive telesurgical training," *IEEE Transactions on Control Systems Technology*, vol. 13, no. 4, pp. 588–592, 2005.

[9] S. Sirouspour and P. Setoodeh, "Adaptive nonlinear teleoperation control in multi-master/multi-slave environments," in *IEEE Conference on Control Applications*. IEEE, 2005, pp. 1263–1268.

[10] P. Malysz and S. Sirouspour, "Dual-master teleoperation control of kinematically redundant robotic slave manipulators," in *IEEE/RSJ International Conference on Intelligent Robots and Systems*. IEEE, 2009, pp. 5115–5120.

[11] B. Khademian and K. Hashtrudi-Zaad, "Novel shared control architectures for enhanced users' interaction in haptic training simulation systems," in *IEEE/RSJ International Conference on Intelligent Robots and Systems*. IEEE, 2009, pp. 886–892.

[12] ——, "A robust multilateral shared controller for dual-user teleoperation systems," in *2008 Canadian Conference on Electrical and Computer Engineering*, 2008.

[13] H. I. Krebs and N. Hogan, "Therapeutic robotics: A technology push," *Proceedings of the IEEE*, vol. 94, no. 9, pp. 1727–1738, 2006.

[14] M. Shahbazi, S. F. Atashzar, and R. V. Patel, "A dual-user teleoperated system with virtual fixtures for robotic surgical training," in *IEEE International Conference on Robotics and Automation*. IEEE, 2013, pp. 3639–3644.

[15] G. Niemeyer and J.-J. E. Slotine, "Telemanipulation with time delays," *The International Journal of Robotics Research*, vol. 23, no. 9, pp. 873–890, 2004.

[16] L. Sciavicco and B. Siciliano, *Modelling and control of robot manipulators*. Springer Science & Business Media, 2012.

[17] A. Shahdi and S. Sirouspour, "Adaptive/robust control for time-delay teleoperation," *IEEE Transactions on Robotics*, vol. 25, no. 1, pp. 196–205, 2009.

[18] M. Shahbazi, S. Atashzar, H. Talebi, and R. Patel, "A multi-master/single-slave teleoperation system," in *ASME 2012 5th Annual Dynamic Systems and Control Conference joint with the JSME 2012 11th Motion and Vibration Conference*. American Society of Mechanical Engineers, 2012, pp. 107–112.

[19] S. Cotin, N. Stylopoulos, M. Ottensmeyer, P. Neumann, D. Rattner, and S. Dawson, "Metrics for laparoscopic skills trainers: the weakest link!" in *Medical Image Computing and Computer-Assisted Intervention—MICCAI*. Springer, 2002, pp. 35–43.

[20] J. E. Colgate, "Robust impedance shaping telemanipulation," *IEEE Transactions on robotics and automation*, vol. 9, no. 4, pp. 374–384, 1993.

[21] R. J. Anderson, "Smart: A modular architecture for robotics and teleoperation," in *IEEE International Conference on Robotics and Automation*. IEEE, 1993, pp. 416–421.

[22] C. A. Desoer and M. Vidyasagar, *Feedback Systems: Input-Output Properties*. Academic Press, 1975.

[23] R. Lozano, B. Brogliato, O. Egeland, and B. Maschke, *Dissipative Systems Analysis and Control. Theory and Applications*. IOP Publishing, 2001.

[24] Y. Ye and P. X. Liu, "Improving trajectory tracking in wave-variable-based teleoperation," *IEEE/ASME Transactions on Mechatronics*, vol. 15, no. 2, pp. 321–326, 2010.

[25] V. Răsvan, S.-I. Niculescu, and R. Lozano, "Input-output passive framework for delay systems," in *IEEE Conference on Decision and Control*, vol. 3. IEEE, 2000, pp. 2823–2828.

[26] A. vd Schaft and A. Schaft, "L2-gain and passivity in nonlinear control," 1999.

[27] A. Talasaz, "Haptics-enabled teleoperation for robotics-assisted minimally invasive surgery," Ph.D. dissertation, The University of Western Ontario, 2012.

Chapter 4

Position-Force Domain Passivity of Human Arm in Telerobotics Systems

The material presented in this chapter has been submitted for publication in the International Journal of Robotics Research (IJRR): Special Issue on Human-Robot Interaction, 2016.

4.1 Introduction

Teleoperation extends an operator's sensing and manipulation capabilities to a remote location. It facilitates off-site robotic performance of a desired task through a user console, and ensures cost-effectiveness, safety and accessibility. Teleoperation systems have been broadly used in a wide range of applications from mining to space and underwater exploration to robotics-assisted minimally invasive surgery [1], [2], robotic surgical training [3, 4], and robotics-assisted rehabilitation therapy [5], [6], [7].

A teleoperation system consists of three main components: 1) A slave robot, performing a desired task on a designated environment, 2) a master console manipulated by an operator, remotely controlling the slave console; and 3) a communication channel to transmit data between the master and the slave [8]. Fig. 4.1 shows the overall scheme of a single-master/single-slave teleoperation system, in which teleoperator refers to the set of communication channels integrated with the master and the slave robots. Long-distance communication can introduce time delays into the system, which can cause instability [9]. To ensure robust stability of

Figure 4.1: The overall scheme of a teleoperation system. The teleoperator includes the communication channel as well as the master and the slave robots. $U = [u_1, u_2]$ and $Y = [y_1, y_2]$ refer to the input and output of the teleoperator, respectively.

the system against communication delays in order to guarantee safe human-robot interaction, passivity-based control methodologies have been developed building on the following passivity theorems:

Theorem I: *A system is passive if it consists solely of passive elements [9].*

Definition I: *A general time-varying n-port network with zero initial energy storage is passive if [10], [11]:*

$$\varepsilon(t) = \int_0^t U^T(\tau) \,.\, Y(\tau) \, \mathrm{d}\tau \geq 0 \tag{4.1}$$

where $U \in R^n$ and $Y \in R^n$ correspond to the input and output of the network, respectively.

Based on *Theorem I* and by the assumption of passivity of the operator and the environment [12], the only element to make passive is the teleoperator (which is equivalent to making the communication channel passive), for which several methodologies have been introduced in the literature. These approaches can be classified into two main categories: 1) Time Domain Passivity Controller (TDPC) [13], [14], and 2) Frequency Domain Passivity Controller (FDPC), which includes Scattering Matrix [9] and Wave Variables [15] approaches.

According to *Definition I*, passivity of a general system can be analyzed based on the input and output of the system, regardless of their nature. In the teleoperation systems literature, all of the existing approaches have addressed the passivity of the communication channel (and therefore, the passivity of the teleoperator) by considering the input-output pair to be velocity and force signals. This has imposed the limitation of having to transmit the velocity signal from the master side to the slave side, rather than transmitting the position signal. Transmission of the velocity signal causes position-error accumulation and position drift, which considerably degrades the position tracking performance of the system [13].

Several techniques have been proposed in the literature in order to address the position drift caused by the FDPCs [16], [17], [18], and a few methods were recently proposed to compensate

for the position drift in TDPC systems [13], [19]. However, these approaches, which mostly modify the conventional passivity controllers, have been mainly developed for addressing the position drift in bilateral Single-Master/Single-Slave (SM/SS) teleoperation systems, and are not straightforwardly applicable to a Multi-Master/Single-Slave (MM/SS) framework, due to the topographical complexities of MM/SS platforms. MM/SS systems have been shown to be useful in supervised robotics-assisted surgical training [3], [4] and rehabilitation [20], [21], where an expert surgeon/therapist can be directly involved in the procedure based on haptic interaction with a trainee/patient. According to a recent study [22], haptics-based interaction with a partner when learning a motor task considerably enhances motor skills compared to when practicing the task alone for the same duration.

Considering the mathematics behind most of the *conventional* passivity controllers proposed in the literature for SM/SS systems, which is fundamentally based on (4.1), the same controller that makes the communication channel passive for the input-output pair of force and velocity (i.e., velocity-force domain) can also make the communication channel passive for the input-output pair of force and position (i.e., position-force domain). This immediately addresses the position-drift issue and may be straightforward to apply to more complex framework such as MM/SS. Although using a Position-force Domain (PD) controller to make the communication channel passive is possible through the existing passivity-based approaches, according to Fig. 4.1, it necessitates the connection terminal of the operator-teleoperator to also remain passive in the position-force domain in order to comply with *Theorem I*. For this purpose, passivity of the operator terminal in the position-force domain, however, is a critical question to be investigated. In fact, passivity of the operator in the velocity-force domain seems to be the main reason behind the development of all the passivity-based controllers to date in the Velocity-force Domain (VD). While there have been a number of studies on the numerical measurement of the endpoint impedance of the arm [23], [24], [25], there are very few studies on PD Passivity (PDP) of the operator. In [26], PD passivity of the human arm was assessed through numerical measurement of the endpoint impedance of the arm. The assessment has been performed over a limited range of frequency and does not discuss the frequency-dependence of PD passivity.

Therefore, in order to facilitate PDP controllers for teleoperation systems regardless of the

complexity of the framework and the number of master and slave robots involved, the main question to answer is whether the operator is passive in the position-force domain as well; and if not, what measures should be taken in order to make the operator termination passive. Consequently, in this chapter, the PDP of the human operator has been investigated through mathematical and experimental analyses as well as statistical user studies involving 12 subjects and 48 trials. It has been shown that, unlike in VD, the operator will not remain passive in PD for all frequency ranges; This implies the need for appropriate control strategies to make the human operator termination passive in PD. For future design of suitable controllers, statistical analyses are conducted to investigate the possible correlation between the levels of PD passivity of the left and right arms of the human participants, and the levels of passivity of the subjects' arms and their physical characteristics, e.g., weight, height, and body mass index. Possible control strategies through which the passivity of the operator termination can be ensured are also discussed.

The rest of the chapter is organized as follows: Section 4.2 analyzes passivity of the operators in PD, mathematically. Section 4.3 gives experimental results in support of the mathematical analysis. Section 4.4 discusses the user trials on humans, and statistically analyzes PD passivity as well as correlations between the subjects' physical features and passivity levels of their arms. Section 4.5 suggests possible control approaches to ensure the PDP of the operator termination, and Section 4.6 concludes the chapter.

4.2 Mathematical Analysis

The dynamics of the human arm can be modeled by a second-order system [27]:

$$M_h\ddot{x}_h(t) + B_h\dot{x}_h(t) + K_h(x_h(t) - x_{h_e}) = f_h(t) \tag{4.2}$$

Here, f_h refers to the force applied to the arm endpoint, x_h is the hand position, and x_{h_e} is the hand equilibrium position commanded by the central nervous system. In addition, M_h, B_h and K_h denote the constant real-valued inertia, damping and stiffness of the arm.

By the change of variables $x = x_h - x_{h_0}$, (4.2) is transformed to:

$$M_h\ddot{x}(t) + B_h\dot{x}(t) + K_h x(t) = f_h(t) \tag{4.3}$$

where x refers to the displacement with respect to the equilibrium point x_{h_0}. Taking the Laplace transform of (4.3) yields

$$(M_h s^2 + B_h s + K_h)X(s) = F_h(s) \tag{4.4}$$

where $F_h(s) = \mathscr{L}\{f_h(t)\}$ and $X(s) = \mathscr{L}\{x(t)\}$, in which $\mathscr{L}$ and s indicate the Laplace operator and the Laplace variable, respectively.

Continuing the analysis in one Degree-Of-Freedom (DOF) in the interest of simplicity and without loss of generality, the admittances of the human arm in the position-force domain, $Y_P(s)$, and in the velocity-force domain, $Y_V(s)$ can be written as follows:

$$Y_P(s) = \frac{X(s)}{F_h(s)} = \frac{1}{M_h s^2 + B_h s + K_h} \tag{4.5}$$

$$Y_V(s) = \frac{V(s)}{F_h(s)} = \frac{s}{M_h s^2 + B_h + K_h} \tag{4.6}$$

where $V(s) = \mathscr{L}\{v(t)\}$ and $v(t) = \dot{x}(t)$.

In order for a transfer function $G(s)$ to represent a passive system, $G(s)$ must be Positive Real (PR) [28] as defined below:

Theorem II: A rational transfer function $G(s)$ is PR if and only if [29]:

1. $G(s)$ does not have poles in the open right half plane,

2. All poles of $G(s)$ on the imaginary axis are simple, and the associated residues are real and non-negative,

3. $G(j\omega) + G(-j\omega) \geq 0$, for all $\omega \geq 0$.

With M_h, B_h and K_h having positive values, both $Y_V(s)$ and $Y_P(s)$ satisfy the first two PR conditions. Investigating the third condition for $Y_V(s)$ in order to investigate the positive-realness

and therefore the passivity of the human arm in the velocity-force domain yields:

$$Y_V(j\omega)+Y_V(-j\omega)=\frac{2B_h\omega^2}{(K_h-M_h\omega^2)^2+(B_h\omega)^2}\geq 0 \tag{4.7}$$

which is always true, as B_h refers to a positive-valued damping term. Therefore, $Y_V(s)$ satisfies the third PR condition as well, which implies the passivity of the human arm with respect to the force-velocity input-output pair. This is completely in agreement with the literature, where the human arm has been considered as a passive system for force-velocity interactions [12].

Investigating the same condition for $Y_P(s)$ leads to

$$Y_P(j\omega)+Y_P(-j\omega)=\frac{2(K_h-M_h\omega^2)}{(K_h-M_h\omega^2)^2+(B_h\omega)^2}\geq 0 \tag{4.8}$$

which is dependent not only on K_h and M_h, but also on the frequency w, and is not true for $\omega>\omega_n=\sqrt{\frac{K_h}{M_h}}$. Therefore, unlike in the velocity-force domain, the human arm does not remain passive in the position-force domain for all frequency ranges.

Remark: *Giving the analysis in one DOF does not affect generality, as the above serves as an counterexample to show the non-passivity of the operator in the position-force domain. The same applies to the second-order model considered for the human arm. Although this model is a simplified model of the human arm's neuro-musculoskeletal structure as detailed in [27], it can still show the position-force domain non-passivity of the human arm as opposed to the velocity-force domain, even for the simplest model.*

What can be inferred from (4.8) is that increased stiffness of the arm can contribute to the passivity of the arm in the position-force domain, while the arm's inertia has an active effect. Moreover, the higher the motion frequency, the higher the possibility of non-passivity. In order to investigate these hypotheses, experiments were conducted as described in the following section.

4.3 Experimental Analysis

In order to investigate the passivating or non-passivating effect of inertia, stiffness and motion frequency, experiments were conducted. The experimental setup, shown in Fig. 4.2, consists of an adjustable custom-built Mass-Spring Array (MSA) connected to a 2-DOF planar Quanser rehabilitation robot (Quanser Consulting Inc., Markham, ON, Canada). The capstan drive mechanism of the Quanser rehabilitation robot makes it back-drivable with low friction and inertia. The robot is capable of exerting forces up to 50 N throughout its semicircular workspace, and the motors encoders provide a resolution of better than 0.002 mm in Cartesian space [26]. The modular structure of the MSA allows us to add external mass and spring elements to examine the effect of various inertia/stiffness values. During the experiments conducted in three scenarios, the MSA's end-point was perturbed by the robot using the following Persistently Exciting (PE) perturbation:

$$P = 0.0025.\sum_{k=1}^{4}\sum_{j=1}^{3} sin(\frac{\omega_i t}{k}) \tag{4.9}$$

where $\omega_1 = 1.2\pi$, $\omega_2 = 2\pi$, and $\omega_3 = 3\pi\ \frac{rad}{s}$. The position of the MSA's endpoint, x_{MSA}, and the force applied to the MSA, f_{MSA}, were measured in 2 Cartesian directions along X and Y axes. In order to measure f_{MSA}, an ATI Gamma force sensor (ATI Industrial Automation Inc., Apex, NC, USA) was placed between the robot's End-Effector (EE) and the MSA. The force sensor has a resolution of 0.0125 N and maximum measurable force of 65 N along X-Y axes. Since the robot's EE was in contact with the MSA's end-point, the position and velocity of the robot's EE captured by applying forward kinematics to the robot's joint positions reading served as those of the MSA's end-point (x_{MSA} and v_{MSA}).

The PD passivity of the MSA system in each experimental trial was investigated using *Definition I* with respect to force-position input-output pair by checking if:

$$\varepsilon_{PD}(t) = \int_0^t x_{MSA}^T(\tau)\ .\ f_{MSA}(\tau)\ \mathrm{d}\tau \geq 0 \tag{4.10}$$

The expression "passivate" has been used as a synonym for "make passive".

Note that MSA was relaxed at $t = 0$, so the initial energy was zero, and therefore the passivity condition given in (4.10) was checked with the right-hand side being zero.

4.3.1 Experimental Scenario I

The first experiment was conducted for a series of mass values, namely, $m_1 = m_0$, $m_2 = m_0 + 230gr$, $m_3 = m_0 + 460gr$, and $m_4 = m_0 + 690gr$ by adding masses to the system, with no springs added; $m_0 > 0$ refers to the mass of the handle between the force sensor and the MSA before adding any external mass to the MSA. Fig. 4.3 shows ε_{PD} calculated for the mass values. As can be seen in this figure, ε_{PD} for all m_i $(i = 1,2,3,4)$ has negative and decreasing value for all $t \geq 0$, which indicates non-passivity of the mass. As can also be seen in this figure, the heavier the mass, the more non-passive behavior it shows, which is in agreement with the mathematical analysis discussed in the previous section.

4.3.2 Experimental Scenario II

The second experiment investigates the effect of stiffness on passivity. For this purpose, stiffness elements were added to the same mass values m_i $(i = 1,2,3,4)$ as in previous scenario by adding a set of springs ($k_1 = 50,\ k_2 = 175,\ k_3 = 190,\ k_4 = 230\ \frac{N}{m}$) to the MSA. Fig. 4.4 shows

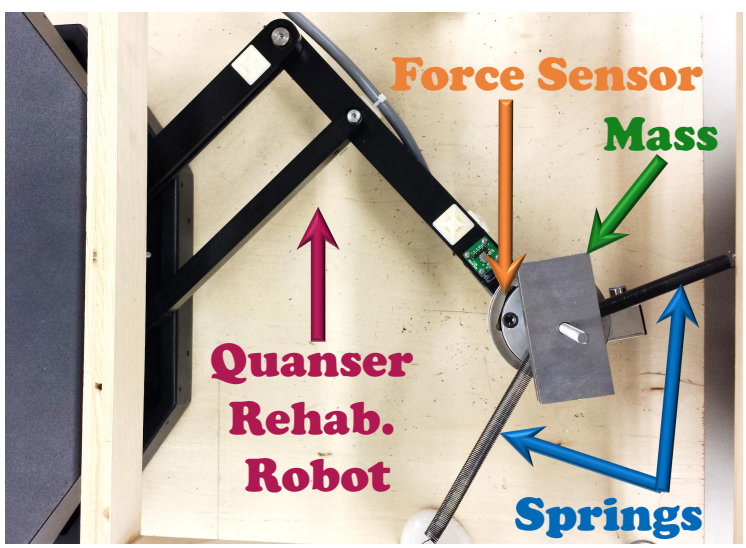

Figure 4.2: The mass-spring array system connected to the 2-DOF planar Quanser rehabilitation robot.

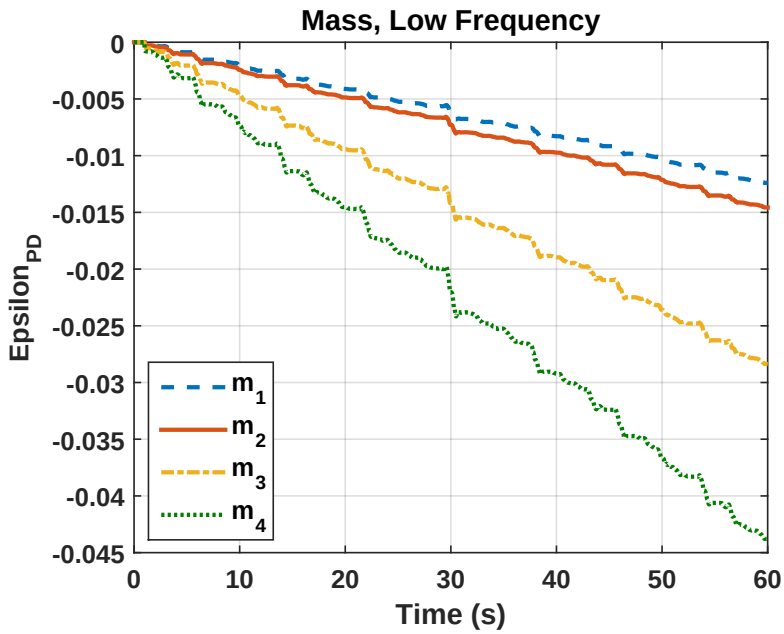

Figure 4.3: Experimental results: effect of inertia on ε_{PD}

ε_{PD} calculated for the sets of mass-spring elements. Comparing Fig. 4.4 with Fig. 4.3, the passivating effect of stiffness components as opposed to mass components can be seen. Although m_i $(i = 1,2,3,4)$ moves the system towards non-passivity (as shown in Fig. 4.3), adding stiffness can reverse the trend and make the system passive. This result is also in agreement with the PD passivity condition derived in the previous section.

4.3.3 Experimental Scenario III

Considering the passivity condition given in (4.8), in addition to mass and stiffness, motion frequency can also play an essential role in passivity of the arm in PD. Therefore, a third experiment is designed to examine the effect of the perturbation's frequency range. For this purpose, experimental scenario I has been repeated for the same circumstances, including the mass values, except for the frequency range of the perturbation signal. In this experiment, the perturbation given in (4.9) has been applied for $\omega_1 = 2\pi$, $\omega_2 = 6\pi$, and $\omega_3 = 10\pi \ \frac{rad}{s}$. Fig. 4.5 shows ε_{PD} calculated for the mass elements perturbed at higher frequencies. Comparing Figs. 4.3 and 4.5, it can be seen that, although the mass elements have shown non-passive behavior in both frequency ranges (experimental scenario I and III), the rate of non-passivity was considerably higher for the higher-frequency perturbation (experimental scenario III). In

60 seconds, ε_{PD} has reached from 0 to -0.045 for the low-frequency perturbation (Fig. 4.3), while during the same time ε_{PD} for the high-frequency perturbation has dropped from 0 to -1.54 (Fig. 4.3).

The experimental results in this section support the mathematical analysis given in Section 4.2. As verified in both Sections 4.2 and 4.3, stiffness can contribute towards passivity in PD, while mass and increased frequency work against passivity of the arm in the position-force domain. The analyses given in Sections 4.2 and 4.3 build upon the second-order model approximation for the human arm. Although the model is very popular in the literature and has been used to a large extent, there still might be a question of accuracy due to the unmodeled dynamics. To address concerns about the thoroughness of the model, a series of user trials has also been conducted as discussed in the following section.

4.4 User Trials and Statistical Analysis

In order to analyze the PD passivity of the human arm without forgoing the analysis accuracy as a result of possible model reduction/uncertainty in the previous section, user trials were conducted.

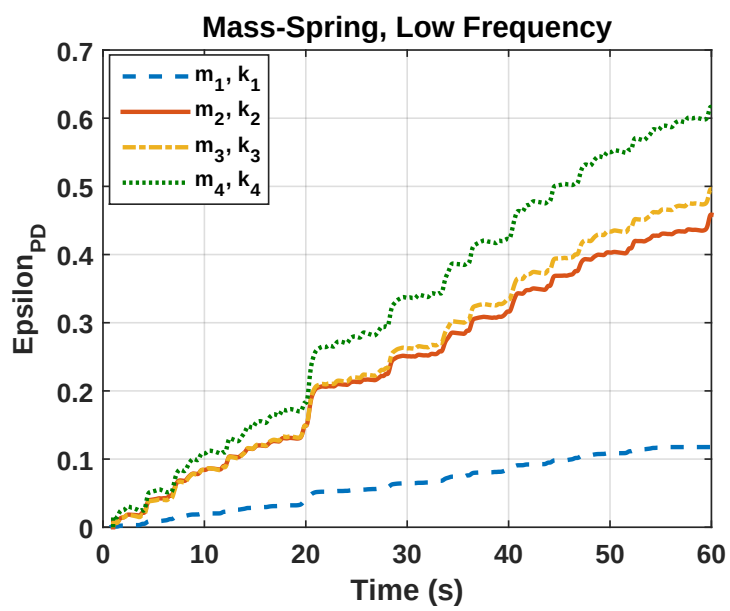

Figure 4.4: Experimental results: effect of stiffness on ε_{PD}

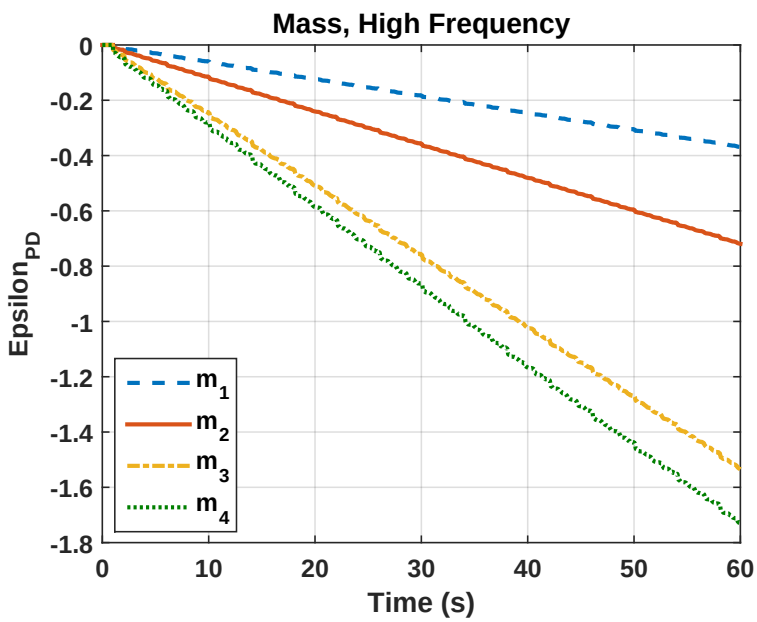

Figure 4.5: Experimental results: effect of motion frequency on ε_{PD}

4.4.1 Subjects

Twelve healthy subjects (5 women, 7 men; mean age, 29 years; age range, 26-40 years) were recruited. Data was collected for both left and right arms of the subjects, giving us 24 sets of data. Two participants were left-handed and 10 right-handed, all with no history of motor impairment. Demographics of all participants are presented in Table 4.1. All participants gave written informed consent to participate in the study. The study was approved by the Research Ethics Board (REB) at the University of Alberta.

4.4.2 Setup and Procedure

As illustrated in Fig. 4.6, each subject sat in front of a Quanser rehabilitation robot and grasped the robot's handle with their hand. They were asked to relax their arm and avoid voluntary intervention as the robot applied perturbations to their arm. All data was collected at test locations in which the subject's forearm formed a right angle with their upper-arm in the interest of consistency. Each trial was repeated four times for each subject, collecting force and position data on both right and left arms with two different frequency ranges of perturbations applied to each side for two minutes. The following PE position perturbation signals were applied to the

Table 4.1: Demographics for all participants

Subject Number	***Sex***	***Age (yr)***	***Handedness***
1	F	27	Right
2	M	27	Right
3	F	30	Right
4	M	28	Right
5	M	27	Left
6	F	28	Right
7	F	26	Left
8	M	28	Right
9	M	27	Right
10	M	40	Right
11	M	29	Right
12	F	26	Right

subject's hand in X and Y directions:

$$\begin{aligned} P_X &= 0.015.\sum_{k=1}^{4}\sum_{j=1}^{3} sin(\frac{\omega_i t}{k})sin(\theta t) \\ P_Y &= 0.015.\sum_{k=1}^{4}\sum_{j=1}^{3} sin(\frac{\omega_i t}{k})cos(\theta t) \end{aligned} \tag{4.11}$$

In (4.11), ω_1, ω_2, ω_3, θ are respectively set to 0, π, 2π and $0.55\pi\ \frac{rad}{s}$ for the lower range of perturbation frequencies, and to 3π, 6π, 12π and $0.35\pi\ \frac{rad}{s}$ for the higher range of perturbation frequencies. The low and high ranges of perturbation frequencies were selected based on a threshold calculated according to the natural frequency of a typical human arm. For this purpose, a stiffness of $K_h = 100\frac{N.s^2}{m}$ and a mass of $M_h = 1Kg$ [26] were considered in (4.2) leading to a natural frequency as $\omega_n = \sqrt{\frac{K_h}{M_h}} = 3.2\pi\frac{rad}{s}$. This shows natural frequency based on the mathematics derived in Section 4.2, may serve as the passivity/non-passivity threshold of the arm. The low-frequency signal was generated such that, while having a rich frequency content, its largest frequency remained below $3.2\pi\frac{rad}{s}$. The high-frequency perturbation signal was also generated such that it contained higher-than-threshold frequencies, while having

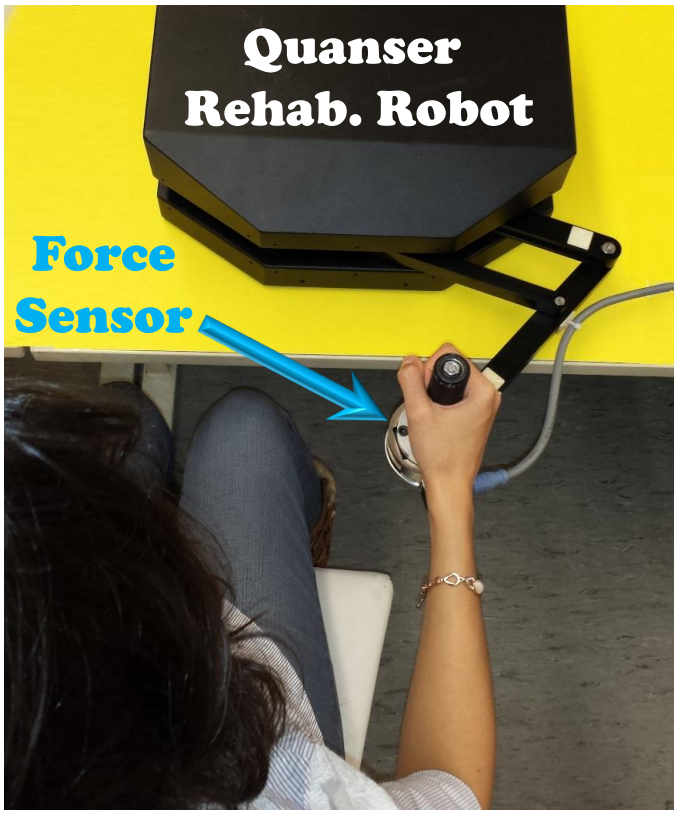

Figure 4.6: The experimental setup used in the user trials.

a rich frequency content.

Figs. 4.7 and 4.8 illustrate a 2-Dimentional (2D) $X-Y$ representation of the perturbation signals with low and high frequencies, respectively. Note that the two-dimensional perturbation would suffice for the analysis of the relative contributions of the shoulder, elbow, and biarticular muscles to the overall limb passivity/activity, without entailing the experimental complexity of a full multi-dimensional evaluation [26] and [23].

During the trials, the forces applied by the subject's hand to the robot's end-effector was measured using the ATI Gamma force sensor located at the robot's EE. The position of the robot's EE also served as the position of the subject's hand endpoint, as the subject were grasping the robot's handle. PD passivity of the subject's arm for each experimental trial was investigated using the general passivity criterion given in (4.1) with respect to force-position input-output pair by calculating $\varepsilon_{PD}(t) = \int_0^t x_h^T(\tau) \,.\, f_h(\tau)\, \mathrm{d}\tau$. It should be noted that using the general input-output-based criterion to investigate the system passivity eliminates any necessity for estimation of the human arm impedance parameters (mass, damping and inertia).

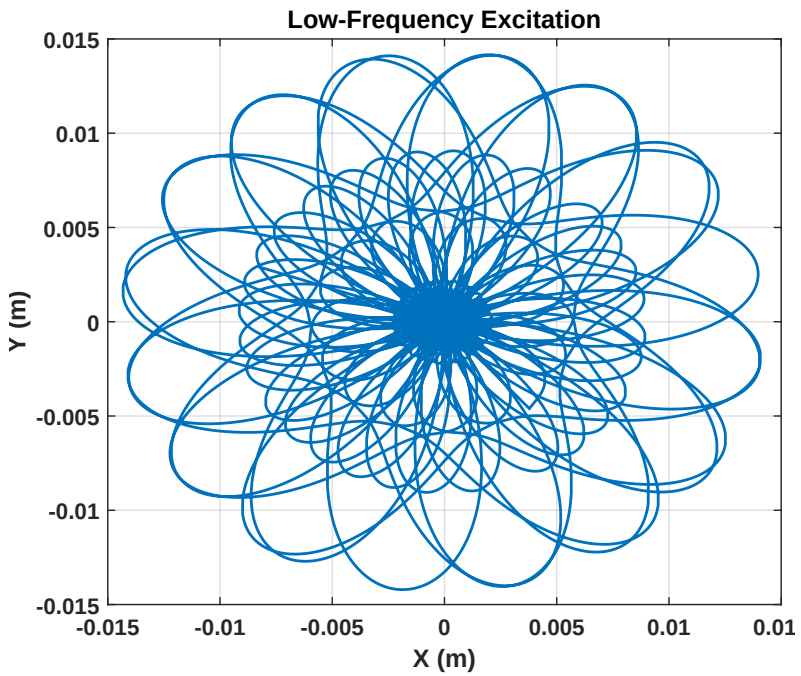

Figure 4.7: Low-frequency 2D X-Y position perturbation

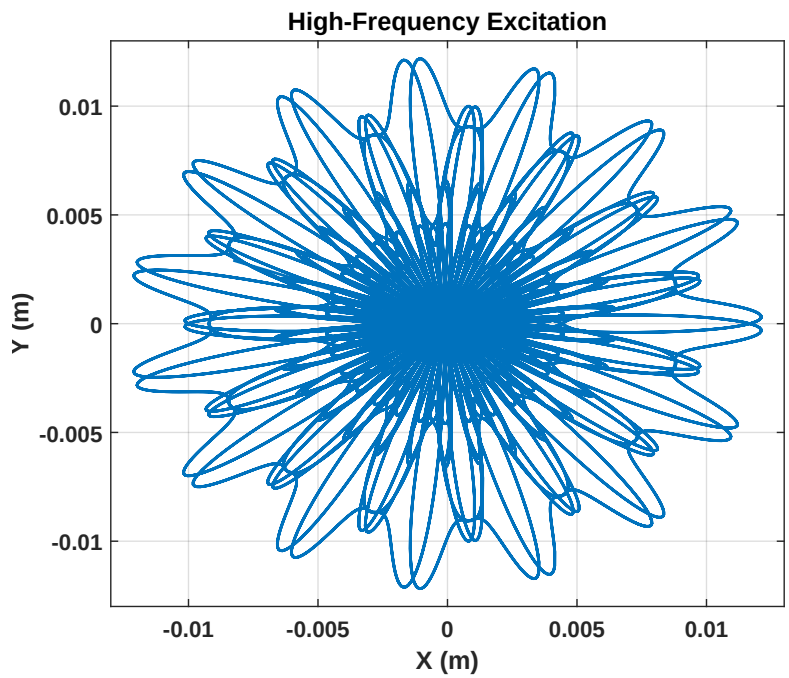

Figure 4.8: High-frequency 2D X-Y position perturbation

Due to its model-free nature, the input-output approach does not suffer from possible inaccuracies/uncertainties of various arm models.

4.4.3 Results

Figs. 4.9-4.12 illustrate ε_{PD} calculated for the subject during the following four sets of trials, respectively; 1) LH-LF: Left Hand, Low-Frequency perturbation; 2) RH-LF: Right Hand, Low-Frequency perturbation; 3) LH-HF: Left Hand, High-Frequency perturbation; and 4) RH-HF: Right Hand, High-Frequency perturbation.

Passivity/Non-passivity in Low-Frequency Trials

As it can be seen in Figs. 4.9 and 4.10, ε_{PD} remained positive for both right and left arms of the subjects during the low-frequency trials. This indicates passivity of the subjects' arms during the low-frequency trials. However, it can also be seen that subject #10 had a fluctuating ε_{PD} with growing oscillations, which could have caused negative ε_{PD} if the trials had lasted longer. Therefore, despite its positive ε_{PD}, we consider the behavior of subject #10 as non-passive. Oscillations can also be seen in the ε_{PD} calculated for subject #5 in the LH-LF trial and subjects #7 and #8 in the RH-LF trial. However, the damped nature of those oscillations eliminates the possibility of ε_{PD} getting non-passive in the long run.

In order to investigate the statistical significance of the result (passivity of the arm in low-frequency ranges), statistical analysis was conducted to illustrate that the high number of passive behaviors during RH-LF and LH-LF did not occur by chance. In this case, an occurrence possibility of 0.5 indicates equal chance of passivity/non-passivity for the subjects during the trials. Based on the high number of passive behaviors during RH-LF and LH-LF, we hypothesize the following:

Hypothesis: Low-frequency perturbations result in passive behavior for the human arm.

To evaluate this hypothesis, a binomial test was carried out to investigate whether the real probability of passive behavior during low-frequency perturbations is greater than 0.5. The binomial test statistically compared the number of successes (the number of passive behaviors during RH-LF and LH-LF trials, i.e., 22), observed in the total number of trials, i.e., 24, with a hypothesized probability of success (that is hypothesized to be greater than 0.5). Based on the aforementioned alternative hypothesis, the null hypothesis is defined as follows:

Null hypothesis: The real probability of passive behaviors in RH-LF and LH-LF trials is **not** greater than 0.5.

Using the binomial test, the null hypothesis is rejected with *p-value* equal to $1.794e-05$, which is well below 0.05, indicating that the true possibility of passive behavior during low-frequency perturbation is significantly greater than 0.5 (the probability of passivity as given by the binomial test is 0.9166). This implies passive behavior of the participants' arms in the presence of low-frequency perturbations.

Passivity/Non-passivity in High-Frequency Trials

Figs. 4.11 and 4.12 illustrate ε_{PD} calculated for left and right arms of the subjects during the high-frequency trials, i.e., RH and LH, respectively. As can be seen in these figures, ε_{PD} had a negative decreasing trend during all the high-frequency trials, except for the right arm of subject #9. This negative ε_{PD} along with its decreasing trend indicates non-passivity of the subjects. This results is in agreement with the mathematics derived in Section 4.2, which associates the higher chance of non-passivity to the higher range of movement frequencies.

The interesting point about the trend of ε_{PD} for subject #9 in the RH trial (Fig. 4.12) is that, although it has shown a passive behavior, the level of passivity has decreased considerably compared to that in the RL trial (Fig. 4.10). This also illustrates the non-passivating effect of the high-frequency perturbation on subject #9, although the perturbation frequency range has yet been low enough for his right arm to behave passively.

In order to investigate the statistical significance of the result (non-passivity of the arm in high-frequency ranges), statistical analysis was conducted to indicate that the high number of non-passive behaviors during RH and LH did not occur by chance. Similar to the previous case, an occurrence possibility of 0.5 indicates equal chance of passivity/non-passivity for the subjects, based on which the hypothesis is defined, as follows:

Hypothesis: High-frequency perturbations can result in non-passive behavior for the human arm.

A binomial test was carried out to evaluate this hypothesis by investigating whether the real probability of non-passive behavior during high-frequency perturbations is greater than 0.5. According to the above alternative hypothesis, the null hypothesis is defined as follows:

Null hypothesis: The real probability of non-passivity during the high-frequency perturbations is **not** greater than 0.5.

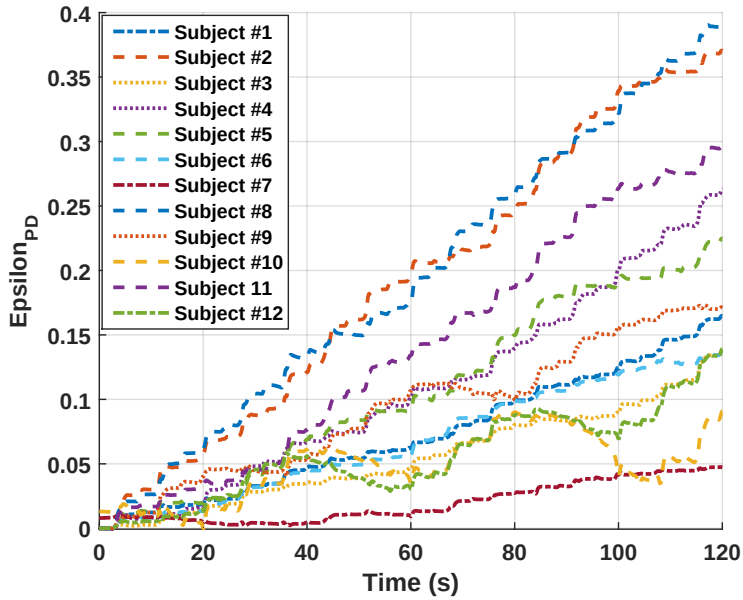

Figure 4.9: ε_{PD} for the left hand of all of the subjects recorded during low-frequency perturbation

Based on the results in Figs. 4.11 and 4.12, the number of successes (that is the number of non-passive behaviors, in this case) was set to 23. The total number of trials was set to 24 and the hypothesized probability of success was set to be greater than 0.5. Using the binomial test, the null hypothesis is rejected with *p-value* equal to $1.49e-06$, which is well below 0.05, indicating that the true possibility of non-passivity during high-frequency perturbation is significantly greater than 0.5 (The probability of non-passivity as given by the binomial test is 0.9583). This implies that the non-passive behavior of the participants' arms has not happened by chance, but as the result of the high-frequency perturbations.

Passivity/Non-passivity Correlation Between Left and Right Arms

Figs. 4.13 and 4.14 compare ε_{PD} for left and right arms of two of the subjects in low-frequency and high-frequency trials, respectively. In both frequency ranges, correlations can be seen between the level of passivity/non-passivity of each subject's left arm and right arm. The level of correlation from one person to another could vary based on the mechanical properties of the person's arms such as muscle density and strength. By looking at the results in Figs. 4.9-4.12, it can be seen that not all of the subjects have shown similar passivity/non-passivity behavior between their left and right arms. In order to investigate the possible correlation between their left

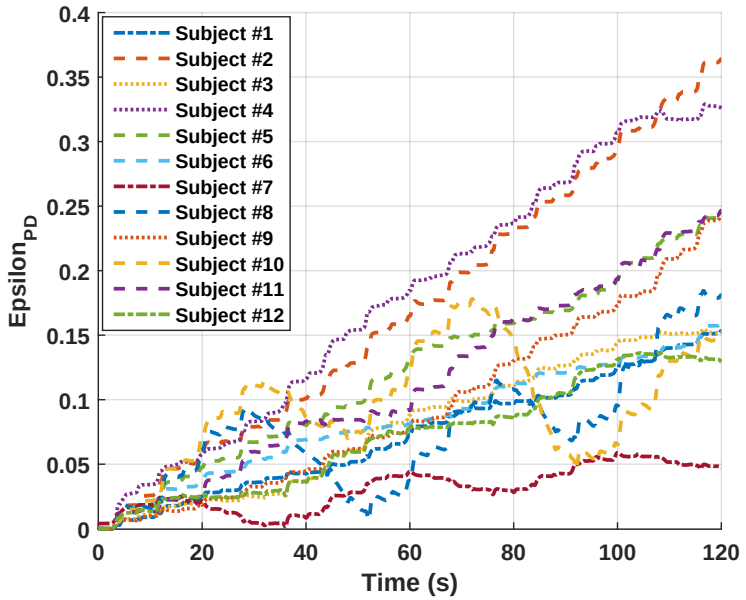

Figure 4.10: ε_{PD} for the right hand of all of the subjects recorded during low-frequency perturbation

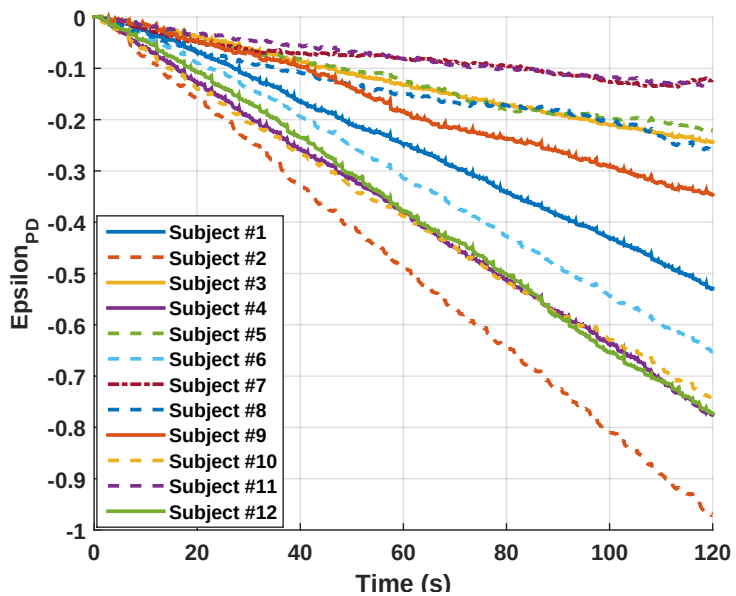

Figure 4.11: ε_{PD} for the left hand of all of the subjects recorded during high-frequency perturbation

and right arms, statistical analysis was carried out. For this purpose, the slope of ε_{PD} calculated for the subjects' arms was used as a metric to quantify the degree of passivity/non-passivity in subject's arms. In order to calculate the average slope of ε_{PD} for each subjects' arms, the linear least-squares curve-fitting method was applied. The slope of the fitted straight-line was

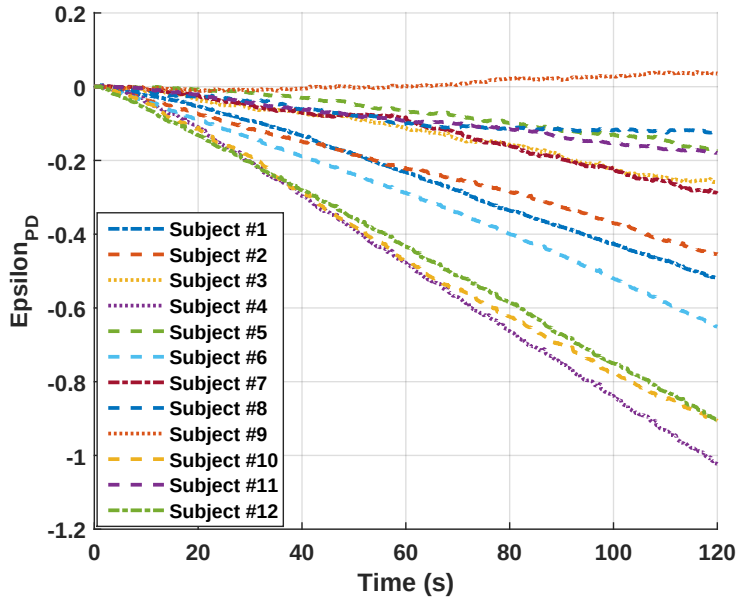

Figure 4.12: ε_{PD} for the right hand of all of the subjects recorded during high-frequency perturbation

Table 4.2: Mean-value and standard deviation of the quantified passivity/non-passivity levels

	LH-LF	***RH-LF***	***LH-HF***	***RH-HF***
Mean	0.0018	0.0017	-0.0040	-0.0039
Standard Deviation	0.0010	0.0009	0.0026	0.0030

recorded for each ε_{PD} as a quantified passivity/non-passivity metric. Fig. 4.15 illustrates the quantified passivity/non-passivity degree for the subjects during the four trials.

Fig. 4.16 shows the distribution of the quantified data for all the subjects during the four sets of trials (LH-LF, RH-LF, LH-HF, RH-HF). The mean-value and standard deviation of the quantified passivity/non-passivity levels for all the trials are given in Table 4.2. Fig. 4.17 also compares the distributions for the Left Hands (LH) and Right Hands (RH), disregarding the frequency range of the perturbations. Both Figs. 4.16 and 4.17 indicate a reasonable correlation between the passivity/non-passivity level of the subjects' left and right arms.

In order to statistically assess the degree of correlation between the left and right arms, the Pearson product-moment Correlation Coefficient (PCC) was calculated. The PCC provides a measure of the linear correlation between two sets of data, where $PCC = 1$ refers to a total

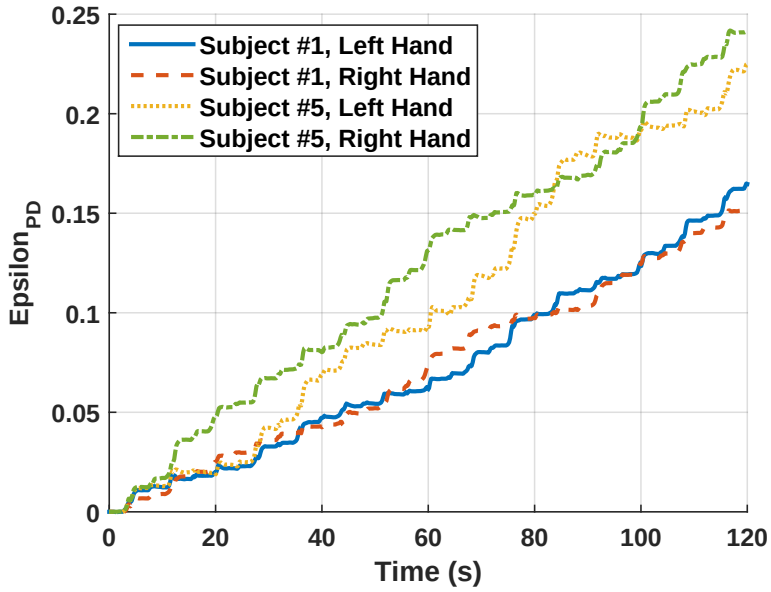

Figure 4.13: ε_{PD} comparison between the left and right hands for subjects #1 and #5 during the low-frequency perturbation.

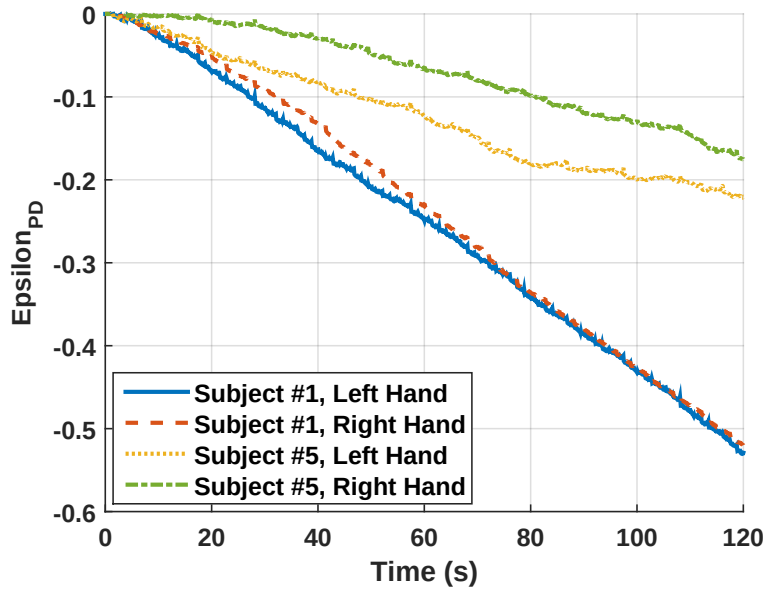

Figure 4.14: ε_{PD} comparison between the left and right hands for subjects #1 and #5 during the high-frequency perturbation.

positive correlation while $PCC = 0$ indicates zero correlation between the data sets. Applying the Pearson test to the data for the subjects' left and right arms, the PCC was calculated to be 0.8240 with a *p-value* equal to $7.4564e-07$ which is well below 0.05, indicating significantly

high levels of correlation between the subjects' left and right arms. It should be noted that the data used in this PCC-based evaluation passed the normality test using the Lilliefors and Jarque-Bera methods.

Remark: *The level of correlation possibly associates with the level of similarities between the mechanical characteristics of the person's arms, despite existing muscle-strength variability as a result of the person's handedness. This association could be helpful in generating a map, based on which the range of passivity/non-passivity degree for one arm of a person can be specified based on that of his/her other arm. Such a correlation map can be specially helpful in designing position-force domain passivity controllers for applications involving bi-manual activities, e.g., in teleoperated robotics surgery. Nevertheless, this would require data collection from an extensive number of subjects in order to generate an accurate correlation map between the left and right arms, which will be part of the future work.*

Correlation Between Passivity/Non-Passivity Levels of the Arm and Physical Features of the Body

An interesting question to answer would be whether the level of passivity of a person's arm can be associated with his/her physical features, e.g. weight and height. If so, a correlation map can be possibly generated, based on which the level of passivity of a person's arm is estimated according to the person's physical features.

In order to address this question, statistical analyses were conducted; and the level of correlation associated with the subjects' weight, height, arm length, and body mass index were investigated. Body Mass Index (BMI) is a quantified value derived based on one's weight and height ($BIM = \frac{Weight_{kg}}{Height_m^2}$), indicating the amount of his/her tissue mass (muscle vs. fat). For this purpose, the Pearson correlation test was applied and the results are as follows: no significant correlation was observed between the subjects' height and the passivity levels of their arms during the low-frequency trials (*p-value*= 0.0744). A significant direct correlation of 0.7393 was, however, observed between the passivity level of their arms and their body weights (*p-value*= 0.0060). A significant direct correlation of 0.7563 was also observed between the subjects' BMI and the passivity level of their arms (*p-value*= 0.0044). This sounds reasonable, as the amount of tissue mass (muscle vs. fat) directly contributes to the mass and

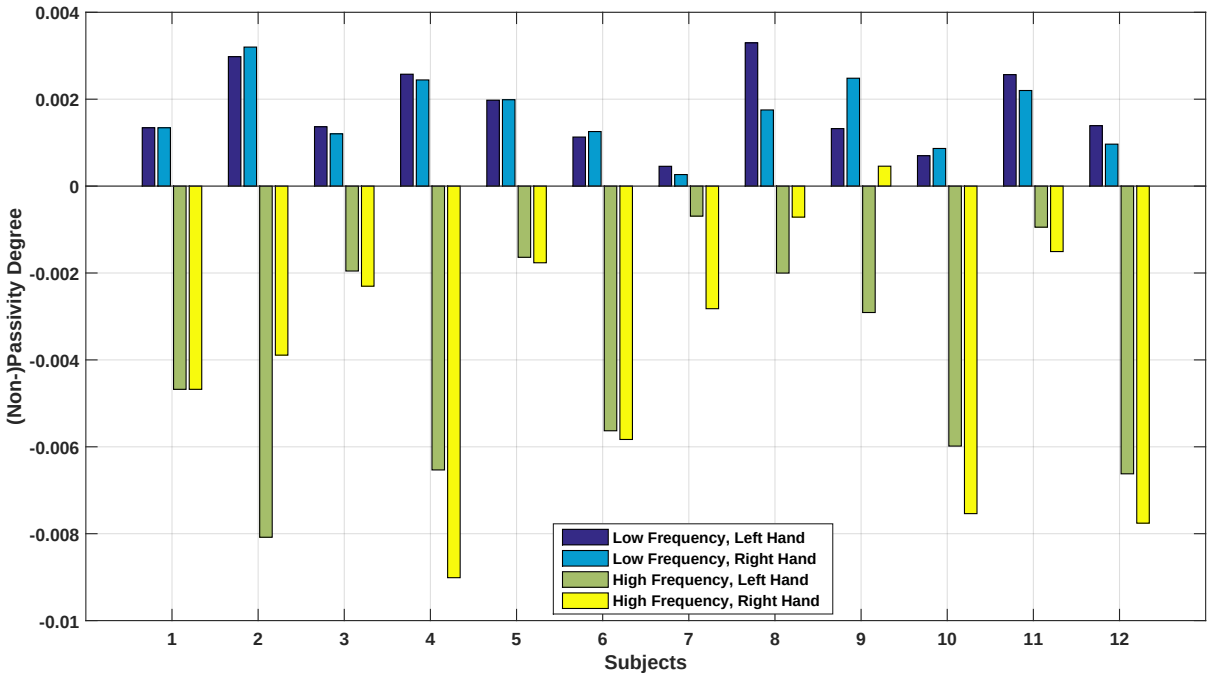

Figure 4.15: Passivity/Non-passivity degrees for all the subjects calculated from the least-squared curves fitted to their ε_{PD}.

stiffness levels of an individual's arm.

Another effective factor could be the individual's arm length, which can affect the end-point impedance of his/her arm with respect to his/her arm impedances at the joints level. Therefore, the combination of the subjects' arm length (L_{Arm}) and their BMI was also tested ($L_{Arm} * BMI$), which resulted in significant direct correlation level of 0.7920 (p-$value$= 0.0021). Among all of the above, the latter metric provides the highest correlation, which can be used for the purpose of generating a correlation map that associates the physical features of an individual to the passivity range of his/her arm. In order to generate an accurate association/correlation map, data collection and analysis should be carried out for a large number of subjects, which will be a part of the future work.

4.5 Discussion

As elaborated earlier, the passivity of the human arm in the position-force domain, unlike in the velocity-force domain, is frequency-dependent and the operator arm may not remain passive

for the high frequency ranges. Therefore, in order to develop position-force domain passivity controllers for MM/SS systems, PD passivity of the operator should be also satisfied in addition to the PD passivity of the communication channel. PD passivity of the communication channel can be realized through the *conventional* passivity controllers in the literature by some change of variables [30]. The important issue, however, will be making the operator in the position-force domain passive for all frequency ranges. Development of an appropriate PD passivity controller for the operator in detail will be part of our future work. However, some of the possible solutions to this problem are briefly discussed below:

1. Filtering out frequencies above the natural frequency of the operator's arm. Considering the fact that the frequency range characteristics of human motion is normally below their natural frequency, the higher frequency ranges of the signals flowing into the system may contain no significant contents. This, though, should be specifically discussed in the context of the application.

2. Virtually increasing the natural frequency of the operator's arm by adding positive stiffness (as a passivating element) into the system through the controller. This approach would be the dual of adding a damping term into the system in the conventional velocity-force domain passivity controllers. The injection of the positive stiffness will shift the ε_{PD} to a higher level and in fact act as an initial positive bias term for the ε_{PD}. Therefore, the combination of the virtual stiffness and the operator's arm can tolerate higher ranges of motion frequencies compared to the operator's arm alone. Although this approach can improve the high-frequency passivity of the system, it may degrade system performance in low-frequency ranges.

3. Canceling out partially the effect of the mass of the operator's arm (the non-passivating element) by virtually injecting a negative mass into the system. This will decrease the total mass value of the combination of the operator's arm and the negative mass, increasing the natural frequency of the system and therefore shifting the boundary of passivity to higher frequency ranges. Unlike the virtual stiffness, the virtual mass will have a frequency-dependent effect on system performance, and will have a less degrading impact in the low-frequency range compared to that in high-frequency range.

Remark: *The combination of the three suggested control approaches may be integrated into a PD passivity-observer/passivity-controller strategy, through which the passivity of the human arm terminal in position-force domain may be guaranteed. To what extent these strategies are helpful along with other possible control strategies are will be investigated in future work.*

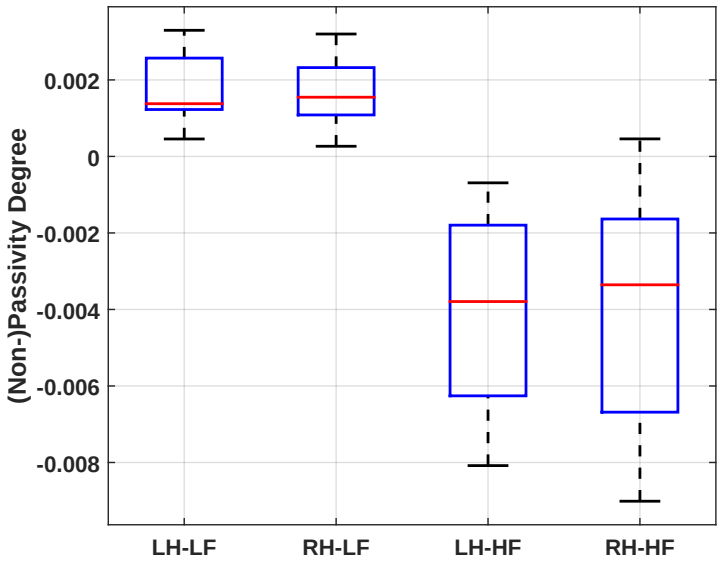

Figure 4.16: The distribution of the passivity/non-passivity degrees for all the subjects during the four trials: LH-LF, RH-LF, LH-HF, RH-HF.

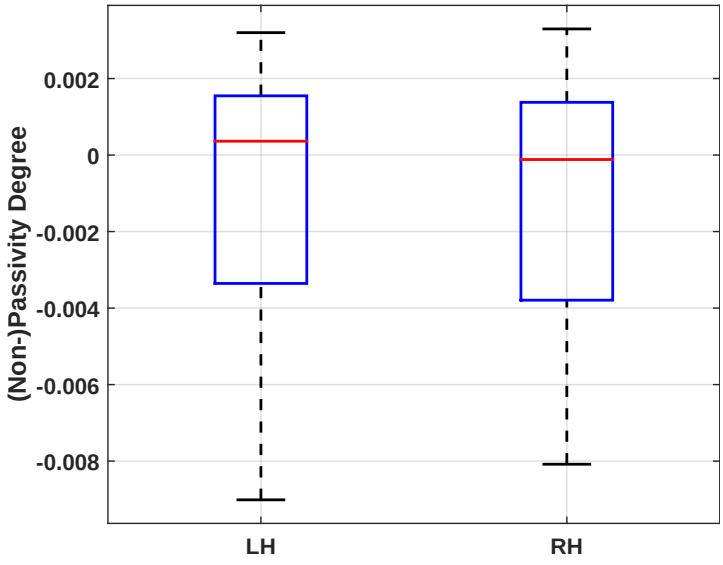

Figure 4.17: The distribution of the passivity/non-passivity degrees for the left hand (LH) and right hand (RH) of the subjects.

4.6 Conclusions

In this chapter, the position-force domain passivity of the human arm was investigated in order to facilitate the development of passivity-based controllers in the position-force domain for teleoperation systems. It was shown through mathematical analysis and experimental results that, unlike the velocity-force domain, the passivity of the human arm in position-force domain is frequency-dependent, and the operator does not remain passive in the position-force domain for all ranges of frequencies. User studies were conducted in support of the proposed hypothesis (frequency-dependent nature of the position-force domain passivity of the human arm), for the purpose of which 12 subjects were recruited. Each subject participated in four trials; data was collected for both their left and right arms for two different ranges of perturbation frequencies. Statistical analysis was performed on the data for 48 trials to validate the proposed hypothesis. Statistical analysis was also conducted to study the correlation between 1) the levels of passivity of the left and the right arms of the subjects; and 2) the level of correlation of the passivity of the subjects' arms and their physical characteristics, e.g., weight, height, and body mass index.

The classic dual-user architecture still has some limitations that make it inadequate for proper motor function (skills) development in RAMT and RAMIS. Consequently, in the next two chapters, the design and implementation of specific supervised trilateral frameworks customized according to the requirements of each application will be discussed.

Bibliography

[1] R. L'Orsa, C. J. Macnab, and M. Tavakoli, "Introduction to haptics for neurosurgeons," *Neurosurgery*, vol. 72, pp. A139–A153, 2013.

[2] J. Burgner, D. C. Rucker, H. B. Gilbert, P. J. Swaney, P. T. Russell, K. D. Weaver, and R. J. Webster, "A telerobotic system for transnasal surgery," *IEEE/ASME Transactions on Mechatronics*, vol. 19, no. 3, pp. 996–1006, 2014.

[3] M. Shahbazi, S. F. Atashzar, and R. V. Patel, "A dual-user teleoperated system with virtual fixtures for robotic surgical training," in *IEEE International Conference on Robotics and Automation (ICRA)*. IEEE, 2013, pp. 3639–3644.

[4] M. Shahbazi, S. F. Atashzar, H. A. Talebi, and R. V. Patel, "An expertise-oriented training framework for robotics-assisted surgery," in *IEEE International Conference on Robotics and Automation (ICRA)*. IEEE, 2014, pp. 5902–5907.

[5] A. Gupta and M. K. O'Malley, "Design of a haptic arm exoskeleton for training and rehabilitation," *IEEE/ASME Transactions on Mechatronics*, vol. 11, no. 3, pp. 280–289, 2006.

[6] P. R. Culmer, A. E. Jackson, S. Makower, R. Richardson, J. A. Cozens, M. C. Levesley, and B. B. Bhakta, "A control strategy for upper limb robotic rehabilitation with a dual robot system," *IEEE/ASME Transactions on Mechatronics*, vol. 15, no. 4, pp. 575–585, 2010.

[7] S. F. Atashzar, I. G. Polushin, and R. V. Patel, "Networked teleoperation with non-passive environment: Application to tele-rehabilitation," in *IEEE/RSJ International Conference on Intelligent Robots and Systems (IROS)*. IEEE, 2012, pp. 5125–5130.

[8] C. Melchiorri, "Robotic telemanipulation systems: An overview on control aspects," in *Proceedings of the 7th IFAC Symposium on Robot Control*, vol. 1, 2003, pp. 707–716.

[9] R. J. Anderson and M. W. Spong, "Bilateral control of teleoperators with time delay," *IEEE Transactions on Automatic Control*, vol. 34, no. 5, pp. 494–501, 1989.

[10] A. Budak, *Passive and active network analysis and synthesis*. Waveland Press Inc, 1991.

[11] C. A. Desoer and M. Vidyasagar, *Feedback systems: input-output properties*. Academic Press, 1975.

[12] P. F. Hokayem and M. W. Spong, "Bilateral teleoperation: An historical survey," *Automatica*, vol. 42, no. 12, pp. 2035–2057, 2006.

[13] V. Chawda and M. K. O'Malley, "Position synchronization in bilateral teleoperation under time-varying communication delays," *IEEE/ASME Transactions on Mechatronics*, vol. 20, no. 1, pp. 245–253, 2015.

[14] J.-H. Ryu, D.-S. Kwon, and B. Hannaford, "Stable teleoperation with time-domain passivity control," *IEEE Transactions on Robotics and Automation*, vol. 20, no. 2, pp. 365–373, 2004.

[15] G. Niemeyer and J.-J. E. Slotine, "Telemanipulation with time delays," *The International Journal of Robotics Research*, vol. 23, no. 9, pp. 873–890, 2004.

[16] ——, "Towards force-reflecting teleoperation over the internet," in *IEEE International Conference on Robotics and Automation*, vol. 3. IEEE, 1998, pp. 1909–1915.

[17] N. Chopra, M. W. Spong, S. Hirche, and M. Buss, "Bilateral teleoperation over the internet: the time varying delay problem," in *Proceedings of the American Control Conference, Denver, USA*, 2003.

[18] N. Chopra, M. W. Spong, R. Ortega, and N. E. Barabanov, "On position tracking in bilateral teleoperation," in *Proceedings of the American Control Conference*, vol. 6. IEEE, 2004, pp. 5244–5249.

[19] J. Artigas, J.-H. Ryu, and C. Preusche, "Position drift compensation in time domain passivity based teleoperation," in *IEEE/RSJ International Conference on Intelligent Robots and Systems (IROS)*. IEEE, 2010, pp. 4250–4256.

[20] M. Shahbazi, S. F. Atashzar, and R. V. Patel, "A framework for supervised robotics-assisted mirror rehabilitation therapy," in *IEEE/RSJ International Conference on Intelligent Robots and Systems (IROS)*. IEEE, 2014, pp. 3567–3572.

[21] M. Shahbazi, S. F. Atashzar, M. Tavakoli, and R. V. Patel, "Therapist-in-the-loop robotics-assisted mirror rehabilitation therapy: An assist-as-needed framework," in *IEEE International Conference on Robotics and Automation (ICRA)*. IEEE, 2015, pp. 5910–5915.

[22] G. Ganesh, A. Takagi, R. Osu, T. Yoshioka, M. Kawato, and E. Burdet, "Two is better than one: Physical interactions improve motor performance in humans," *Scientific Reports, Nature Publishing Group*, vol. 4: 3824, 2014.

[23] N. Hogan, "The mechanics of multi-joint posture and movement control," *Biological Cybernetics*, vol. 52, no. 5, pp. 315–331, 1985.

[24] F. A. Mussa-Ivaldi, N. Hogan, and E. Bizzi, "Neural, mechanical, and geometric factors subserving arm posture in humans," *The Journal of Neuroscience*, vol. 5, no. 10, pp. 2732–2743, 1985.

[25] T. Tsuji, P. G. Morasso, K. Goto, and K. Ito, "Human hand impedance characteristics during maintained posture," *Biological Cybernetics*, vol. 72, no. 6, pp. 475–485, 1995.

[26] M. Dyck, A. Jazayeri, and M. Tavakoli, "Is the human operator in a teleoperation system passive?" in *World Haptics Conference (WHC)*. IEEE, 2013, pp. 683–688.

[27] J. M. Dolan, M. B. Friedman, and M. L. Nagurka, "Dynamic and loaded impedance components in the maintenance of human arm posture," *IEEE Transactions on Systems, Man and Cybernetics*, vol. 23, no. 3, pp. 698–709, 1993.

[28] N. Kottenstette and P. J. Antsaklis, "Relationships between positive real, passive dissipative, & positive systems," in *American Control Conference (ACC)*. IEEE, 2010, pp. 409–416.

[29] S. S. Haykin, *Active network theory*. Addison-Wesley, 1970, vol. 2680.

[30] M. Shahbazi, H. A. Talebi, and R. V. Patel, "Networked dual-user teleoperation with time-varying authority adjustment: A wave variable approach," in *IEEE/ASME International Conference on Advanced Intelligent Mechatronics (AIM)*. IEEE, 2014, pp. 415–420.

Chapter 5

Robotics-Assisted Mirror Rehabilitation Therapy: A Therapist-in-the-Loop Assist-as-Needed Architecture

The material presented in this chapter was published in the IEEE/ASME Transactions on Mechatronics, vol. 21, no. 14, pp. 1954 - 1965, 2016.

5.1 INTRODUCTION

Annually 15 million people worldwide suffer from stroke. With a survival rate of about 70%, stroke is known to be a major leading cause of long-term disabilities and severe impairments [1, 2]. The significant number of patients recovering from stroke, in addition to other neurological disorders, has led to a growing need for rehabilitation services to induce neuroplasticity in patients. Neuroplasticity is referred to as the reorganization ability of the brain by developing new neural connections through sensory input, experience, and learning, which allows the brain's neurons to compensate for injury and disease [3]. Achieving brain neuroplasticity from rehabilitation therapy is a labor-intensive process, which necessitates not only a therapist's expertise and knowledge, but also reproducible movements and stereotyped

©[2016] IEEE. Reprinted, with permission, from [M. Shahbazi, S.F. Atashzar, M. Tavakoli and R.V. Patel, "Robotics-Assisted Mirror Rehabilitation Therapy: A Therapist-in-the-Loop Assist-as-Needed Architecture", IEEE/ASME Transactions on Mechatronics, vol. 21, no. 14, pp. 1954 - 1965, 2016].

exercises. This has led to a paradigm shift towards robotics-assisted rehabilitation therapy, offering novel recovery-assessment approaches along with patient-targeted rehabilitation therapies [4, 5].

Robotics-assisted mirror therapy, a recent form of robotic rehabilitation, has received a great deal of attention during the past decade [6] . This type of therapy is particularly useful for patients with hemiparesis [7], the most common movement impairment. Hemiparesis refers to one-sided weakness and affects about 80% of stroke survivors [8]. Effectiveness of mirror therapy has been also shown for patients suffering from unilateral neglect after stroke [9]. Unilateral neglect, also known as hemispatial neglect, is a symptom of a brain damage in which the person experiences a deficit in attention to and awareness of one side of his/her body and anything in the external world on the same side. A patient with this neurological condition is unable to perceive and process stimuli on that side of the body or the environment, while that inability is not due to a lack of sensation [10].

During robotics-assisted mirror therapy, motions of the Patient's Functional Limb (PFL) are mirrored through a telerobotic medium to the Patient's Impaired Limb (PIL), promoting the functional recovery of the impaired/affected limb through the spatial coupling effect between the two limbs. This results from the tendency of one limb to adopt the spatial features of the other limb [11–13]. Through mirror-symmetric (or any other coordinated bimanual) movement pattern for the two limbs in mirror therapy, the unimpaired hemisphere of the brain interacts with the impaired hemisphere, thereby inducing reorganization of the motor cortex networks and facilitating cortical neuroplasticity [11, 14]. The effectiveness of mirror-symmetric *bimanual* therapy has been shown in comparison with conventional *unimanual* therapy to result in an increase in the functional ability as well as a decrease in movement completion times for the PIL [15]. Mirror therapy has also been shown to be effective in terms of improving the accuracy, active range of motion, dexterity and grip strength of the limb [16–19].

Existing robotics-assisted mirror-therapy systems, such as MIME [20], provide a unilateral Single-Master/Single-Slave (SM/SS) telerobotic framework in order for the PIL to move in accordance with the mirror-image motions of the PFL. This gives patients some level of control over the therapy through the involvement of their functional limb. However, due to the inherently restrictive structure of SM/SS systems [21], the PIL interacting with the slave robot

can only receive commands from the PFL interacting with the master robot. This means that a therapist cannot be directly involved in the rehabilitation loop to apply corrective movements or to monitor/assess the PIL performance through haptic feedback. Fig. 5.1 shows the overall scheme of a conventional robotics-assisted mirror therapy system. Presence of an expert in the loop of the therapy can play an essential role in promoting the patient's functional recovery. Based on a recent study published [22], haptics-based interaction with a partner when learning a motor task considerably enhances the motor skills compared to when practicing the task alone for the same duration. Therefore, haptics-based interaction of a therapist with a patient can be effective not only because of the therapist's knowledge and expertise, but also due to his/her positive effect on the patient's learning curve as a result of the interaction. Capitalizing on the impact of therapist-patient haptics-based interaction, in this chapter a Therapist-In-the-Loop (TIL) framework is proposed for robotics-assisted mirror therapy based on a *supervised trilateral* telerobotic system integrated with adaptive Assist-as-Needed Therapy (ANT) that is adjusted based on the impairment and disability level of the patient's affected limb. The overall scheme of the proposed framework is shown in Fig. 5.2. The proposed architecture offers the following innovations:

(1) Therapist-in-the-loop MT,

(2) PFL-mediation,

(3) Haptic feedback to the therapist,

(4) Adaptive GVF,

(5) Task-independent and patient-specific motor-function assessment,

(6) Closed-loop stability analysis,

which are discussed below.

The architecture establishes a mirroring behavior between the patient's two limbs, while the desired trajectories are provided by a therapist supervising the therapy. This is expected to enhance the treatment by bringing the therapist's expertise directly into the treatment. The framework is designed such that the trajectories desired for the PIL are commanded by the therapist through the PFL, where the PFL has the ability to modify/update the trajectory. Therefore, having the PFL as a medium between the therapist and the PIL, the therapist-commanded trajectories can be conditioned before being passed on to the PIL. Benefiting from the pa-

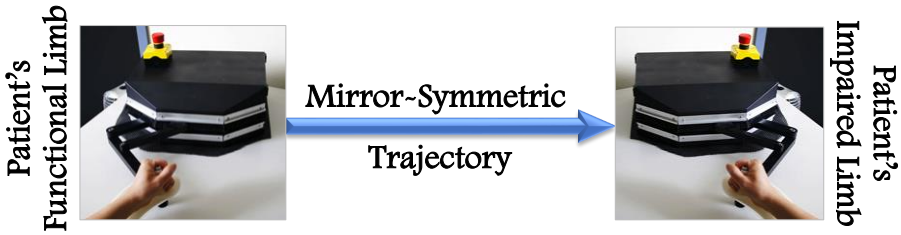

Figure 5.1: The overall scheme of the conventional robotics-assisted MT.

tient's proprioceptive knowledge and self-awareness of workspace limitations, the proposed PFL-mediated approach enables the patient to modify the therapist-commanded trajectories in order to avoid painful/uncomfortable maneuvers for the PIL, of which the therapist may not be aware. Based on how closely the therapist-commanded trajectories are followed by the PIL, which may have been modified by the PFL in the interest of patient safety and comfort, the system also provides the therapist with haptic feedback. This would allow the therapist to better decide on the intensity of the therapy administered to and acceptable for the patient.

The framework also provides the patient with *adaptive* Assist-as-Needed Therapy (ANT) using a time-varying Guidance Virtual Fixture (GVF). A GVF is a suitable approach for providing kinesthetic guidance along desired trajectories [23]. In this thesis, the intensity/forcefulness of the GVF is proposed to be adaptively adjusted based on the patient's impairment/performance level perceived during the therapy.

For this purpose, benefiting from the presence of the PFL in the therapy loop, a novel performance assessment framework (called *performance symmetry* (PS)) is proposed for mirror therapy, based on which the adaptive GVF is adjusted in real time. PS provides a relative quantifiable assessment of the PIL performance by comparing it to the PFL performance as the patient's gold standard. Unlike the absolute assessment metrics currently available in the literature [5, 24], the proposed PS metric takes the performance level of the PFL into account for each patient when assessing the PIL performance for the same patient. Consequently, the quantified assessment results will be more objective, easier to interpret, and adjusted to the inevitable intra-patient variability in motor deficiency.

In addition to PS, another metric is also proposed based on the *Level Of Guidance* (LOG) provided to the PIL during the treatment. Using this metric in parallel with other performance metrics enables the assessment process to distinguish between performance improvements due to the patient's functional recovery vs. those due to the GVF-based assistance to the patient

during the treatment. The aforementioned PS and LOG metrics, along with two other metrics from the literature, are used to develop an adaptation law for updating the adaptive ANT based on the impairment level of the PIL.

As there are three sets of local sub-systems (PIL, PFL and therapist), globally interacting through a trilateral telerobotic architecture, stability of the closed-loop system should be investigated in order to guarantee system stability. For this purpose, a combination of the Circle Criterion and the Small-Gain Theorem is applied and a set of sufficient stability conditions is derived. The proposed stability analysis addresses instabilities caused by communication delays between the therapist and the patient. This facilitates the case of haptics-enabled bilateral tele-rehabilitation, which is suitable for applications such as in-home rehabilitation [25], [26]. Incorporating the Circle Criterion into the Small-Gain Theorem, the proposed procedure also addresses extra stability-analysis challenges raised by the integration of the time-varying nonlinear GVF element into the delayed closed-loop system.

Through the proposed trilateral framework, the patient benefits from an enhanced motor-recovery process as a result of integrating the following characteristics: (a) the cross-cortex coupling effect between limbs induced by the mirror therapy; (b) the expertise and direct supervision of, along with the haptic feedback delivered to, the therapist in the loop over the treatment to provide appropriate corrective movements; (c) the supervision/impact of the patient over the treatment through the PFL-mediated feature, which guarantees the patient's safety and comfort by avoiding the application of excessive pressure and pain on the PIL; and (d) active involvement of the patient in the treatment through the adaptive GVF-based ANT.

The rest of this chapter is organized as follows: Section 5.2 presents the proposed architecture. Section 5.3 discusses the metrics proposed and the adaptation law developed for ANT. Section 5.4 presents the closed-loop stability of the system in the presence of communication delays. Experimental results are given in Section 5.5, and Section 5.6 concludes the chapter.

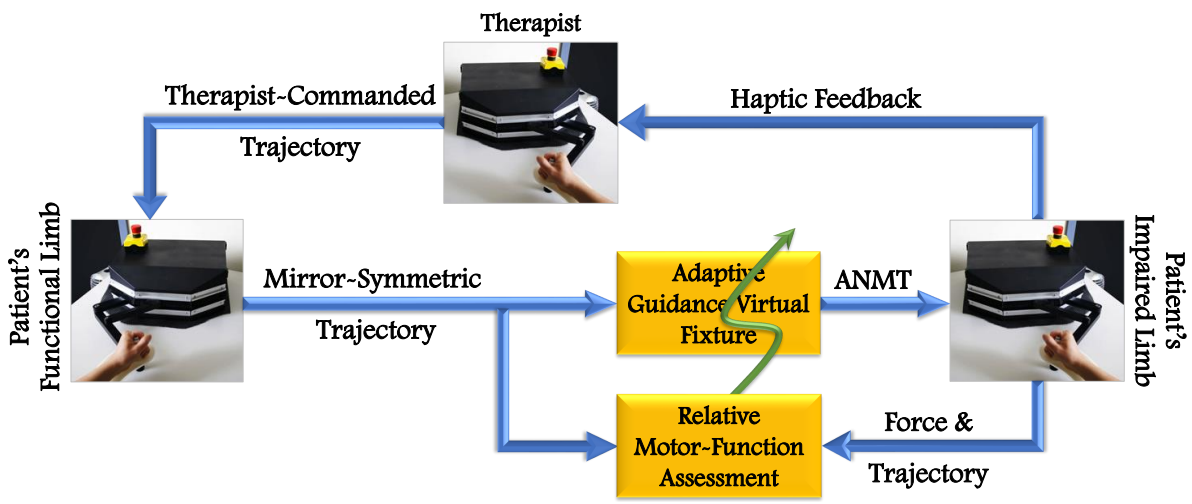

Figure 5.2: The overall scheme of the supervised trilateral telerobotic framework proposed for Assist-as-Needed Mirror Therapy (ANMT).

5.2 THE PROPOSED FRAMEWORK

5.2.1 Architecture for the PIL/Robot Interaction

In order for the PIL to undergo mirror therapy, its desired position $x_{des,PIL}$ is defined to be the mirror image of PFL's position, x_{PFL}, as follows:

$$x_{des,PIL}(t) = \beta \cdot x_{PFL}(t) \tag{5.1}$$

where $\beta = diag(\beta_1, ..., \beta_n)$ refers to the mirroring matrix, accommodating for the mirroring effect between the functional and the impaired limb across the sagittal plane; the subscript n indicates the number of Degrees of Freedom (DOF). Depending on the mirroring plane, β_i $(i = 1, 2, \cdots, n)$, which is the mirroring coefficient for the ith DOF, can be set to either +1 or -1. For example, for mirroring along the x-axis, β_1 will be set to -1, while β_i $(i \neq 1)$ will be set to +1 in order to accommodate for the same-directional/parallel trajectories along other axes. By setting all the elements of the mirroring matrix to +1, the framework can be used for bilateral parallel therapy, which has also been shown to be effective in inducing neuroplasticity [6].

In order to provide the PIL with an assist-as-needed therapy to *actively* engage the patient in the treatment process, an adaptive GVF is proposed, the stiffness of which can be adaptively

adjusted according to the impairment/disability level of the PIL. The higher level of impairment the PIL shows, the more strict and enforcing the GVF becomes to provide the patient with a higher level of assistance. The GVF is designed such that if the PIL remains within a specific range of its desired trajectory, i.e., inside a specific spherical volume centered at the desired trajectory point $x_{des,PIL}$, no GVF force will be applied to it. However, if the deviation error between the PIL and the mirror image of the PFL (the desired trajectory for PIL) exceeds a certain threshold, the GVF will apply force to the PIL in order to assist the PIL with accomplishing the trajectory. The allowable range of the deviation error is set to be up to R_{GVF}. Exceeding the allowable range of position error, i.e., $\left|x_{des,PIL} - x_{PIL}\right| > R_{GVF}$, will cause the PIL to receive the following GVF force:

$$F_{GVF,PIL}(t) = K_{GVF,PIL}(t)(x_{des,PIL}(t) - x_{PIL}(t)) \tag{5.2}$$

where $K_{GVF,PIL}(t) \in [\kappa_{min}, \kappa_{max}]$ refers to the adaptive stiffness of the GVF, to be adjusted according to the impairment level of the PIL, the design of which including the patient's motor-function assessment is discussed in Section 5.3. κ_{min} and κ_{max} indicate some positive lower and upper bounds to be considered in the design procedure for $K_{GVF,PIL}$. It should be noted that various motor-function assessment metrics, including but not limited to movement accuracy, motion smoothness, movement velocity and grip strength, can be used in order to design the variation profile of the adaptive GVF's stiffness.

In order for the patient to transparently feel the desired GVF force applied by the robot on his/her PIL, it is required to have:

$$F_{PIL}(t) = -F_{GVF,PIL}(t) \tag{5.3}$$

where F_{PIL} refers to the force applied by the PIL to its corresponding robot. Note that the minus sign is to account for the direction of forces, i.e., applied by the robot to the PIL or vice versa. However, as will be discussed in Section 5.4, similar to any other telerobotic system [27], ensuring closed-loop stability may degrade the system transparency and performance. Thus, to guarantee closed-loop stability in the presence of communication delays, a modified impedance surface is defined as the desired closed-loop system at the PIL robot, through which the GVF

force $F_{GVF,PIL}$ is applied to the PIL by its corresponding robot:

$$\begin{gathered} F_{PIL}(t) = -F_{GVF,PIL}(t) + \\ M_{\vartheta,PIL} \cdot \ddot{x}_{PIL}(t) + B_{\vartheta,PIL} \cdot \dot{x}_{PIL}(t) + K_{\vartheta,PIL} \cdot x_{PIL}(t) \end{gathered} \tag{5.4}$$

where $M_{\vartheta,PIL}$, $B_{\vartheta,PIL}$ and $K_{\vartheta,PIL}$ stand for mass, damping and stiffness, respectively, to be used as the local control parameters at the PIL robot. From the performance viewpoint, the control parameters are desired to be set to zero, which results in $F_{PIL}(t) = -F_{GVF,PIL}(t)$ as in (5.3). However, it will be shown in Section 5.4 how positive values for these parameters will contribute to closed-loop stability in the presence of communication time delay between the therapist and the patient in order to facilitate the case of tele and in-home rehabilitation.

5.2.2 Architecture for the PFL/Robot Interaction

The architecture at the PFL robot is designed such that the PFL receives commands (desired trajectories) from the therapist, but is able to deviate from them. This PFL-mediated platform allows the patient to alter the therapist-commanded trajectory, if the trajectories are felt to be painful or uncomfortable for the PIL. To realize this goal, a position-error impedance surface is designed for the PFL:

$$\begin{gathered} F_{PFL,des}(t) = M_{des,PFL}(\ddot{x}_T^*(t) - \ddot{x}_{PFL}(t)) + \\ B_{des,PFL}(\dot{x}_T^*(t) - \dot{x}_{PFL}(t)) + K_{des,PFL}(x_T^*(t) - x_{PFL}(t)) \end{gathered} \tag{5.5}$$

where x_{PFL} indicates the trajectory generated by the PFL and x_T^* refers to the mirror image of the therapist-commanded trajectory. Note that since the PIL will move based on the mirror-image of the PFL, while the therapist will provide the trajectory desired for the PIL, the PFL should receive the mirror-symmetric image of the trajectory commanded for the PIL by the therapist, i.e., to receive $x_T^* = \beta \cdot x_T$, where β indicates the mirroring matrix. $M_{des,PFL}$, $B_{des,PFL}$ and $K_{des,PFL}$ refer to the desired mass, damping and stiffness, respectively, through which the PFL can alter the desired trajectories received from the therapist in the interest of safety and comfort. In addition, $F_{PFL,des}$ stands for the desired force applied by the robot to the PFL as a result of interaction with the therapist. In order for the PFL to receive $F_{PFL,des}$, it is desired to

have:

$$F_{PFL} = -F_{PFL,des}, \tag{5.6}$$

where F_{PFL} indicates the force applied by the PFL to the robot. Consequently, and based on the desired impedance surface defined in (5.5), the position of the functional limb will be:

$$X_{PFL}(s) = \frac{F_{PFL}(s)}{Z_{des,PFL}(s)} + \beta \cdot X_T(s) \tag{5.7}$$

where $Z_{des,PFL}(s) = M_{des,PFL}s^2 + B_{des,PFL}s + K_{des,PFL}$. Here, s indicates the Laplace transform variable. Thus, the PFL can follow the mirrored image of therapist's trajectories βx_T by applying minimal F_{PFL}. However, if the patient considers the therapist-commanded trajectories to be painful or uncomfortable for the PIL, s/he can apply enough force F_{PFL}, des, to make x_{PFL} deviate from the therapist mirrored trajectory βx_T. The PFL as a medium to convey desired trajectories from the therapist to the PIL increases the patient safety and comfort.

With the same reasoning as for (5.4), for the sake of closed-loop stability, the desired behavior $F_{PFL} = -F_{PFL,des}$ is replaced by an impedance surface as the desired closed-loop system at the PFL robot, through which the desired force $F_{PFL,des}$ is applied to the PFL by some modification:

$$\begin{gathered} F_{PFL} = -F_{PFL,des}(t) + \\ M_{\vartheta,PFL} \cdot \ddot{x}_{PFL}(t) + B_{\vartheta,PFL} \cdot \dot{x}_{PFL}(t) + K_{\vartheta,PFL} \cdot x_{PFL}(t) \end{gathered} \tag{5.8}$$

where $M_{\vartheta,PFL}$, $B_{\vartheta,PFL}$ and $K_{\vartheta,PFL}$ refer to the mass, damping and stiffness to be used as the local control parameters at the PFL robot. These parameters are desired to be zero for the purpose of performance, i.e., the PFL feels $F_{PFL,des}$, entirely. However, as discussed in Section 5.4, setting them to non-zero values will help with stabilizing the entire closed-loop system.

5.2.3 Architecture for the Therapist/Robot Interaction

As described earlier, in the interest of the patient's safety and comfort, the framework enables the PFL to alter the therapist-commanded trajectory, x_T, when necessary, before passing it on to the PIL. Therefore, the trajectories eventually followed by the PIL may not be exactly similar to those created by the therapist. Therefore, it is required for the therapist to receive haptic feedback about the PIL movements in relation to the therapist-commanded movements. For

this purpose, position-error-based haptic feedback, $F_{\varphi,T}$, is designed to be sent to the therapist by his/her corresponding robot, as follows:

$$\begin{aligned} F_{\varphi,T}(t) = M_{\varphi,T}(\ddot{x}_{PIL}(t) - \ddot{x}_T(t)) + \\ B_{\varphi,T}(\dot{x}_{PIL}(t) - \dot{x}_T(t)) + K_{\varphi,T}(x_{PIL}(t) - x_T(t)) \end{aligned} \tag{5.9}$$

where $M_{\varphi,T}$, $B_{\varphi,T}$ and $K_{\varphi,T}$ denote the mass, damping and stiffness of the position-error-based haptic feedback, respectively. With the same reasoning for (5.4) and (5.8), an impedance surface is defined for the desired closed-loop behavior at the therapist side, through which the haptic force feedback $F_{\varphi,T}$ is applied by the robot to the therapist by the modification:

$$\begin{aligned} F_T = -F_{\varphi,T}(t) + \\ M_{\vartheta,T} \cdot \ddot{x}_T(t) + B_{\vartheta,T} \cdot \dot{x}_T(t) + K_{\vartheta,T} \cdot x_T(t) \end{aligned} \tag{5.10}$$

where $M_{\vartheta,T}$, $B_{\vartheta,T}$ and $K_{\vartheta,T}$ stand for the desired mass, damping and stiffness to be used as the local control parameters at the therapist's robot. In addition, F_T refers to the force applied to the robot by the therapist. The force F_T applied by the therapist to the corresponding robot, as well as the forces F_{PIL} and F_{PFL} applied by the PIL and PFL to their corresponding robots can be modeled by second-order LTI systems [28]:

$$\begin{aligned} F_\Theta(t) = F^*_\Theta(t) - M_\Theta \cdot \ddot{x}_\Theta(t) - B_\Theta \cdot \dot{x}_\Theta(t) \\ -K_\Theta \cdot (x_\Theta(t) - x_{\Theta_0})) \end{aligned} \tag{5.11}$$

where F^*_Θ, for $\Theta = PIL,\ PFL,\ T$, denote the exogenous force applied by the operator, which is either the patient or the therapist. M_Θ, B_Θ and K_Θ stand for mass, damping and stiffness of the limb, respectively; and x_{Θ_0} indicates the initial position of the therapist's limb, x_Θ.

5.3 Adaptive Assist-as-Needed Therapy

A patient-specific treatment practice that actively engages the patient in the treatment by adapting to his/her motor capability enhances the degree of recovery, compared to a non-adaptive training scenario [29, 30].

In order to promote patient active involvement, the framework provides the PIL with ANT, the level of which is decided by the GVF adjusted adaptively based on the PIL's level of impairment. In order to realize the proposed ANT strategy, objective assessment of the PIL's motor-function is essential.

5.3.1 Motor Function Assessment

By development of robotics-assisted rehabilitation, quantified evaluation of patient's motor performance and recovery has been also made possible [31], providing *objective* assessment results compared to the traditional subjective assessment approaches, e.g. Fugl Meyer [32], Motor Assessment Scale [33] and Motricity Index [34]. For this purpose, various objective and quantitative evaluation metrics have been used in the literature such as movement smoothness, movement accuracy, active range of motion, peak and mean velocity, task completion time, etc. [5, 24, 35].

Although the above metrics provide useful quantified information about a patient's motor function, they could still be challenging, due to the intra-patient variability, to interpret and to correlate with the impairment severity of every patient regardless of their age, gender and their before-stroke baseline muscle strength. Intra-task variability is also another issue when assessing a patient's motor-function, as not every daily activity can be linked to a quantified baseline performance level. Having a baseline performance level for every single task and every single patient can be challenging, as a result of which a wide range of daily tasks cannot be included in the patient's treatment and evaluation practice.

In this thesis, we take advantage of having both functional and impaired limbs of the patient involved in order to propose a novel motor function assessment metric for mirror therapy, which addresses both intra-task variability and intra-patient variability. The proposed metric, called *Performance Symmetry* can reflect the nature of any of the current metrics in the literature, but also provides a task-independent and patient-specific evaluation. In hemiparetic patients, regardless of their age, gender, baseline muscle strength, and for any type of practice tasks, the motor performance of their functional limb can reflect the ideal level of performance their impaired limb should achieve. Therefore, the performance of the PFL can be considered as the patient-specific baseline in evaluation of the PIL performance. Accordingly, unlike the

absolute assessment metrics in the literature, we propose a normalized *relative* quantifying assessment metric, PS, for mirror therapy in order to provide more objective, patient-specific, and easier-to-interpret evaluation results, as follows:

$$PS_{\Omega}(t) = 1 - \left| \frac{\Omega_{PFL}(t) - \Omega_{PIL}(t)}{\Omega_{PFL}(t) + \Omega_{PIL}(t)} \right| \tag{5.12}$$

where Ω can be any quantified metric used in conventional robotics-assisted rehabilitation. Here, we have used two of these metrics to incorporate in the PS assessment:

Movement Smoothness (MS)

which is shown to be correlated with the patient's level of temporal coordination and the extent of jerky movements. Following a stroke, movements made by the affected limb are composed of sub-movements with poor temporal coordination, resulting in jerky movements. The higher the motor recovery, the smoother the movements become [24]. In order to incorporate MS into PS, it is required to calculate MS for both PFL and PIL (MS_{η} for $\eta = PFL$ and PIL), which can be performed as per the definition

$$MS_{\eta}(t) = \frac{1}{t} \int_0^t \sqrt{(\frac{\mathrm{d}^3 x_{\eta,x}}{\mathrm{d}\,\tau^3})^2 + (\frac{\mathrm{d}^3 x_{\eta,y}}{\mathrm{d}\,\tau^3})^2 + (\frac{\mathrm{d}^3 x_{\eta,z}}{\mathrm{d}\,\tau^3})^2}\ \mathrm{d}\,\tau \tag{5.13}$$

where the subscripts x, y and z refer to positions along the x, y and z directions, respectively. Calculating MS_{PFL} and MS_{PIL} based on (5.13), and incorporating them into (5.12), the movement-smoothness symmetry (PS_{MS}) will be specified as

$$PS_{MS}(t) = 1 - \left| \frac{MS_{PFL}(t) - MS_{PIL}(t)}{MS_{PFL}(t) + MS_{PIL}(t)} \right| \tag{5.14}$$

This provides a normalized objective assessment of the PIL's movement smoothness without any *a priori* knowledge about the task.

Total Path Length (TPL)

which is the total distance traveled by the patient's limb from movement onset. Comparing the TPL traveled by the PIL and the PFL gives a measure of the deviation error to indicate

how accurately the PIL has been able to follow the mirrored-image of the PFL. The higher the motor recovery, the more similar the distance traveled. The total path length TPL_η for both PFL and PIL ($\eta = PFL, PIL$) can be calculated based on

$$TPL_\eta(t) = \int_0^t \sqrt{(\frac{\mathrm{d}x_{\eta,x}}{\mathrm{d}\tau})^2 + (\frac{\mathrm{d}x_{\eta,y}}{\mathrm{d}\tau})^2 + (\frac{\mathrm{d}x_{\eta,z}}{\mathrm{d}\tau})^2}\ \mathrm{d}\tau \tag{5.15}$$

Calculating TPL_{PIL} and TPL_{PFL} based on (5.15) and incorporating them into (5.12) gives the normalized measure of symmetry for the PIL deviation error, as follows:

$$PS_{TPL}(t) = 1 - \left|\frac{TPL_{PFL}(t) - TPL_{PIL}(t)}{TPL_{PFL}(t) + TPL_{PIL}(t)}\right| \tag{5.16}$$

For any quantifying metric, the same process can be repeated to calculate the patient-specific symmetry level for that metric.

In addition to the proposed PS measure, a motor-function metric is also proposed based on the level of guidance provided to the PIL during the therapy. Most of the metrics in the literature, which are mainly meant for assessing performance, cannot distinguish in real-time whether an improved performance has been due to the patient's functional recovery or as a result of the haptic assistance guiding the patient's limb toward the practice trajectory. Therefore, we are proposing a novel metric based on the LOG provided to the PIL through the adaptive GVF during the treatment, which is beneficial in updating the quantified performance assessment based on the actual contribution and active involvement of the patient. The higher the level of guidance and assistance provided to the PIL to accomplish the task, the lower the level of functional ability scored for the PIL. For this purpose, the normalized GVF-based LOG metric is defined as follows:

$$\psi_{GVF}(t) = 1 - \frac{\int_0^t \left|F_{GVF,PIL}(\tau)\right| \mathrm{d}\tau}{\left|F_{GVF,max}\right| * t} \tag{5.17}$$

where $F_{GVF,PIL}$ refers to the adaptive GVF force applied to the PIL, and $F_{GVF,max}$ indicates the maximum level of GVF force considered to apply to the PIL during a treatment session. Incorporating this metric in parallel with other performance metrics, the patient's functional improvement as well as his/her own level of contribution to the movements can be quantified.

5.3.2 Adaptive GVF Design

To incorporate the three assessment metrics PS_{MS}, PS_{TPL} and ψ_{GVF} for the purpose of updating the stiffness of the adaptive GVF applied to the PIL, given in (5.2), the metrics are integrated using the following fusion law:

$$\Lambda_{PIL}(t) = \frac{1}{2}\psi_{GVF}(t) \cdot (PS_{MS}(t) + PS_{TPL}(t)) \tag{5.18}$$

which combines the metrics derived based on the performance symmetry with the proposed GVF-based LOG metric in parallel, resulting in a normalized single metric between 0 and 1 to be used as an adaptive coefficient in order to update the adaptive stiffness of the GVF, $K_{GVF,PIL}$:

$$K_{GVF,PIL}(t) = \kappa_{min} + (\kappa_{max} - \kappa_{min})(1 - \Lambda_{PIL}(t)) \tag{5.19}$$

where κ_{min} and κ_{max} refer to the lower and upper bounds of the GVF's stiffness, $K_{GVF,PIL}$, preset based on the level of guidance forces desired to be applied to the PIL during a treatment session. Note that having $0 \leq \Lambda_{PIL} \leq 1$ ensures that $K_{GVF,PIL}$ remains between the desired boundaries $[\kappa_{min}, \kappa_{max}]$. It should be noted that, setting $\kappa_{min} = \kappa_{max}$, would set $K_{GVF,PIL}$ to a constant value κ_{min}, which bypasses the real-time adaptation.

5.4 Closed-loop Stability Analysis

In order to satisfy the local desired closed-loop system defined for each robot as in (5.4), (5.8) and (5.10), a decentralized impedance controller adopted from [36] is applied. By satisfying these impedance surfaces, the closed-loop system will be decoupled in various DOFs. Therefore, stability of each DOF can be analyzed independently. By some mathematical manipulations, the proposed architecture defined in (5.1)-(5.11) can be modeled as in Fig. 5.3 for each DOF, and then transformed to Fig. 5.4 without affecting the outputs y_1 and y_2; τ_1 and τ_2 refer to communication delays from the patient to the therapist and vice versa, and

$$\Xi_1(s) = \frac{Z_{des,PFL}(s)}{Z_{\vartheta,PFL}(s) + Z_{des,PFL}(s) + Z_{PFL}(s)} \tag{5.20}$$

$$\Xi_2(s) = \frac{1}{Z_{\vartheta,PIL}(s) + Z_{PIL}(s)} \tag{5.21}$$

$$\Xi_3(s) = -\frac{Z_{\varphi,T}(s)}{Z_{\vartheta,T}(s) + Z_{\varphi,T}(s) + Z_T(s)} \tag{5.22}$$

$$\Xi_4(s) = \frac{1}{Z_{\varphi,T}(s)} \tag{5.23}$$

$$\Xi_5(s) = \frac{1}{Z_{des,PFL}(s)} \tag{5.24}$$

$$\Xi_6(s) = (\Xi_1 \cdot \beta_i)^{-1} \tag{5.25}$$

$$Z_{(.)}(s) = M_{(.)}s^2 + B_{(.)}s + K_{(.)}; \;\; M_{(.)}, B_{(.)}, K_{(.)} > 0 \tag{5.26}$$

In order to analyze the stability of the system, a combination of the Small-Gain Theorem and the Circle Criterion is applied.

Theorem I [37]: *The delayed feedback system given in Fig. 5.5 is Input-Output Stable*

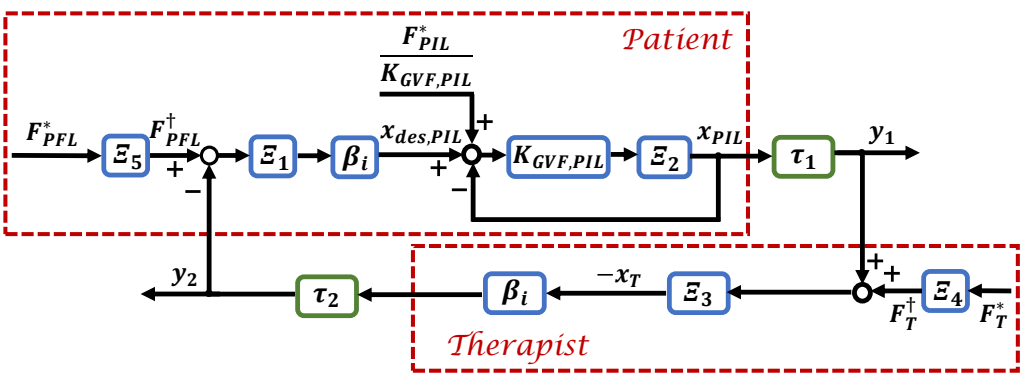

Figure 5.3: The overall closed-loop system

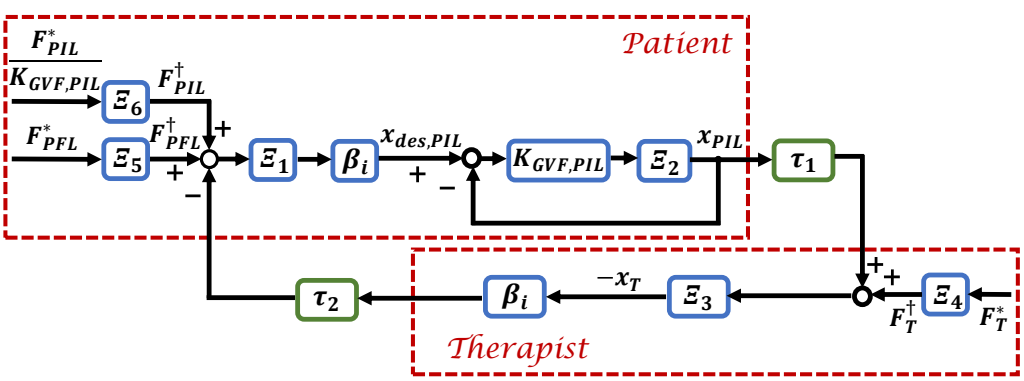

Figure 5.4: The overall closed-loop system

(IOS) if:

$$u_1 \in L_\infty \ , \ u_2 \in L_\infty \tag{5.27}$$

$$\zeta_1 \in [0,\infty) \ , \ \zeta_2 \in [0,\infty) \tag{5.28}$$

$$\zeta_1 \cdot \zeta_2 \leqslant 1 \tag{5.29}$$

where, ζ_1 and ζ_2 in (5.28)-(5.29) stand for the IOS gain of sub-systems Σ_1 and Σ_2, respectively, as per the following definition given for the IOS gain.

Definition I: *The IOS gain of a system with the input-output relation $y(t) = \Sigma u(t)$, where Σ is a mapping or operator that specifies y in terms of u, is a nonnegative constant ζ such that:*

$$\sup_{t\geqslant 0} |y(t)| \leqslant \zeta \cdot \sup_{t\geqslant 0} |u(t)| + \varepsilon;$$

where ε is a nonnegative constant bias term.

Therefore, in order for the closed-loop system given in Fig. 5.4 to remain stable, the three small-gain conditions given in (5.27)-(5.29) should be met. Based on the first condition, it is required to have

$$u_1 = F^{\dagger}_{PFL} + F^{\dagger}_{PIL} \in L_\infty \ , \ u_2 = F^{\dagger}_{T} \in L_\infty \tag{5.30}$$

$F^*_T(t)$, $F^*_{PFL}(t)$ and $F^*_{PIL}(t)$ refer to the exogenous forces applied by the therapist and the patient, which belong to the L_∞ space [37], while $F^{\dagger}_T(t)$, $F^{\dagger}_{PFL}(t)$ and $F^{\dagger}_{PIL}(t)$ indicate the outputs of the systems $\Xi_4(s)$, $\Xi_5(s)$ and $\Xi_6(s)$ for inputs $F^*_T(t)$, $F^*_{PFL}(t)$ and $\frac{F^*_{PIL}(t)}{K_{GVF,des}(t)}$, respectively. Having $0 < \kappa_{min} < K_{GVF,PIL}$ from the previous section, the input $\frac{F^*_{PIL}(t)}{K_{GVF,des}(t)}$ is also bounded and belongs to the L_∞ space. Considering the structure of systems $\Xi_4(s)$, $\Xi_5(s)$ and $\Xi_6(s)$, which are stable and proper transfer functions belonging to the L_1 space, they map inputs in L_∞ to outputs in L_∞. Consequently, $F^{\dagger}_T(t)$, $F^{\dagger}_{PFL}(t)$ and $F^{\dagger}_{PIL}(t)$ belong to L_∞, satisfying (5.27).

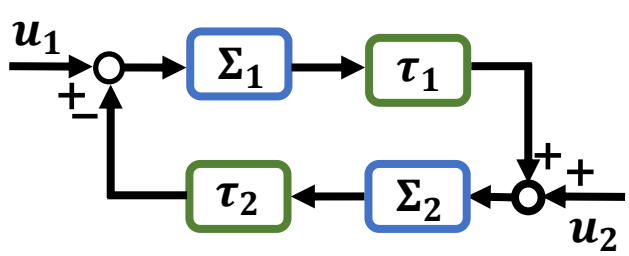

Figure 5.5: Small-Gain Theorem

The next step in analyzing closed-loop stability is to check whether the IOS gains of the feedforward and the feedback paths in Fig. 5.4 satisfy the next two sets of conditions in (5.28) and (5.29). To calculate the IOS gain of the feedforward loop, first let us consider the local feedback loop in the feedforward path, from x_{PIL} to $x_{des,PIL}$. In this feedback loop, $K_{GVF,PIL}$ is a time-varying parameter belonging to $[\kappa_{min}, \kappa_{max}]$, as defined in the previous section. This parameter refers to the stiffness of the GVF, to be adjusted adaptively. Without the need to go into details about how to update $K_{GVF,PIL}$, it can be assumed to belong to sector $(0, \rho]$ per the following definition:

Definition II [38]: *A memoryless function $h : [0,\infty) \times R^P \longrightarrow R^P$ is said to belong to the sector $(0,\rho]$* with $\rho = \rho^T > 0$ if $h(t,u)^T[h(t,u) - \rho u] \leqslant 0$.

Stability of the local feedback loop from x_{PIL} to $x_{des,PIL}$ can be analyzed using the Circle Criterion, as described next. Previously, Miandashti [39] used the Circle Criterion to study the stability of sampled-data bilateral teleoperation systems.

Theorem II [38]: *The feedback connection of a linear dynamical system $G(s)$ and a nonlinear element ξ, as shown in Fig. 5.6, is stable if $\xi \in [\xi_1, \xi_2]$, with $\xi_2 - \xi_1 > 0$, and $[I + \xi_2 G(s)][I + \xi_1 G(s)]^{-1}$ is Strictly Positive Real (SPR).*

Using a type II loop transformation [38], and considering that $\xi = K_{GVF,PIL}(t)$ is a mapping such that $K^{-1}_{GVF,PIL}$ is causal, $K_{GVF,PIL} \cdot K^{-1}_{GVF,PIL} = I$, and both $K_{GVF,PIL}$ and $K^{-1}_{GVF,PIL}$ have finite gains, the feedback connection in Fig. 5.6 can be transformed into the feedback system in Fig. 5.7. Since $0 < \kappa_{min} < K_{GVF,PIL}(t) < \kappa_{max}$, $\xi^{-1} = K^{-1}_{GVF,PIL}$ in the feedforward path of Fig. 5.7 does not affect the system's stability. Therefore, the system in Fig. 5.7 is identical to the feedback connection in Fig. 5.8 in terms of stability, which in turn is similar to that for the local feedback loop in the feedforward path, from x_{PIL} to $x_{des,PIL}$, in Fig. 5.4. Therefore, considering that $K_{GVF,PIL} \in [\kappa_{min}, \kappa_{max}]$ and based on Theorem II, the local feedback system, from x_{PIL} to $x_{des,PIL}$, in Fig. 5.4 is stable if $[I + \kappa_{max}\Xi_2(s)][I + \kappa_{min}\Xi_2(s)]^{-1}$ is SPR. We also

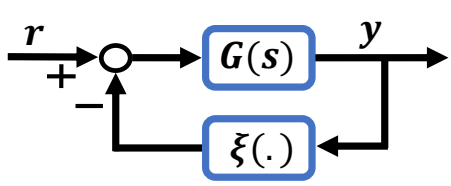

Figure 5.6: Feedback connection used in the Circle Criterion

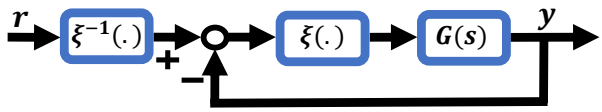

Figure 5.7: Feedback connection based on the type II loop transformation [38]

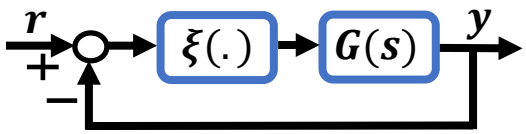

Figure 5.8: Modified feedback connection used in the Circle Criterion

need the following definitions:

Definition III [38]: *The transfer function $H(s)$ is SPR if $H(s-\varepsilon)$ if Positive Real (PR) for some $\varepsilon > 0$.*

Definition IV [38]: *The transfer function $H(s)$ is PR if:*

- *poles of $H(s)$ are in $Re(s) < 0$*
- *for all real ω for which $j\omega$ is not a pole of $H(s)$, $H(s)+H^T(s^*)$ is positive semi-definite, and*
- *any pure imaginary pole $j\omega$ of $H(s)$ is a simple pole and the residue $lim_{s\to j\omega}(s-j\omega)H(s)$ is positive semidefinite Hermitian.*

According to *Definitions III* and *IV*, and considering the structure of $\Xi_2(s)$, which is a stable and strictly proper transfer function, $[I+\kappa_{max}\Xi_2(s)][I+\kappa_{min}\Xi_2(s)]^{-1}$ is SPR if

$$(1+\kappa)(K_\Upsilon+\kappa_{min})+B_\Upsilon^2\omega^2 > (1+\kappa)M_\Upsilon\omega^2 \tag{5.31}$$

where $\kappa = \kappa_{max}-\kappa_{min} > 0$, $M_\Upsilon = M_{\vartheta,PIL}+M_{PIL}$, $B_\Upsilon = B_{\vartheta,PIL}+B_{PIL}$ and $K_\Upsilon = K_{\vartheta,PIL}+K_{PIL}$. Therefore, by proper adjustment of local control parameters at the PIL side ($M_{\vartheta,PIL}$, $B_{\vartheta,PIL}$ and $K_{\vartheta,PIL}$), stability of the local feedback loop from x_{PIL} to $x_{des,PIL}$ can be guaranteed. Having the local feedback loop stable, it can be shown that the loop has its highest input-output gain when $K_{GVF,PIL}$ is at its maximum level, i.e., $K_{GVF,PIL} = \kappa_{max}$. Therefore, the IOS gain of the local feedback loop in the presence of time-varying $K_{GVF,PIL}$ will be equivalent to the IOS gain of the same loop when $K_{GVF,PIL}$ has been set to κ_{max}. Therefore, we can continue the stability

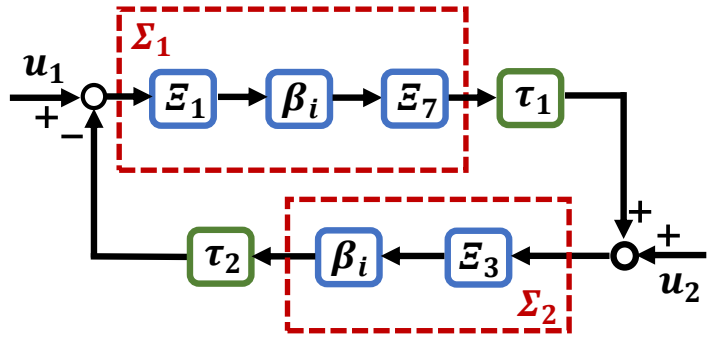

Figure 5.9: The closed-loop system transformed based on the Circle Criterion

analysis of the overall closed-loop system by replacing the time-varying $K_{GVF,PIL}$ by its upper bound κ_{max}, which represents the worst case. Consequently, Fig. 5.4 can be transformed to Fig. 5.9, where $\Xi_7(s) = \dfrac{\kappa_{max} \cdot \Xi_2(s)}{1 + \kappa_{max} \cdot \Xi_2(s)}$. Comparing Fig. 5.9 with Fig. 5.5, Σ_1 and Σ_2 can be written as

$$\Sigma_1(s) = \Xi_1(s) \cdot \beta_i \cdot \Xi_7(s) = \frac{\beta_i \cdot \kappa_{max}}{Z_{\vartheta,PIL}(s)+Z_{PIL}(s)+\kappa_{max}} \cdot \frac{Z_{des,PFL}(s)}{Z_{\vartheta,PFL}(s)+Z_{des,PFL}(s)+Z_{PFL}(s)} \tag{5.32}$$

$$\Sigma_2(s) = \beta_i \cdot \Xi_3(s) = -\frac{\beta_i \cdot Z_{\varphi,T}(s)}{Z_{\vartheta,T}(s)+Z_{\varphi,T}(s)+Z_T(s)} \tag{5.33}$$

The next step is to investigate the condition given in (5.28), i.e., to have the IOS gains of $\Sigma_1(s)$ and $\Sigma_2(s)$ belong to $[0,\infty)$. Since $\Sigma_1(s)$ and $\Sigma_2(s)$ indicate transfer functions representing two LTI systems, the IOS gain is equal to the L_1 norm of the two systems; L_1 norm of transfer function $\Sigma(s)$ is defined according to the formula $\|\Sigma(s)\|_{L_1} = \int_0^{+\infty} |\sigma(\tau)| \, d\tau$, $\sigma(t) = L^{-1}[\Sigma(s)]$. Therefore, (5.28) is equivalent to $\Sigma_1(s) \in L_1$ and $\Sigma_2(s) \in L_1$. Considering the structure of $\Sigma_1(s)$ and $\Sigma_2(s)$, which are stable and proper transfer functions, and knowing that β_i and κ_{max} are bounded parameters, both $\Sigma_1(s)$ and $\Sigma_2(s)$ belong to L_1. The last condition given in (5.29) necessitates

$$\begin{aligned} &\left| \frac{\beta_i \cdot \kappa_{max}}{Z_{\vartheta,PIL}(s)+Z_{PIL}(s)+\kappa_{max}} \cdot \frac{Z_{des,PFL}(s)}{Z_{\vartheta,PFL}(s)+Z_{des,PFL}(s)+Z_{PFL}(s)} \right|_{L_1} \cdot \\ &\left| -\frac{\beta_i \cdot Z_{\varphi,T}(s)}{Z_{\vartheta,T}(s)+Z_{\varphi,T}(s)+Z_T(s)} \right|_{L_1} \leq 1 \end{aligned} \tag{5.34}$$

which can be transformed into three conservative conditions, as follows:

$$\left| \frac{\beta_i \cdot \kappa_{max}}{Z_{\vartheta,PIL}(s) + Z_{PIL}(s) + \kappa_{max}} \right|_{L_1} \leq 1 \tag{5.35}$$

$$\left|\frac{Z_{des,PFL}(s)}{Z_{\vartheta,PFL}(s)+Z_{des,PFL}(s)+Z_{PFL}(s)}\right|_{L_1} \leq 1 \tag{5.36}$$

$$\left|-\frac{\beta_i \cdot Z_{\varphi,T}(s)}{Z_{\vartheta,T}(s)+Z_{\varphi,T}(s)+Z_T(s)}\right|_{L_1} \leq 1 \tag{5.37}$$

An approach to guarantee that (5.35)-(5.37) are satisfied is to ensure that the magnitude of each transfer function inside the brackets is not greater than one for all $s = j\omega$, i.e.,

$$|\kappa_{max}| \leq \left|Z_{\vartheta,PIL}(s)+Z_{PIL}(s)+\kappa_{max}\right| \tag{5.38}$$

$$\left|Z_{des,PFL}(s)\right| \leq \left|Z_{\vartheta,PFL}(s)+Z_{des,PFL}(s)+Z_{PFL}(s)\right| \tag{5.39}$$

$$\left|Z_{\varphi,T}(s)\right| \leq \left|Z_{\vartheta,T}(s)+Z_{\varphi,T}(s)+Z_T(s)\right| \tag{5.40}$$

These three inequalities along with the one given in (5.31) represent the stability criteria for the closed-loop system in the presence of communication time delays between the patient and the therapist. As can be seen, the control parameters $M_{\vartheta,\Delta}$, $B_{\vartheta,\Delta}$ and $K_{\vartheta,\Delta}$; $\Delta = PIL, PFL, T$ appear in all four conditions, through which the stability conditions can be satisfied.

Remark: The proposed stability analysis platform can be applied to general *non-rehabilitation* teleoperation applications, as well. The framework itself can be considered as a new triple-user hierarchical/supervised leader-follower system.

5.5 Experiments

In order to evaluate the performance of the proposed framework, three sets of experiments were conducted. The experimental setup consists of one Quanser HD^2 haptic device acting as the therapist's robot; and two Quanser upper-extremity rehabilitation robots serving as the PIL and PFL robots. The User Datagram Protocol (UDP) was used to transmit data between the master robots and the slave robot. All controllers and the communication between the robots were implemented using the QuaRC Real-Time system at a sampling frequency of 1 kHz. Fig. 5.10 shows the experimental setup.

The experiments were performed in two DOFs, along the sagittal-transverse plane. The mirroring between the PIL and the PFL was implemented across the sagittal plane. In these

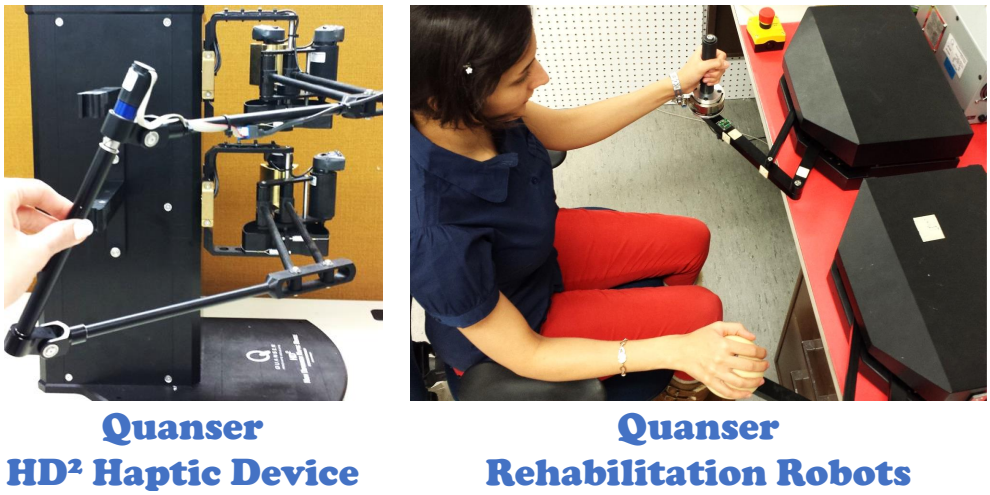

Figure 5.10: Experimental Setup

experiments, two operators were asked to simulate behaviors of a typical patient and a typical therapist in three distinctive scenarios in order to evaluate various features of the proposed system. The operators were familiar with the setup.

5.5.1 Scenario I: PFL-mediated Mirror Therapy

The first scenario consisted of two phases to evaluate 1) the mirroring effect between the PIL and the PFL, and 2) the impact of the PFL as a medium on the Therapist-Commanded Trajectory (TCT) received at the PIL robot. The therapist was asked to generate and repeat a squared trajectory during both phases of the experiment. The patient was asked to consider the TCT as "comfortable" in Phase I ($t = 0 - 80s$) and "uncomfortable" in Phase II ($t = 80 - 160s$), and react accordingly. Therefore, she was supposed to intentionally alter the TCT by her PFL in Phase II, where the motions were defined as "uncomfortable". A time-varying profile was set for $K_{GVF,des}$, such that $\kappa_{min} = 350$ and $\kappa_{min} = 400$. Round-trip communication delay of 200 ms was also introduced between the therapist's robot and the patient's robots.

The results are given in Figs. 5.11-5.13. Fig. 5.11 shows the 2D representation of the trajectories for the therapist, the PFL and the PIL. As can be seen, the therapist provided squared trajectories. The PFL followed the mirror-image of the Therapist-Commanded Trajectory (TCT), which in turn caused the PIL to follow the TCT in the same direction, as expected. In the second phase of the experiment, where the PFL was asked to resist the TCT due to the

motions being considered as "uncomfortable" for the PIL, the amplitude of the PIL motion was also reduced through the PFL-mediated architecture to avoid the painful and/or uncomfortable trajectory for the PIL. As can be seen, the framework also ensured the mirroring effect between the PIL and the PFL in both phases. Fig. 5.12 shows the same trajectory results in 1D, across

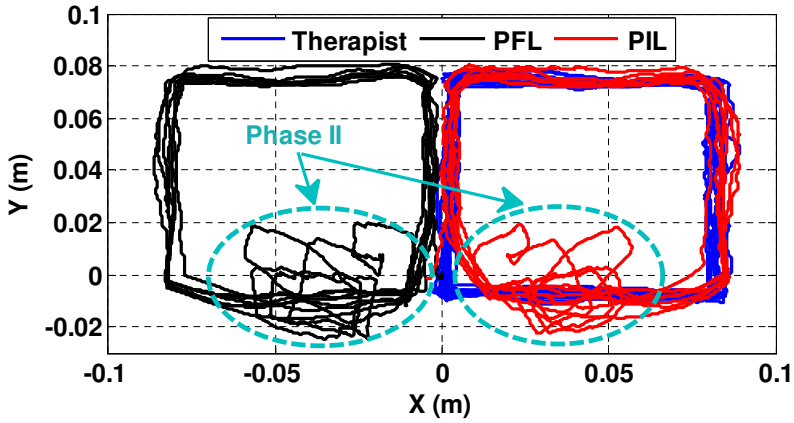

Figure 5.11: Experimental scenario #1: 2D plot of trajectories

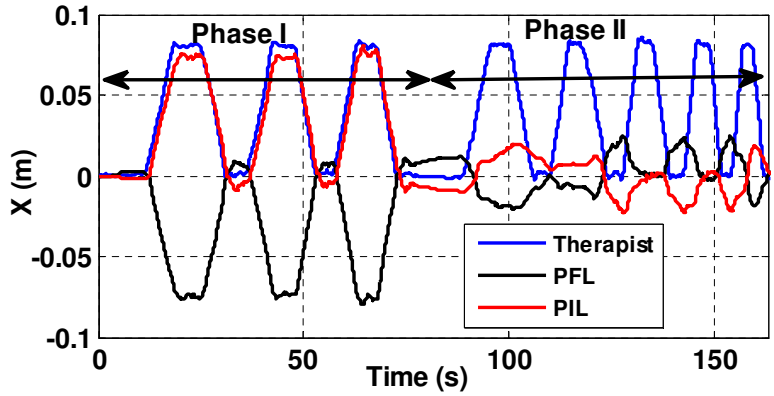

Figure 5.12: Experimental scenario #1: 1D plot of trajectories across the mirroring plane

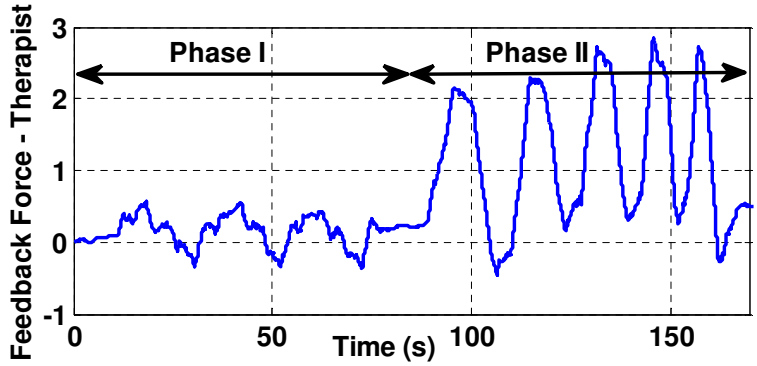

Figure 5.13: Experimental scenario #1: Haptic feedback provided to the therapist

the mirroring plan with respect to time. The force feedback provided to the therapist during the experiment is shown in Fig. 5.13. As can be seen, in Phase II, the therapist received considerable force on his hand informing him of the "discomfort" felt by the patient. This feature helps the therapist to be aware of and ensure the patient's safety during the therapy.

5.5.2 Scenario II: How Time-Varying Assistance Helps

The second scenario was designed to investigate the effect of the time-varying virtual fixture gain $K_{GVF,des}$ on the PIL performance. For this purpose, a time-varying profile was set for $K_{GVF,des}$, increasing from $\kappa_{min} = 1$ to $\kappa_{max} = 400$ during the experiment. The round-trip communication time delay between the patient's robots and the therapist's robot was $200ms$. To simulate an impaired PIL, a 2-DOF mass-spring array was used in order to represent non-symmetric spasticity in a PIL. Spasticity, also referred to as an unusual stiffness, tightness, or pull of muscles, is a feature of altered skeletal muscle performance as a result of damage to the brain or the spinal-cord including that resulting from stroke.

For this purpose, the 2-DOF asymmetric mass-spring array was connected to the PIL robot, as shown in Fig. 5.14, simulating an impaired PIL affected by spasticity. Similar to the first scenario, the therapist was asked to generate squared trajectories, while the PFL was asked to consider the TCT as comfortable, thereby transferring the TCT to the PIL with no conditioning. Fig. 5.15 illustrates the 2-DOF time-based trajectory generated by the therapist and the trajectory followed by the simulated impaired PIL as a result of the time-varying GVF assistance force applied to the impaired PIL. As can be seen, at the beginning of the experiment, where $K_{GVF,des}$ was at its lowest value $K_{GVF,des} = \kappa_{min}$, the GVF provided minimal assistance to the PIL, thus the PIL was not able to follow the therapist-commanded trajectory. By increasing $K_{GVF,des}$ during the experiment, the level of assistance provided to the PIL increased such that during the last $50s$ of the experiment, the impaired PIL fully tracked the desired TCT.

Fig. 5.16 shows a 2D planar view of the same trajectories, where the smaller squares correspond to the lower levels of assistance by the GVF. As can be seen, at the beginning of the experiment, the simulated impaired PIL was not only unable to generate the desired amplitudes of the trajectory due to the low level of the GVF assistance, but also had an undesired rotational shift due to the asymmetry of the PIL. Towards the end of the experiment, increasing levels of

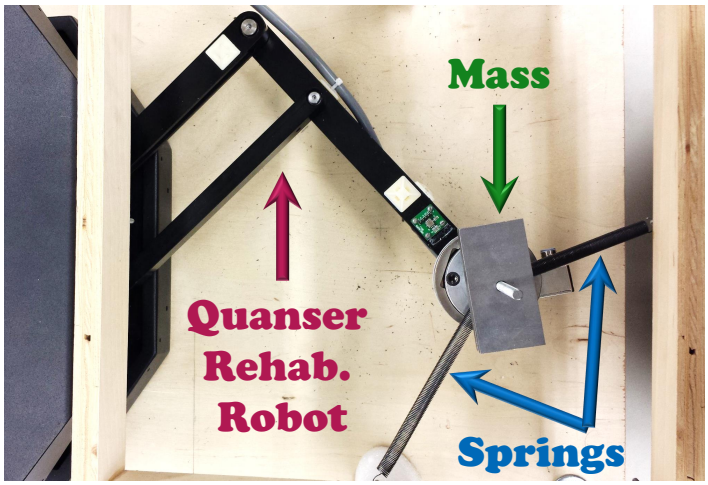

Figure 5.14: The 2-DOF mass-spring array connected to the PIL robot

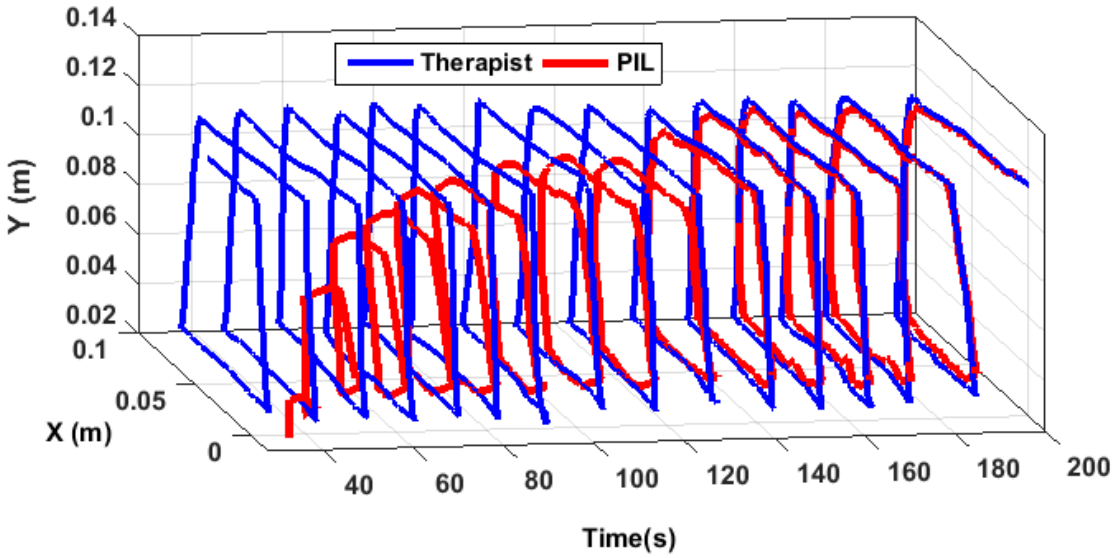

Figure 5.15: Experimental scenario #2: 2D trajectories with respect to time

the GVF corrected for both amplitude and rotational-shift of the trajectories. The time-varying GVF assistance enables the *adaptive* ANT in order to *actively* engage the patient in the therapy.

5.5.3 Scenario III: Adaptive Patient-Targeted ANT

The third scenario was designed in three phases to evaluate various aspects of the proposed adaptive ANT strategy updated based on the patient's motor-function ability. For this purpose, the patient was asked to simulate three different motor-function levels in three Phases, as fol-

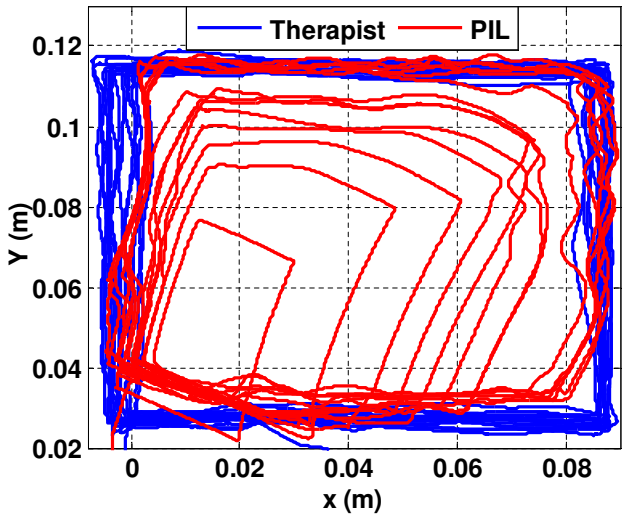

Figure 5.16: Experimental scenario #2: 2D plot of trajectories

lows:

Phase I ($t = 0 - 45s$)**:** extensively impaired and unable to move. To emphasize the high level of impairment, the user was asked not to follow the PFL's mirrored movement, but to add some level of resistance to her PIL's movement (not allowing the GVF guiding her PIL along the TCT) in order to simulate a "heavy" PIL.

Phase II ($t = 45 - 85s$)**:** moderately impaired with some weakness, requiring some level of assistance from the GVF in order to complete the task.

Phase III ($t = 85 - 130s$)**:** slightly impaired, able to generate the mirror image of the PFL's movement with minimum assistance from the GVF.

The scenario's pattern can be also seen in Fig. 5.17, which shows a comparison between the therapist-commanded trajectory and the one made by the PIL. In phase I, the low amplitude of the PIL's movement is due to the resistance the user was asked to make to the GVF, although the GVF was trying to make her follow the TCT. In the second phase, a tracking improvement happened because the user did not resist the GVF (yet showing a moderate impairment on her PIL), enabling the GVF to assist as needed. In Phase III, the enhanced tracking was due to the ability of the PIL in following the TCT with minimum assistance from the GVF.

The results for this experiment are given in Fig. 5.18-Fig. 5.20. Fig. 5.18 illustrates the proposed normalized motor-function metrics, PS_{MS}, PS_{TPL} and ψ_{GVF} (LOG), for the PIL calculated during the experiment in real-time. As can be seen, the two metrics PS_{MS} and PS_{TPL}

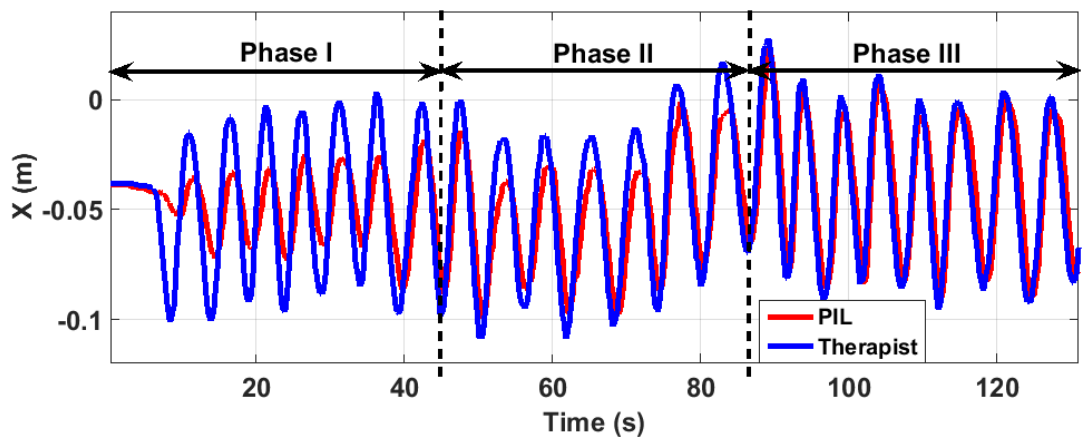

Figure 5.17: Experimental scenario #3: PIL's trajectory compared with the TCT

refer to a relatively low level of motor-function for the PIL during Phase I, due to the undesirable tracking performance. The metric LOG also represents a low level of functional ability, zero at most of the time-range, as the PIL was not able to accomplish the task even with the help of the GVF; as mentioned, this phase was included to emphasize the feature of a "heavy" hand with high level of impairment, in order to provide a comparison platform for the other two phases of the experiment. In Phases II and III, the performance metrics PS_{MS} and PS_{TPL} increased considerably, which indicates the improved performance for the PIL, as expected. However, an interesting difference can be seen at the level of the functional ability shown by the metric LOG between these two phases. Although in both Phases II and III, the PIL has shown tracking improvement, the metric LOG refers to higher level of motor-function in phase III, compared to Phase II. This is a remarkable feature of the proposed LOG metric, which can distinguish between an improved performance induced by the GVF's assistance (as in Phase II) and an improvement due to the actual functional recovery of the PIL (as in Phase III).

Fig. 5.19 shows the adaptive stiffness of the GVF, K_{GVF} resulting from the parallel combination of the LOG with performance metrics PS_{MS} and PS_{TPL}. As can be seen, in the first phase, the system increased the K_{GVF} to its maximum level ($\kappa_{max} = 500N/m$) to assist the extensively-impaired and unable-to-move PIL. In the second phase, the stiffness was adjusted by the system to a medium level to help the moderately-impaired PIL; while in the third phase, the stiffness was reduced considerably, as the PIL's functional assessment assigned a high level of functional ability for the PIL.

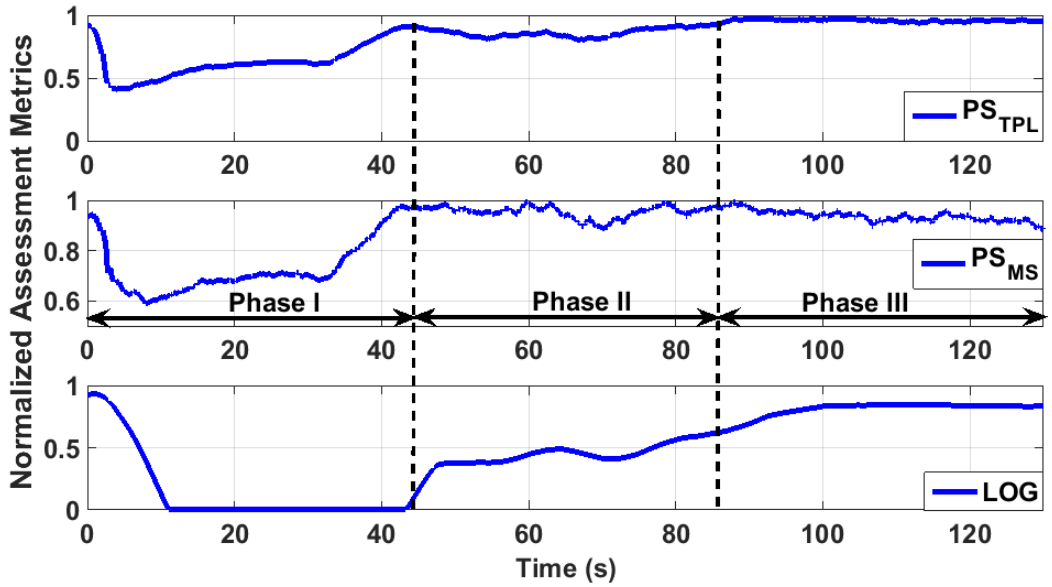

Figure 5.18: Experimental scenario #3: Motor-function assessment metrics

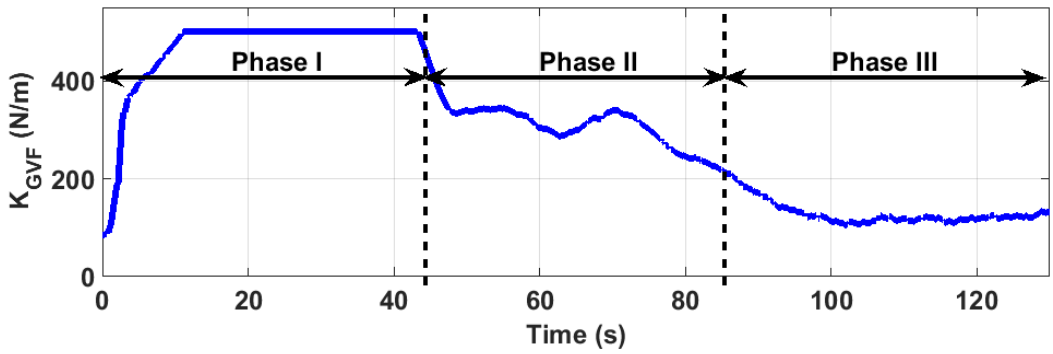

Figure 5.19: Experimental scenario #3: Adaptive GVF's stiffness adjusted according to the PIL impairment level

Fig. 5.20 shows the GVF assistance provided to the PIL based on the adaptive GVF stiffness derived in accordance with the PIL's functional ability. In Phase I, the PIL was provided with a high level of GVF assistance (about 20N peak-to-peak), due to the poor motor-function. During Phase II, the GVF assistance reduced considerably (to about 9N peak-to-peak), as the PIL was able to partially perform the task and required less level of assistance. In Phase III, a slight level of GVF force was applied to the PIL (about 2N peak-to-peak), as a result of the enhanced motor-function illustrated by the PIL.

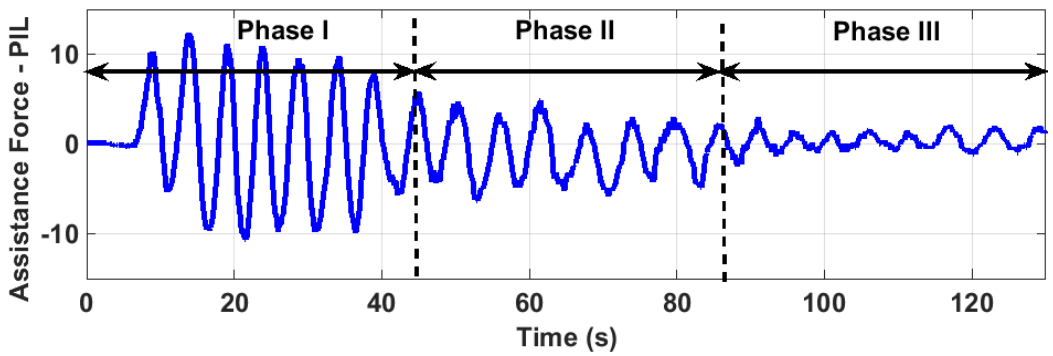

Figure 5.20: Experimental scenario #3: ANT provided to the PIL

5.6 Conclusions

A therapist-in-the-loop framework was presented for mirror rehabilitation therapy. Integrating an adaptive assist-as-needed training approach, the patient's impaired limb receives personalized therapy according to their level of impairment and disability. This enables the patient's impaired limb to be actively involved in the therapy. The expectation is that this will play an important role in promoting functional recovery and motor learning, as opposed to moving passively. Using the proposed framework, the desired therapy trajectories are transferred from the therapist to the patient's impaired limb after being conditioned by the patient's functional limb especially when trajectories that are painful or uncomfortable for the impaired limb are prescribed by the therapist. In order to inform the therapist about any discomfort at the patient's side causing alteration in the desired trajectories, haptic feedback from the patient's impaired limb is provided to the therapist. A criterion was also developed for updating the adaptive ANT implemented by the guidance virtual fixture, based on the patient's impairment level. Two assessment metrics, Performance Symmetry (PS) and Level Of Guidance (LOG), were developed to facilitate the patient-targeted therapy and evaluation. Stability of the closed-loop system was investigated using a combination of the Circle Criterion and the Small-Gain Theorem. The stability analysis took into account the *adaptive* assist-as-needed therapy as well as communication time-delays between the patient and the therapist, facilitating tele and in-home rehabilitation applications. The proposed stability analysis platform can be possibly applied to general non-rehabilitation teleoperation applications, as well. Experimental results were reported to show the performance of the proposed framework.

While this chapter presented the design and implementation of the supervised dual-console

architecture proposed for motor function restoration using mirror rehabilitation therapy, the next chapter will discuss the framework proposed for motor skills development in robotic minimally invasive surgery.

Bibliography

[1] http://www.strokecenter.org/patients/about-stroke/stroke-statistics/. [Online]. Available: http://www.strokecenter.org/patients/about-stroke/stroke-statistics/

[2] A. Otten, C. Voort, A. Stienen, R. Aarts, E. van Asseldonk, and H. Kooij, "Limpact: A hydraulically powered self-aligning upper limb exoskeleton," *IEEE/ASME Transactions on Mechatronics*, vol. 20, no. 5, pp. 2285–2298, 2015.

[3] B. B. Johansson, "Brain plasticity and stroke rehabilitation the willis lecture," *Stroke*, vol. 31, no. 1, pp. 223–230, 2000.

[4] H. I. Krebs, N. Hogan, M. L. Aisen, and B. T. Volpe, "Robot-aided neurorehabilitation," *IEEE Transactions on Rehabilitation Engineering*, vol. 6, no. 1, pp. 75–87, 1998.

[5] R. Colombo, F. Pisano, S. Micera, A. Mazzone, C. Delconte, M. C. Carrozza, P. Dario, and G. Minuco, "Robotic techniques for upper limb evaluation and rehabilitation of stroke patients," *IEEE Transactions on Neural Systems and Rehabilitation Eng.*, vol. 13, no. 3, pp. 311–324, 2005.

[6] S. Hesse, G. Schulte-Tigges, M. Konrad, A. Bardeleben, and C. Werner, "Robot-assisted arm trainer for the passive and active practice of bilateral forearm and wrist movements in hemiparetic subjects," *Archives of physical medicine and rehabilitation*, vol. 84, no. 6, pp. 915–920, 2003.

[7] H. I. Krebs and N. Hogan, "Therapeutic robotics: A technology push," *Proceedings of the IEEE*, vol. 94, no. 9, pp. 1727–1738, 2006.

[8] http://www.stroke.org/site/pageserver?pagename=hemiparesis. [Online]. Available: http://www.stroke.org/site/PageServer?pagename=hemiparesis

[9] C. Dohle, J. Püllen, A. Nakaten, J. Küst, C. Rietz, and H. Karbe, "Mirror therapy promotes recovery from severe hemiparesis: a randomized controlled trial," *Neurorehabilitation and neural repair*, vol. 23, no. 3, pp. 209–217, 2009.

[10] A. Parton, P. Malhotra, and M. Husain, "Hemispatial neglect," *J. of Neurology, Neurosurgery & Psychiatry*, vol. 75, no. 1, pp. 13–21, 2004.

[11] H. Kim, L. M. Miller, I. Fedulow, M. Simkins, G. M. Abrams, N. Byl, and J. Rosen, "Kinematic data analysis for post-stroke patients following bilateral versus unilateral rehabilitation with an upper limb wearable robotic system," *IEEE Transactions on Neural Systems and Rehabilitation Engineering*, vol. 21, no. 2, pp. 153–164, 2013.

[12] A. R. Luft, S. McCombe-Waller, J. Whitall, L. W. Forrester, R. Macko, J. D. Sorkin, J. B. Schulz, A. P. Goldberg, and D. F. Hanley, "Repetitive bilateral arm training and motor cortex activation in chronic stroke: a randomized controlled trial," *The J. of the American Med. Association*, vol. 292, no. 15, pp. 1853–1861, 2004.

[13] M. E. Michielsen, M. Smits, G. M. Ribbers, H. J. Stam, J. N. van der Geest, J. B. Bussmann, and R. W. Selles, "The neuronal correlates of mirror therapy: an fMRI study on mirror induced visual illusions in patients with stroke," *J. of Neurol., Neurosurg. & Psychiat.*, vol. 82, no. 4, pp. 393–398, 2011.

[14] J. H. Cauraugh and J. J. Summers, "Neural plasticity and bilateral movements: a rehabilitation approach for chronic stroke," *Progress in neurobiology*, vol. 75, no. 5, pp. 309–320, 2005.

[15] J. J. Summers, F. A. Kagerer, M. I. Garry, C. Y. Hiraga, A. Loftus, and J. H. Cauraugh, "Bilateral and unilateral movement training on upper limb function in chronic stroke patients: a TMS study," *Journal of the neurological sciences*, vol. 252, no. 1, pp. 76–82, 2007.

[16] E. L. Altschuler, S. B. Wisdom, L. Stone, C. Foster, D. Galasko, D. M. E. Llewellyn, and V. S. Ramachandran, "Rehabilitation of hemiparesis after stroke with a mirror," *The Lancet*, vol. 353, no. 9169, pp. 2035–2036, 1999.

[17] J. A. Stevens and M. E. P. Stoykov, "Using motor imagery in the rehabilitation of hemiparesis," *Archives of physical medicine and rehabilitation*, vol. 84, no. 7, pp. 1090–1092, 2003.

[18] ——, "Simulation of bilateral movement training through mirror reflection: a case report demonstrating an occupational therapy technique for hemiparesis," *Topics in stroke rehabilitation*, vol. 11, no. 1, pp. 59–66, 2004.

[19] K. Sathian, A. I. Greenspan, and S. L. Wolf, "Doing it with mirrors: a case study of a novel approach to neurorehabilitation," *Neurorehabilitation and Neural Repair*, vol. 14, no. 1, pp. 73–76, 2000.

[20] P. Lum, C. G. Burgar, M. Van der Loos, P. Shor, M. Majmundar, and R. Yap, "The mime robotic system for upper-limb neuro-rehabilitation: results from a clinical trial in subacute stroke," in *9th International Conf. on Rehabilitation Robotics*, 2005, pp. 511–514.

[21] M. Shahbazi, S. F. Atashzar, H. A. Talebi, and R. V. Patel, "Novel cooperative teleoperation framework: Multi-master/single-slave system," *IEEE/ASME Transactions on Mechatronics*, vol. 20, no. 4, pp. 1668–1679, 2015.

[22] G. Ganesh, A. Takagi, R. Osu, T. Yoshioka, M. Kawato, and E. Burdet, "Two is better than one: Physical interactions improve motor performance in humans," *Scientific reports, Nature Pub. Group*, vol. 4, 2014.

[23] R. Prada and S. Payandeh, "A study on design and analysis of virtual fixtures for cutting in training environments," in *First Joint Eurohaptics Conference and Symposium on Haptic Interfaces for Virtual Environment and Teleoperator Systems, World Haptics*, 2005, pp. 375–380.

[24] B. Rohrer, S. Fasoli, H. I. Krebs, R. Hughes, B. Volpe, W. R. Frontera, J. Stein, and N. Hogan, "Movement smoothness changes during stroke recovery," *The J. of Neuroscience*, vol. 22, no. 18, pp. 8297–8304, 2002.

[25] C. R. Carignan and H. I. Krebs, "Telerehabilitation robotics: bright lights, big future?" *Journal of rehabilitation research and development*, vol. 43, no. 5, p. 695, 2006.

[26] S. F. Atashzar, I. G. Polushin, and R. V. Patel, "Networked teleoperation with non-passive environment: Application to tele-rehabilitation," in *IEEE/RSJ International Conference on Intelligent Robots and Systems*, 2012, pp. 5125–5130.

[27] A. Haddadi, K. Razi, and K. Hashtrudi-Zaad, "Operator dynamics consideration for less conservative coupled stability condition in bilateral teleoperation," *IEEE/ASME Transactions on Mechatronics*, vol. 20, no. 5, pp. 2463–2475, 2015.

[28] M. Dyck and M. Tavakoli, "Measuring the dynamic impedance of the human arm without a force sensor," in *Int. Conf. Rehab. Robotics*, 2013.

[29] N. Hogan, H. I. Krebs, B. Rohrer, J. J. Palazzolo, L. Dipietro, S. E. Fasoli, J. Stein, R. Hughes, W. R. Frontera, D. Lynch *et al.*, "Motions or muscles? some behavioral factors underlying robotic assistance of motor recovery," *Journal of rehabilitation research and development*, vol. 43, no. 5, p. 605, 2006.

[30] M. Ferraro, J. Palazzolo, J. Krol, H. Krebs, N. Hogan, and B. Volpe, "Robot-aided sensorimotor arm training improves outcome in patients with chronic stroke," *Neurology*, vol. 61, no. 11, pp. 1604–1607, 2003.

[31] A. U. Pehlivan, F. Sergi, and M. K. OMalley, "A subject-adaptive controller for wrist robotic rehabilitation," *IEEE/ASME Transactions on Mechatronics*, vol. 20, no. 3, pp. 1338–1350, 2015.

[32] A. R. Fugl-Meyer, L. Jääskö, I. Leyman, S. Olsson, and S. Steglind, "The post-stroke hemiplegic patient. 1. a method for evaluation of physical performance." *Scandinavian journal of rehabilitation medicine*, vol. 7, no. 1, pp. 13–31, 1974.

[33] J. H. Carr, R. B. Shepherd, L. Nordholm, and D. Lynne, "Investigation of a new motor assessment scale for stroke patients," *Physical therapy*, vol. 65, no. 2, pp. 175–180, 1985.

[34] C. Collin and D. Wade, "Assessing motor impairment after stroke: a pilot reliability study." *Journal of Neurology, Neurosurgery & Psychiatry*, vol. 53, no. 7, pp. 576–579, 1990.

[35] A. L. Trejos, "A sensorized instrument for minimally invasive surgery for the measurement of forces during training and surgery: development and applications," *Western University*, 2012.

[36] M. Shahbazi, H. A. Talebi, S. F. Atashzar, F. Towhidkhah, R. V. Patel, and S. Shojaei, "A novel shared structure for dual user systems with unknown time-delay utilizing adaptive impedance control," in *2011 IEEE Int. Conf. on Robotics and Automation*, 2011, pp. 2124–2129.

[37] I. Polushin, H. J. Marquez, A. Tayebi, and P. X. Liu, "A multichannel IOS small gain theorem for systems with multiple time-varying communication delays," *IEEE Transactions on Automatic Control*, vol. 54, no. 2, pp. 404–409, 2009.

[38] H. K. Khalil and J. Grizzle, *Nonlinear systems*. Prentice Hall, Upper Saddle River, 2002, vol. 3.

[39] N. Miandashti and M. Tavakoli, "Stability of sampled-data, delayed haptic interaction and teleoperation," in *2014 IEEE Haptics Symposium*, 2014, pp. 215–220.

Chapter 6

Multimodal Sensorimotor Integration for Expert-in-the-Loop Telerobotic Surgical Training

The material presented in this chapter has been submitted for publication in IEEE Transactions on Robotics (TRO), 2016.

6.1 INTRODUCTION

Robotics-Assisted Minimally Invasive Surgery (RAMIS) has emerged during the last few decades, building on the advantages of Minimally Invasive Surgery (MIS), while addressing several challenges facing traditional MIS. Besides the benefits provided to patients, i.e., less post-operative pain and significantly faster recovery time as result of reduced trauma, and improved cosmesis, RAMIS also offers several advantages to surgeons by 1) improving dexterity in manipulating surgical instruments, 2) providing High-Definition (HD) stereovision capabilities, 3) filtering out their hand tremor, and 4) scaling down their hand motions resulting in enhanced precision [1], [2]. The improved dexterity and precision offered by RAMIS enables surgeons to perform operations that would previously have been difficult to perform via conventional MIS, especially for morbidly-obese patients [3]. The *da Vinci*® surgical system [4] is the first FDA-approved RAMIS system and is used in more than 500,000 procedures annually [5].

While RAMIS offers significant advantages, it could be challenging for novice surgeons and residents to perform, and achieving technical competence requires a well-planned learning strategy. For successful RAMIS, effective surgical training is necessary for novices to acquire appropriate psychomotor skills [6]. There have been several RAMIS-related adverse events reported to the FDA during the past 15 years [7]. One reason cited for this is a lack of proper training; affirming the necessity of developing appropriate RAMIS training frameworks.

In order to provide on-demand training to RAMIS trainees, robotic surgery simulators have been developed, e.g., RoSS™ (Simulated Surgical Systems, LLC) [8], RobotiX Mentor™ (3D Systems, Inc.) [9], and dV-Trainer® [10]. The simulators interface with a Virtual Reality (VR) environment and provide task-based (e.g. ring transfer and suturing) and procedure-based training modules [5]. Although simulators can serve as a bridge between preclinical and clinical training, they still fall short of providing realistic tissue-behavioral characteristics [11].

By development of the dual-console *da Vinci® Si* surgical system [12], a new teaching paradigm has evolved, which addresses questions that normally arise regarding fidelity of the VR-based simulation environment by enabling a trainee to be involved in an actual surgical procedure. This system offers two master consoles, each manipulated individually by a surgeon, one of which can be a trainee. However, at each time, the slave console receives commands only from one master console. Therefore, to involve the trainee in the procedure, it is required to switch from the expert's console to the trainee's. Therefore, when the trainee has control over the procedure, the expert does not have any authority over the surgery, which may increase potential risks to the patient. This constraint is mainly imposed due to the inherent Single-Master/Single-Slave (SM/SS) structure of the system. Although two master consoles are incorporated into the system, the whole framework is a combination of two SM/SS systems independently working in series/parallel, rather than a cohesive and integrated Dual-Master/Single-Slave framework.

Moreover, the dual-console *da Vinci® Si* system provides the training based on a *see-and-repeat* model [12], with no direct supervision and control on the trainee through haptic-based interaction between the expert and the trainee. Haptics-based interaction with a partner when learning a motor task has been proved highly effective in enhancing the motor skills as compared to practicing the task alone for the same duration [13].

Haptic interaction between an expert and a trainee could also provide an effective approach to deliver real-time feedback to the trainee. As Fitts and Posner proposed [14], there are three phases involved in acquisition of any motor skill: 1) cognitive phase, in which the learner intellectualizes the task and understands the mechanics of the skill; 2) integrative phase, in which knowledge is translated into appropriate motor behavior, yet with lack of fluidity; and 3) autonomous phase, in which independent learning occurs with no supervision or guidance, and smooth performance evolves [15]. During the integrating phase, in which the trainee develops motor behaviors, coaching and immediate feedback must accompany performance in order to avoid acquisition of incorrect motor habits, as undesirable motor patterns are difficult to eliminate once they are established. In fact, there is little benefit but great potential side-effect for a trainee to practice a task without receiving proper real-time feedback, i.e., knowing if they are performing correctly and what they must perform differently [16].

Providing the trainee with solely verbal feedback or a *see-and-repeat* guidance/instruction from an expert may have limited effectiveness; since the expert no longer views the task as an intellectual problem broken down into steps, while the learner may not have achieved adequate proficiency to perceive the important elements of the expert motion through merely observation. Therefore, the expert may not be able to verbalize the guidance beyond a global statement, while visual demonstration of the expert movement may not be sufficiently enlightening for the trainee [16]. Furthermore, the *see-and-repeat* approach is only suitable for trainees who have enough level of expertise to perform the procedure, at least partially, on their own. In fact, they should possess a reasonably high level of motor skills to qualify to operate the surgical system. This makes it insufficient for less-skilled trainees.

Therefore, in this chapter an Expert-In-the-Loop (EIL) haptics-enabled training framework is proposed for dual-console surgical robotic systems to deliver feedback and guidance through a fusion of multiple sensorimotor modalities, rather than a stand-alone vision modality. The framework includes a Fuzzy Interface System (FIS) to provide the trainee with expertise-oriented guidance, such that the more expertise the trainee shows, the lower level of haptic guidance will be provided. The proposed expertise-oriented framework can be used by trainees at any stage of motor-skills development without jeopardizing patient safety.

Another safety aspect that must be ensured in any haptics-enabled teleoperation system

is closed-loop stability to guarantee safe and reliable human-robot interaction [17]. Therefore, closed-loop stability of the framework is investigated using the Circle Criterion and it is shown that the proposed framework is *unconditionally* stable. The framework is implemented on a dual-console surgical system consisting of a classic *da Vinci*® surgical system and a dV-Trainer®. As indicated by several studies, the dV-Trainer® provides the look and feel of the *da Vinci*® master console [10], and together with the classic *da Vinci*® surgical system, they provide the key features of a dual-console surgical robotic system in terms of workspace, number of Degrees-Of-Freedom (DOFs) and user interface. Experimental evaluations are given in three separate scenarios in support of the proposed platform.

Remark: *To the best knowledge of the authors, the implemented setup serves as 1) the first research platform for dual-console studies and development on the classic da Vinci® surgical system, and 2) the first haptics-enabled training platform based on HOH guidance/cueing for such a system.*•

The rest of the chapter is organized as follows: Section 6.2 presents the overall framework with multimodal sensorimotor integration for dual-console surgical robotic systems. Section 6.3 discusses the adaptive adjustment process of a trainee's level of engagement in terms of their authority over the procedure and the haptic guidance provided based on their level of proficiency in real-time. Section 6.4 presents a stability analysis for the closed-loop system. Experimental results are given in Section 6.5. Sections 6.6 and 6.7 discuss two further extensions, and Section 6.8 concludes the chapter.

6.2 Sensorimotor Integration for Dual-Console Surgical Robotic Systems

Kinesthetic Hand-Over-Hand (HOH) guidance can be applied to trainees' hands in order to teach them the optimal movement synergies required for performing a task without "wasting movements". Teaching optimal synergies from early stages of surgical robotic skills acquisition, before the trainee establishes incorrect or inefficient movements and motor habits that could be difficult to unlearn, can speed up the learning process while decreasing the practice-related fatigue [16].

The presence of an expert in the loop, realized through the dual-console framework (such as the *da Vinci® Si* surgical system) can provide an appropriate desired reference of the movement synergy for the trainee. Therefore, as a result of the proposed EIL architecture, without requiring any task prediction or any *a priori* information about the surgical task, the trainee can receive real-time kinesthetic HOH guidance along with the visual cues already available on the dual-console system. A possible realization of the HOH guidance force, f_Γ, applied to the trainee's hands through the corresponding master console is defined as follows:

$$f_\Gamma(t) = k_\Gamma(t)(x_E(t) - x_T(t)) \tag{6.1}$$

where x_T and x_E refer to the trajectories of the master consoles manipulated by the trainee and the expert, respectively; x_E serves as the real-time desired trajectory for the trainee; $k_\Gamma \in [0, \kappa]$ indicates the stiffness of the "virtual elastic bond" between the trainee's and the expert's hands, based on which the trainee is cued to follow the optimal motion of the expert. Also, κ is the maximum level of k_Γ, the variation profile of which can be set in real-time based on the expertise level of the trainee, as discussed in the next section. The more skilled the trainee is, the less the level of HOH guidance provided to preserve their freedom of motion. It should be noted that the HOH guidance induces a 1-way haptic interaction (from the expert to the trainee) that does not affect surgical performance and movements of the expert surgeon, and therefore does not impose any risk with regard to patient safety.

Depending on the skills level of the trainee, it may also be desirable for the expert in the loop to provide a sufficiently skilled trainee with some level of control over the surgical procedure in order to speed up the trainee's learning process. The current architecture of the dual-console *da Vinci® Si* system allows either zero or full transfer of control over the slave console to the trainee, i.e., $x_{S,Des}(t) = x_E(t)$ or $x_{S,Des}(t) = x_T(t)$, respectively; where $x_{S,Des}$ refers to the desired trajectory of the slave manipulator. A more general and flexible configuration would be to provide the trainee with partial authority over the procedure, so that the expert's continuous involvement is preserved:

$$x_{S,Des}(t) = \alpha_E(t) \cdot x_E(t) + \alpha_T(t) \cdot x_T(t) \tag{6.2}$$

where $0 \leq \alpha_E \leq 1$ and $0 \leq \alpha_T \leq 1$ denote the authority level (dominance factor) over the slave console for the expert and the trainee, respectively, such that $\alpha_E + \alpha_T = 1$. This configuration keeps the expert involved in the loop of surgery while the sufficiently skilled trainee performs a part of the surgical operation. The authority level of the trainee can be either set directly by the expert, or adapted automatically based on the trainee's level of expertise, as elaborated in the next section. Note that two special cases of (6.2) would be to have: 1) $\alpha_E = 1$, $\alpha_T = 0$, and 2) $\alpha_E = 0$, $\alpha_T = 1$. These cases provide the trainee with zero and full authority over the slave console, respectively, which are the only two configurations available in the current architecture of the *da Vinci® Si* system.

Through the proposed framework, a trainee can benefit in several ways:

1. real-time feedback as a result of the expert-in-the-loop configuration;
2. sensorimotor integration by incorporating haptic modality with the visual modality;
3. progressive training through the adaptive expertise-oriented scheme.

6.3 Adaptive Expertise-Oriented Engagement

In the previous section, an overview of the proposed framework was presented. In this section, the adjustment process for the stiffness of the HOH force provided to the trainee, k_Γ, as well as their level of control over the operation, α_T, based on the trainee's level of proficiency will be discussed. Although this process can also be manually performed in an offline manner by the expert, online adaptation of the parameters helps engage the trainee in an intermittent interaction, which has been shown to significantly enhance and speed up motor learning [13]. *Automatic*, yet *supervised*, adaptation of k_Γ and α_T facilitates their real-time adjustment without imposing an extra processing burden on the expert surgeon in the loop. Therefore, to incorporate the element of the expert's supervision into the automatic online adaptation process, the adjustment profiles of k_Γ and α_T are defined as follows:

$$\alpha_T(t) = \zeta \cdot \hat{\alpha}_T(t) \tag{6.3}$$

$$k_\Gamma(t) = \kappa \cdot \hat{k}_\Gamma(t) \tag{6.4}$$

where $0 \leq \hat{\alpha}_T(t) \leq 1$ and $0 \leq \hat{k}_\Gamma(t) \leq 1$ denote the adaptive elements of the online adjustment process. In addition, $0 \leq \kappa$ and $0 \leq \zeta \leq 1$ are supervisory elements set by the expert surgeon, which enable the expert to confine α_T and k_Γ within his/her preferable range. Unlike the adaptive elements which are automatically updated in real-time, the supervisory elements can be adjusted offline or at much lower rates, so that the expert is not burdened with unnecessary multitasking. In order to adjust the adaptive elements ($\hat{\alpha}_T$ and $\hat{k}_\Gamma$) based on the trainee's level of proficiencies, an FIS is designed as described below. Fuzzy Logic (FL) provides a powerful flexible approach in dealing with the imprecision, vagueness and subjectivity of surgical motor-skills assessment [18].

6.3.1 Task-Independent Skills Assessment

The first step in the development of the expertise-oriented FIS is to assess the trainee's proficiency level objectively and in real-time. Since it is not possible to quantitatively express the desired maneuvers of a complex and multi-step surgical operation in advance, using the traditional absolute assessment approaches, a desired quantitative performance cannot be determined with respect to which the trainee's performance can be assessed. Therefore, the skills assessment approach should be task-independent, yet objective, so that it can be used in real-time surgical scenarios. Having an expert in the loop as a result of the dual-console framework, the performance of the expert serves as a desired reference for the trainee in real-time. For this purpose, a normalized task-independent metric, Φ, is defined, based on which the performance of the trainee can be determined in relation to that of the expert in the loop.

$$\Phi_\Delta(t) = 1 - \left| \frac{\Delta_E(t) - \Delta_T(t)}{\Delta_E(t) + \Delta_T(t)} \right| \tag{6.5}$$

where Δ_E and Δ_T denote absolute skills-assessment metrics calculated for the expert and the trainee, individually. The absolute metric, Δ, can be any of the existing quantitative gold-standard metrics in the literature, two of which are used in this chapter, as described below.

Total Path Length (TPL)

denotes the length of the curved path traversed by the operator's hand, which is equal to the TPL traveled by her/his corresponding master manipulator. To perform a similar task, in contrast with that performed by a novice, an expert will have a smaller TPL due to optimized movement characteristics and coordination. The TPL, ρ, for an operator is calculated as follows [19]:

$$\rho_{\nu} = \int_0^t \sqrt{\left(\frac{dx_{\nu,x}}{d\tau}\right)^2 + \left(\frac{dx_{\nu,y}}{d\tau}\right)^2 + \left(\frac{dx_{\nu,z}}{d\tau}\right)^2} d\tau \tag{6.6}$$

where ρ_E $(\nu = E)$ and ρ_T $(\nu = T)$ denote the TPL for the expert and the trainee respectively; subscripts x, y and z refer to position elements along x, y and z directions respectively. Having ρ_E and ρ_T calculated for the expert and trainee in real time, the normalized TPL can be calculated for the trainee relative to that of the expert using (6.5), as follows:

$$\Phi_{\rho}(t) = 1 - \left|\frac{\rho_E(t) - \rho_T(t)}{\rho_E(t) + \rho_T(t)}\right| \tag{6.7}$$

which provides an online task-independent measure for the trainee's performance.

Motion Smoothness (MS)

can be quantified based on the time-integrated squared jerk, where jerk refers to the third derivative of the manipulator's end-effector position. Maximally smooth movements have minimal time-integrated jerks, which makes the metric appropriate for quantitative skills assessment [19], [20]. The metric representing MS, δ, is defined as follows:

$$\delta_{\nu} = \int_0^t \sqrt{\left(\frac{d^3x_{\nu,x}}{d\tau^3}\right)^2 + \left(\frac{d^3x_{\nu,y}}{d\tau^3}\right)^2 + \left(\frac{d^3x_{\nu,z}}{d\tau^3}\right)^2} d\tau \tag{6.8}$$

Calculating δ_E $(\nu = E)$ and δ_T $(\nu = T)$ for the expert and the trainee and incorporating them into (6.5) gives the normalized MS for the trainee relative to that of the expert as follows:

$$\Phi_{\delta}(t) = 1 - \left|\frac{\delta_E(t) - \delta_T(t)}{\delta_E(t) + \delta_T(t)}\right| \tag{6.9}$$

Level Of Guidance (LOG)

The same process can be repeated in order to task-independently normalize any quantitative *performance* metric for the trainee relative to that of the expert. This relative approach of performance assessment specifies how closely the trainee has been able to follow the desired trajectory generated by the expert. In order to determine whether a good performance of the trainee has been due to the trainee's actual proficiency over the task or resulted from the presence of HOH haptic guidance, a linear metric based on the LOG provided to the trainee is also incorporated into the skills assessment process. The LOG metric, Φ_η, determines how attentively the trainee has followed guidance cues provided to their hand through the HOH haptic force.

$$\Phi_\eta = \begin{cases} 1 - \dfrac{f_\Gamma}{f_\kappa} & \text{if } f_\Gamma \leq f_\kappa; \\ 0 & \text{if } f_\Gamma > f_\kappa. \end{cases} \tag{6.10}$$

where f_κ denotes the maximum level of HOH force to be applied to the trainee's hand.

6.3.2 The Fuzzy Interface System Design

In order to adjust the adaptive elements of the architecture, $\hat{\alpha}_T(t)$, $\hat{k}_\Gamma(t)$, based on the proficiency level of the trainee, an FIS is designed. The FIS fuses and utilizes the three proficiency assessment metrics (Φ_ρ, Φ_δ and Φ_η) as inputs in order to adaptively update $\hat{\alpha}_T(t)$, and $\hat{k}_\Gamma(t)$ in real time. For this purpose, the proficiency level of a trainee is categorized into four divisions: 1) Beginner, 2) Intermediate, 3) Advanced, and 4) Skilled (BIAS).

Moving from a beginner trainee to a skilled trainee, the FIS should increase the adaptive portion of the trainee's authority level over the task, $\hat{\alpha}_T(t)$. Note that according to (6.3), the overall authority level of the trainee, α_T, is restricted to the maximum allowable level set by the expert, ζ, which retains the expert's desirable authority level over the operation to ensure patient safety.

The FIS should also provide a higher level of HOH guidance to a beginner, compared to an intermediate/advanced trainee, by increasing the adaptive portion of the HOH stiffness, $\hat{k}_\Gamma(t)$, while decreasing the LOG for trainees with higher proficiency levels. Note that according to (6.4), the overall stiffness of the HOH guidance, $k_\Gamma(t)$, is limited by the maximum allowable

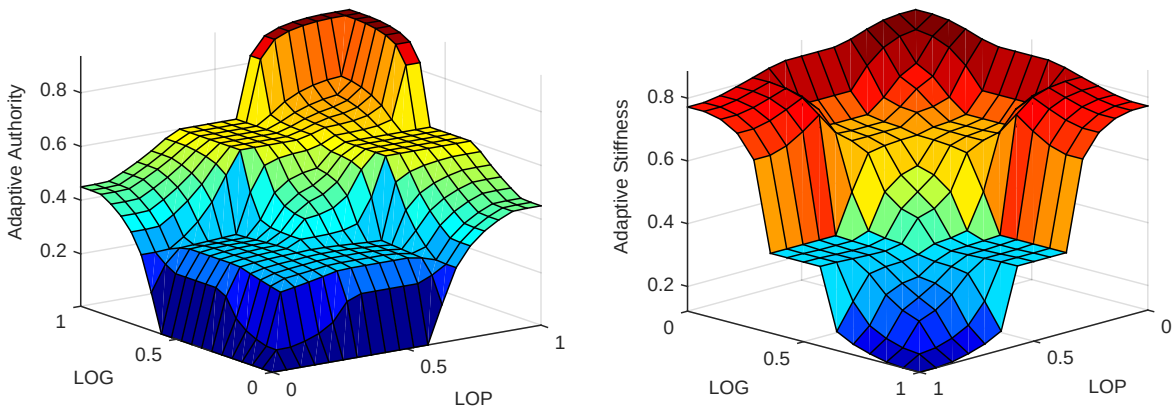

Figure 6.1: The FIS output surfaces with respect to inputs LOP and LOG- Left: $\hat{\alpha}_T$, Right: $\hat{k}_\Gamma$.

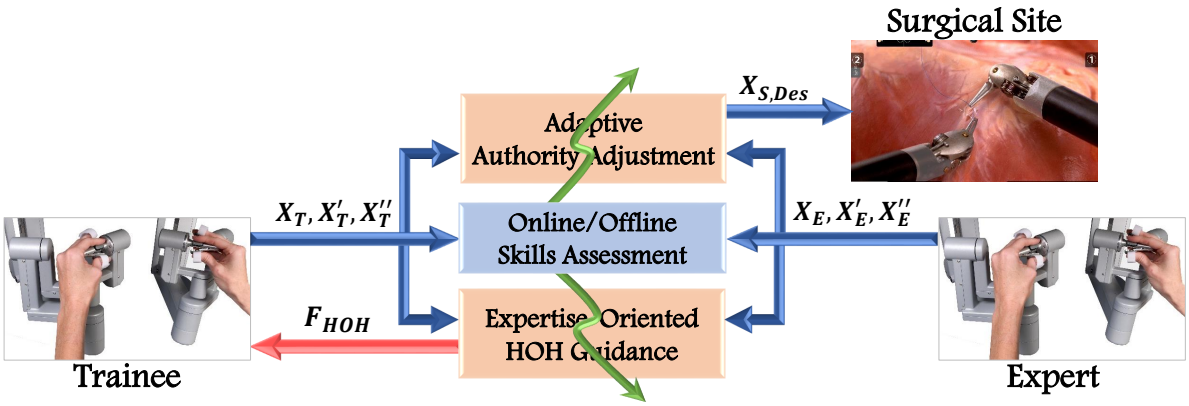

Figure 6.2: The overall scheme of the closed-loop system in the absence of tool-tissue interaction haptic feedback. Image derived from photographs of masters and EndoWrist™-Instruments provided by Intuitive Surgical, Inc. [©2006].

stiffness level set by the expert, κ, while the FIS specifies its adaptive variation profile, $\hat{k}_\Gamma(t)$.

To accomplish the requirements desired for the training system, the fuzzy rules are defined as follows:

- If the trainee level is Beginner, significantly decrease $\hat{\alpha}_T(t)$ and significantly increase $\hat{k}_\Gamma(t)$;
- If the trainee level is Intermediate, slightly decrease $\hat{\alpha}_T(t)$ and slightly increase $\hat{k}_\Gamma(t)$;
- If the trainee level is Advanced, slightly increase $\hat{\alpha}_T(t)$ and slightly decrease $\hat{k}_\Gamma(t)$;
- If the trainee level is Skilled, significantly increase $\hat{\alpha}_T(t)$ and significantly decrease $\hat{k}_\Gamma(t)$.

To design the FIS, the MATLAB Fuzzy Logic Toolbox is used. An average sum of the two performance metrics Φ_ρ and Φ_δ along with Φ_η are fuzzified as the inputs of the FIS using "Trapezoidal-shaped" and "Triangular-shaped" membership functions. The same membership functions are also used for the purpose of defuzzification at the output. Note that Φ_ρ and Φ_δ are combined into a single input, quantifying the performance level of the trainee, called the Level Of Performance (LOP), while LOG (Φ_η) is used as the second input in parallel to indicate if a skilled behavior of the trainee is a result of their good performance or due to the presence of HOH guidance. Using the average/weighted summation of *performance* metrics as a single input allows for straightforwardly integrating other quantitative performance metrics into the process without the necessity of redesigning the FIS. The resulting output surfaces with respect to the two inputs LOP and LOG are shown in Fig. 6.1.

6.4 Closed-Loop Stability Analysis

Fig. 6.2 illustrates the overall scheme of the proposed framework. As can be seen, there is a feedback loop at the trainee's side, the effect of which on stability of the overall system should be investigated. Ensuring closed-loop stability in any haptics-enabled teleoperation system is a necessity in order to guarantee the safety and reliability of the human-robot interaction [21]. Therefore, in this section, closed-loop stability of the framework is analyzed.

The dynamics of a trainee's arm can be modeled by a second-order system as follows [22]:

$$\begin{aligned} f_\Upsilon(t) = f_T^*(t) - M_T \cdot \ddot{x}_T(t) - B_T \cdot \dot{x}_T(t) \\ -K_T \cdot (x_T(t) - x_{T_0})) \end{aligned} \tag{6.11}$$

where f_Υ refers to the force applied by the trainee at his/her corresponding master console, and $f_\Upsilon = -f_\Gamma$; f_T^* denotes the exogenous force applied by the trainee; M_T, B_T and K_T stand for the mass, damping and stiffness of the trainee's hand respectively; and x_{T_0} indicates the initial position of the trainee's hand, x_T.

Combining (6.1) and (6.11) , the resulting system at the trainee side is shown in Fig. 6.3. The closed-loop system is a feedback connection of the linear dynamical system $Z_T^{-1}(s)$ and the nonlinear time-varying element $K_\Gamma(t)$, the stability of which can be analyzed using the

Circle Criterion. The Circle Criterion is an appropriate analysis tool for linear systems subject to a nonlinear feedback element [23]. In Fig. 6.3, $Z_T(s)$ denotes the impedance characteristics of the trainee's hand in the Laplace domain, such that $Z_T(s) = M_T s^2 + B_T s + K_T$; where s indicates the Laplace Transform variable.

Theorem I [23]: *The feedback connection of a linear dynamical system $G(s)$ and a nonlinear element ξ is stable if for $\xi \in [\xi_1, \xi_2]$, with $\xi_2 - \xi_1 > 0$, $[I + \xi_2 G(s)][I + \xi_1 G(s)]^{-1}$ is Strictly Positive Real (SPR).*•

Considering that $K_\Gamma \in [0, \kappa]$ and based on Theorem I, the feedback system, from output x_T to input $f_T^* + K_\Gamma x_E$, is stable if $[I + \kappa Z_T^{-1}(s)]$ is SPR. We also need the following definitions:

Definition I [23]: *The transfer matrix $H(s)$ is SPR if $H(s - \varepsilon)$ is Positive Real (PR) for some $\varepsilon > 0$.*•

Definition II [23]: *The transfer matrix $H(s)$ is PR if:*

- *the poles of all elements of $H(s)$ are in $Re(s) < 0$*
- *for all real ω for which $j\omega$ is not a pole of $H(s)$, $H(s) + H^T(-s)$ is positive semi-definite, and*
- *any pure imaginary pole $j\omega$ of $H(s)$ is a simple pole and the residue $lim_{s \to j\omega}(s - j\omega)H(s)$ is positive semi-definite Hermitian.*•

Considering that $0 < \kappa$, and $Z_T(s) = M_T s^2 + B_T s + K_T$ denotes the impedance characteristics of the trainee's hand such that M_T, B_T and $K_T > 0$, the first and the third conditions of strictly positive realness are automatically satisfied for $[I + \kappa Z_T^{-1}(s)]$. In order for the second condition to be satisfied, $[I + \kappa Z_T^{-1}(s)] + [I + \kappa Z_T^{-1}(-s)]^T$, which can be simplified to (6.12),

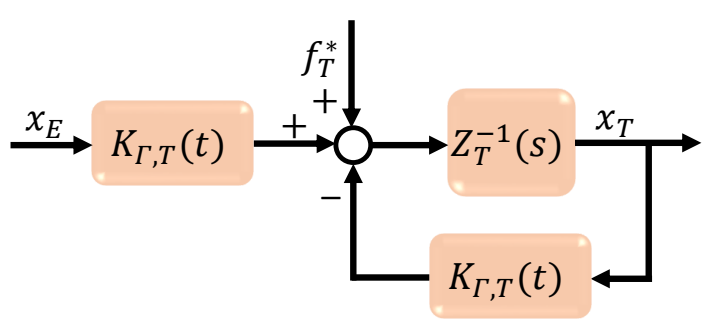

Figure 6.3: The closed-loop system at the trainee side.

should be Positive Semi-Definite (PSD).

$$\begin{aligned}
&[I+\kappa Z_T^{-1}(s)]+[I+\kappa Z_T^{-1}(-s)]^T = \\
&[I+\kappa Z_T^{-1}(s)]+[I^T+\kappa Z_T^{-T}(-s)] = \\
&2I+\kappa(Z_T^{-1}(s)+Z_T^{-T}(-s))
\end{aligned} \tag{6.12}$$

Assuming that the admittance characteristic of the human hand, Z_T^{-1}, is an SPR system, $Z_T^{-1}(s)+Z_T^{-T}(-s)$ is a PSD matrix; which, considering that $0<\kappa$, implies that (6.12) is PSD, as well. Hence, all the conditions in Theorem I are satisfied and the closed-loop system shown in Fig. 6.3 is stable. Note that f_T^* and x_E are the trainee's exogenous force and the expert-generated position, respectively, which are bounded signals; and considering that $K_\Gamma \in [0,\kappa]$, $f_T^*+K_\Gamma x_E$ is a bounded input to the system. This guarantees boundedness of x_T in the presence of HOH guidance. Satisfying (6.2) for the slave console, and considering that $0 \leq \alpha_E$, $\alpha_T \leq 1$, boundedness of $x_{s,Des}$ is also guaranteed, which implies *unconditional* stability of the proposed framework.

Remark: *The admittance characteristic of the human arm in the velocity-force domain is an SPR system. In position-force domain, there exists a frequency-dependent condition on the arm's characteristics for the human arm to remain SPR. However, in most telerobotic applications, including surgical, the frequencies of motions generated by operators are normally below the natural frequency of their arm characteristic. By considering this assumption, the admittance characteristic of the human arm in the position-force domain is also an SPR system.*•

6.5 Experimental Evaluations

6.5.1 Setup Design and Implementation

To evaluate the proposed framework, a dual-console platform was set up. The platform consists of 1) a first generation *da Vinci*® surgical robotic system, integrated with the *da Vinci*® Research Kit (dVRK) motor controllers (by Johns Hopkins University, Baltimore, MD; Worcester Polytechnic Institute, Worcester, MA; and Intuitive Surgical, Inc., Sunnyvale, CA, USA) [24]; and 2) a dV-Trainer® console. The dV-Trainer® provides the look and feel of the *da Vinci*® master console [10], and together with the *da Vinci*® result in a dual-console RAMIS system

in terms of workspace, number of DOFs and user interface. In addition to haptics-enabled training based on HOH guidance/cueing, the implemented setup also provides an appropriate research and development testbed for the dual-console surgical robotic systems, including the *da Vinci*® *Si* system.

In this setup, each of the *da Vinci*'s two Master Tool Manipulators (MTMs) and two Patient Side Manipulators (PSMs) are connected to an individual dVRK motor controller, consisting of a pair of Quad Linear Amplifiers (QLAs) and IEEE-1394 FPGA boards [24]. The dVRK enables us to transmit force commands to the MTMs. This results in the MTMs being haptic-enabled. High level control computations are performed on a Linux computer which communicates with the motor controllers via a low-latency Firewire (IEEE-1394a) bus. The application software for dVRK is written in C++ using the component-based *cisst* libraries [25] and the Surgical Assistant Workstation (SAW) package [26].

Fig. 6.4 illustrates the experimental setup along with the schematic connections between components. In this figure, Computer I is responsible for interfacing with the dV-Trainer® using a C++ API provided by Mimic Technologies. Computer I also serves as the processing core for the proposed framework, on which the adaptive FIS-based parameters are generated in MATLAB Simulink integrated with Quarc real-time software (by Quanser Inc.). Computer II runs a modified version of the dVRK teleoperation application and interfaces with the dVRK motor controllers. The modified dVRK teleoperation application runs at a sampling rate of 500Hz, where at each sample the Cartesian position of both the MTMs and PSMs as well as the gripper and pedal states of the MTMs and grasper angle of the PSMs are measured and sent to Computer I. This information along with that received from the dV-Trainer® is processed by the FIS-based processing core on Computer I. The resulting desired position for the PSMs and the desired HOH force are re-transmitted to Computer II. When received, the former (position) is set by the original dVRK teleoperation control implementation as the desired position for the PSMs, while the latter (force) is mapped and applied to the haptics-enabled MTMs. The two computers communicate via the User Datagram Protocol (UDP) over a Local Area Network (LAN). VGA multiplexers are used to share the endoscopic cameras' outputs between the stereo viewers on the two master consoles. In this configuration, the *da Vinci*® master console was utilized as the trainee's console, while the dV-Trainer® was used as the expert's console.

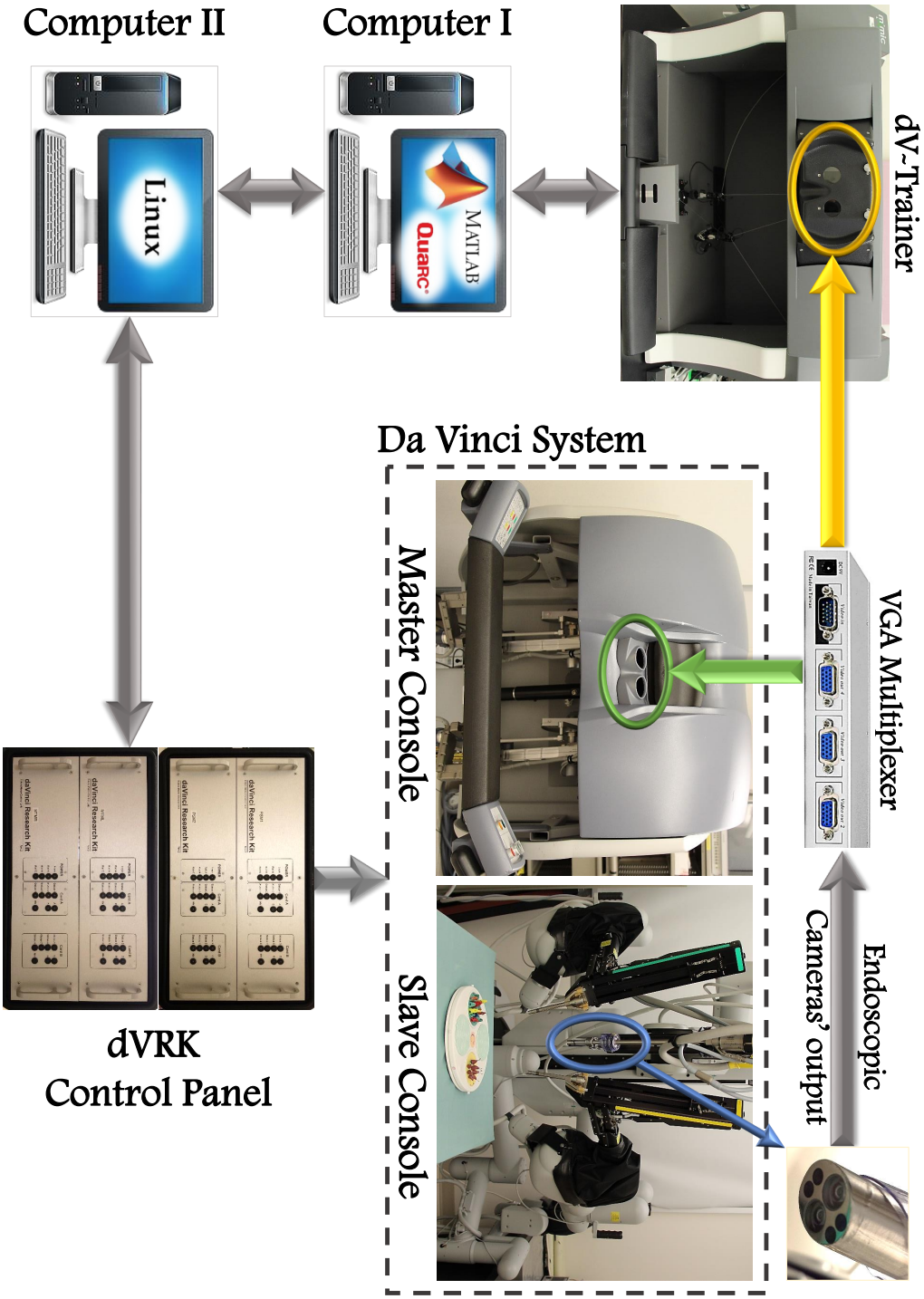

Figure 6.4: The experimental platform.

6.5.2 Experimental Results

In order to evaluate various aspects of the framework, three sets of experiments were conducted. The experiments, discussed below, examine the architecture when the trainee is given zero, constant and time-varying adaptive authority levels over the task, respectively.

Scenario I

This experiment evaluates the adaptation process of the HOH guidance provided to the trainee, while the expert has full control over the procedure. This mode allows training a *novice* trainee concurrently with the performance of a surgical procedure by an expert surgeon, without jeopardizing patient safety due to the trainee's inexpertise. For this purpose, it is sufficient to set ζ, the expert's supervisory element over the trainee's authority level, to zero, resulting in $\alpha_T = 0$ and $\alpha_E = 1$. In order to study the behavior of the system in various situations, the experiment was conducted in three phases:

Phase #1 $(t = 0 - 50s)$**:** the trainee was asked to simulate skilled behavior by following the desired trajectory also followed by the expert.

Phase #2 $(t = 55 - 110s)$**:** the trainee was asked to follow the desired trajectory not very accurately, but with some errors, while paying moderate attention to the HOH force provided to him and allowing the HOH force to guide him to *some extent*.

Phase #3 $(t = 115 - 165s)$ the trainee was asked to simulate unskilled behavior by keeping his master console at a fixed location, while completely ignoring the desired trajectory generated by the expert or the HOH guidance provided to him.

In this experiment, κ was set to 250 N/m as the maximum allowable level of HOH stiffness. The results are given in Fig. 6.5. Fig. 6.5a shows the trajectories in the Y direction for the expert's and the trainee's master consoles as well as the desired trajectory generated for the slave console. As can be seen in this figure, in all three phases and as a result of $\alpha_E = 1$, the slave robot followed the expert's trajectory regardless of the level of expertise shown by the trainee. Fig. 6.5b shows the three normalized proficiency metrics Φ_ρ, Φ_δ and Φ_η calculated for the trainee in real-time. As can be seen, in the first phase of the experiment, when the trainee was behaving as an expert, all three measures refer to his high level of expertise. During the second phase, a slight reduction of Φ_ρ, Φ_δ can be seen as a result of small errors generated by the

trainee, while they still refer to an acceptable level of performance for him. However, Φ_η has dropped considerably during the second phase. Comparing the first and the second phases, this indicates that although the trainee has shown quite similar levels of performance (in terms of trajectory tracking) in both phases, his good performance during the first phase has been as a result of his expertise, while he has relied more on the HOH guidance force during the second phase in order to retain his performance level. During the third phase of the experiment, all three metrics dropped considerably, as the trainee completely ignored the expert's trajectory and the HOH guidance force.

Fig. 6.5c illustrates the adaptive HOH stiffness generated by the FIS for the trainee according to his proficiency level during the experiment. As can be seen in this figure, the lowest and the highest levels of stiffness were set for the trainee during the first and the last phases, respectively, while providing him with a moderate level of assistance during the second phase.

Scenario II

This experiment investigates the effect of a constant authority level for the trainee and illustrates how undesirable a non-adaptive approach could be. For this purpose, the trainee's authority level, α_T, was set to 0.5, allocating equal levels of control over the task for the trainee and the expert. The experiment was conducted in three phases, as describe below:

Phase #1 $(t = 0 - 60s)$**:** The expert was asked to generate the desired trajectory as an oval-shape path traversed four times. The trainee's role was defined to simulate a proficient performance by following the desired trajectory generated by the expert.

Phase #2 $(t = 60 - 110s)$**:** The trainee was asked to simulate a non-expert by following a trajectory completely different from that of the expert in the loop. The trainee was instructed to move his hand at a normal pace.

Phase #3 $(t = 110 - 165s)$**:** The trainee was asked to repeat the actions of Phase #2, but also generate non-smooth and abrupt movements in order to exaggerate undesirable movements.

Fig. 6.6 shows 2D representation of trajectories in the X-Y plane. As can be seen, during the first phase, the slave manipulator followed the average of the expert's and the trainee's trajectories. During the second phase, the trainee created smaller trajectories than the desired

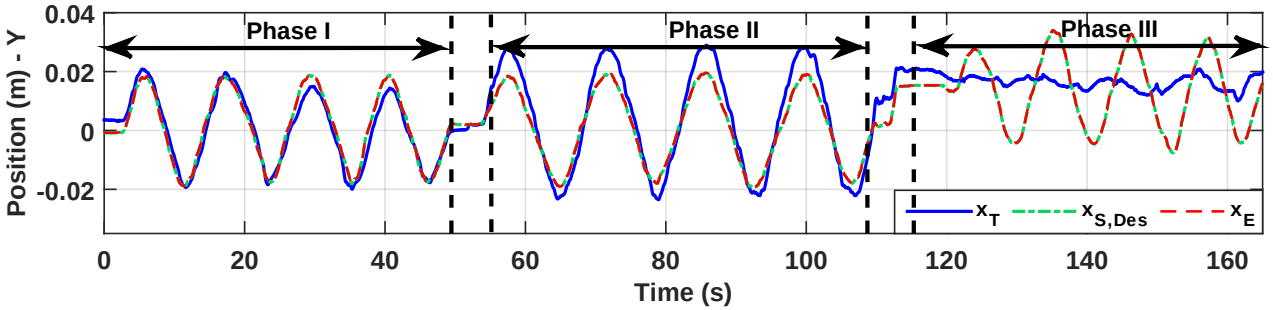

(a) Position comparison

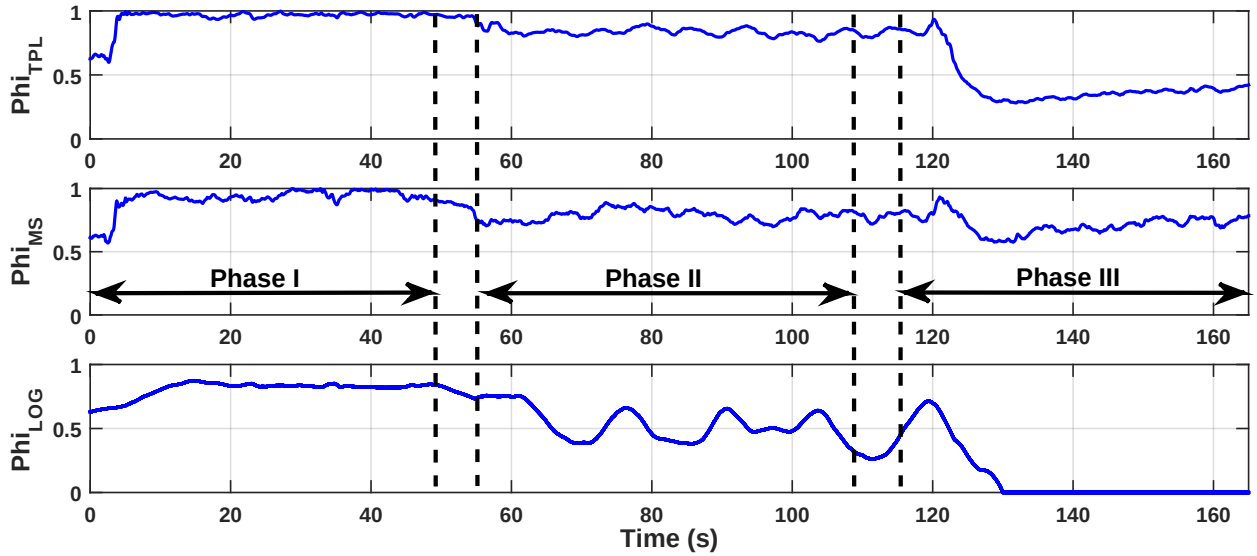

(b) Normalized proficiency metrics Φ_ρ (TPL), Φ_δ (MS) and Φ_η (LOG)

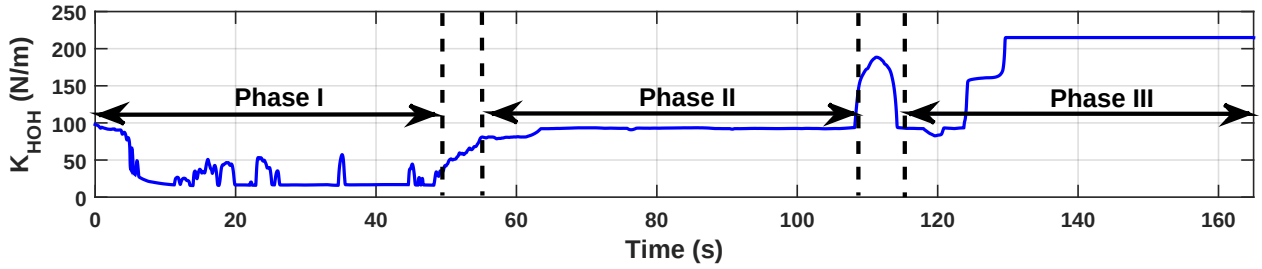

(c) Stiffness of HOH guidance (k_Γ) adaptively adjusted by the FIS based on the trainee's performance

Figure 6.5: Experimental results, scenario #1; $\alpha_T = 0$, $\alpha_E = 1$.

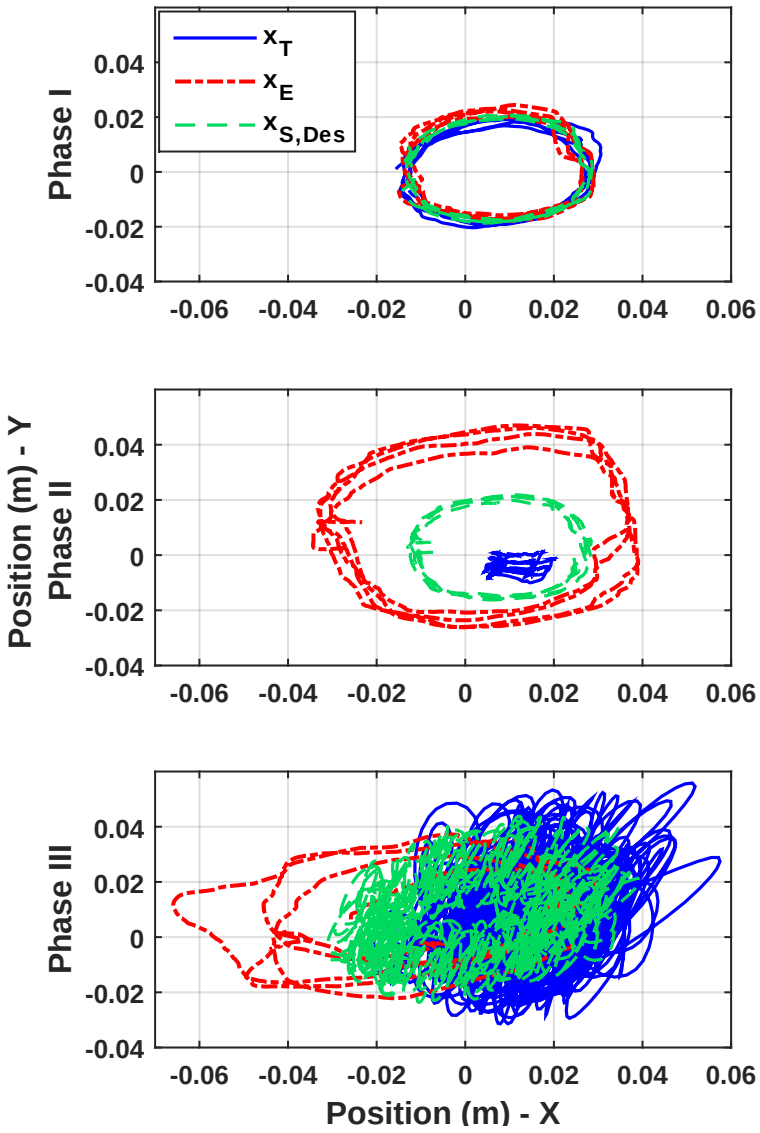

Figure 6.6: Experimental results, scenario #2: position comparison, 2D representation; $\alpha_T = \alpha_E = 0.5$.

oval-shape generated during the previous phase. Therefore, the expert had to increase the movement range of her hand to compensate for the undesired performance of the trainee in order to make the slave robot follow the oval-shaped trajectory. In fact, as a result of the non-zero authority level of the expert, she was still able to handle the trainee's inexpertise, although with extra effort. While this situation (resulting from partial but non-adaptive authority allocation for the trainee) is far from ideal, it may be a safer approach than transferring full authority to the trainee (as in the current architecture for the dual-console *da Vinci® Si*), since the expert still has some level of control over the task. However, as shown in the third phase, providing the trainee with partial but *non-adaptive* authority over the task is insufficient in terms of ensuring patient's safety. As can be seen in Fig. 6.6, during the third phase, the trainee created exaggerated non-smooth and abrupt movements. Despite the expert's effort to suppress the trainee's undesirable performance, the expert was not able to compensate for the trainee's inexpertise. Therefore, the trajectory set for the slave robot was far from the desired oval-shaped path. Although transferring *partial*, rather than full, authority over the task to the trainee can enhance safety, the *offline* adjustment process is still insufficient.

Scenario III

Online adjustment of the trainee's authority level during the operation can be either done by the expert in the loop, which might impose extra load and stress on the expert, or performed adaptively but *semi-autonomously*. In this experiment, the full architecture including the expertise-oriented online adaptation process of the trainee's authority level along with adaptive HOH guidance force is evaluated. In order to make the experiment's conditions comparable to those of the previous experiment, ζ (the expert's supervisory element over the trainee's authority level) was set to 0.5, while enabling the online adaptation feature. The trainee was also asked to repeat all the phases performed in experimental scenario #2, simulating 1) a skilled trainee ($t = 0 - 65s$), 2) a novice trainee, while making normally-paced movements ($t = 65 - 125s$), and 3) a novice trainee, while creating non-smooth and abrupt movements ($t = 125 - 170s$). In addition, the trainee was instructed to forcefully ignore and resist the HOH guidance force applied to his hand during the novice phases (#2 and #3) of the experiment. The expert's supervisory element for the HOH force, κ, was set to 250 N/m, indicating the maximum allowable

stiffness of the HOH force to be applied to the trainee's hand. Fig. 6.7 illustrates the results of this experiment.

Fig. 6.7a shows the three normalized proficiency metrics Φ_ρ, Φ_δ and Φ_η calculated for the trainee in real-time. As can be seen, all three metrics refer to a high level of expertise for the trainee during Phase #1. Therefore, as shown in Fig. 6.7b, the system provided the trainee with a high level of authority (about 0.4 out of the maximum allowable level $\zeta = 0.5$) during this phase. During both second and third phases, the proficiency metrics dropped considerably as a result of the inexpertise shown by the trainee. Comparing Φ_δ (quantifying the level of motion smoothness of the trainee's movement) for Phases #2 and #3, Φ_δ dropped in the third phase due to the non-smooth and wobbly movements of the trainee, as expected. In addition, in both phases, the LOG metric (Φ_η) plunged, indicating that the trainee had ignored the HOH forces applied to his hand.

Consequently, the trainee was rated as a beginner by the FIS during Phases #2 and #3, setting his authority level over the task to zero (Fig. 6.7b). Fig. 6.7c also illustrates the HOH stiffness, k_Γ, adaptively adjusted for the trainee by the FIS. As can be seen, during phases #2 and #3, k_Γ was set to a very high level (215 out of the maximum allowable level $\kappa = 250$), increasing the HOH force applied to the trainee's hand (Fig. 6.7d).

Fig. 6.8 compares the trainee's and the expert's trajectories as well as the desired trajectory set for the slave console. As can be seen, the slave robot has followed the weighted summation of the expert's and the trainee's trajectories during the first phase. However, in phases #2 and #3, the zero authority provided to the trainee by the PIS as a result of his lack of proficiency resulted in the slave console to completely ignore the trainee's trajectory and follow the expert's. Comparing this result with Fig. 6.6 (the position diagram of scenario #2), the effectiveness of the expertise-oriented adaptive adjustment approach is clear. Using the adaptive framework, while a *skilled* trainee can participate in the surgical procedure, a *novice* trainee can receive HOH guidance in order to develop adequate sensorimotor skills, without jeopardizing patient safety.

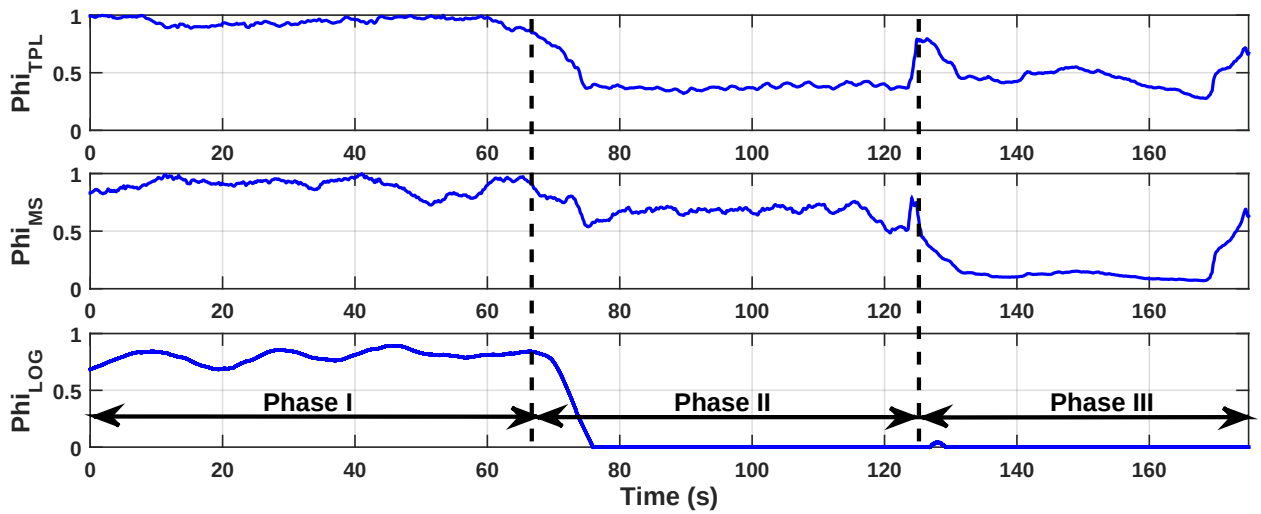

(a) Normalized proficiency metrics Φ_ρ (TPL), Φ_δ (MS) and Φ_η (LOG).

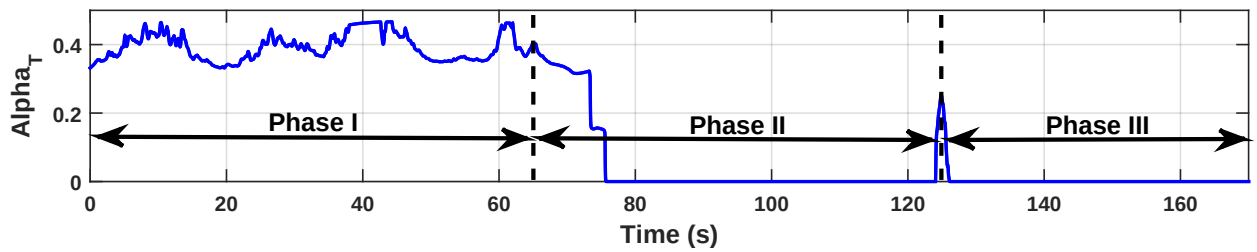

(b) The authority level of the trainee (α_T) adaptively adjusted by the FIS based on the trainee's performance.

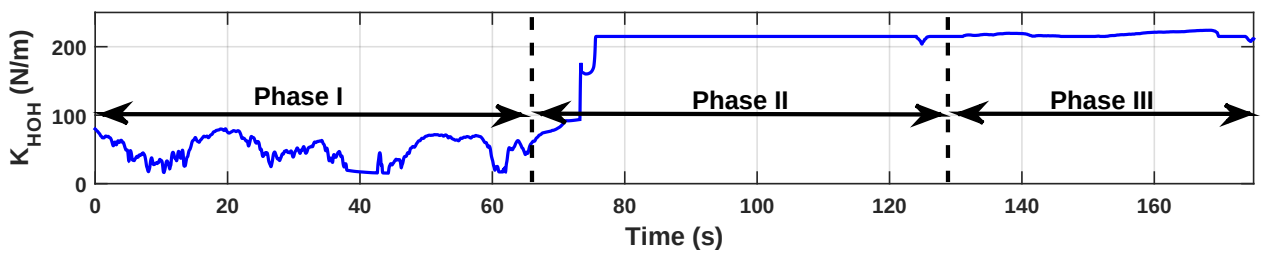

(c) Stiffness of HOH guidance (k_Γ) adaptively adjusted by the FIS based on the trainee's performance.

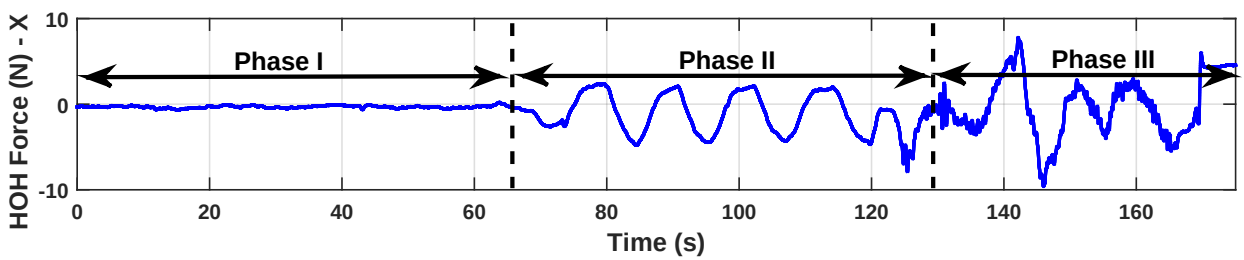

(d) HOH guidance force (f_Γ) provided to the trainee.

Figure 6.7: Experimental results, scenario #3; $\zeta = 0.5$

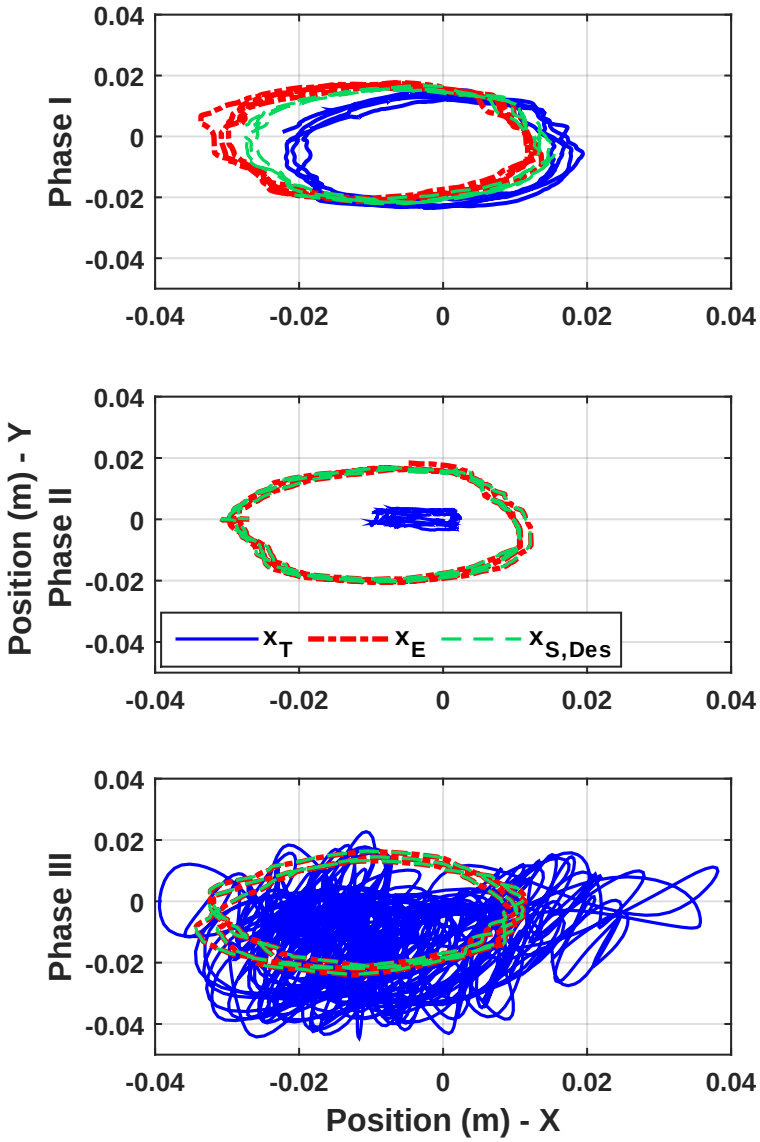

Figure 6.8: Experimental results, scenario #3: position comparison, 2D representation; $\zeta = 0.5$.

6.6 Extension: Integration of Haptic Feedback of Tool-Tissue Interaction Forces

During the late stages of learning, when the trainee has achieved a reasonable level of motor skills in manipulating the robotic console, familiarization with Tool-Tissue Interaction (TTI) forces should be the next step. Directing the trainee's focus on the effect of the movement, i.e., the TTI force, has been shown to be effective in facilitating automaticity in motor control

and enhancing movement efficiency [27]. TTI force estimation/measurement in surgical robots including the *da Vinci® Si* has not, however, fully evolved [28], [29]. Development of an appropriate force sensor for RAMIS is still an open problem due to constraints on size, geometry and cost along with the necessity for biocompatibility and sterilizability [30], [31]. Nonetheless, assuming the availability of accurate TTI force measurement technology for RAMIS in the near future, the training haptic force provided to the trainee through the master console, f_T (equal to $f_\Gamma(t)$ in the previous case), can be modified such that an *advanced* trainee feels TTI haptic forces on their hands rather than HOH haptic guidance. For this purpose, the haptic force provided to the trainee, f_T, can be defined as:

$$f_T(t) = \beta_\Gamma . f_\Gamma(t) + \beta_\Omega . f_\Omega(t) \tag{6.13}$$

where f_Ω denotes the TTI haptic force; β_Γ and β_Ω refer to activation coefficients of forces f_Γ and f_Ω, respectively. β_Γ and β_Ω can have a value of 0 or 1 such that $\beta_\Gamma + \beta_\Omega = 1$. They can be adjusted by the expert (for example using a foot pedal) or automatically through the FIS depending on the learning need as well as the learning phase of the training. For the latter case, the fuzzy rule should be defined as follows:

- If the trainee is at the Beginner level, significantly decrease $\hat{\alpha}_T(t)$ and significantly increase $\hat{k}_\Gamma(t)$;
- If the trainee is at the Intermediate level, slightly decrease $\hat{\alpha}_T(t)$ and slightly increase $\hat{k}_\Gamma(t)$;
- If the trainee is at the Advanced level, slightly increase $\hat{\alpha}_T(t)$ and significantly decrease $\hat{k}_\Gamma(t)$;
- If the trainee is at the Skilled level, significantly increase $\hat{\alpha}_T(t)$ and provide them with TTI haptic feedback, rather than HOH guidance force, i.e., switching from β_Γ to β_Ω.

This provides the trainee with expertise-oriented training in the sense that the type of haptic guidance (HOH vs. TTI) will be specified based on their level of expertise as well as their phase of learning. Assuming the availability of accurate TTI force measurement, the expert

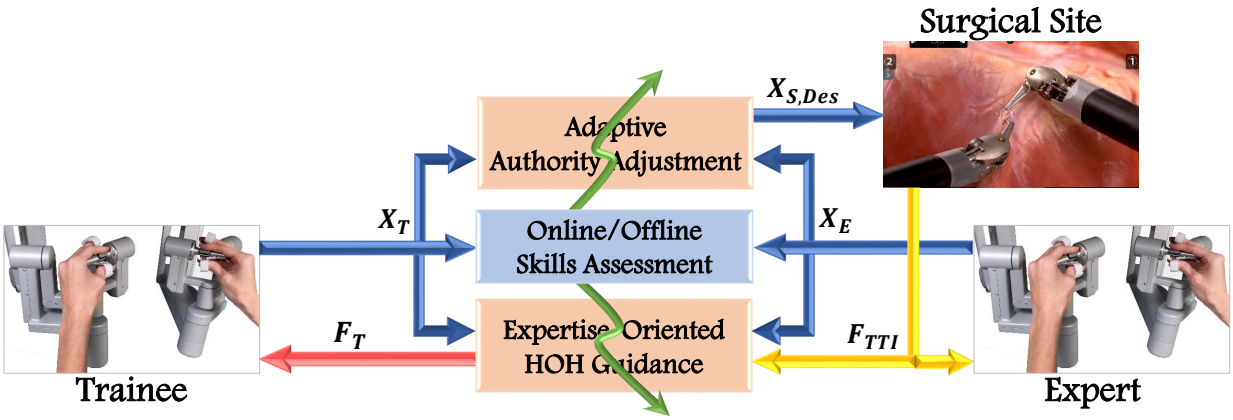

Figure 6.9: The overall scheme of the closed-loop system in the presence of TTI haptic feedback.

surgeon can also be provided with TTI haptic feedback, as follows, in order to enhance their surgical performance:

$$f_E(t) = f_\Omega(t) \tag{6.14}$$

where F_E indicates the force applied to the expert's hand by their corresponding master console. Augmenting TTI feedback adds extra loops into the system that, as shown below, will impose stability conditions to be satisfied and the closed-loop stability will not necessarily be unconditional anymore.

6.6.1 Stability Analysis in the Presence of TTI Force Feedback

Incorporating TTI feedback to the system will transform the framework to Fig. 6.9, and the closed-loop system into:

$$\begin{cases} f_T(t) = \beta_\Gamma . f_\Gamma(t) + \beta_\Omega . f_\Omega(t) \\ x_{S,Des}(t) = \alpha_E(t).\, x_E(t) + \alpha_T(t).\, x_T(t) \\ f_E(t) = f_\Omega(t) \end{cases} \tag{6.15}$$

Now, by modeling the operators (the trainee and the expert) as well as the environment (generating the TTI force on the slave manipulator) by second-order linear time-invariant sys-

tems [32], we have:

$$\begin{cases} f_{h_\Lambda}(t) = f^*_{h_\Lambda}(t) - M_\Lambda \ddot{x}_\Lambda(t) - B_\Lambda \dot{x}_\Lambda(t) - K_\Lambda\left(x_\Lambda(t) - x_\Lambda\right)) \\ f_\Omega(t) = M_\Omega \ddot{x}_S(t) + B_\Omega \dot{x}_S(t) + K_\Omega\left(x_S(t) - x_{S_0}\right)) \end{cases} \tag{6.16}$$

where f_{h_Λ} $(\Lambda : T,\ E)$ denotes the force applied by the trainee $(\Lambda : T)$ and by the Expert $(\Lambda : E)$ to their corresponding master console, where $f_{h_T} = -f_T$ and $f_{h_E} = -f_E$. Also, M_Λ, B_Λ and K_Λ indicate mass, damping and stiffness of their hand, respectively; and x_{Λ_0} indicates the initial position of the their hand, x_Λ. In addition, f_Ω denotes the TTI force applied by the environment to the tool; M_Ω, B_Ω and K_Ω indicate mass, damping and stiffness of the environment, respectively. Also, x_{S_0} denotes the initial value of x_S, the end-effector position of the slave manipulator in contact with the environment.

In order to analyze the stability of the closed-loop system, the Small-Gain Theorem is applied.

Theorem II [33]: *The feedback interconnection of systems Σ_1 and Σ_2 is Input-Output Stable (IOS) if:*

$$u_1 \in L_\infty \ \ , \ \ u_2 \in L_\infty \tag{6.17}$$

$$\Sigma_1 \in L_1 \ \ , \ \ \Sigma_2 \in L_1 \tag{6.18}$$

$$\vartheta_1 \cdot \vartheta_2 \leqslant 1 \tag{6.19}$$

where, ϑ_1 and ϑ_2 in (6.18)-(6.19) denote the IOS gain of sub-systems Σ_1 and Σ_2, respectively, as per the following definition given for IOS gain.

Definition III: *The IOS gain of a system with the input-output relation $y(t) = \Sigma u(t)$, where Σ is an operator or a mapping that specifies y in terms of u, is a nonnegative constant ς such that:*

$$\sup_{t \geqslant 0} |y(t)| \leqslant \varsigma \cdot \sup_{t \geqslant 0} |u(t)| + \varepsilon;$$

where ε is a nonnegative constant bias term.•

The closed-loop framework can be transformed into the format given in Fig. 6.10. Since $0 \leq \alpha_E, \alpha_T \leq 1, \alpha_T$ and $\alpha_E = 1 - \alpha_T$ introduce the maximum gain 1 to inputs x_T and x_E. Therefore, in the worst case, α_T and α_E can be replaced by 1, as shown in Fig. 6.11. It should

be noted that in reality α_T and α_E do not become equal to 1 simultaneously. Therefore, this worst case considered in Fig. 6.11 leads to a conservative stability condition. By substituting f_Ω and f_{h_Λ} $(\Lambda : T, E)$ from (6.16) into the closed-loop system given in (6.15), considering the worst case condition and by some mathematical manipulations, Z_Ω, Π_1, Π_2 and U_1 are calculated as follows:

$$Z_\Omega = M_\Omega \cdot s^2 + B_\Omega \cdot s + K_\Omega \tag{6.20}$$

$$\Pi_1 = \frac{1}{Z_E} \tag{6.21}$$

$$\Pi_2 = \frac{\beta_\Omega Z_E + \beta_\Gamma K_{HOH}}{Z_E \cdot (Z_T + \beta_\Gamma K_{HOH})} \tag{6.22}$$

$$U_1 = \frac{Z_T + \beta_\Gamma K_{HOH}}{\Xi} \cdot F_E^* + \frac{\beta_\Omega Z_E + \beta_\Gamma K_{HOH}}{\Xi} \cdot F_T^* \tag{6.23}$$

where $\Xi = Z_T + \beta_\Omega Z_E + 2\beta_\Gamma K_{HOH}$, $Z_E = M_E s^2 + B_E s + K_E$, and $Z_T = M_T s^2 + B_T s + K_T$.

Based on the Small-Gain Theorem, it is required to investigate the following conditions for ensuring stability of the closed-loop system in the presence of the TTI force:

$$U_1 \in L_\infty \tag{6.24}$$

$$\Sigma_1 = \Pi_1 + \Pi_2 \in L_1 \ \ , \ \ \Sigma_2 = Z_\Omega \in L_1 \tag{6.25}$$

$$\vartheta_1 \cdot \vartheta_2 \leqslant 1, \ where \ \vartheta_1 = ||\Sigma_1||_{L_1}, \ \vartheta_2 = ||\Sigma_2||_{L_1} \tag{6.26}$$

$F_{h_\Lambda}^*$ $(\Lambda : T,\ E)$, which denotes the hand exogenous forces applied by the trainee and the expert belonging to L_∞ [33]. In addition, Z_Λ $(\Lambda : T,\ E)$ corresponds to their hand dynamics with positive and bounded coefficients. As a result, while also having K_{HOH} as a positive and bounded parameter, U_1 belongs to L_∞, i.e., the first stability condition given by (6.24) is satisfied.

For the second stability condition given by (6.25), we have $\Sigma_1 = \Pi_1 + \Pi_2$, which results in $\Sigma_1 = \dfrac{Z_T + \beta_\Omega Z_E + 2\beta_\Gamma K_{HOH}}{Z_E(Z_T + \beta_\Gamma K_{HOH})}$, belonging to L_1. However, $\Sigma_2 = Z_\Omega$ does not belong to L_1 due to its improper dynamics. In order to address this issue, as elaborated in [33], it is sufficient to apply a low-pass filter $\psi = \dfrac{1}{\psi_2 s^2 + \psi_1 s + \psi_0}$ to the TTI force, before transmitting it to the operators' master consoles, in order to transform Σ_2 to a proper dynamics. Applying the filter results in $\Sigma_2 = Z_\Omega \cdot \psi = \dfrac{M_\Omega s^2 + B_\Omega s + K_\Omega}{\psi_2 s^2 + \psi_1 s + \psi_0} \in L_1$. Therefore, the second stability condition

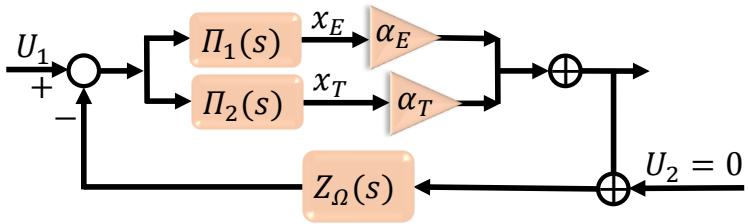

Figure 6.10: The schematic of the closed-loop system transformed based on the Small-Gain Theorem.

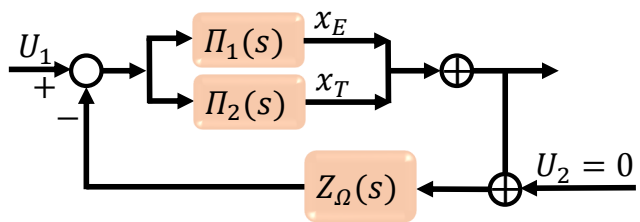

Figure 6.11: A general worst-case scheme of the closed-loop system transformed based on the Small-Gain Theorem.

given by (6.25) is also fulfilled.

For the third stability condition given by (6.26), and based on the definition of the L_1-norm, we have:

$$||\Sigma_1||_{L_1} = \int_{-\infty}^{+\infty} \left| \frac{Z_T + \beta_\Omega Z_E + 2\beta_\Gamma K_{HOH}}{Z_E(Z_T + \beta_\Gamma K_{HOH})} \right| d\omega \tag{6.27}$$

$$||\Sigma_2||_{L_1} = \int_{-\infty}^{+\infty} \left| \frac{M_\Omega s^2 + B_\Omega s + K_\Omega}{\psi_2 s^2 + \psi_1 s + \psi_0} \right| d\omega \tag{6.28}$$

Using the above definitions, and considering that ψ is a user-defined filter which can be designed such that $||\psi||_{L_1} \leq 1$, a sufficient condition to guarantee the third stability criterion given in (6.26) can be defined as follows:

$$\left| \frac{Z_T + \beta_\Omega Z_E + 2\beta_\Gamma K_{HOH}}{Z_T + \beta_\Gamma K_{HOH}} \right| \leq \left| \frac{Z_E}{Z_\Omega} \right| \tag{6.29}$$

It should be noted that, as a result of considering the worst case scenario when calculating the IOS gain for the feedforward path in Fig. 6.10, the above condition is a sufficient condition for the closed-loop system to remain stable in the presence of the TTI haptic force feedback.

As can be seen, the derived stability condition depends on the impedance values of the

operator's hand and the environment. In order to add some level of control over the stability condition, the desired closed-loop system defined in (6.15) can be modified to:

$$\begin{cases} f_T(t) = \beta_\Gamma . f_\Gamma(t) + \beta_\Omega . f_\Omega(t) \\ x_{S,Des}(t) = \alpha_E(t).\, x_E(t) + \alpha_T(t).\, x_T(t) \\ f_E(t) = f_\Omega(t) - (M_c \ddot{x_E}(t) + B_c \dot{x_E}(t) + K_c x_E(t)) \end{cases} \tag{6.30}$$

where M_c, B_c and K_c denote controller parameters through which the stability condition can be guaranteed, disregarding the impedance characteristics of the operators' hand and those of the environment. This, however, results in transparency degradation for the expert, causing them to feel the TTI feedback force with an error equal to $M_c \ddot{x_E}(t) + B_c \dot{x_E}(t) + K_c x_E(t)$. Stability-transparency trade-off in TTI-force-reflective teleoperation systems is an inherent challenge of such frameworks [34]. Repeating the same stability analysis process for the modified closed-loop system given by (6.30), the stability condition given by (6.29) will be transformed to:

$$\left| \frac{Z_T + \beta_\Omega Z_E + 2\beta_\Gamma K_{HOH}}{Z_T + \beta_\Gamma K_{HOH}} \right| \leq \left| \frac{Z_E + Z_c}{Z_\Omega} \right| \tag{6.31}$$

where $Z_c = M_c s^2 + B_c s + K_c$ provides control over the stability condition, disregarding the impedance characteristics of the environment and the operators' hand.

6.7 Future Work: Sensorimotor Integration for Haptics-Enabled Simulators

A RAMIS simulator mainly consists of a haptics-enabled master console integrated with a VR-based simulated environment. Although RAMIS simulators have been shown to be effective in surgical skills acquisition, the process can be accelerated through sensorimotor integration. Some simulators, e.g. the dVTrainer from Mimic, have enabled visual guidance by visually illustrating for the trainee the desired configuration of the simulated master console in the VR environment. The visual cue is meant to guide/help the trainee in aligning the master console with the desired configuration in order to speed up the learning process. However, manipulating a master console in 6-DOF is often quite complicated so that solely a visual cue may not be

enough to guide the novice toward the desired configuration. Although visual guidance shows ***where*** to move the tool's tip, it does not show ***how*** to manipulate the master console to achieve that desired configuration. In order to address this issue, the proposed hand-over-hand guidance can also be integrated into RAMIS simulators, as discussed below.

6.7.1 Integration of HOH Guidance into RAMIS Simulators

Incorporation of HOH guidance into RAMIS simulators enables the novice to observe the desired configuration along with receiving haptic cues that direct their attention towards the way of reaching that configuration and serves as online performance feedback. For this purpose, the HOH guidance force f_{ϖ} to be applied to the trainee's hand is defined as follows:

$$f_{\varpi}(t) = k_{\varpi}(t)(x_{\varpi,Des}(t) - x_{\varpi}(t)) \tag{6.32}$$

where x_{ϖ} refers to the endpoint position of the master console projected onto the tool tip in the VR environment; $x_{\varpi,Des}$ indicates the desired configuration of the tool tip to align with. In addition, k_{ϖ} refers to the positive elasticity of the virtual bond established between the trainee's hand and the desired configuration. The stiffer the virtual bond, the stronger the guidance or cueing HOH force will be.

Specifying the desired configuration or trajectory in simple tasks, e.g., ring transfer, cutting and needle handling, is pretty straightforward, since the task itself implies the desired trajectory. Therefore, the optimal trajectory can be automatically detected. However, specifying the desired trajectory for more complex training tasks may not be as straightforward to automatically detect in real-time. In order to address this issue, we propose to pre-record the trajectories made by an expert surgeon to be used later as the desired reference trajectory for novices. In fact, because of the simulated environment, a specific task has consistent goals from one session to another. Therefore, the performance of an expert surgeon with sufficiently developed motor skills and optimal movement synergy can be used as the reference performance for the novice trainee who later practices the same task. By using pre-recorded trajectories of an expert as the desired reference trajectory for trainees, the stiffness k_{ϖ} resembles a virtual bond between the trainee's hand and that of the expert's in real-time, without the physical presence

of the expert during the trainee's practice session. In fact, this approach enables an expert-in-the-loop training with real-time feedback which provides the novice with a fusion of visual and haptic sensorimotor modalities. This feature can be added to any haptics-enabled RAMIS simulator in order to accelerate the trainees learning speed through multimodal sensorimotor integration.

After sufficiently developing the trainee's motor skills, the next phase of the learning procedure would be to familiarize the trainee with forces applied to the virtual tool's tip to represent tool-tissue interaction in the VR environment. It should be mentioned that due to the complexity of accurately modeling tissue dynamics [11], estimation of the TTI force in the VR environment could be inaccurate; however, the incorporation of haptic information in the VR environment may prove useful in determining how integration of this additional sensing modality helps in the learning process.

6.8 Conclusions

A novel expert-in-the-loop framework integrated with multiple sensorimotor modalities was presented for training on dual-console surgical robotic systems, such as the *da Vinci® Si* surgical system. In order to provide the trainee with adaptive expertise-oriented training in real-time which actively engages them in the training session, a Fuzzy Interface System (FIS) was incorporated into the architecture. The FIS adjusts the trainee's authority level over the procedure as well as the level of kinesthetic hand-over-hand guidance and cueing provided to the trainee based on their level of proficiency. Capitalizing on the presence of an expert in the loop as well as the expertise-oriented design of the framework, concurrent performance of a surgical procedure by an expert while providing multimodal training to a trainee at any stage of motor-skills learning can be realized without jeopardizing patient safety. Closed-loop stability of the overall system was analyzed using the Circle Criterion, and it was shown that, unlike many haptics-enabled teleoperation systems, the proposed framework is *unconditionally* stable. In order to evaluate the architecture, a dual-console platform was designed and implemented, consisting of the classic *da Vinci®* surgical system and the dV-Trainer® console. The implemented setup serves not only as the first research platform for dual-console studies on the classic *da Vinci®*

surgical system, but also the first training platform integrated with haptic guidance and cueing for such a system. Experimental evaluations were conducted in three distinct scenarios and the overall performance of the proposed platform was investigated.

The dual-console telerobotic architectures mentioned in this and the previous chapters provide expert-in-the-loop motor function training to one patient (trainee) at each time. In order to save on the therapist (surgeon) time, the dual-console architectures can be extended to accommodate for multiple patients (trainees). The first step in doing this is the development of a multi-master/single-slave telerobotics framework, which is discussed in the next chapter.

Bibliography

[1] A. Talasaz, "Haptics-enabled teleoperation for robotics-assisted minimally invasive surgery," Ph.D. dissertation, Western University, 2012.

[2] A. Takhmar, I. G. Polushin, A. Talasaz, and R. V. Patel, "Cooperative teleoperation with projection-based force reflection for MIS," *IEEE Transactions on Control Systems Technology*, vol. 23, no. 4, pp. 1411–1426, 2015.

[3] A. L. Smith, E. M. Scott, T. C. Krivak, A. B. Olawaiye, T. Chu, and S. D. Richard, "Dual-console robotic surgery: a new teaching paradigm," *Journal of Robotic Surgery*, vol. 7, no. 2, pp. 113–118, 2013.

[4] http://www.intuitivesurgical.com/products/skills_simulator/.

[5] A. M. Jarc and I. Nisky, "Robot-assisted surgery: an emerging platform for human neuroscience research," *Frontiers in Human Neuroscience*, vol. 9, p. 315, 2015.

[6] C. Feng, H. Haniffa, J. Rozenblit, J. Peng, A. Hamilton, and M. Salkini, "Surgical training and performance assessment using a motion tracking system," in *Proceedings of the 2nd European Modeling and Simulation Symposium*, 2006, pp. 647–652.

[7] H. Alemzadeh, R. K. Iyer, Z. Kalbarczyk, N. Leveson, and J. Raman, "Adverse events in robotic surgery: A retrospective study of 14 years of FDA data," *ArXiv Preprint ArXiv:1507.03518*, 2015.

[8] http://www.simulatedsurgicals.com.

[9] http://simbionix.com/simulators/robotixmentor.

[10] http://www.mimicsimulation.com/products/dv-trainer/.

[11] C. D. Lallas, Davis, and J. W. Members of the Society of Urologic Robotic Surgeons, "Robotic surgery training with commercially available simulation systems in 2011: a current review and practice pattern survey from the society of urologic robotic surgeons," *Journal of Endourology*, vol. 26, no. 3, pp. 283–293, 2012.

[12] http://www.intuitivesurgical.com/products/davinci_surgical_system/da vinci_surgical_system_si/ dualconsole.html.

[13] G. Ganesh, A. Takagi, R. Osu, T. Yoshioka, M. Kawato, and E. Burdet, "Two is better than one: Physical interactions improve motor performance in humans," *Scientific reports, Nature Publishing Group*, vol. 4, 2014.

[14] P. M. Fitts and M. I. Posner, *Human performance*. Brooks/Cole, 1967.

[15] M. Cox, D. M. Irby, R. K. Reznick, and H. MacRae, "Teaching surgical skills—changes in the wind," *New England Journal of Medicine*, vol. 355, no. 25, pp. 2664–2669, 2006.

[16] J. A. Kopta, "The development of motor skills in orthopaedic education." *Clinical Orthopaedics and related research*, vol. 75, pp. 80–85, 1971.

[17] J. Li, M. Tavakoli, and Q. Huang, "Absolute stability of multi-dof multilateral haptic systems," *IEEE Transactions on Control Systems Technology*, vol. 22, no. 6, pp. 2319–2328, 2014.

[18] M. Riojas, C. Feng, A. Hamilton, and J. Rozenblit, "Knowledge elicitation for performance assessment in a computerized surgical training system," *Applied Soft Computing*, vol. 11, no. 4, pp. 3697–3708, 2011.

[19] S. Cotin, N. Stylopoulos, M. Ottensmeyer, P. Neumann, D. Rattner, and S. Dawson, "Metrics for laparoscopic skills trainers: the weakest link!" in *Medical Image Computing and Computer-Assisted Intervention*. Springer, 2002, pp. 35–43.

[20] N. Hogan and T. Flash, "Moving gracefully: quantitative theories of motor coordination," *Trends in Neurosciences*, vol. 10, no. 4, pp. 170–174, 1987.

[21] A. Aziminejad, M. Tavakoli, R. V. Patel, and M. Moallem, "Transparent time-delayed bilateral teleoperation using wave variables," *IEEE Transactions on Control Systems Technology*, vol. 16, no. 3, pp. 548–555, 2008.

[22] J. M. Dolan, M. B. Friedman, and M. L. Nagurka, "Dynamic and loaded impedance components in the maintenance of human arm posture," *IEEE Transactions on Systems, Man and Cybernetics*, vol. 23, no. 3, pp. 698–709, 1993.

[23] H. K. Khalil, *Nonlinear Systems*. Prentice Hall, Upper Saddle River, 2002, vol. 3.

[24] P. Kazanzidesf, Z. Chen, A. Deguet, G. S. Fischer, R. H. Taylor, and S. P. DiMaio, "An open-source research kit for the da vinci® surgical system," in *IEEE International Conference on Robotics and Automation*, 2014, pp. 6434–6439.

[25] M. Y. Jung, A. Deguet, and P. Kazanzides, "A component-based architecture for flexible integration of robotic systems," in *IEEE/RSJ International Conference on Intelligent Robots and Systems*, 2010, pp. 6107–6112.

[26] P. Kazanzides, S. DiMaio, A. Deguet, B. Vagvolgyi, M. Balicki, C. Schneider, R. Kumar, A. Jog, B. Itkowitz, C. Hasser *et al.*, "The Surgical Assistant Workstation (SAW) in minimally-invasive surgery and microsurgery," in *MICCAI Workshop on Systems and Arch. for Computer Assisted Interventions*, 2010.

[27] G. Wulf, C. Shea, and R. Lewthwaite, "Motor skill learning and performance: a review of influential factors," *Medical Education*, vol. 44, no. 1, pp. 75–84, 2010.

[28] O. Mohareri, C. Schneider, and S. Salcudean, "Bimanual telerobotic surgery with asymmetric force feedback: A davinci® surgical system implementation," in *2014 IEEE/RSJ International Conference on Intelligent Robots and Systems*, 2014, pp. 4272–4277.

[29] A. Trejos, R. Patel, and M. Naish, "Force sensing and its application in minimally invasive surgery and therapy: a survey," *Proceedings of the Institution of Mechanical Engineers, Part C: Journal of Mechanical Engineering Science*, vol. 224, no. 7, pp. 1435–1454, 2010.

[30] A. M. Okamura, "Haptic feedback in robot-assisted minimally invasive surgery," *Current Opinion in Urology*, vol. 19, no. 1, p. 102, 2009.

[31] O. Mohareri, S. E. Salcudean, and C. Nguan, "Asymmetric force feedback control framework for teleoperated robot-assisted surgery," in *2013 IEEE International Conference on Robotics and Automation (ICRA)*, 2013, pp. 5800–5806.

[32] A. Shahdi and S. Sirouspour, "Adaptive/robust control for time-delay teleoperation," *IEEE Transactions on Robotics*, vol. 25, no. 1, pp. 196–205, 2009.

[33] I. Polushin, H. J. Marquez, A. Tayebi, and P. X. Liu, "A multichannel IOS small gain theorem for systems with multiple time-varying communication delays," *IEEE Transactions on Automatic Control*, vol. 54, no. 2, pp. 404–409, 2009.

[34] C. A. L. Martínez, R. van de Molengraft, S. Weiland, and M. Steinbuch, "Switching robust control for bilateral teleoperation," *IEEE Transactions on Control Systems Technology*, vol. 24, no. 1, pp. 172–188, 2016.

Chapter 7

Multi-Master/Single-Slave Teleoperation Framework

The material presented in this chapter was published in the IEEE/ASME Transactions on Mechatronics, vol. 20, no. 4, pp. 1668-1679, 2014.

7.1 Introduction

Providing operators with safety and accessibility, teleoperation systems allow remote performance of a desired task through a set of robotic consoles. In a Single-Master/Single-Slave (SM/SS) teleoperation system, a master console is manipulated by an operator in order to perform a desired task in a remote environment through a slave console [1], [2]. In order to transmit data between master and slave consoles that may be located at a considerable distance, a communication channel is also required [3]. As a manifest feature of data-transmission, mainly at long distances, communication delays are inevitable. These can lead to undesired effects on the system in terms of stability and transparency [4], [5]. To address this issue, several control methodologies were introduced for SM/SS systems.

In [6], a control law was designed to ensure closed-loop passivity in the presence of constant communication time-delays. System passivity was shown using scattering theory. In [7],

©[2014] IEEE. Reprinted, with permission, from [M. Shahbazi, S.F Atashzar, H.A. Talebi, R.V. Patel, "Novel Cooperative Teleoperation Framework: Multi-Master/Single-Slave System", IEEE/ASME Transactions on Mechatronics, vol. 20, no. 4, pp. 1668-1679, 2014].

a scattering-based approach was extended to address the problem of time-varying communication delays. Wave variables were defined in [8] as another systematic approach to guarantee closed-loop stability.

In [9], transparency of various SM/SS structures was discussed and a transparency-optimized architecture was designed. The architecture requires a two-way transmission of force and velocity. In [10], Hashtrudi-zaad introduced two classes of three-channel architectures which require transmission of three signals, rather than all four signals that are required in the four-channel architecture, that ensure transparency in the presence of negligible time delays. In [11] and [12], further development introduced two-channel architectures that also ensure system transparency. Several other control methodologies were introduced for SM/SS system, some of which have been summarized in [13].

SM/SS teleoperation systems have been extensively used in a wide range of applications from mining, space and under-water exploration to telesurgery, Robotics-Assisted Minimally Invasive Surgery (RAMIS) [14], [15], [16], [17] and rehabilitation [18], [19], [20]. However despite the promising advantages, the SM/SS structure does not offer the opportunity of cooperative task-performance to multiple operators. In some applications, e.g., RAMIS, the operator needs to perform a task while training a non-expert person simultaneously, as training is essential to highly develop the trainee's psychomotor skills in a robotics-assisted task [21]. To address the issue, a dual-user teleoperation system, as in the case of the new *da Vinci Si* from Intuitive Surgical Inc. [22], could be used in which two surgeon's consoles are available, one operated by an expert and the other by a trainee to manipulate the slave robotic system at the environment side. In [23], the authors proposed a novel dual-user teleoperation framework, through which the performance of a surgical operation concurrently with training a non-expert trainee is possible. The framework allows adaptive adjustment of the trainee's level of involvement in the task, according to his/her level of expertise over the operation.

Another application for a dual-user teleoperation system is in two-handed tele-rehabilitation therapy, where the patient involves his/her healthy arm to cooperate with the therapist's arm in order to train the patient's impaired arm [24]. This approach, which increases the effectiveness of the therapy, necessitates two master consoles, one held by the therapist and the other by the patient's healthy arm in order to manipulate a slave robot held by the patient's impaired arm.

With regard to the emerging applications of a dual-user teleoperation system, several studies have been performed on dual-user systems. In [25], adaptive nonlinear control architectures were developed for dual-user haptic interaction compatible with impedance and admittance dynamic simulations. However, the given stability analysis did not address communication time-delays. In [26], a six-channel multilateral shared control architecture was presented for a delay-free dual-user system and a number of performance measures were extended/proposed to analyze the kinesthetic performance of the controller. In [27], a μ-synthesis-based robust controller was proposed for dual-user systems in the presence of known communication delays. In [28], a sliding-mode-based controller was proposed to overcome the undesired effects of time delays on stability of a dual-user system, though a stability condition was derived for the system which necessitates numerical computation to determine system stability. An adaptive impedance controller was presented in [29] to stabilize a dual-user system in the presence of constant time-delays, while a comprehensive stability analysis was given for the closed-loop system. In [30], the effect of environmental factors on the user's performance were investigated in a dual-user system where a trainee and a trainer were able to collaboratively perform a common task in a virtual environment.

Although various control frameworks have been presented for the dual-user system, this category is a very special class of Multi-Master/Single-Slave (MM/SS) teleoperation system. The general format of the MM/SS system with more than two operators has received very little attention. A general MM/SS system would be beneficial in training scenarios (e.g. surgical) allowing multiple-trainees to be involved in the training procedure. For example in a surgical training case, this would allow a surgical task to be performed concurrently with training several trainees, while adaptively adjusting the involvement level of each trainee in the task according to his/her level of expertise. Without regarding the involvement level of the trainees in the task, trainees would still be able to feel the environment force on their hands, and learn about the various ranges of force interactions with various types of tissues in a surgical task. As a future application, in order to provide force reflection, haptic gloves along with visuo-haptic displays can be used to expand the force-feedback capabilities that would allow trainees to feel the environment in a much more natural way [31], [32]. In addition to the benefit for trainees, the architecture would also be convenient for experts in enabling them to work with

several trainees at the same time. Another possible application of an MM/SS system architecture could also be a multilateral haptic system, in which multiple master robots control a higher degrees-of-freedom slave robot to enable several human operators to collaboratively perform a dexterous task [33].

Therefore, this thesis takes a further step and proposes an MM/SS teleoperation system for the general case of "n" operators $(n \geq 2)$. In this chapter, a set of desired objectives for an MM/SS system is proposed. The passivity of the closed-loop system is investigated and it is shown that unlike a traditional SM/SS system, an ideal MM/SS system with the proposed structure is not passive (even when communication delays are negligible), which, as elaborated later, is a consequence of the way the system's desired objectives are defined. An impedance-based control methodology is adopted to satisfy the system objectives. The small-gain theorem is then used to investigate closed-loop stability in the presence of communication delays, resulting in a sufficient condition to guarantee system stability. Finally experimental results are given to evaluate the performance of the proposed methodology.

The rest of the chapter is organized as follows: The dynamics of an MM/SS teleoperation system are given in Section 7.2. The desired objectives for the MM/SS system are proposed in Section 7.3. In Section 7.4, passivity of the ideal MM/SS system is investigated and discussed. Sections 7.5 and 7.6 present the control methodology and stability analysis, respectively. Experimental results are presented in Section 7.7 and Section 7.8 concludes the chapter.

7.2 Dynamics of MM/SS Teleoperation Systems

7.2.1 Master Consoles

A general MM/SS system consists of "n" master robots manipulated by "n" operators in order to control a slave robot. Each master robot has nonlinear dynamics as follows [34]:

$$D_{m_i}(x_{m_i})\ddot{x}_{m_i} + C_{m_i}(x_{m_i}, \dot{x}_{m_i})\dot{x}_{m_i} + G_{m_i}(x_{m_i}) = F_{c,m_i} - F_{ext,m_i} \tag{7.1}$$

where x_{m_i} $(i = 1, .., n)$ is the end-effector position of master #i. $D_{m_i}(x_{m_i})$ is the mass matrix, while $C_{m_i}(x_{m_i}, \dot{x}_{m_i})$ and $G_{m_i}(x_{m_i})$ represent velocity-dependent elements and position-

dependent forces such as gravity, respectively. Moreover, F_{c,m_i} and F_{ext,m_i} are the control signal and the external force acting at the robot end-effector. Since, the external force, F_{ext,m_i}, acting on each master robot is applied by its corresponding operator, we have:

$$F_{ext,m_i} = -F_{h_i} \tag{7.2}$$

While the operators' hand forces $F_{h_i}(i = 1,2,\ldots,n)$ can be modeled as second-order time-invariant systems as follows [35]:

$$F_{h_i} = F^*_{h_i} - M_{h_i}\ddot{x}_{h_i} - B_{h_i}\dot{x}_{h_i} - K_{h_i}[x_{h_i} - x_{h_i0}] \tag{7.3}$$

where M_{h_i}, B_{h_i}, K_{h_i} and $F^*_{h_i}$ denote the mass, damping, stiffness, and the users' exogenous force, respectively. In addition, x_{h_i} and x_{h_i0} show the hand position of operator #i and the initial value for x_{h_i}, respectively. Note that each master robot is held by a corresponding operator resulting in $x_{h_i} = x_{m_i}$. It is worth mentioning that the operators' hand dynamics will be used in the stability analysis in Section 7.6.

7.2.2 Slave Console

Similar to the master robots, the slave robot can be described by nonlinear dynamics as follows:

$$D_s(x_s)\ddot{x}_s + C_s(x_s,\dot{x}_s)\dot{x}_s + G_s(x_s) = F_{c,s} - F_{ext,s} \tag{7.4}$$

where x_s denotes the end-effector position for the slave robot. Similarly, $D_s(x_s)$ is the mass matrix, $C_s(x_s,\dot{x}_s)$ corresponds to the velocity dependent elements and $G_s(x_s)$ represents position-dependent forces such as gravity. $F_{c,s}$ and $F_{ext,s}$ denote the control signal and the external force acting on the end-effector of the slave robots. The external force acting on the slave robot corresponds to the environment force, F_e, which can be modeled by a second-order time-invariant system as follows [35]:

$$F_{ext,s} = F_e = M_e\ddot{x}_e + B_e\dot{x}_e + K_e[x_e - x_{e0}] \tag{7.5}$$

where M_e, B_e, K_e and x_e denote the environment mass, damping, stiffness and position, respectively. In addition, x_{e0} refers to the initial value for x_e. Note that since the slave robot is interacting with the environment, we have $x_s = x_e$.

7.3 Desired Objectives for the MM/SS System

As mentioned earlier, an MM/SS teleoperation system provides a cooperative environment for multiple operators, enhancing the quality of the task performance. In addition, an MM/SS architecture allows performance of an operation, e.g. surgery, simultaneously with training of multiple trainees. This coincidence provides trainees with hands-on training on a real environment, rather than virtual simulated environments currently used for training. An MM/SS system is also useful for remote performance of delicate tasks such as telesurgery, in which a communication network failure could cause serious problems. Using an MM/SS system, if any failure occurs for one operator's network, the other operator(s) involved in the procedure can easily take over the control of the slave system. Accordingly, in an MM/SS system, each operator is desired to have a level of authority to affect the task based on his/her level of expertise and experiences. To address this issue, the desired position for the slave robot is proposed as follows:

$$x_{sd} = \alpha_1 x_{m_1} + \alpha_2 x_{m_2} + \ldots + \alpha_n x_{m_n} \tag{7.6}$$

where x_{sd} shows the desired position for the slave robot; x_{m_i} shows the position of master #i. Moreover, $\alpha_i (i = 1, 2, \ldots, n)$, the "dominance factor", specifies authority level of operator #i over the task. Therefore, authority of each operator over the task is adjustable through his/her corresponding dominance factor, which varies between 0 and 1, and:

$$\sum_{i=1}^{n} \alpha_i = 1, \ \alpha_i \geq 0 \tag{7.7}$$

In an MM/SS system, it is also desired for each user to feel the environment force for having an ideal transparent operation. Therefore, in addition to the objectives defined for the slave robot in (7.6), the objectives are defined for the operators as follows, specifying the desired force to

be exerted on their hands:

$$\begin{cases} F_{h_1 d} = F_e \\ F_{h_2 d} = F_e \\ \quad \vdots \\ F_{h_n d} = F_e \end{cases} \tag{7.8}$$

where $F_{h_i d}$ shows the desired value for the force to be exerted on operator #i's hand. By defining the desired objectives as given by (7.6)-(7.8), each operator can have an impact over the task according to his/her authority based on his/her level of expertise. At the same time, he/she is able to feel the environment force completely, without regarding his/her level of authority over the task. This definition makes the system appropriate for training applications such as surgery. As an example, consider the expert as the operator #j, α_j in (7.6) can be set to 1 and $\alpha_i (i = 1, \ldots, n \neq j)$ to 0, which leads the desired position of the slave robot to be equal to the end-effector position of master-console #j manipulated by the mentor, operator #j. This authority adjustment eliminates the impact of other operators, which could be novice trainees. However, considering (8), they are still capable of feeling the force reflected back from the environment. This allows the trainees to get trained on the interaction-force ranges for different environment types, e.g. different tissue types in surgical operations. Of course, using the proposed structure, a trainee who does have sufficient skills level could still be given some authority over the task, if desired.

It should be noted that in this framework, in addition to multiple trainees, multiple experts could also be given authority over the task according to various factors, e.g. their skills level and the communication network quality through which each operator is transmitting data to/from the slave robot. The quality of the communication network is an essential factor to be considered, especially in remote performance of delicate operations such as surgery, in which any network failure could be a real challenge. Adjustment of the operators' authority levels in an MM/SS system is a topic worth investigating further. Preliminary steps have been taken by the authors for a specific case of a dual-user system in [23], [36].

7.4 Passivity of an Ideal MM/SS System

In a traditional SM/SS system, the passivity theorem is an approach used to investigate stability of the closed-loop system. It has been shown that in the presence of negligible communication delay, the SM/SS system is passive and consequently stable [37]. However, as shown in this section, the general MM/SS system does not exhibit this property. In fact, due to its specific structure imposed by the way the system's desired objectives are defined in (7.6)-(7.8), the closed-loop system is not passive. To show this, a hybrid matrix is defined for the proposed MM/SS system and the passivity theorem is applied as discussed below.

An MM/SS system with n operators is an $(n+1)$-port network. Therefore, a hybrid matrix can be derived by defining the input U and the output Y for the network as follows:

$$U = \begin{bmatrix} \dot{x}_{m_1} \\ \dot{x}_{m_2} \\ \vdots \\ \dot{x}_{m_n} \\ -F_e \end{bmatrix}_{(n+1)\times 1} , \quad Y = \begin{bmatrix} F_{h_1} \\ F_{h_2} \\ \vdots \\ F_{h_n} \\ \dot{x}_s \end{bmatrix}_{(n+1)\times 1} \tag{7.9}$$

The hybrid matrix $H_{(n+1)\times(n+1)}$ for an MM/SS system can be defined as follows:

$Y = HU$, where $H_{(n+1)\times(n+1)} =$

$$\begin{bmatrix} \left.\frac{F_{h_1}}{\dot{x}_{m_1}}\right|_{\dot{x}_{m_1}\neq 0, OTIN=0} & \cdots & \left.\frac{F_{h_1}}{\dot{x}_{m_n}}\right|_{\dot{x}_{m_n}\neq 0, OTIN=0} & \left.\frac{F_{h_1}}{-F_e}\right|_{\dot{x}_{m_i}=0} \\ \vdots & \ddots & \vdots & \vdots \\ \left.\frac{F_{h_n}}{\dot{x}_{m_1}}\right|_{\dot{x}_{m_1}\neq 0, OTIN=0} & \cdots & \left.\frac{F_{h_n}}{\dot{x}_{m_n}}\right|_{\dot{x}_{m_n}\neq 0, OTIN=0} & \left.\frac{F_{h_n}}{-F_e}\right|_{\dot{x}_{m_i}=0} \\ \left.\frac{\dot{x}_s}{\dot{x}_{m_1}}\right|_{\dot{x}_{m_1}\neq 0, OTIN=0} & \cdots & \left.\frac{\dot{x}_s}{\dot{x}_{m_n}}\right|_{\dot{x}_{m_n}\neq 0, OTIN=0} & \left.\frac{\dot{x}_s}{-F_e}\right|_{\dot{x}_{m_i}=0} \end{bmatrix} \tag{7.10}$$

where OTIN refers to other elements of the network input, U. In other words, $\dot{x}_{m_1} \neq 0, OTIN = 0$ means that all elements of U except $\dot{x}_{m_i}$ are set to zero.

Considering the desired objectives defined for the system in (7.6)-(7.8), the desired hybrid

matrix is given by:

$$H_{desired} = \begin{bmatrix} 0 & \dots & 0 & -1 \\ \vdots & \ddots & \vdots & \vdots \\ 0 & \dots & 0 & -1 \\ \alpha_1 & \dots & \alpha_n & 0 \end{bmatrix}_{(n+1)\times(n+1)} \tag{7.11}$$

The desired hybrid matrix is satisfied if the desired objectives for the system are satisfied. Consequently, $H_{desired}$ is an illustration of ideal transparency for the system. In order to investigate passivity of the system, $H_{desired}$ is examined through the passivity theorem, as follows:

Theorem 1: A linear time-invariant n-port network possessing a general hybrid matrix, which is analytic in the open Right Half Plane (RHP), is passive if and only if the general hybrid matrix is positive real [38].

Theorem 2: The matrix H is positive real if and only if [38], [39]:

1. *H is analytic in the open RHP.*
2. $\overline{H(s)} = H(\bar{s})$ *for all s in the open RHP.*
3. *The Hermitian part of H is Positive Semi-Definite (PSD) for all s in the open RHP.*

Considering Theorems 1 and 2, in order for the proposed MM/SS system to be passive, the Hermitian part of $H_{desired}$, denoted by H_{hermit}, is required to be positive semi-definite, which is equivalent to having all eigenvalues of $H_{hermit} \geq 0$, where:

$$H_{hermit} = \frac{1}{2}(H_{desired} + H^*_{desired}) \tag{7.12}$$

Calculating the eigenvalues of H_{hermit} we have:

$$eig(H_{hermit}) = \begin{cases} 0 \\ \vdots \\ 0 \\ \pm\frac{1}{2}\sqrt{\sum_{i=1}^{n}(\alpha_i - 1)^2}. \end{cases} \tag{7.13}$$

As can be seen, considering (7.7), H_{hermit} has $n-1$ zero eigenvalues, while one of the other two is always negative. The only case in which all the eigenvalues are zero is when $n =$

1, causing $\sum_{i=1}^{n}(\alpha_i - 1)^2 = 0$, which is in fact equivalent to an SM/SS system. However, for the general MM/SS system with $n \geq 2$, disregarding the value of α_i, H_{hermit} has always one negative eigenvalue. This implies that $H_{desired}$ is not Positive Real. Consequently, unlike a traditional SM/SS system, the proposed closed-loop MM/SS system is not passive (even when communication delays are negligible), due to its specific structure imposed by the way the system's desired objectives are defined in (7.6)-(7.8). The non-passivity of the proposed general MM/SS system means that it generates more energy than it consumes. The reason can be intuitively described by taking a look on what each operator injects into the *n-port* network and what he/she receives from the network. As can be seen in (7.6)-(7.8), each master robot has a partial effect on the slave robot proportional to the corresponding operator's authority level. Therefore, the slave robot is partially controlled by each operator. On the other hand, each operator receives the environment force reflected back from the slave side. The environment force is the result of the slave's full motion in the environment. This full motion is in fact a combination of the partial motions injected by all operators. Therefore, each operator is injecting partial motion into the system, while he/she is receiving the environment force caused by the full motion of the slave robot. This generates negative energy flow into the network, causing non-passivity of the system. This non-passivity is a result of the way the system transparency is defined, as all the users are desired to feel the environment force completely. Depending on application, the desired objectives can be also defined in such a way that the system remains passive. For example, by reflecting back to each operator a scaled version of the environment force proportional to his/her dominance factor, the hybrid matrix will be transformed to (7.14). Using Theorems 1 and 2, it can be shown that this represents a passive network.

$$H_{desired} = \begin{bmatrix} 0 & \dots & 0 & -\alpha_1 \\ \vdots & \ddots & \vdots & \vdots \\ 0 & \dots & 0 & -\alpha_n \\ \alpha_1 & \dots & \alpha_n & 0 \end{bmatrix}_{(n+1)\times(n+1)} \tag{7.14}$$

Reflecting back an α_i-based ratio of the environment force means that each operator will feel the portion of environment force generated solely from his/her motion. This structure is not a suitable approach for training, since a trainee with zero authority will feel zero force reflected

back from the environment. The framework could still be useful in some applications such as cooperative task performance, the discussion of which is outside the scope of this thesis. In the following sections, we will focus on the system introduced in (7.6)-(7.8), addressing the control methodology and stability analysis for the closed-loop system in the presence of communication time-delays.

7.5 Control Methodology

Communication time-delays can destabilize an MM/SS teleoperation system. Therefore, a control methodology is required, using which the closed-loop stability can be assured. For this purpose, a methodology previously presented by the authors in [28] for a dual-user system is extended here for the general case of MM/SS with n operators. In this impedance-based structure, the following $n+1$ impedance surfaces are defined as the desired closed-loop system:

$$\begin{cases} M_{1,d}\ddot{x}_{m_1} + B_{1,d}\dot{x}_{m_1} + K_{1,d}x_{m_1} = F_{h_1d} - F_e \\ M_{2,d}\ddot{x}_{m_2} + B_{2,d}\dot{x}_{m_2} + K_{2,d}x_{m_2} = F_{h_2d} - F_e \\ \vdots \\ M_{n,d}\ddot{x}_{m_n} + B_{n,d}\dot{x}_{m_n} + K_{n,d}x_{m_n} = F_{h_nd} - F_e \end{cases} \tag{7.15}$$

$$x_s = \alpha_1 x_{m_1} + \alpha_2 x_{m_2} + \ldots + \alpha_n x_{m_n} \tag{7.16}$$

In (7.15), the equation with the index i shows the desired impedance surface defined for master console #i. In this equation, $M_{i,d}$, $B_{i,d}$ and $K_{i,d}$ denote the desired mass, damping and stiffness respectively for the master console #i. Also (7.16) defines the desired impedance surface defined for the slave console. By setting $M_{i,d}$, $B_{i,d}$ and $K_{i,d}(i = 1,2,\ldots,n)$ to 0 in (7.15), it can be seen that the proposed desired impedance-based closed-loop system, (7.15) and (7.16), will be ideally equivalent to the system desired objectives defined by (7.6) and (7.8). However, it will be shown in the next section that these parameters play a significant role in ensuring closed-loop system stability although they may degrade the system transparency.

In order to satisfy the defined impedance surfaces as the closed-loop system, an impedance controller is designed to locally control each master and slave console. It should be noted that to implement the controller, each master console requires the environment force to be sent from

the slave side. Moreover, the slave console requires the position of the master consoles to be sent. In the presence of communication delays, the signals transmitted from one console to another are received in their delayed format. Therefore, the closed-loop system can be expressed by (7.17) and (7.18) below, when the communication delay is not negligible.

$$\begin{cases} M_{1,d}\ddot{x}_{m_1} + B_{1,d}\dot{x}_{m_1} + K_{1,d}x_{m_1} = F_{h_1d} - F_e^{d_1} \\ M_{2,d}\ddot{x}_{m_2} + B_{2,d}\dot{x}_{m_2} + K_{2,d}x_{m_2} = F_{h_2d} - F_e^{d_2} \\ \vdots \\ M_{n,d}\ddot{x}_{m_n} + B_{n,d}\dot{x}_{m_n} + K_{n,d}x_{m_n} = F_{h_nd} - F_e^{d_n} \end{cases} \tag{7.17}$$

$$x_s = \alpha_1 x_{m_1}^{d_1} + \alpha_2 x_{m_2}^{d_2} + \ldots + \alpha_n x_{m_n}^{d_n} \tag{7.18}$$

where the $d_i (i = 1, 2, \ldots, n)$ shows the value of the time-delay for the communication channel #i, through which the data between the slave console and master console #i is transmitted. In addition, the signal Δ^{d_i} corresponds to the delayed format of Δ, i.e., $\Delta(t - d_i)$. For example, $x_{m_i}^{d_i} = x_{m_i}(t - d_i)$.

7.6 Closed-Loop Stability Analysis

This section discusses stability analysis for the proposed MM/SS system in the presence of communication time-delays. For this purpose, the small-gain theorem, a tool for studying stability of interconnected systems [40], is applied to obtain a sufficient stability condition for the system. The derivation of a stability condition for a general MM/SS system is considerably more complicated than that for an SM/SS or a dual-user system, as it should address the issue for a general case of n operators, while n can take any positive integer value.

Theorem 3: According to the small-gain theorem, the feedback system in Fig. 7.1 is Input-Output Stable (IOS) if [40], [41]:

$$u_1 \in L_\infty \ \& \ u_2 \in L_\infty \tag{7.19}$$

$$\Sigma_1 \in L_1 \ \& \ \Sigma_2 \in L_1 \tag{7.20}$$

$$\gamma_1.\gamma_2 \leq 1 \textit{ where } \gamma_1 = ||\Sigma_1||_{L_1}, \ \gamma_2 = ||\Sigma_2||_{L_1} \tag{7.21}$$

In Fig. 7.1, T_1 and T_2 correspond to time-varying communication delays satisfying the following conditions:

1. *$\Xi_l > 0$ and a piecewise continuous function $\Xi_u : R \to R_+$ satisfying $\Xi_u(\tau_2) - \Xi_u(\tau_1) \leq \tau_2 - \tau_1$ exist, such that the following inequalities hold for all $t \geq 0$:*

   $\Xi_l \leq min\{T_1(t), T_2(t)\} \leq max\{T_1(t), T_2(t)\} \leq \Xi_u$

2. $t - max\{T_1(t), T_2(t)\} \to +\infty$ *as* $t \to +\infty$

In real-world communication networks, these assumptions can always be satisfied. Assumption #1 implies the existence of an upper-bound for delays that does not grow faster than the time itself. Assumption #2 can also be satisfied using standard techniques such as sequence numbering and/or time-stamping and by assigning a maximal packet lifetime, when transmitting the data [41].

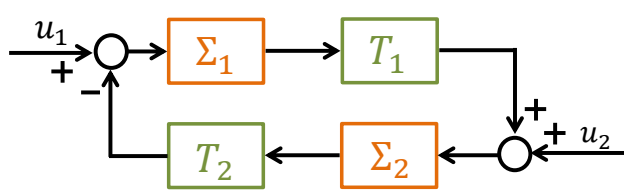

Figure 7.1: General scheme of a feedback system with time delays.

In order for the small-gain theorem to be applicable to the MM/SS system, it is required to transform the system into the format given in Fig. 7.1. For this purpose, by substituting F_e and $F_{h_i}(i = 1, 2, \ldots, n)$ from (7.3) and (7.5) into the closed-loop MM/SS system given by (7.17) and (7.18), the system can be modeled as given in Fig. 7.2. In this figure, $F^*_{h_i}$, $(i = 1, 2, \ldots, n)$ shows the exogenous force exerted on master #i by operator #i. Also $\Psi_i = \alpha_i(Z_{h_i} + Z_{i,d})^{-1}$, and $\Sigma_2 = \Sigma_e$, where:

$$Z_{h_i} = M_{h_i}s^2 + B_{h_i}s + K_{h_i} \tag{7.22}$$

$$Z_{i,d} = M_{i,d}s^2 + B_{i,d}s + K_{i,d} \tag{7.23}$$

$$Z_e = M_e s^2 + B_e s + K_e \tag{7.24}$$

In addition, d_i and $d_i^{'}$ show the time delays between the master console #i and the slave console and vice versa, respectively.

In this model, let $T_1 = max(d_1, d_2, ..., d_n)$ and $T_2 = max(d_1^{'}, d_2^{'}, ..., d_n^{'})$. Now let's define ζ_i

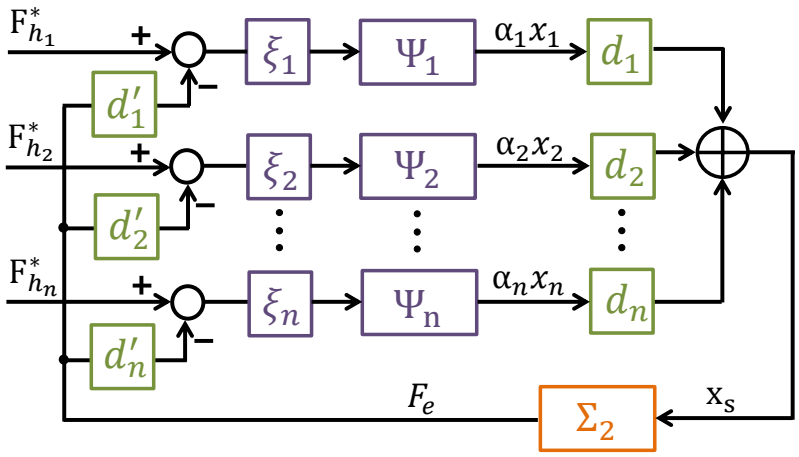

Figure 7.2: General scheme of the MM/SS system in the presence of delays.

and ξ_i, for $i = 1, 2, \ldots, n$, as $\zeta_i = d_i - T_1$ and $\xi_i = d_i^{'} - T_2$. With regard to the fact that $T_1 \geq d_i$ and $T_2 \geq d_i^{'}$, ζ_i and ξ_i characterize lead blocks with the values of $T_1 - d_i$ and $T_2 - d_i^{'}$. It should be noted that although ζ_i and ξ_i are non-causal, they can be used in the analysis procedure. Using the given definitions, the system given in Fig. 7.2 can be transformed to one given in Fig. 7.3, where δ_i $(i = 1, 2, \ldots, n)$ illustrate delay blocks with the value of $T_2 - d_i^{'}$.

Now, we take a further step by defining F_δ^* as given in 7.25, which allows simplification of Fig. 7.3 to Fig. 7.4.

$$F_\delta^* = \frac{F_1^*\Psi_1 + F_2^*\Psi_2 + ... + F_n^*\Psi_n}{\Psi_1 L(\xi_1) + \Psi_2 L(\xi_2) + ... + \Psi_n L(\xi_n)} \tag{7.25}$$

where $L(\xi_i)$ represents a lead operator with the value of ξ_i.

By naming the block shown by the dashed line as Σ_1, which is a combination of n separate systems in parallel, Fig. 7.4 will have a similar format as Fig. 7.1. Therefore, to investigate the system stability, it is required to examine the small-gain stability conditions given by (7.19)-(7.21). For this purpose, the two cases of constant and time-varying delay are discussed separately.

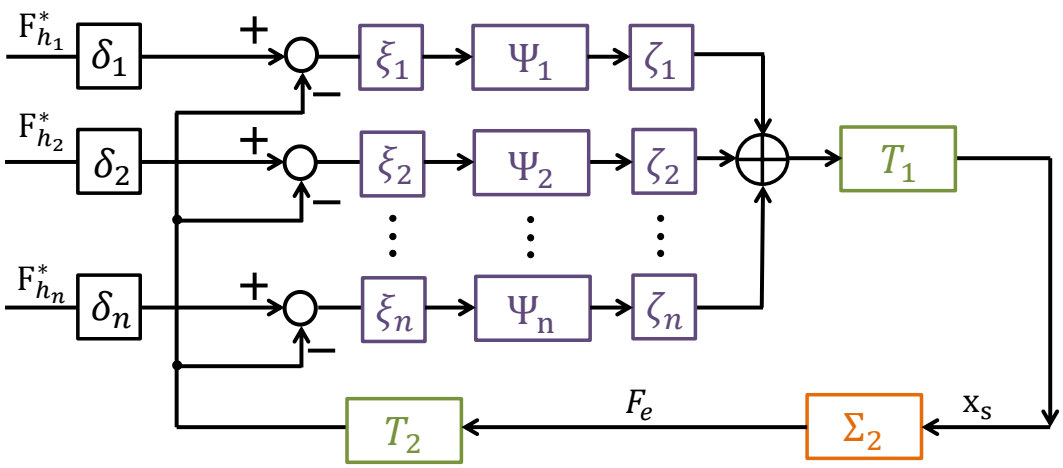

Figure 7.3: General scheme of the MM/SS system after some manipulations

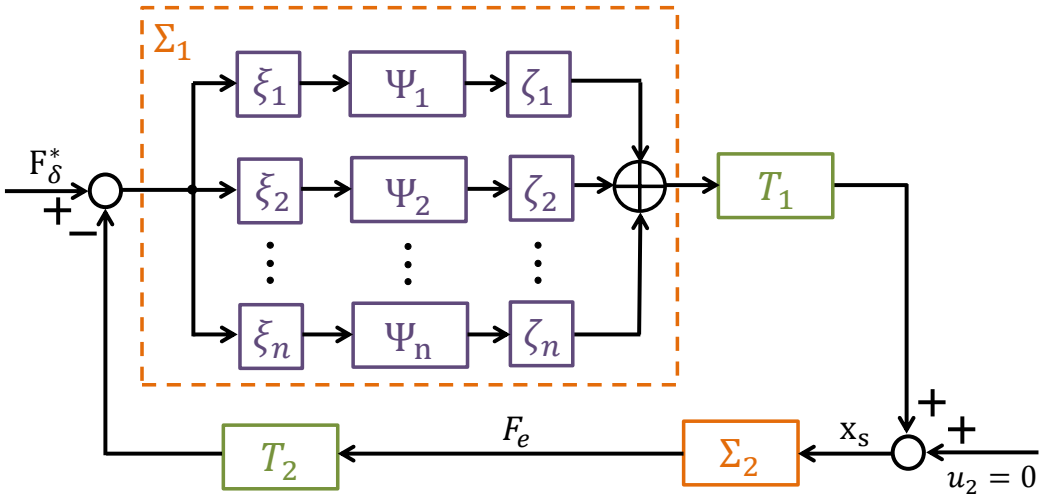

Figure 7.4: General scheme of the MM/SS system transformed so as to match with Fig. 7.1.

7.6.1 Constant Communication Delay

In the case of constant communication delay, ζ_i and ξ_i, for $i = 1, 2, \ldots, n$, have constant values. Therefore, using the Laplace transform, they can be modeled as $e^{\zeta_i s}$ and $e^{\xi_i s}$ in the frequency domain. To investigate input-to-output stability of the closed-loop system, as the first condition given by (7.19) implies, the inputs F^*_δ and u_2 are needed to be bounded, that is $F^*_\delta \in L_\infty$ & $u_2 \in L_\infty$. According to the system structure, $u_2 \in L_\infty$. To investigate $F^*_\delta \in L_\infty$, by some algebraic manipulations, (7.25) can be transformed to:

$$F^*_\delta = \sum_{k=1}^{n} \frac{F^*_k . \alpha_k . \prod_{j \neq k} \left(Z_{h_j} + Z_{j,d}\right)}{\sum_{i=1}^{n} \alpha_i . \left[\prod_{j \neq i} (Z_{h_j} + Z_{j,d})\right] . e^{\xi_i s}} \tag{7.26}$$

By defining $\varpi_k = \dfrac{\alpha_k . \prod_{j\neq k}\left(Z_{h_j}+Z_{j,d}\right) . e^{\xi_k s}}{\sum_{i=1}^{n}\alpha_i . \left[\prod_{j\neq i}(Z_{h_j}+Z_{j,d})\right] . e^{\xi_i s}}$ for $k=1,\ldots,n$, (7.26) can be written as:

$$F_\delta^* = \sum_{k=1}^{n}(F_k^* . e^{-\xi_k s}).\varpi_k \tag{7.27}$$

In this equation, F_k^* for $k=1,2,\ldots,n$, which is the hand exogenous force for operator #k in the frequency space belongs to L_∞ [41]. Therefore, $F_k^* . e^{-\xi_k s}$ also belongs to L_∞, since the time delay does not change the L_∞-norm. In addition, n , the number of the involved operators, is a bounded value. Therefore, to satisfy $F_\delta^* \in L_\infty$, it is sufficient for ϖ_k no matter of the causality issue, to be bounded, i.e., to be a proper transfer function with no poles on $j\omega$ axis. For $k=1,\ldots,n$, $e^{\xi_k s}$ can be modeled by a λ-order *Padé* approximation as follows:

$$e^{\xi_k s} = \frac{1-\imath_{1,k}s+\imath_{2,k}s^2+\ldots\pm\imath_{\lambda,k}s^\lambda}{1+\imath_{1,k}s+\imath_{2,k}s^2+\ldots+\imath_{\lambda,k}s^\lambda} \tag{7.28}$$

where $\imath_{\vartheta,k}$ $(\vartheta=1,\ldots,\lambda)$ are constant parameters proportional to ξ_k. By substituting $e^{\xi_k s}$ from (7.28), ϖ_k will be transformed to:

$$\varpi_k = \frac{\alpha_k . \left[\prod_{j\neq k}\left(Z_{h_j}+Z_{j,d}\right)\right] . \left(\dfrac{1-\imath_{1,k}s+\imath_{2,k}s^2+\ldots\pm\imath_{\lambda,k}s^\lambda}{1+\imath_{1,k}s+\imath_{2,k}s^2+\ldots+\imath_{\lambda,k}s^\lambda}\right)}{\sum_{i=1}^{n}\left[\alpha_i . \left[\prod_{j\neq i}(Z_{h_j}+Z_{j,d})\right] . \left(\dfrac{1-\imath_{1,i}s+\imath_{2,i}s^2+\ldots\pm\imath_{\lambda,i}s^\lambda}{1+\imath_{1,i}s+\imath_{2,i}s^2+\ldots+\imath_{\lambda,i}s^\lambda}\right)\right]} \tag{7.29}$$

By some algebraic manipulation, it can be shown that ϖ_k, $(k=1,\ldots,n)$, is a proper transfer function, belonging to L_∞. Therefore, the first stability condition given by (19) is fulfilled. The next step is investigating the second stability condition, given in (7.20). According to the definition Σ_1 and Σ_2, $\|\Sigma_1\|_{L_1}$ and $\|\Sigma_2\|_{L_1}$ are as follows:

$$\|\Sigma_1\|_{L_1} = \left\|\sum_{i=1}^{n}\Psi_i\, e^{(\zeta_i+\xi_i)s}\right\|_{L_1} = \left\|\sum_{i=1}^{n}\alpha_i(Z_{h_i}+Z_{i,d})^{-1}\, e^{(\zeta_i+\xi_i)s}\right\|_{L_1} \tag{7.30}$$

$$\|\Sigma_2\|_{L_1} = \|Z_e\|_{L_1} \tag{7.31}$$

According to the definition of the L_1-norm in the frequency domain, $\|\Sigma_1\|_{L_1}$ can be written as:

$$\begin{aligned}\|\Sigma_1\|_{L_1} &= \int_{-\infty}^{+\infty} \left| \sum_{i=1}^{n} \alpha_i (Z_{h_i} + Z_{i,d})^{-1} \; e^{(\zeta_i+\xi_i)s} \right| d\omega \\ &\leq \int_{-\infty}^{+\infty} \sum_{i=1}^{n} \left| \alpha_i (Z_{h_i} + Z_{i,d})^{-1} \; e^{(\zeta_i+\xi_i)s} \right| d\omega \\ &= \int_{-\infty}^{+\infty} \sum_{i=1}^{n} \left| \alpha_i (Z_{h_i} + Z_{i,d})^{-1} \right| \left| e^{(\zeta_i+\xi_i)s} \right| d\omega\end{aligned} \tag{7.32}$$

Considering the fact that $\left| e^{(\zeta_i+\xi_i)j\omega} \right|_{i=1,2,\ldots,n} = 1$, the right-hand side of the above inequality can be simplified as follows:

$$\begin{aligned}\|\Sigma_1\|_{L_1} &\leq \int_{-\infty}^{+\infty} \sum_{i=1}^{n} \left| \alpha_i (Z_{h_i} + Z_{i,d})^{-1} \right| d\omega \\ &= \sum_{i=1}^{n} \int_{-\infty}^{+\infty} \left| \alpha_i (Z_{h_i} + Z_{i,d})^{-1} \right| d\omega \\ &= \sum_{i=1}^{n} \left\| \alpha_i (Z_{h_i} + Z_{i,d})^{-1} \right\|_{L_1}\end{aligned} \tag{7.33}$$

Therefore, an upper-bound for $\|\Sigma_1\|_{L_1}$ is calculated as:

$$\|\Sigma_1\|_{L_1} \leq \sum_{i=1}^{n} \left\| \alpha_i (Z_{h_i} + Z_{i,d})^{-1} \right\|_{L_1} \tag{7.34}$$

As given in (7.22) and (7.23), Z_{h_i} and $Z_{i,d}$ represent impedances. Therefore, $(Z_{h_i} + Z_{i,d})^{-1}$ is a strictly-proper transfer function. Since $0 \leq \alpha_i \leq 1$, $\|\alpha_i (Z_{h_i} + Z_{i,d})^{-1}\|_{L_1}$ has an upper bound. Calling the upper-bound β_i, inequality (7.34) can be written as:

$$\begin{aligned}\|\Sigma_1\|_{L_1} &\leq \sum_{i=1}^{n} \left\| \alpha_i (Z_{h_i} + Z_{i,d})^{-1} \right\|_{L_1} \\ &\leq n * max(\beta_i)_{i=1,2,\ldots,n}\end{aligned} \tag{7.35}$$

where n represents the number of master consoles. As a result, $\|\Sigma_1\|_{L_1}$ has an upper bound, $n * max(\beta_i)_{i=1,2,\ldots,n}$, which implies $\Sigma_1 \in L_1$ as a part of the second stability condition given by (7.20).

As given by (7.20), for the second stability condition of the small-gain theorem, it is required to have $\Sigma_2 \in L_1$. Considering the definition of $\Sigma_2 = Z_e$, where Z_e is the environment impedance which is an improper dynamics, it is clear that Σ_2 does not belong to L_1. In order to transform Σ_2 to a proper dynamics, a low-pass filter $\Pi(s) = \dfrac{1}{\phi_1 s^2 + \phi_2 s + \phi_3}$ can be applied to the environment force, before sending it to the master robots sides, which is a typical approach in the small-gain-based teleoperation systems as elaborated in [20]. The applied filter may introduce undesired lag into the system and alleviate the high-frequency component of the reflected environment-force, degrading the transparency. However, these undesired effects can be decreased by setting the filter's poles far enough. By applying the filter $\Pi(s)$, Σ_2 will be transformed to $Z_e(s)\Pi(s) = \dfrac{M_e s^2 + B_e s + K_e}{\phi_1 s^2 + \phi_2 s + \phi_3}$ which belongs to L_1 space and consequently, the second part of the first stability condition given by (7.20) is satisfied.

The third stability condition given by (7.21) requires to have $\gamma_1.\gamma_2$, where $\gamma_1 = \|\Sigma_1\|_{L_1}$, $\gamma_2 = \|\Sigma_2\|_{L_1}$. Using the derived inequality in (7.34), the stability condition can be written as follows to achieve a sufficient stability condition:

$$\begin{aligned} \gamma_1.\gamma_2 &= \|\Sigma_1\|_{L_1}\|\Sigma_2\|_{L_1} \\ &\leq \left(\int_{-\infty}^{+\infty}\sum_{i=1}^{n}\left|\alpha_i(Z_{h_i}+Z_{i,d})^{-1}\right|d\omega\right).\|\Sigma_2\|_{L_1} \leq 1 \end{aligned} \tag{7.36}$$

Simplifying $(\int_{-\infty}^{+\infty}\sum_{i=1}^{n}\left|\alpha_i(Z_{h_i}+Z_{i,d})^{-1}\right|d\omega).\|\Sigma_2\|_{L_1} \leq 1$, a sufficient stability condition is derived as follows:

$$\frac{M_e s^2 + B_e s + K_e}{\phi_1 s^2 + \phi_2 s + \phi_3} \leq \left|\frac{1}{\sum_{i=1}^{n}\left|\alpha_i(Z_{h_i}+Z_{i,d})^{-1}\right|}\right| \tag{7.37}$$

Using the inequality $\sum_{i=1}^{n}\left|\alpha_i(Z_{h_i}+Z_{i,d})^{-1}\right| \leq \left|\sum_{i=1}^{n}\alpha_i(Z_{h_i}+Z_{i,d})^{-1}\right|$, the sufficient stability condition given in (7.37), derived for the MM/SS system in the presence of constant time-delay, can be transformed to:

$$\frac{Z_e}{\phi_1 s^2 + \phi_2 s + \phi_3} \leq \left|\frac{1}{\sum_{i=1}^{n}\alpha_i(Z_{h_i}+Z_{i,d})^{-1}}\right| \tag{7.38}$$

As can be seen, system stability can be ensured by appropriate adjustment of the desired impedance parameters, $M_{i,d}$, $B_{i,d}$ and $K_{i,d}$, where $Z_{i,d} = M_{i,d}s^2 + B_{i,d}s + K_{i,d}$, meaning that in order to guarantee system stability the parameters may be needed to be set to non-zero values.

However, referring to the desired impedance surfaces defined in (7.15) and (7.16), it is obvious that setting $M_{i,d}$, $B_{i,d}$ and $K_{i,d}$ to non-zero values causes the system transparency to deviate from the ideal situation. However, the compromise between system stability and transparency is essential in an MM/SS system, as it is also the case in SM/SS, the traditional category of teleoperation system.

By setting the number of users to 1, and also setting the filter poles sufficiently far, the stability condition derived in (7.38) will be transformed to $|Z_e| \leq |(Z_{h_i} + Z_{i,d})|$, which is in accordance with the condition derived in the literature for the traditional SM/SS system.

It is noteworthy that to ensure system stability, proper adjustment of the desired impedance parameters, $M_{i,d}$, $B_{i,d}$ and $K_{i,d}$, is an important issue to focus on. For this purpose, either a rough estimation of the operator's hand impedance, or a rough upper-bound estimation would suffice, ensuring system stability in a conservative manner. There has been some research aimed at providing measures of an operator's hand impedance with/without force sensors [42], [43], [44] This topic will be studied in more depth as a part of our future work.

7.6.2 Time-Varying Communication Delay

In order to analyze system stability in case of time-varying communication delays, the following assumption is made: $d_1 = d_2 = ... = d_i$ and $d_1^{'} = d_2^{'} = ... = d_n^{'}$, which means equal delays between the slave console and the master consoles. By making this assumption, T_1 and T_2 will be transformed to $T_1 = d_i$ and $T_2 = d_i^{'}$, which leads to $\zeta_i = \xi_i = 0$. Following the same procedure for constant time-delay, (7.26)-(7.38), it can be seen that (7.38) will also be a sufficient stability condition for the system in the presence of equal time-varying delays.

An approach to satisfy the above assumption is to locate all the master consoles, and consequently the operators, at the same site. In training applications, such as in surgery, this assumption is not restricting since the expert and the class of trainees can be located at the same site. However, for more flexibility, our future work will focus on relaxing the assumption made for the time-varying delay case.

7.7 Experiments

7.7.1 Experimental Setup

In order to evaluate the proposed methodology, a set of experiments were conducted. The experimental setup consists of two customized Quanser Haptic Wands and a Quanser HD^2 as the master consoles and one Mitsubishi PA10-7C robot as the slave console.

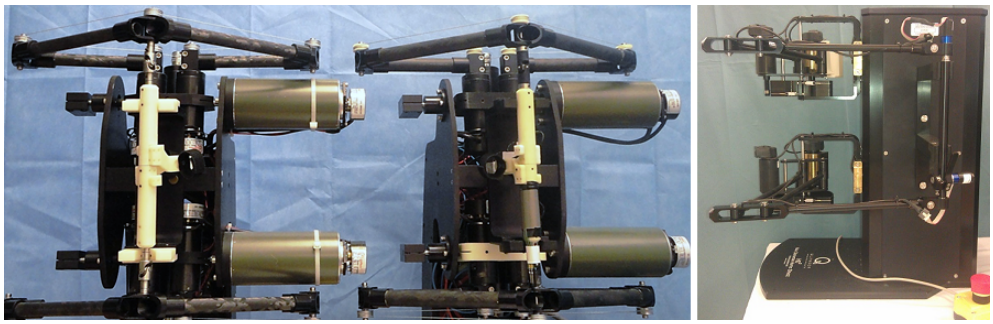

(a) Customized Quanser haptic wands, and Quanser HD^2

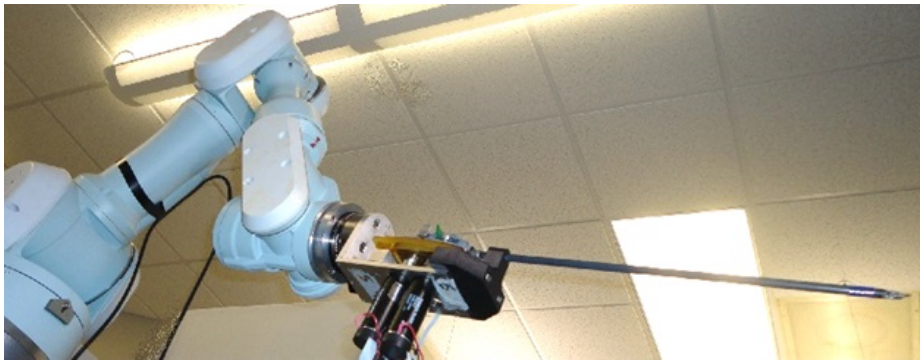

(b) Mitsubishi PA10-7C slave robot and *da Vinci* tool.

Figure 7.5: The experimental setup.

Fig. 7.5 shows the experimental setup. The controller for each robot was implemented on a computer and the Real-Time QuaRC software was used to automatically generate real-time code directly from MATLAB Simulink. The User Datagram Protocol (UDP) was used for communication between the master consoles and the slave console. In order to expose the system to random time-varying communication delays, delay blocks from MATLAB Simulink were used. The round-trip time-varying delay between the slave robot and master robot #1, #2, and #3 were set to $T_1 = 260 \pm 40ms$, $T_2 = 280 \pm 40ms$, and $T_3 = 220 \pm 40ms$, respectively. All controllers and the communication between the robots were implemented at a sampling frequency of 1 kHz.

7.7.2 Experimental Results

The experiments consisted of two main scenarios. In the first scenario, the behavior of the system in the presence of various sets of dominance factors was investigated. For this purpose, three experiments were performed in which the dominance factors were set as follows: 1) $\alpha_1 = \alpha_2 = 0.333$, $\alpha_3 = 0.334$, allocating equal authority level for the operators, 2) $\alpha_1 = \alpha_2 = 0.5$, $\alpha_3 = 0$, allocating some authority level for operators #1 and #2, while setting zero authority for operator #3, and 3) $\alpha_1 = \alpha_2 = 0$, $\alpha_3 = 1$, giving full authority to operator #3, while setting zero authority for operator #1 and #2. The results for these experiments are given in Fig. 7.6-Fig. 7.8. In these experiments, $M_{i,d} = 0.3\ kg$ and $B_{i,d} = 0.6\ N.s/m$ and the task was defined to move in both free motion and in-contact motion interacting with soft tissue. As can be seen in Fig. 7.6a, each of the master robots had some level of authority over the slave robot. To clearly show this, the experiment was conducted in four segments: $0-25s$, $25-55s$, $55-90s$ and $90-125s$. In the first three sections, one operator was asked to move the corresponding master robot at each time range, while the other two operators were asked to keep their master robots firmly at a fix position. It can be seen that the operators were able control the slave robot proportional to their authority level, $\alpha_1 = \alpha_2 = 0.333$, $\alpha_3 = 0.334$. In the last episode of the experiment, the three operators were asked to manipulate their master robots concurrently. As can be seen, the slave robot moved in accordance with the combination of their positions based on their authority level. In addition, Fig. 7.6b shows the force profile for the environment and the operators' hands. As shown in this figure, without regarding the authority level of the operators, each operator was able to feel the environment force, although with a delay. Note that as discussed earlier, due to the considerable amount of communication delays, the transparency level is not ideal. However, a delayed format of the environment force can be reflected on the operators' hands, which is the case in this experimental result.

The second experiment conducted for the first scenario, the results of which are shown in Fig. 7.7, investigates a different set of authority levels for the operators, where $\alpha_1 = \alpha_2 = 0.5$, $\alpha_3 = 0$. As can be seen in Fig. 7.7a between $t = 0s$ and $t = 30s$, although operator #3 moved his corresponding master robot, the slave robot remained stationary which is due to the zero authority level set for operator #3. However, both operators #1 and #2 had control over the slave robot proportional to their authority level, as can be seen from $t = 30s$ onwards. Moreover,

without regarding the levels of authority set for the operators, as shown in Fig. 7.7b, they were all able to feel the delayed environment force reflected back on their hand.

Another set of authority levels, $\alpha_1 = \alpha_2 = 0$, $\alpha_3 = 1$, was set for the operators, the results of which are shown in Fig. 7.8. This experiment was performed to show the system behavior as an SM/SS system, which is an especial case of the general MS/SS system. For this purpose, the authority of the two operators was set to zero, whereas the third one was given full authority. As shown in Fig. 7.8a, operators #1 and #2 had no authority over the slave robot, while operator #3 was fully controlling the task. As shown in Fig. 7.8b, all the operators were able to feel the environment force, even though two of them did not have any involvement in the task.

With regard to the precision of the slave robot's end-effector, consider Fig. 7.8a as a specific example. In this figure, by setting $\alpha_1 = \alpha_2 = 0$, $\alpha_3 = 1$, the slave robot was set to follow the movements made by the end-effector of master robot #3. The results show that x_s tracks x_{m_3} accurately indicating good tracking performance for the slave robot's end-effector.

In the second experimental scenario, the effect of the desired impedance parameters on the system behavior was investigated. For this purpose, a heavy hard object was used as the environment and the task was defined to interact with the object, which could possibly lead to instability in the system. In this scenario, two experiments were conducted, focusing on the effect of the desired impedance parameters on system stability. In both experiments, the authority levels for the operators were set similarly to $\alpha_1 = \alpha_2 = 0.1, \alpha_3 = 0.8$, in order to create a comparable condition between the two experiments. In the first experiment the result of which is shown in Fig. 7.9, $M_{i,d}$ and $B_{i,d}$, $(i = 1,2,3)$ were set to 0.3 kg and 0.6 $N.s/m$, respectively. As shown in Fig. 7.9, these parameters were not high enough to satisfy the closed-loop stability condition and consequently were not able to stabilize the system. Therefore, the system behavioral trend was towards instability.

In the next experiment, $M_{i,d}$ and $B_{i,d}$, $(i = 1,2,3)$ were set to 1.2 kg and 2.4 $N.s/m$, while the other factors were kept similar to those of the previous experiment. As shown in Fig. 7.10, the closed-loop stability condition was satisfied and the system behaved in a stable manner. As can be seen in Fig. 7.10a, the slave robot tracked an α_i-based combination of the three master robots. In addition, all the operators were able to feel the force reflected back from the environment.

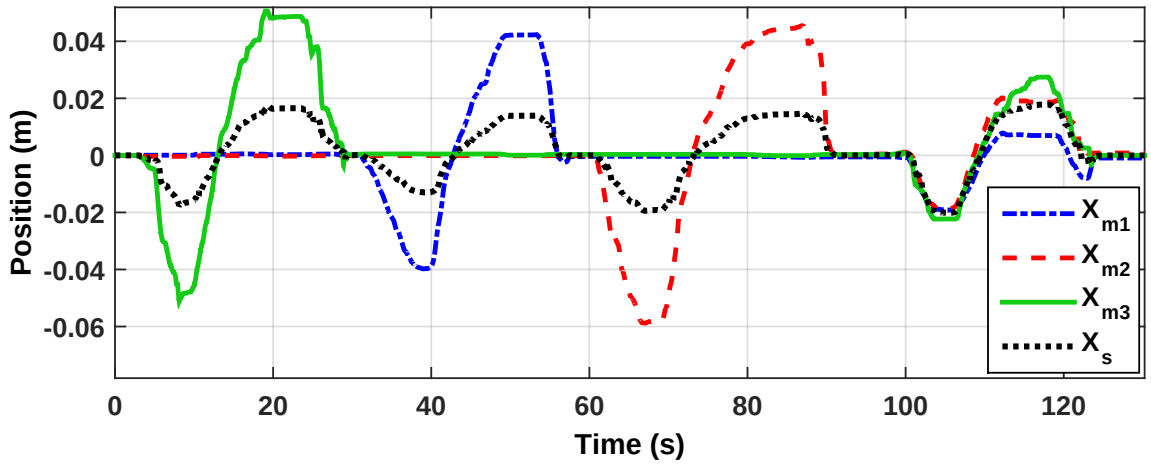

(a) Position comparison

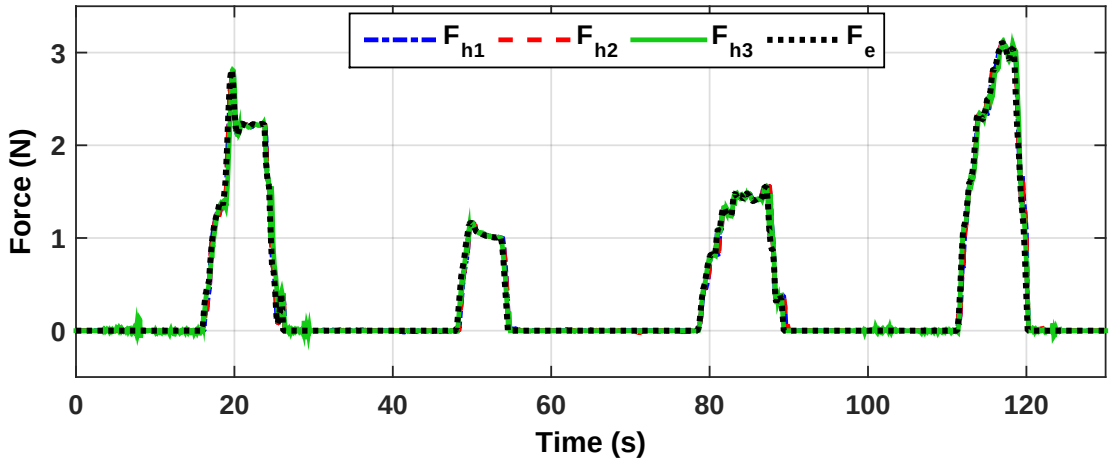

(b) Force comparison

Figure 7.6: Experimental results for the first scenario, $\alpha_1 = \alpha_2 = 0.333$, $\alpha_3 = 0.334$, $M_{i,d} = 0.3\ kg$ and $B_{i,d} = 0.6\ N.s/m$.

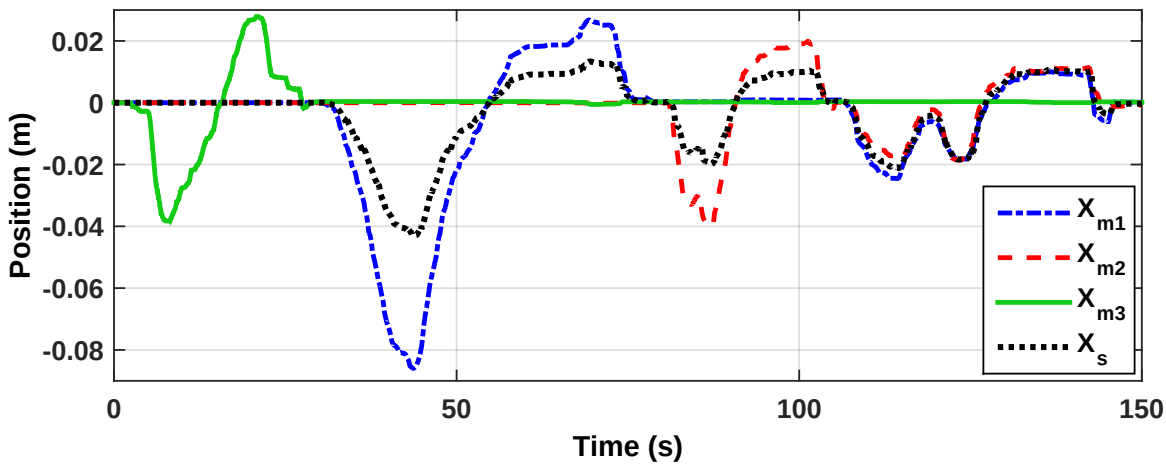

(a) Position comparison

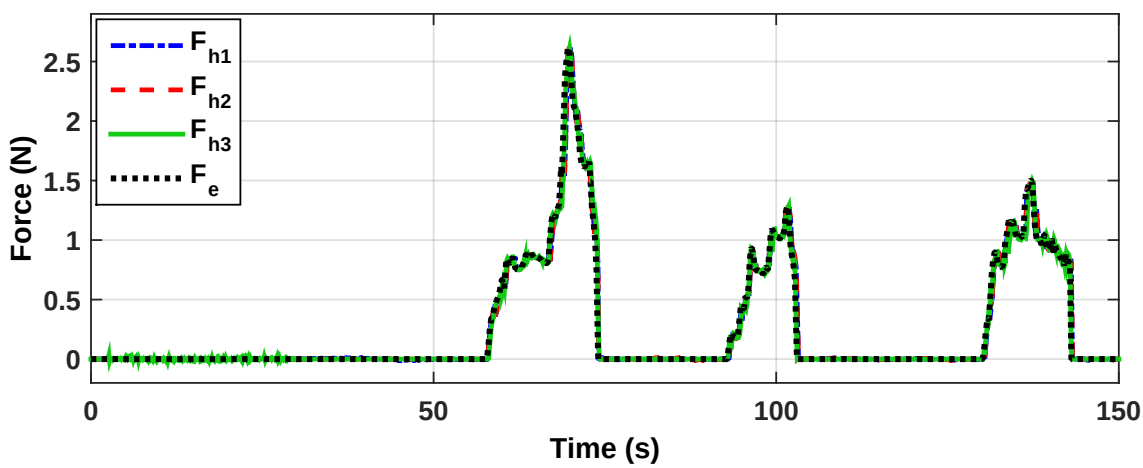

(b) Force comparison

Figure 7.7: Experimental results for the first scenario, $\alpha_1 = \alpha_2 = 0.5$, $\alpha_3 = 0$, $M_{i,d} = 0.3\ kg$ and $B_{i,d} = 0.6\ N.s/m$.

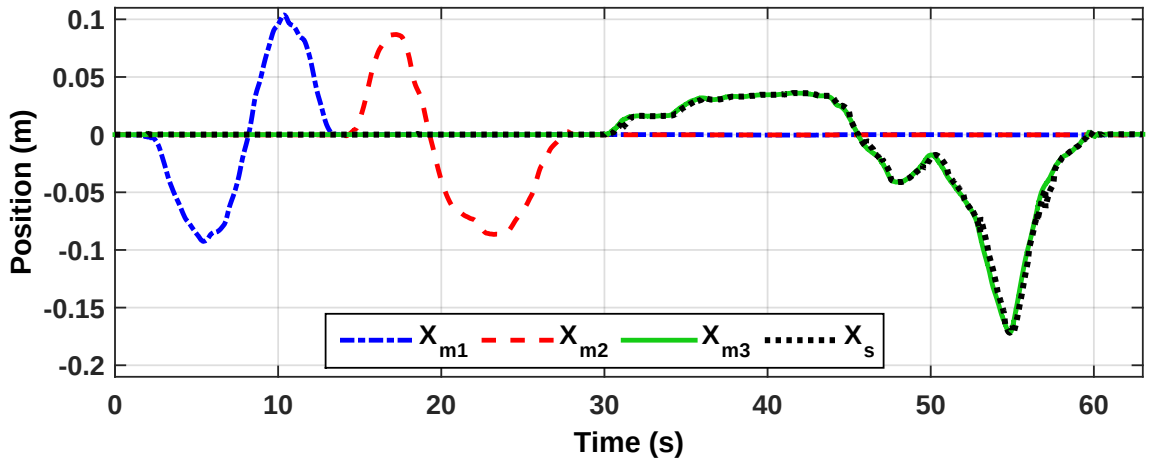

(a) Position comparison

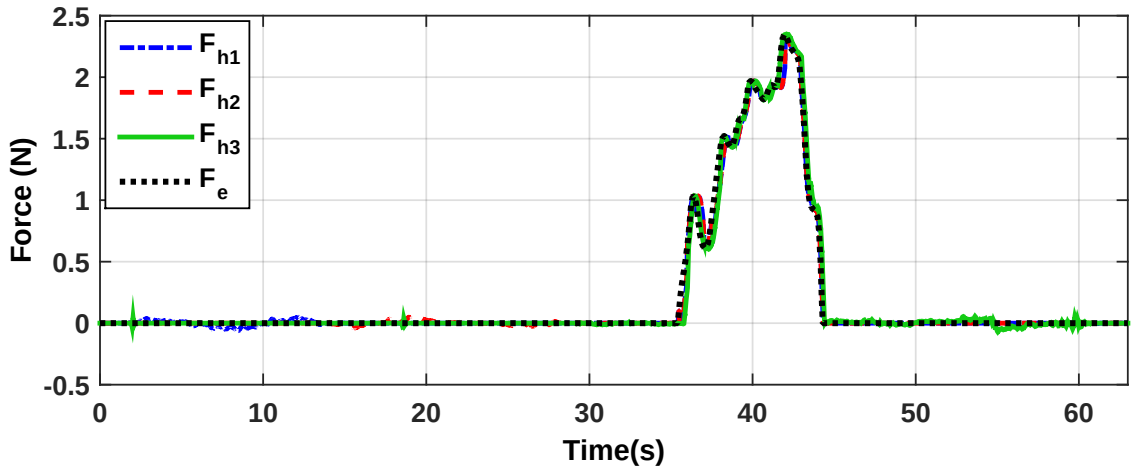

(b) Force comparison

Figure 7.8: Experimental results for the first scenario, $\alpha_1 = \alpha_2 = 0$, $\alpha_3 = 1$, $M_{i,d} = 0.3\ kg$ and $B_{i,d} = 0.6\ N.s/m$.

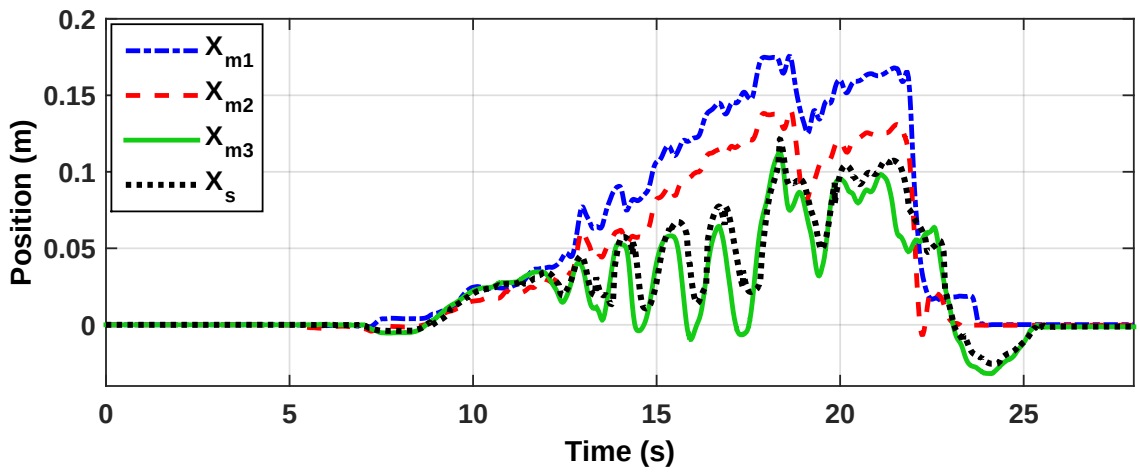

(a) Position comparison

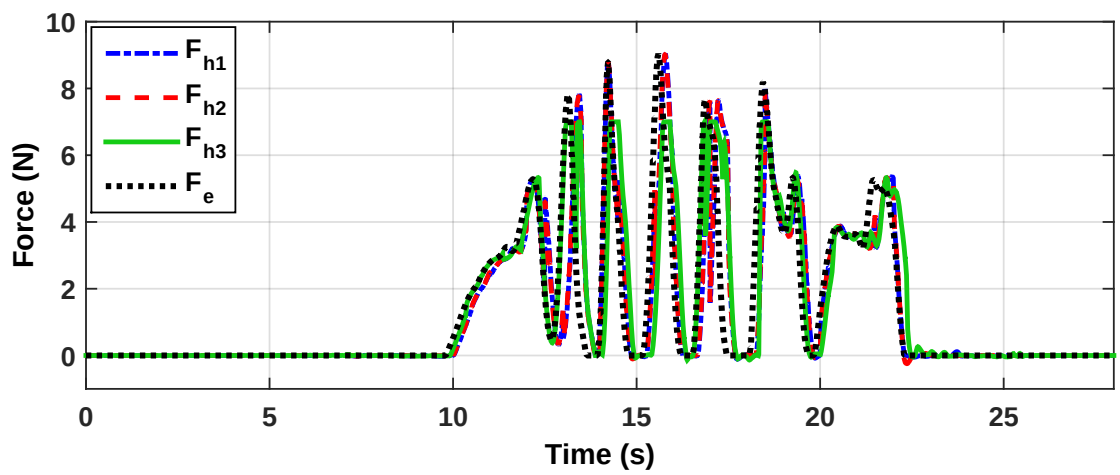

(b) Force comparison

Figure 7.9: Experimental results for the second scenario, $\alpha_1 = \alpha_2 = 0.1$, $\alpha_3 = 0.8$, $M_{i,d} = 0.3\ kg$ and $B_{i,d} = 0.6\ N.s/m$.

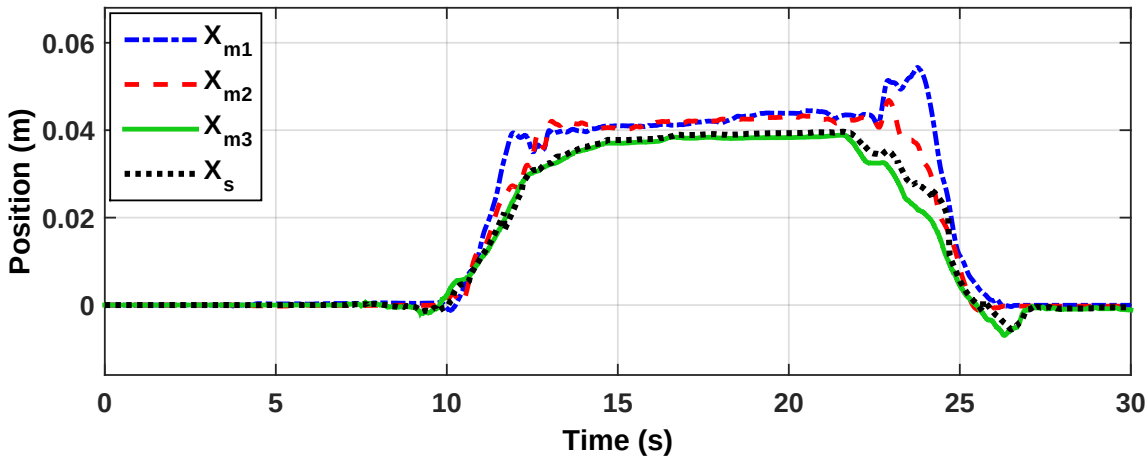

(a) Position comparison

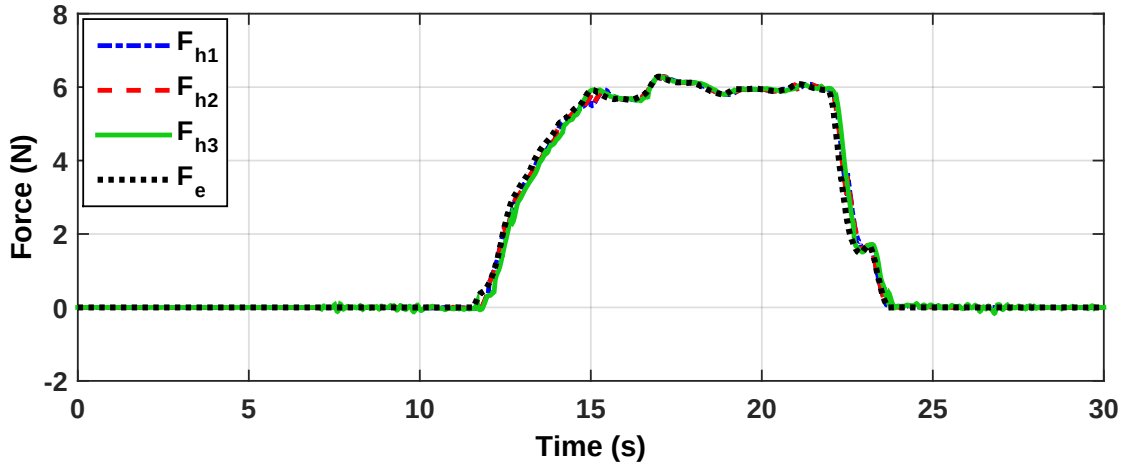

(b) Force comparison

Figure 7.10: Experimental results for the second scenario, $\alpha_1 = \alpha_2 = 0.1$, $\alpha_3 = 0.8$, $M_{i,d} = 1.2\ kg$ and $B_{i,d} = 2.4\ N.s/m$.

7.8 Conclusions

In this chapter, a general MM/SS teleoperated system was proposed. A set of desired objectives for the MM/SS system were presented in such a way that both cooperative and training applications, e.g. surgical teleoperation and surgical training, can benefit. Using the passivity theorem, it was shown that an ideal MM/SS system is not passive unlike the traditional SM/SS system. To satisfy the desired objectives, an impedance-based control methodology was adopted. Stability of the closed-loop system in the presence of communication delay was investigated using the small-gain theorem and a sufficient condition was derived to ensure system stability. Experimental results on an MM/SS system were given to evaluate the proposed methodology.

Bibliography

[1] Y. Ye and P. X. Liu, "Improving trajectory tracking in wave-variable-based teleoperation," *IEEE/ASME Transactions on Mechatronics*, vol. 15, no. 2, pp. 321–326, 2010.

[2] V. Chawda and M. K. OMalley, "Position synchronization in bilateral teleoperation under time-varying communication delays," *IEEE/ASME Transactions on Mechatronics*, vol. 20, no. 1, pp. 245–253, 2015.

[3] S. Islam, P. X. Liu, A. El Saddik, and Y. B. Yang, "Bilateral control of teleoperation systems with time delay," *IEEE/ASME Transactions on Mechatronics*, vol. 20, no. 1, pp. 1–12, 2015.

[4] S. Munir and W. J. Book, "Internet-based teleoperation using wave variables with prediction," *IEEE/ASME Transactions on Mechatronics*, vol. 7, no. 2, pp. 124–133, 2002.

[5] D. A. Lawrence, "Stability and transparency in bilateral teleoperation," *IEEE Transactions on Robotics and Automation*, vol. 9, no. 5, pp. 624–637, 1993.

[6] R. J. Anderson and M. W. Spong, "Bilateral control of teleoperators with time delay," *IEEE Transactions on Automatic Control*, vol. 34, no. 5, pp. 494–501, 1989.

[7] R. Lozano, N. Chopra, and M. W. Spong, "Passivation of force reflecting bilateral teleoperators with time varying delay," in *Proceedings of the 8th Mechatronics Forum*. Citeseer, 2002, pp. 954–962.

[8] G. Niemeyer and J.-J. E. Slotine, "Towards force-reflecting teleoperation over the internet," in *IEEE International Conference on Robotics and Automation, 1998*, vol. 3. IEEE, 1998, pp. 1909–1915.

[9] D. A. Lawrence, "Stability and transparency in bilateral teleoperation," *IEEE Transactions on Robotics and Automation*, vol. 9, no. 5, pp. 624–637, 1993.

[10] K. Hashtrudi-Zaad and S. E. Salcudean, "Transparency in time-delayed systems and the effect of local force feedback for transparent teleoperation," *IEEE Transactions on Robotics and Automation*, vol. 18, no. 1, pp. 108–114, 2002.

[11] E. Naerum and B. Hannaford, "Global transparency analysis of the lawrence teleoperator architecture," in *IEEE International Conference on Robotics and Automation*. IEEE, 2009, pp. 4344–4349.

[12] S. F. Atashzar, M. Shahbazi, H. A. Talebi, and R. V. Patel, "Control of time-delayed telerobotic systems with flexible-link slave manipulators," in *IEEE/RSJ International Conference on Intelligent Robots and Systems*. IEEE, 2012, pp. 3035–3040.

[13] P. F. Hokayem and M. W. Spong, "Bilateral teleoperation: An historical survey," *Automatica*, vol. 42, no. 12, pp. 2035–2057, 2006.

[14] C. Melchiorri and A. Eusebi, "Telemanipulation: System aspects and control issues," *Proc. Model. Cont. Mechan. Robot*, pp. 149–183, 1996.

[15] M. Tavakoli, *Haptics for teleoperated surgical robotic systems*. New Frontiers in Robotics series, World Scientific., 2008.

[16] A. D. Greer, P. M. Newhook, and G. R. Sutherland, "Human–machine interface for robotic surgery and stereotaxy," *IEEE/ASME Transactions on Mechatronics*, vol. 13, no. 3, pp. 355–361, 2008.

[17] J. Burgner, D. C. Rucker, H. B. Gilbert, P. J. Swaney, P. T. Russell, K. D. Weaver, and R. J. Webster, "A telerobotic system for transnasal surgery," *IEEE/ASME Transactions on Mechatronics*, vol. 19, no. 3, pp. 996–1006, 2014.

[18] A. Gupta and M. K. O'Malley, "Design of a haptic arm exoskeleton for training and rehabilitation," *IEEE/ASME Transactions on Mechatronics*, vol. 11, no. 3, pp. 280–289, 2006.

[19] P. R. Culmer, A. E. Jackson, S. Makower, R. Richardson, J. A. Cozens, M. C. Levesley, and B. B. Bhakta, "A control strategy for upper limb robotic rehabilitation with a dual robot system," *IEEE/ASME Transactions on Mechatronics*, vol. 15, no. 4, pp. 575–585, 2010.

[20] S. F. Atashzar, I. G. Polushin, and R. V. Patel, "Networked teleoperation with non-passive environment: Application to tele-rehabilitation," in *IEEE/RSJ International Conference on Intelligent Robots and Systems*. IEEE, 2012, pp. 5125–5130.

[21] S. S. Nudehi, R. Mukherjee, and M. Ghodoussi, "A shared-control approach to haptic interface design for minimally invasive telesurgical training," *IEEE Transactions on Control Systems Technology*, vol. 13, no. 4, pp. 588–592, 2005.

[22] [Online]. Available: http://www.intuitivesurgical.com/products/davinci_surgical_system/davinci_surgical_system_si/

[23] M. Shahbazi, S. F. Atashzar, and R. V. Patel, "A dual-user teleoperated system with virtual fixtures for robotic surgical training," in *IEEE International Conference on Robotics and Automation*. IEEE, 2013, pp. 3639–3644.

[24] H. I. Krebs and N. Hogan, "Therapeutic robotics: A technology push," *Proceedings of the IEEE*, vol. 94, no. 9, pp. 1727–1738, 2006.

[25] S. Moghimi, S. Sirouspour, and P. Malysz, "Haptic-enabled collaborative training with generalized force and position mappings," in *symposium on Haptic interfaces for virtual environment and teleoperator systems*. IEEE, 2008, pp. 287–294.

[26] B. Khademian and K. Hashtrudi-Zaad, "Dual-user teleoperation systems: New multilateral shared control architecture and kinesthetic performance measures," *IEEE/ASME Transactions on Mechatronics*, vol. 17, no. 5, pp. 895–906, 2012.

[27] M. Shahbazi, H. Talebi, and F. Towhidkhah, "A robust control architecture for dual user teleoperation system with time-delay," in *36th Annual Conference on IEEE Industrial Electronics Society*. IEEE, 2010, pp. 1419–1423.

[28] M. Shahbazi, S. F. Atashzar, H. A. Talebi, F. Towhidkhah, and M. Yazdanpanah, "A sliding-mode controller for dual-user teleoperation with unknown constant time delays," *Robotica*, vol. 31, no. 04, pp. 589–598, 2013.

[29] M. Shahbazi, H. A. Talebi, S. F. Atashzar, F. Towhidkhah, R. V. Patel, and S. Shojaei, "A novel shared structure for dual user systems with unknown time-delay utilizing adaptive impedance control," in *IEEE International Conference on Robotics and Automation*. IEEE, 2011, pp. 2124–2129.

[30] B. Khademian, J. Apkarian, and K. Hashtrudi-Zaad, "Assessment of environmental effects on collaborative haptic guidance," *Presence: Teleoperators and Virtual Environments*, vol. 20, no. 3, pp. 191–206, 2011.

[31] S. Yun, S. Park, B. Park, S. K. Park, H. Prahlad, P. Von Guggenberg, and K.-U. Kyung, "Polymer-based flexible visuo-haptic display," *Mechatronics, IEEE/ASME Transactions on*, vol. 19, no. 4, pp. 1463–1469, 2014.

[32] Z. Ma and P. Ben-Tzvi, "Rml glove—an exoskeleton glove mechanism with haptics feedback," *Mechatronics, IEEE/ASME Transactions on*, vol. 20, no. 2, pp. 641–652, 2015.

[33] J. Li, M. Tavakoli, and Q. Huang, "Absolute stability of multi-dof multilateral haptic systems," *Control Systems Technology, IEEE Transactions on*, vol. 22, no. 6, pp. 2319–2328, 2014.

[34] L. Sciavicco and B. Siciliano, *Modelling and control of robot manipulators*. Berlin, Germany: Springer-Verlag, 2000.

[35] A. Shahdi and S. Sirouspour, "Adaptive/robust control for time-delay teleoperation," *IEEE Transactions on Robotics*, vol. 25, no. 1, pp. 196–205, 2009.

[36] M. Shahbazi, S. F. Atashzar, H. A. Talebi, and R. V. Patel, "An expertise-oriented training framework for robotics-assisted surgery," in *IEEE International Conference on Robotics and Automation*. IEEE, 2014, pp. 5902–5907.

[37] D. Lee and M. W. Spong, "Passive bilateral teleoperation with constant time delay," *Robotics, IEEE Transactions on*, vol. 22, no. 2, pp. 269–281, 2006.

[38] S. S. Haykin, *Active network theory*. Addison-Wesley, Boston, Massachusetts, USA, 1970.

[39] T. Koga, "Synthesis of finite passive n-ports with prescribed positive real matrices of several variables," *IEEE Transactions on Circuit Theory*, vol. 15, no. 1, pp. 2–23, 1968.

[40] C. A. Desoer and M. Vidyasagar, *Feedback systems: input-output properties*. SIAM, 2009, vol. 55.

[41] I. Polushin, H. J. Marquez, A. Tayebi, and P. X. Liu, "A multichannel IOS small gain theorem for systems with multiple time-varying communication delays," *IEEE Transactions on Automatic Control*, vol. 54, no. 2, pp. 404–409, 2009.

[42] P. K. Artemiadis, P. T. Katsiaris, M. V. Liarokapis, and K. J. Kyriakopoulos, "Human arm impedance: Characterization and modeling in 3d space," in *IEEE/RSJ International Conference on Intelligent Robots and Systems*. IEEE, 2010, pp. 3103–3108.

[43] K. Park and P. H. Chang, "Stochastic estimation of human shoulder impedance with robots: An experimental design," in *IEEE International Conference on Rehabilitation Robotics*. IEEE, 2011, pp. 1–8.

[44] M. Dyck and M. Tavakoli, "Measuring the dynamic impedance of the human arm without a force sensor," in *IEEE International Conference on Rehabilitation Robotics*. IEEE, 2013, pp. 1–8.

Chapter 8

Conclusions and Future Work

The work presented in this thesis was aimed at design and development of supervised telerobotic platforms that facilitate further investigations on the nature of human motor learning and retention in both Robotics-Assisted Mirror Therapy (RAMT) and Robotics-Assisted Minimally Invasive Surgery (RAMIS) applications. To this end, a wave-variable controller was proposed to ensure closed-loop stability of a classical trilateral teleoperation system in the presence of a time-varying dominance factor. Time-varying dominance factors in multilateral teleoperation platforms enable active participation and involvement of the trainee and thereby accelerate the motor learning process. In order to enable straightforward application of the proposed wave-variable control to Position-force Domain (PD), passivity of the human arm in PD was investigated using mathematical analyses, experimentation as well as user studies involving 12 participants and 48 trials. Implementing wave-variable controllers in PD eliminates inaccuracies due to position-error accumulation and position drift.

The results, in conjunction with the proposed wave-variable approach, can be used to guarantee closed-loop PD stability of the supervised trilateral teleoperation system in its classical format. Classic dual-user teleoperation frameworks do not, however, fully satisfy the requirements for properly inducing motor function in Robotics-Assisted Mirror Rehabilation Therapy (RAMRT) and Robotics-Assisted Minimally invasive Surgical Training (RAMIST). Therefore, novel supervised trilateral frameworks were designed and developed for inducing motor learning in RAMRT and RAMIST, each customized according to the requirements of the application. The frameworks enable time-varying involvement of the patient and trainee, adaptive and

skills-oriented adjustment of hand-over-hand haptic guidance for active immersion, as well as data transfer through communication networks with time delays for facilitating tele- and in-home rehabilitation and tele-surgical training. Finally, a multi-master/single-slave telerobotic framework was also proposed in order to accommodate for motor function training simultaneously for a class of patients or trainees. The next section discusses the contributions in further details.

8.1 Contributions

The main contributions of the thesis are as follows:

- A wave variable control approach was developed for conventional haptics-enabled dual-user teleoperation systems such that system stability is guaranteed in the presence of a time-varying dominance factor as well as communication time delays. The proposed controller includes a local impedance-based controller adopted from the literature for each robot and a wave transformation modified for the dual-user system with a time-varying dominance-factor. In order to investigate closed-loop stability, passivity theory was applied and it was shown that the proposed wave-variable controller guarantees system stability in the presence of a time-varying dominance factor, while the communication channels have constant time delays. Validity of the controller was demonstrated via experiments.

- Passivity of the human arm in position-force domain was investigated through mathematical analysis, experimentation and statistical user studies. It was shown that, unlike in the Velocity-force Domain (VD), passivity of the human arm in the position-force domain is frequency-dependent. This implies the necessity of making the human-arm terminal passive in addition to ensuring teleoperator passivity in PD, as opposed to that in VD, in which passivity of the human-arm terminal is assumed to inherently be the case. For future design of suitable controllers, statistical analyses were conducted to investigate correlations between the levels of PD passivity of the left and the right arms of the human participants, as well as the levels of passivity of their arms and their physical characteristics, e.g., weight, height, and body mass index. Possible control strategies

through which the passivity of the operator termination can be guaranteed in PD were also discussed.

- A trilateral teleoperation framework was developed for robotics-assisted mirror rehabilitation therapy, providing the following innovations:
  - Therapist-in-the-loop Mirror Therapy (MT), which enhances the motor recovery process for the patient's Impaired Limb (PIL) through the cross-cortex coupling effect between limbs, as well as the expertise and direct supervision of the therapist over the treatment to provide appropriate corrective movements.
  - Patient's Functional Limb (PFL)-mediation, which allows for the supervision/impact of the patient over the treatment through their PFL medium in order to guarantee the patient's safety and comfort by avoiding the application of excessive pressure and pain on the PIL.
  - Haptic feedback to the therapist from the patient side, which allows the therapist to decide on the intensity of the therapy administered to the patient;
  - Assist-as-needed therapy realized through an adaptive Guidance Virtual Fixture (GVF) which promotes active involvement of the patient in the treatment.
  - Task-independent and patient-specific motor-function assessment, which facilitates the adaptive adjustment of the therapy based on the patient's impairment level.

  Closed-loop stability of the proposed framework was rigorously investigated using a combination of the Circle Criterion and the Small-Gain Theorem, deriving a set of sufficient stability conditions. The proposed stability analysis also addresses instabilities caused by communication delays between the therapist and the patient, thereby, facilitates haptics-enabled tele/in-home rehabilitation. The proposed procedure also addresses extra stability challenges raised by the integration of the time-varying nonlinear GVF element into the delayed closed-loop system. Several experiments were conducted in order to evaluate the proposed framework.

- A trilateral teleoperation framework was developed for robotics-assisted minimally invasive surgical training, providing the following innovations:

- Expert-in-the-loop surgical training with multimodal sensorimotor integration to speed up the learning curve through haptic interaction between the novice and the expert.
- Adaptive expertise-oriented training– realized through a Fuzzy Interface System (FIS), which actively engages the trainee, while providing them with appropriate level/format of training, depending on their level of proficiency over the task.
- Task-independent motor skills assessment to facilitates adaptive expertise-oriented training.
- Haptic feedback from the surgical site to the expert surgeon which enables the expert to transparently perceive the surgical environment, disregarding the trainee's level of skills and participation.
- Conduct of a surgical procedure by an expert concurrent with providing multimodal training to a trainee at any stage of motor-skills learning, without jeopardizing patient safety.

Closed-loop stability of the proposed architecture was investigated using the Circle Criterion, in the presence and absence of tool-tissue interaction haptic feedback, and sufficient stability conditions were derived. In addition to the time-varying elements of the system, the stability analysis approach also addressed communication time delays, facilitating tele-surgical training. Experimental evaluations were presented in support of the proposed platform through the implementation of a dual-console surgical setup consisting of the classic *da Vinci*® surgical system (Intuitive Surgical, Inc., Sunnyvale, CA) and the dV-Trainer® master console (Mimic Technology Inc., Seattle, WA). The implemented setup serves as 1) the first research platform for dual-console studies and development on the classic *da Vinci*® surgical system, and 2) the first haptics-enabled training platform based on hand-over-hand guidance and cueing for such a system.

- A novel multi-master/single-slave telerobotics framework was designed. The desired objectives for the MM/SS system were presented such that both cooperative and training applications, e.g. surgical teleoperation and surgical training, can benefit. Passivity of the system was investigated and it was shown that, unlike a conventional SM/SS system,

an ideal MM/SS system, depending on its structure, may not always be passive. An impedance-based control methodology was developed to satisfy the desired objectives of the MM/SS system in the presence of communication delays. The Small-Gain theorem was applied to analyze closed-loop stability in the presence of time delays and a sufficient condition was derived. Experimental results on an MM/SS system were presented to evaluate the performance of the proposed methodology.

8.2 Future Work

Based on the work described in this thesis, there are several research directions that can be explored, as summarized below:

- The wave variable controller proposed for conventional trilateral frameworks in VD can be integrated with the results of the Position-force Domain Passivity (PDP) study of the human arm in order to directly apply the controller in PD. For this purpose, appropriate controllers to make the human-arm terminal passive in PD should be developed. Toward this end, the solutions suggested in Chapter 4 can be implemented and compared in terms of performance for various ranges of frequencies, identifying the approaches best fitting to the application. The results can also be used in conjunction with other VD passivity-based approaches in order to realize PD versions of such controllers.

  Based on the results derived in Chapter 4 from statistical studies on correlation between the PDP of the participant's arm and their physical characteristics, and through further user studies on a larger group of participants, passivity maps of the human arm in relation to their physical characteristics can be generated. Towards this end, appropriate artificial neural networks may be designed to associate the input data with the output data. The input data can include physical characteristics of the participants, e.g., weight, height, gender and BMI; The output data can be the frequency range over which their arm terminal remains passive. Such passivity maps would enable development of user-independent PD controllers that do not require identification of the impedance characteristics of the operator in teleoperation applications.

- Besides facilitating controller design in PD, PD passivity analysis of the arm terminal

for patients with hemiparesis may also serve as an appropriate metric to quantify the disability level as well as longitudinal functional recovery of their impaired limb. Irrespective of their gender and their baseline muscular strength, a patient's functional limb can serve as an ideal reference for their impaired limb in terms of maneuverability, range of motion and stiffness. Therefore, having a passivity map associated with dominant and non-dominant limbs of a group of healthy control participants can enable passivity-based assessment of the functional ability of a patient's impaired limb relative to that of their functional limb. The outcome can also be integrated with the relative skills assessment approach in Chapter 5 in order to enhance the efficacy of the proposed adaptive assist-as-needed therapy for RAMRT.

- Exploring the effectiveness of the framework proposed for RAMRT through clinical studies would be another direction for further research. A user study can be conducted to compare the proposed framework with conventional robotic rehabilitation and mirror therapy approaches in terms of efficacy in motor function development and retention in patients with hemiparesis. In this context, in addition to haptics-enabled assistance, visual and auditory modalities can be also integrated and evaluated. Accordingly, an optimal multimodal sensorimotor integration pattern may be designed to maximize the development rate of motor function in patients with disabilities. Identifying the optimal profile of haptics-enabled assistance would also be another aspect to explore. The optimal profile may differ from one patient to another depending on their extent of disabilities, due to the possible variations in their levels of perceivable haptic forces.

- While the classical form of mirror rehabilitation therapy focuses on the mirroring effect between symmetric limbs (arm-arm or leg-leg), asymmetric mirror therapy (arm-leg) may also be effective in inducing motor function. This is a question that can be answered through a teleoperation-based mirror therapy framework. Using such a platform, asymmetric mirror therapy can be implemented and examined in terms of possible benefits to hemiparetic patients.

- Effectiveness of the framework designed for RAMIST in accelerating motor skills development can be examined through user studies. For this purpose, the dual-console da

Vinci-based platform developed in Chapter 6 can be used to involve an expert surgeon and a trainee simultaneously. The effect of various factors on the learning curve of the trainee can be examined. Some of these factors include: type and complexity levels of the tasks to be practiced; expertise level of the trainee; as well as format and intensity level of guidance to be provided to the trainee.

Effect of various formats of guidance - including haptic, vibratory tactile, visual, and auditory – can be evaluated and compared to design the optimal integration degree of multiple modalities into the guidance profile. Optimal intensity of the haptic guidance can be investigated such that it can convey enough cues to the trainee, without spoiling their active participation. That can also involve optimal design of membership functions for the FIS through user studies.

The modular design of FIS allows for integration of multiple skills assessment metrics. Therefore, in addition to the metrics described here, other measures can be straightforwardly incorporated. An avenue to explore would be to study and develop skills assessment measures based on some biological measurements. Examples of such biometrics are heart rate, oxygen and carbon dioxide saturation level, respiratory rate and EEG-based brain activity. Such biometrics could provide trainee-specific measurements such as their level of stress and concentration over the task. As an ongoing part of this study, we have started investigating possible correlations between the expertise level of trainees and their level of stress and concentration during robotic surgical tasks. For this purpose, we have been conducting user trials involving 40 participants with expertise levels varying from novice to expert robotics surgeons. In this ongoing study, participants are asked to perform several tasks on the *da Vinci* surgical system as well as the dv-Trainer, while some of their biometrics are recorded. These biometrics include heart rate, oxygen saturation and EEG signals. The tasks varies from easy to complex and includes pick and place, rope walk, ring walk, suturing and tube anastomosis, as well as energized dissection. A partial goal of this study would be to explore any possible correlations between the expertise levels of the surgeons and their levels of stress and concentration during a robotic surgical task. The outcome will be used later to develop surgical assessment metrics based on biological measurements, which can be integrated into the supervised

training platform proposed in this thesis.

Another aspect to investigate through user studies would be to compare the impact of haptic interaction with an expert in real-time with that with a virtual expert. A virtual expert refers to movements of an expert recorded prior to and replayed during the training session. A combination of the above studies will help to provide in-depth understanding of the nature of human motor learning during robotics-assisted surgical tasks. The outcome, in turn, will specify appropriate measures to be taken towards optimizing the training framework for robotics-assisted minimally invasive surgery.

- Another direction would be to equip haptics-enabled RAMIS simulators with haptic guidance. Some simulators, e.g. the dV-Trainer from Mimic, have enabled visual guidance by visually illustrating for the trainee the desired configuration of the simulated master console in the VR environment. The visual cue is meant to guide/help the trainee in aligning the master console with the desired configuration in order to speed up the learning process. However, manipulating a master console in 6-DOF is often quite complicated so that a visual cue by itself may not be enough to guide the novice toward the desired configuration. Although visual guidance shows ***where*** to move the tool's tip, it does not show ***how*** to manipulate the master console to achieve that desired configuration. Therefore, hand-over-hand guidance and cueing can also be integrated into such simulators to speed up the trainee's motor learning.

- The frameworks proposed for both RAMRT and RAMIST in Chapters 5 and 6 are designed and analyzed in the presence of communication time delays. Therefore, they can be used for tele/in-home rehabilitation and tele-mentoring. The stability analyses provided for both architectures make it possible to investigate the impact of communication delay on the human learning curve. Studies can be conducted to find the sensitivity to delay of human motor learning through haptic guidance. A delay threshold may be obtained to denote the level up to which the learning ability is preserved. This threshold may be different for rehabilitation purposes and surgical training due to cognitive and physical differences between healthy and impaired participants.

- Finally, the MM/SS teleoperation framework proposed in Chapter 7 can be customized

to specifically address the requirements for RAMRT and RAMIST applications. The framework should be modified such that each patient or trainee receives an appropriate level and format of guidance, without affecting the inputs to other patients or trainees. The outcome would enable rehabilitation and surgical training for a class of patients and trainees, while saving on the time of the therapist/expert. This will be helpful in considerably reducing treatment and training costs for such applications, while providing patients and trainees with higher quality of therapy and training.

Curriculum Vitae

Name:	Mahya Shahbazi
Post-Secondary Education and Degrees:	K.N. Toosi University of Technology Tehran, Iran 2004 - 2008 B.Sc. Electrical Engineering Amirkabir University of Technology Tehran, Iran 2008 - 2011 Ph.D. Mechatronics Engineering University of Western Ontario London, ON, Canada 2011 - 2016 Ph.D. Electrical and Computer Engineering
Honours and Awards:	Ontario Graduate Scholarship (OGS), **International-Students** Competition, 2014-2015, $15000 NSERC CREATE program in Computer-Assisted Medical Interventions (CAMI) Western University, 2012 - 2014, $15000 per year Western Graduate Research Scholarship (WGRS), Western University, 2011-2015, $12000 per year. Selected Course Project, "Singularity-Free Robust Control of a Redundant 7-DOF Robot", Amirkabir University of Technology, Tehran, Iran, 2009, $150 Ranked 3rd in RoboCup Iran-Open Competition, Small-Size League, Iran, 2009 Participation in RoboCup Competition, Small-Size League, Austria, 2009 Ranked among top 1% nationwide in university entrance exam, Iran, 20004

Related Work Experience:

Teaching Assistant
Electrical and Computer Engineering Department, Western University
2012 - 2015

Teaching Assistant
Department of Electrical Engineering, K.N. Toosi University of Technology
2008 - 2009

Research Assistant
Canadian Surgical Technologies and Advanced Robotics (CSTAR)
Department of Electrical and Computer Engineering, Western University
2011 - 2016

Visiting Research Scholar
Department of Electrical and Computer Engineering, University of Alberta
Jun - Dec., 2014

Other Scientific Activities

Workshop Co-organizer of:
AIM workshop on "Advanced Intelligent Mechatronics for Neuromuscular Rehabilitation and Recovery Assessment",
Co-organized with S.F. Atashzar, M. Tavakoli, R.V. Patel
Banff, AB, Canada, 2016

Lab Tutor of:
"The 3rd North American Summer School on Image Guided Interventions, Surgical Robotics and Simulation",
CSTAR, Western University, Canada, 2012

Project Judge at:
WE FIRST Lego League Robotics Competition
London, ON, Canada, 2016

Robot Design Judge at:
WE FIRST Lego League Robotics Competition
London, ON, Canada, 2015

Physical Science Judge at:
Thames Valley Science and Engineering Fair
London, ON, Canada, 2015

Technical Reviewer of:

- IEEE Robotics and Automation Letters, 2017
- Control Engineering Practice, 2016
- International Journal of Control, 2016
- IEEE Transactions on Haptics, 2015
- Mechatronics, 2015
- Journal of Intelligent and Robotic Systems, 2015
- IEEE Int. Conf. on Robotics and Automation, 2013-2017
- IEEE/RSJ Int. Conf. on Intelligent Robots and Systems, 2013-2015
- Robotics: Science and Systems Conference, 2015
- American Control Conference, 2011-2016
- World Congress of the Int. Federation of Automatic Control, 2014
- Robotica, 2012, 2013
- IEEE World Haptics Conference, 2011
- Conference on Decision and Control, 2010

Publications:

Peer-Reviewed Journal Papers

Mahya Shahbazi, S. Farokh Atashzar, Mahdi Tavakoli and Rajni V. Patel, "Robotics-Assisted Mirror Rehabilitation Therapy: A Therapist-in-the-Loop Assist-as-Needed Architecture", *IEEE/ASME Transactions on Mechatronics*, vol. 21, no.4, pp. 1954 - 1965, 2016.

Mahya Shahbazi, S. Farokh Atashzar, Mahdi Tavakoli and Rajni V. Patel, "Position-Force Domain Passivity of Human Arm in Telerobotics Systems", Submitted to the *International Journal of Robotics Research: Special Issue on Human-Robot Interaction*, 2016.

Mahya Shahbazi, Rajni V. Patel, "A Systematic Review of Multilateral Teleoperation Systems", To be submitted to *IEEE Transactions on Haptics*, 2016.

S.F. Atashzar, **Mahya Shahbazi**, M. Tavakoli and R.V. Patel, "A Supervised Therapist-in-the-Loop Technique for Training of Haptics-enabled Robotic Rehabilitation Systems", Submitted to *IEEE Transactions on Human-Machine Systems*, 2016.

S.F. Atashzar, **Mahya Shahbazi**, C. Ward, O. Samotus, M. Delrobaei, F. Rahimi, J. Lee, M. Jackman, M. Jog, R.V. Patel, "Haptic Feedback Manipulation During Botulinum Toxin Injection Therapy for Focal Hand Dystonia Patients: A Possible New Assistive Strategy", *IEEE Transactions on Haptics, Special Issue on Haptics in Neuroscience*, DOI. 10.1109/TOH.2016.2601605, 2016.

M. Jackman, M. Delrobaei, F. Rahimi, S.F. Atashzar, **Mahya Shahbazi**, Rajni Patel, and M.

Jog, "Predicting Improvement in Writer's Cramp Symptoms Following Botulinum Neurotoxin Injection Therapy", *Tremor Other Hyperkinetic Movements*, DOI. 10.7916/D82Z15Q5, 2016.

S.F. Atashzar, **Mahya Shahbazi**, Mahdi Tavakoli and Rajni V. Patel, "A Grasp-based Passivity Signature for Haptics-enabled Human- Robot Interaction: Application to Design of a New Safety Mechanism for Robotic Rehabilitation", *International Journal of Robotics Research: Special Issue on Human-Robot Interaction*, 2016, Accepted subject to minor revisions.

M. Delrobaei, F. Rahimi, M.E. Jackman, S.F. Atashzar, **Mahya Shahbazi**, R.V. Patel, M. Jog, "Kinematic and Kinetic Assessment of Upper Limb Movements in Patients with Writer's Cramp", *J. of NeuroEngineering and Rehabilitation*, DOI: 10.1186/s12984-016-0122-0, 2016.

S. Farokh Atashzar, **Mahya Shahbazi**, O. Samotus, M. Tavakoli, M. Jog, and R.V. Patel, "Characterization of Upper-limb Pathological Tremors: Application to Design of an Augmented Haptic Rehabilitation System", *IEEE Journal of Selected Topics in Signal Processing: Special Issue on Person-Centered Signal Processing for Assistive, Rehabilitative and Wearable Health Technologies*, vol. 10, no. 5, pp. 888 – 903, 2016.

S. F. Atashzar, N. Jafari, **Mahya Shahbazi**, H. Janz, M. Tavakoli, R.V. Patel, K. Adams, "Telerobotics-assisted Platform for Enhancing Interaction with Physical Environments for People Living with Cerebral Palsy", *Journal of Medical Robotics Research*, 2016, In press.

S. F. Atashzar, **Mahya Shahbazi**, M. Tavakoli, R.V. Patel, "A Passivity-based approach for Stable Patient-Robot Interaction in Haptics-enabled Rehabilitation Systems: Modulated Time-domain Passivity Control (M-TDPC)", *IEEE Transactions on Control*, DOI: 10.1109/TCST.2016.2594584, 2015.

Mahya Shahbazi, S.F. Atashzar, H.A. Talebi, R.V. Patel, "Novel Cooperative Teleoperation Framework: Multi-Master/Single-Slave System", *IEEE/ASME Transactions on Mechatronics*, vol. 20, no. 4, pp. 1668-1679, 2014.

Mahya Shahbazi, H.A. Talebi, S.F. Atashzar, F. Towhidkhah and M.J. Yazdanpanah, "A Sliding-Mode Controller for Dual User Teleoperation with Unknown Time Delay", *Robotica*, vol. 31, no. 4, pp. 589-598, 2013.

S. F. Atashzar, H.A. Talebi, **Mahya Shahbazi** and F. Towhidkhah, "A Force Observation Methodology for Tracking Control of Flexible Link Manipulators", *Robotica*, vol. 31, no. 4, pp. 669-677, 2013.

H.D. Taghirad, S. F. Atashzar and **Mahya Shahbazi**, "A Robust Solution to 3D Pose Estimation Using Composite Extended Kalman Observer and Kalman Filter", *IET Computer Vision*, vol. 6, no. 2, pp. 140-52, 2012.

S. F. Atashzar, H.A. Talebi, **Mahya Shahbazi**, M.J. Yazdanpanah and F. Towhidkhah, "Robust Trajectory Modification for Tip Position Tracking of Flexible-Link Manipulators", *Journal of*

Systems and Control Engineering (IMECHE-Part I), vol. 226, no. 4, pp. 523-536, 2012.

M. Vaezzadeh and Q. Wang, M. Shahbazi, S. F. Atashzar, "The alternating electrostatic force needed to optimize growth of a carbon nanotube", *Journal of Computational and Theoretical Nanoscience*, Vol.5, No. 11, pp. 2170-2175, 2008.

Peer-Reviewed Conference Papers

Mahya Shahbazi, S. Farokh Atashzar, Mahdi Tavakoli and Rajni V. Patel, "Therapist-In-The-Loop Robotics-Assisted Mirror Rehabilitation Therapy: An Assist-As-Needed Framework", IEEE International Conference on Robotics and Automation (ICRA), 2015.

S. Farokh Atashzar, **Mahya Shahbazi**, Mahdi Tavakoli and Rajni V. Patel, "A New Passivity-Based Control Technique for Safe Patient-Robot Interaction in Haptics-Enabled Rehabilitation Systems", IEEE/RSJ International Conference on Intelligent Robots and Systems (IROS), 2015.

Mahya Shahbazi, S.F. Atashzar, and R.V. Patel, "A Framework for Supervised Robotics-Assisted Mirror Rehabilitation Therapy", IEEE/RSJ International Conference on Intelligent Robots and Systems (IROS), 2014.

S.F. Atashzar, A. Saxena, **Mahya Shahbazi**, R.V. Patel, "Involuntary Movement during Haptics-enabled Robotic Rehabilitation: Analysis and Control Design", IEEE/RSJ International Conference on Intelligent Robots and Systems (IROS), 2014.

Mahya Shahbazi, H.A. Talebi, R.V. Patel, "Networked Dual-User Teleoperation with Time-Varying Authority Adjustment: A Wave Variable Approach", IEEE/ASME International Conference on Advanced Intelligent Mechatronics (AIM), 2014.

Mahya Shahbazi, S.F. Atashzar, H.A. Talebi and R.V. Patel, "An Expertise-Oriented Training Framework for Robotics-Assisted Surgery", IEEE International Conference on Robotics and Automation (ICRA), 2014.

M. Delrobaei, M. Jog., F. Rahimi, M.E. Jackman, S.F. Atashzar, **Mahya Shahbazi**, R.V. Patel, "Simultaneous Arm Joint Angles and Force Changes in Writer's Cramp", 21th Iranian Conference on Biomedical Engineering (ICBME), pp. 229 – 234, 2014.

Mahya Shahbazi, S.F. Atashzar, and R.V. Patel, "A dual-user teleoperated system with Virtual Fixtures for robotic surgical training", IEEE International Conference on Robotics and Automation (ICRA), pp. 3639-3644, 2013.

Mahya Shahbazi*, S. F. Atashzar*, I. Khalaji*, R.V. Patel, M. Naish, A. Talasaz, "Robot-assisted lung motion compensation during needle insertion", IEEE International Conference on Robotics and Automation (ICRA), 2013. (*contributed equally to the work).

Mahya Shahbazi*, S.F. Atashzar*, F. Rahimi, M. Delrobaei, J. Lee, R.V. Patel, and M. Jog, ”Effect of kinesthetic force feedback and visual sensory input on writer’s cramp”, International IEEE/EMBS Conference on Neural Engineering, pp. 883-886, 2013. (*contributed equally to the work).

F. Rahimi, M. Delrobaei, S.F. Atashzar, **Mahya Shahbazi**, J. Lee, M.E. Jackman, R.V. Patel, and M. Jog, ”Sensory manipulation in writer’s cramp: Possibilities for rehabilitation”, International IEEE/EMBS Conference on Neural Engineering, pp. 303-306, 2013.

Mahya Shahbazi, S.F. Atashzar, H.A. Talebi, R.V. Patel, “A Multi-Master /Single-Slave Teleoperation System”, ASME Dynamic Systems and Control Conference (DSCC), 2012.

S.F. Atashzar, **Mahya Shahbazi**, H.A. Talebi, R.V. Patel, “Control of Time-Delayed Telerobotic Systems with Flexible-Link Slave Manipulators,” IEEE/RSJ International Conference on Intelligent Robots and Systems (IROS), 2012.

Mahya Shahbazi, H.A. Talebi, S.F. Atashzar, F. Towhidkhah, R.V. Patel, S. Shojaei, “A Novel Shared Structure for Dual User Systems with Unknown Time-Delay Utilizing Adaptive Impedance Control”, IEEE International Conference on Robotics and Automation (ICRA), 2011.

Mahya Shahbazi, H.A. Talebi, S. F. Atashzar, F. Towhidkhah, R.V. Patel and S. Shojaei, “A new set of desired objectives for dual-user systems in the presence of unknown communication delay”, IEEE/ASME International Conf. on Advanced Intelligent Mechatronics (AIM), 2011.

S. F. Atashzar, H.A. Talebi, **Mahya Shahbazi**, Farzad Towhidkhah, Rajni Patel, “Time Delayed Non-minimum Phase Slave Telerobotics”, 50th IEEE Conf. on Decision and Control (CDC), 2011.

S. F. Atashzar, H.A. Talebi, **Mahya Shahbazi**, Farzad Towhidkhah, Rajni Patel, S. Shojaei, “Control Challenges in Non-minimum Phase Telerobotics Systems,” IEEE/ASME International Conf. on Advanced Intelligent Mechatronics (AIM), 2011.

Mahya Shahbazi, H.A. Talebi, and M.J. Yazdanpanah, “A control architecture for dual user teleoperation with unknown time delays: A sliding mode approach”, IEEE/ASME International Conference on Advanced Intelligent Mechatronics (AIM), 2010.

Mahya Shahbazi, H. A. Talebi and F. Towhidkhah “A Robust Control Architecture for Dual User Teleoperation System with Time-Delay”, 36th Annual Conference of the IEEE Industrial Electronics Society (ISIE), 2010.

S. F. Atashzar, H.A. Talebi, and **Mahya Shahbazi**, “Tracking Control of Flexible-Link Manipulators Based on Environmental Force Disturbance Observer”, 49th IEEE Conference on Decision and Control (CDC), 2010.